Technical Report 1179
LL-6

Dynamically Stable Legged Locomotion

Marc H. Raibert
H. Benjamin Brown, Jr.
Michael Chepponis
Jeff Koechling
Jessica K. Hodgins
Diane Dustman
W. Kevin Brennan
David S. Barrett
Clay M. Thompson
John Daniell Hebert
Woojin Lee
Lance Borvansky

MIT Artificial Intelligence Laboratory

This blank page was inserted to preserve pagination.

Dynamically Stable Legged Locomotion

Report LL–6

Marc H. Raibert, H. Benjamin Brown, Jr., Michael Chepponis
Jeff Koechling, Jessica K. Hodgins, Diane Dustman
W. Kevin Brennan, David S. Barrett, Clay M. Thompson
John Daniell Hebert, Woojin Lee, Lance Borvansky

The Leg Laboratory

Artificial Intelligence Laboratory
Massachusetts Institute of Technology
Cambridge, Massachusetts

September 1989

This research was sponsored by contract MDA903-85-K-0179 from the Defense Advanced Research Projects Agency, Information Sciences Technology Office, and by a grant from the System Development Foundation.

Massachusetts Institute of Technology
Copyright © 1988 by Oliver R. Mitchell
All rights reserved. Published by ____.
Printed in the United States of America

Abstract

This report documents our study of active balance in dynamic legged systems. The purpose of this research is to build a foundation of knowledge that can lead both to the construction of useful legged vehicles and to a better understanding of animal locomotion. In this report we focus on the control of biped locomotion, the use of terrain footholds, running at high speed, biped gymnastics, symmetry in running, and the mechanical design of articulated legs:

- Planar Biped—Control principles originally developed for one-legged hopping were extended to control biped running. A planar biped machine uses this approach to run with an alternating gait, to hop on one leg, and to switch between gaits.
- Rough Terrain—The ability to place the feet on specific footholds is essential to locomotion on rough terrain. We have explored three methods for controlling the length of the step in order to control foot placement. This work allows the planar biped to negotiate obstacles and climb stairs.
- Top Running Speed—The running speed of a legged system can be limited by the strength, length, and stiffness of the legs, the range of joint motion, and the actuator force-velocity characteristics. In the course of experimenting with these parameters, the planar two-legged robot has reached a top speed of 5.9 m/s (13.1 mph).
- Biped Gymnastics—The planar biped has done front flips and aerials. The control program that produces flips uses open-loop actuation patterns in conjunction with the algorithms for normal running.
- Trot, Pace, Bound—We have generalized algorithms for one-legged running to the control of a four-legged running machine. One set of control programs generates three running gaits: trotting, pacing, and bounding. The machine can switch between some of the gaits while running.
- Articulated Legs—We expect legs that use rotary joints to be better than telescoping legs. They will have lower moment of inertia, less unsprung mass, a larger range of motion, better ruggedness, and will be easier to build. Tests on a simple articulated leg indicate that it has superior mechanical characteristics, but it is more difficult to control.
- Passive Dynamic Running—We are interested in the possibility of designing legged systems whose intrinsic mechanical behavior is very close to the behavior needed for locomotion. We have simulated a passive legged system composed entirely of springs, masses, and linkages. It runs passively when supplied with suitable initial conditions.

- Internal Combustion Actuators—A typical mobile hydraulic power supply consists of an engine, pump, drivetrain, and actuators. Can the combustions that normally occur in the engine be moved to the actuator, thereby eliminating the engine, pump, and drivetrain?
- Zero Gravity Running—It is possible to run in the absence of gravity by traveling between two rebound surfaces. We have explored zero-gravity running for the case of a planar one-legged, two-footed machine. The one-g balance algorithms are effective in zero-g without fundamental modification.

Contents

This empty page was substituted for a blank page in the original document.

Chapter 1

Introduction and Summary

This is the sixth in a series of reports describing research on the dynamics of legged locomotion. The work was done in the Leg Laboratory, located at Carnegie-Mellon University from 1981–1986, and at the Massachusetts Institute of Technology from 1987–present. The premise for this research is that active balance and dynamics are important for the control of legged systems, robots and animals alike. Systems that balance actively can use footholds that are widely separated or erratically placed, and they can move along narrow paths where a broad base of support is not available. They can locomote when support is available only intermittently. Dynamics is already a key ingredient in the behavior of animals and it will weigh heavily in the development of useful legged vehicles.

A dynamic treatment need not be an intractable treatment. We have found that simple algorithms can provide balance and control for a variety of dynamic legged systems. The machines we have studied include a planar one-legged hopping machine, a three-dimensional one-legged hopping machine, a planar biped running machine, a quadruped, a monopod with a rotary leg joint, and a zero-gravity one-legged two-footed running machine. The techniques used to control each of these machines derive from a single set of control algorithms, modified in various ways. These algorithms have been adapted for hopping, pronking, biped running, fast running, trotting, pacing, bounding, and simple gymnastic maneuvers. The ability of simple algorithms to operate under these diverse circumstances suggests the algorithm's fundamental nature.

The remainder of this report is a collection of papers that describes these projects. They are summarized in the following paragraphs.

Planar Biped Running Machine

The algorithms used to control machines that hop on one leg were extended to control a planar biped, which runs on two legs. The basic approach is for the control system to designate an active leg and an idle leg. Because there is just one active leg at a time, the one-leg algorithms can be used to control the biped's behavior. These algorithms focus on controlling hopping height, forward running speed, and body posture. The idle leg is kept short while it is made ready for the next step. Using this approach, the planar biped

Table 1–1: Summary of Research at the Leg Laboratory

1982	Planar one-legged machine hops in place, travels at a specified rate, keeps its balance when disturbed, and jumps over small obstacles.
1983	Three-dimensional one-legged machine runs and balances on an open floor.
1983	Simulations reveal passively stabilized bounding gait for quadruped-like model.
1984	Data from cat and human runners exhibit symmetries like those used to control running machines.
1984	Quadruped running machine runs with trotting gait. The one-leg algorithms are extended to control this machine.
1985	Planar biped runs with one- and two-legged gaits and changes between gaits.
1986	Planar biped does flips and aerials.
1986	Planar biped sets new speed record of 5.2 m/s (11.5 mph).
1987	Quadruped runs with trotting, pacing, and bounding gaits.
1988	Planar biped adjusts stride to place feet on footholds. This allows jumping over obstacles and climbing stairs.
1988	Planar biped runs with longer legs, increasing top speed to 5.9 m/s (13.1 mph.
1988	Quadruped demonstrates rudimentary ability to change between running gaits.
1988	Simulations show energy conservative running motion for simple one- and two-legged systems.
1988	Computer simulation shows running in zero-g by bouncing between two floors.

runs with an alternating gait or a hopping gait, and can change gaits while running. We have used the planar biped to study locomotion on rough terrain, running at high speed, and gymnastic maneuvers. See figure 1–2. The control program that produces a flip uses open-loop control patterns in conjunction with the algorithms for normal running.

Controlling Step Length for Rough Terrain

Legged vehicles will be useful when they are able to travel on rough terrain. Jessica Hodgins is studying the control of dynamic legged locomotion on rough terrain. She addresses the problem of controlling the length of each step to position the feet on particular footholds on the ground. She has explored three approaches to manipulating step length. One approach adjusts the duration of the flight phase, holding the duration of stance and the forward speed constant. A second approach adjusts the stiffness of the leg to change the duration of the stance phase, holding the duration of flight and forward speed constant. The third approach adjusts forward running speed, holding cadence constant. Measurements show

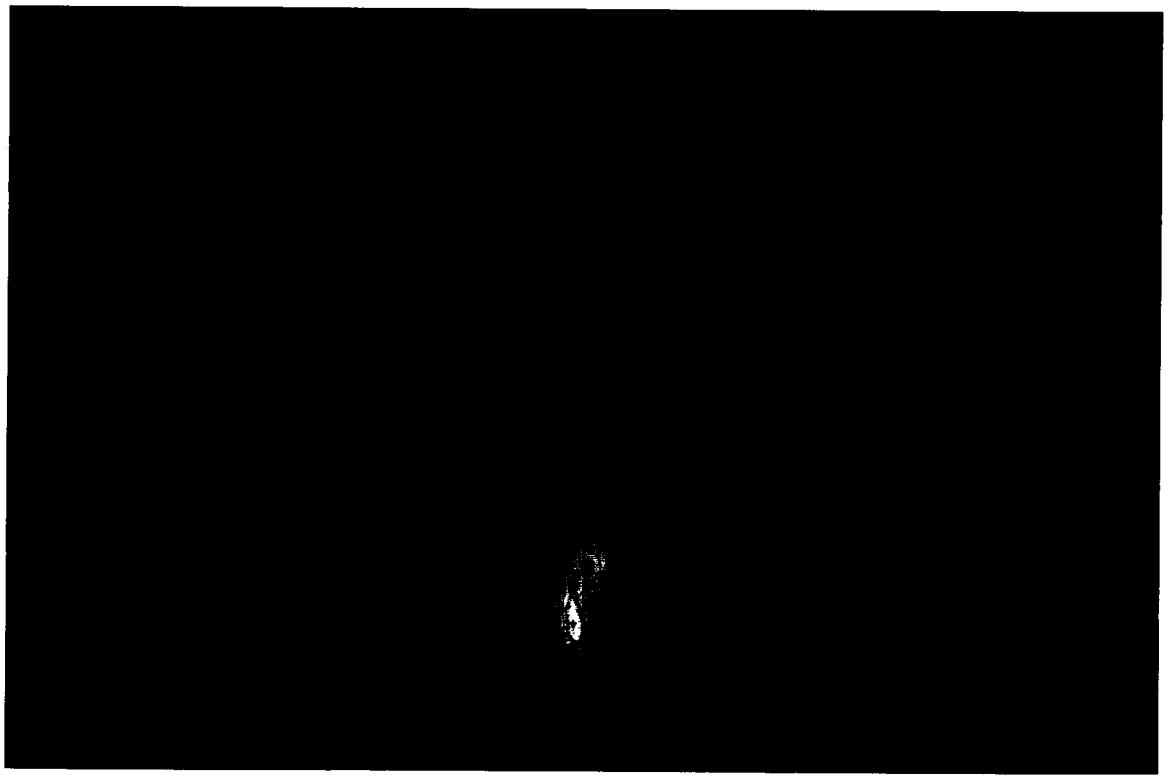

Figure 1–1: Photograph of the planar biped running up and down a short flight of stairs. The machine adjusts the length of each step as it approaches the stairs, in order to place the feet properly with respect to the stairs. The machine is shown running from left to right, with the lines indicating the paths of the feet.

that all three control methods were successful in manipulating step length, but the forward speed method provided accurate control of step length (average absolute error 0.07 m) and the widest range of step lengths (0.1 m and 1.1 m). A practical system running on rough terrain might combine these and other techniques for manipulating the length of its steps. So far we have studied the methods in isolation to understand them better. Using these methods to control step length, the planar biped has climbed stairs, jumped over obstacles, and jumped through a hoop.

Fast Running

What are the basic factors that limit speed in legged locomotion? What limits top speed for the specific case of the planar biped? Energy, control, mechanical design, and computing are broad candidates. Jeff Koechling developed a dependency tree that expresses the speed of a running system in terms of its physical parameters and constraints on the control. The tree suggests that a robot should have long, strong, stiff legs, and actuators with high peak velocity in order to run fast. These efforts have resulted in a substantial increase in top running speed for the planar biped, which now stands at 5.9 m/s (13.1 mph).

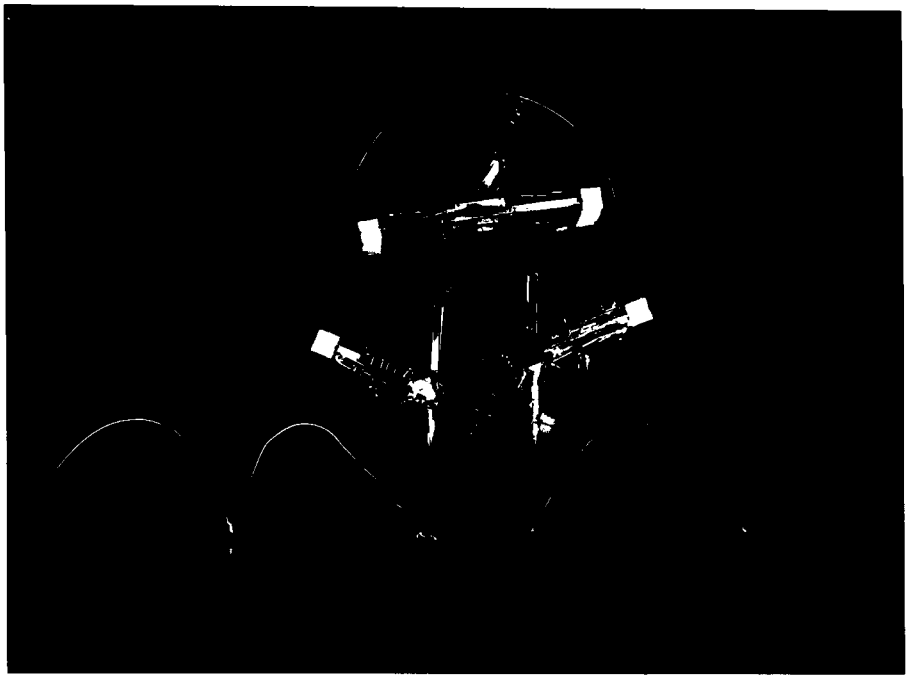

Figure 1–2: Three images of the planar biped as it does a flip. The flash was synchronized with liftoff, peak altitude during flip, and touchdown. The machine ran from right to left.

Articulated Legs

How can we build legs that are stronger, lighter, faster, and more reliable than those used on previous running machines? One approach is to use rotary joints rather than linear telescoping joints. In previous work we built four machines that ran successfully on telescoping legs. However the mass and moment of inertia of these legs was high, their reliability was low, and they were difficult to build. We believe that articulated legs, those that use rotary joints, can be designed to solve some of these problems. One hurdle is to incorporate the elastic storage elements vital to good dynamic behavior, without making the leg too difficult to control. A first design is shown in figure 1–3. The tests we have done show that it performs quite well as part of a planar hopping machine, though its asymmetry and high natural frequency pose new locomotion control problems. This work is aimed at designing an articulated leg for a quadruped.

Passive Dynamic Running

The legged robots we studied previously used springs in their legs to drive the vertical motion of the body. A springy leg allows the vertical motion to be based on a spring-mass oscillation that recycles energy from one step to the next. Can a springy hip be used to improve the efficiency of the legs' fore and aft motions too? To explore this question we

Figure 1–3: Photograph of monopod with articulated leg. The foot is a fiberglass leaf-spring. Hydraulic actuators drive the hip joint and pulls on a tendon attached to the foot.

have done computer simulations of a simple hopping machine made up entirely of passive elements, such as springs, masses, and linkages, with no actuators. One spring in the leg allows vertical oscillations while a second spring in the hip allows the leg to swing fore-aft in a passive oscillation. By tuning the mechanical parameters of the system, we have found reentrant trajectories for the system that coordinate the vertical body motions with the leg sweeping motions, and that accommodate the ground interaction constraints. Whereas physical implementations of passive dynamic running will require a source of control for stability and a source of energy to make up for losses, good passive behavior will reduce the energetic cost of locomotion, especially at high speeds.

Internal Combustion Actuator

A typical self-contained power supply for a hydraulic robot includes a gas tank, an internal combustion engine, a linkage, a hydraulic pump, plumbing, servovalve, and a piston driven actuator. Can the internal combustions that occur in the engine be moved to the actuator, so we can eliminate the tank, engine, linkage, and pump? To do so would require a degree of control over the combustions that is not found in existing engines. Furthermore, the output impedance of the combustion actuator would have to be matched to the input impedance of the robot linkage. If these problems can be solved, the result would be a self-contained system with high power to weight ratio. So far we have built a hydrogen powered internal combustion actuator that operates on the workbench. Running machines that use internal combustion actuation are in the planning stage.

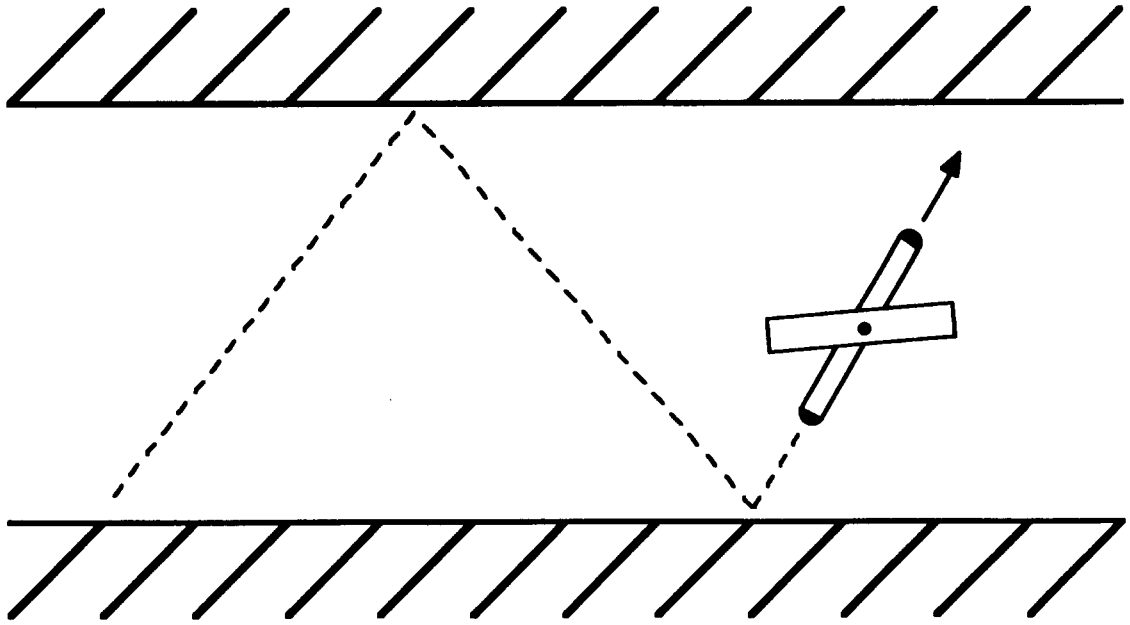

Figure 1–4: Zero gravity running. The pattern of motion exhibited by a system running between two parallel walls.

Zero Gravity Running

Normally it is not possible to run without gravity, because the upward motion that initiates the flight phase can not be reversed once contact with the ground is lost. One way to overcome this limitation is to run between two parallel rebound surfaces. In this case, the supporting forces generated in the collision with one surface reverse the vertical velocity generated during collision with the other surface. Such a configuration for running might occur in a space station, where the walls could act as the rebound surfaces. To test running between two walls, we simulated a planar machine with one leg and two feet. See figure 1–4. We found that one-leg algorithms function well in the simulated zero-g environment.

The work reported in this document focuses on principles of legged systems, including their mechanical design, approaches to sensing and control, and the computations needed for effective locomotion. Progress in developing these principles can lead to better understanding of animal locomotion and to the construction of useful legged vehicles. We also believe that progress in legged locomotion can contribute more generally to the development of dynamic robots, and to other forms of physical systems.

Leg Laboratory Bibliography

More background information for the work described in this report can be found in the following publications.

Brown, H. B. Jr., Raibert M. H. 1986. Leg that deform elastically, In *Theory and Practice of Robots and Manipulators, Proceedings of RoManSy'86*, A. Morecki, G. Bianchi, K. Kedzior (eds.) (MIT Press, Cambridge).

Goldberg, K. Y., Raibert, M. H. 1987. Conditions for symmetric running in single and double support. *Proceedings of IEEE International Symposium on Robotics*, Raleigh, North Carolina.

Hodgins, J. 1988. Legged robots on rough terrain: experiments in adjusting step length. In *Proceedings of the IEEE International Conference on Robotics and Automation* Philadelphia, March 1988.

Hodgins, J. 1989. *Legged Robots on Rough Terrain: Experiments in Adjusting Step Length.* Ph.D Thesis, Computer Science, Carnegie Mellon University, Pittsburgh, Pennsylvania.

Hodgins, J., Raibert, M. H. 1987. Planar Biped Goes Head Over Heels. In *Proceedings ASME Winter Annual Meeting* Boston, December, 1987.

Hodgins, J., Raibert, M. H. 1987. Biped Gymnastics, In *Fourth International Symposium of Robotics Research*, B. Bolles, B. Roth (eds.), (MIT Press, Cambridge).

Hodgins, J., Raibert, M. H. In Press. Biped gymnastics, *International J. Robotics Research.*

Hodgins, J., Raibert, M. H., Adjusting step length for rough terrain locomotion, Submitted to *IEEE J. Robotics and Automation*, August, 1989.

Hodgins, J., Koechling, J., Raibert, M. H. 1986. Running experiments with a planar biped. *Third International Symposium on Robotics Research*, G. Giralt, M. Ghallab (eds.). (MIT Press, Cambridge).

Hodgins, J., Koechling, J., Raibert, M. H. "Planar biped locomotion", Submitted to *IEEE Trans. Systems, Man and Cybernetics.* June, 1989.

Koechling, J. 1989. *The Limits of Running Speed: Experiments with a Legged Robot.* Ph.D Thesis, Mechanical Engineering Department, Carnegie Mellon University, Pittsburgh, Pennsylvania.

Koechling, J. and Raibert, M. 1988. How fast can a legged robot run? In: *Symposium in Robotics, DSC-Vol. 11*, K. Youcef-Toumi, H. Kazerooni (eds.). (American Society of Mechanical Engineers, New York).

Murphy, K. N., Raibert, M. H. 1985. Trotting and bounding in a planar two-legged model. In *Theory and Practice of Robots and Manipulators, Proceedings of RoManSy'84*, A. Morecki, G. Bianchi, K. Kedzior (eds.). (MIT Press, Cambridge), 411–420.

Murthy, S. S., Raibert, M. H. 1983. 3D balance in legged locomotion: modeling and simulation for the one-legged case. In *Inter-Disciplinary Workshop on Motion: Representation and Perception*, ACM.

Raibert, M. H. 1983. Dynamic stability and resonance in a one-legged hopping machine. In *Theory and Practice of Robots and Manipulators, Proceedings of RoManSy'81*, A. Morecki, G. Bianchi, K. Kedzior (eds.). Warsaw: Polish Scientific Publishers. 352–367.

Raibert, M. H. 1984. Hopping in legged systems—Modeling and simulation for the 2D one-legged case. *IEEE Trans. Systems, Man, and Cybernetics* 14:451–463.

Raibert, M. H. 1985. Four-legged running with one-legged algorithms. In *Second International Symposium on Robotics Research*, H. Hanafusa, H. Inoue (eds.), (MIT Press, Cambridge), 311–315.

Raibert, M. H. 1986. *Machines That Run (Videotape)*, (MIT Press: Cambridge Mass.)

Raibert, M. H. 1986. *Legged Robots That Balance* (MIT Press, Cambridge).

Raibert, M. H. 1986. Symmetry in running. *Science*, 231:1292–1294.

Raibert, M. H. 1986. Legged robots. *Communications of the ACM* 29:499–514.

Raibert, M. H. 1986. Running with symmetry. *International Journal of Robotics Research* 5:3–19.

Raibert, M. H., In Press. Trotting, pacing, and bounding by a quadruped robot, *Journal of Biomechanics.*

Raibert, M. H., Brown, H. B., Jr. 1984. Experiments in balance with a 2D one-legged hopping machine. *ASME J. Dynamic Systems, Measurement, and Control* 106:75–81.

Raibert, M. H., Sutherland, I. E. 1983. Machines that walk. *Scientific American* 248:44–53.

Raibert, M. H., Wimberly, F. C. 1984. Tabular control of balance in a dynamic legged system. *IEEE Trans. Systems, Man, and Cybernetics* 14:334–339.

Raibert, M. H., Brown, H. B., Jr., Murthy, S. S. 1984. 3D balance using 2D algorithms? In *First International Symposium of Robotics Research*, M. Brady, R. P. Paul (eds.), (MIT Press, Cambridge), 279–301.

Raibert, M. H., Brown, H. B., Jr., Chepponis, M. 1984. Experiments in balance with a 3D one-legged hopping machine. *International J. Robotics Research* 3:75–92.

Raibert, M. H., Chepponis, M., Brown, H. B. Jr. 1986. Running on four legs as though they were one. *IEEE J. Robotics and Automation*, 2:70–82.

Raibert, M. H., Brown, H. B., Jr., Chepponis, M., Hastings, E., Shreve, S. T., Wimberly, F. C. 1981. *Dynamically Stable Legged Locomotion, First Annual Report.* CMU–RI–81–9, Robotics Institute, Carnegie-Mellon University.

Raibert, M. H., Brown, H. B., Jr., Chepponis, M., Hastings, E., Murthy, S. S., Wimberly, F. C. 1983. *Dynamically Stable Legged Locomotion–Second Annual Report.* CMU–RI–TR–83–1, Robotics Institute, Carnegie-Mellon University.

Raibert, M. H., Brown, H. B. Jr., Chepponis, M., Hastings, E., Koechling, J., Murphy, K. N., Murthy, S. S., Stentz, A. 1983. *Dynamically Stable Legged Locomotion—Third Annual Report.* CMU–RI–TR–83–20, Robotics Institute, Carnegie-Mellon University.

Raibert, M. H., Brown, H. B., Jr., Chepponis, M., Hodgins, J., Koechling, J., Miller, J., Murphy, K. N., Murthy, S. S., Stentz, A. J. 1985. *Dynamically Stable Legged Locomotion—Fourth Annual Report.* CMU–LL–4–1985, Carnegie-Mellon University.

Thompson, C. M., Raibert, M. H., 1989. Passive dynamic running, In *International Symposium of Experimental Robotics*, Hayward, V., Khatib, O. (eds.), (Springer-Verlag, New York).

Chapter 2

Experiments with a Planar Biped

Jessica K. Hodgins, Jeff Koechling, and
Marc H. Raibert

2.1 Abstract

Bipeds typically run with an alternating gait, using only one leg at a time for support. This characteristic of bipedal running suggests that a biped could be controlled by algorithms designed for one-legged hopping. With this approach, the leg providing support is considered to be active, while the other leg is considered idle. The one-leg algorithms control the position, thrust, and hip torque of the active leg, while they keep the idle leg short and out of the way. Laboratory experiments with a planar biped running machine were used to verify the approach. The machine maintains its balance while it runs in place, travels at specified speeds, and changes between running and hopping gaits. The approach has also been used to study high-speed running, travel over rough terrain, and simple gymnastic maneuvers.

2.2 Introduction

Bipedal locomotion is a behavior that humans and animals perform with agility, grace, and speed, but robots have not yet mastered. In this paper we examine bipedal locomotion by exploring the control and coordination of a two-legged laboratory robot. Our approach takes advantage of the fact that a biped frequently runs with a gait that uses one leg at a time for support. For such a gait, the support leg can be controlled as though it were the only leg in the system, while the other leg is kept immobile so that it acts like part of the body. This approach allows algorithms developed to control one-legged hopping to be

extended for two-legged running.

The algorithms for hopping on one leg consist of separate control laws that regulate hopping height, body attitude, and running speed. These algorithms are adequate to provide dynamic balance for planar and three-dimensional one-legged hopping machines (Raibert and Brown 1984, Raibert, Brown, and Chepponis 1984). To extend the one-legged hopping algorithms for bipedal running, we added a bookkeeping mechanism so that the legs take turns providing support, and a controller for the idle leg to ensure that it does not collide with the ground.

We built a planar bipedal robot to test our approach to bipedal running. We simplified the problem by constraining the biped to move in a plane, and by using an off-board computer and power supply. The machine runs in place, travels at specified speeds, maintains balance when disturbed, and changes gaits between running and one-legged hopping. The one-leg hopping algorithms are adequate to control biped running, but we found that performance is improved when the idle leg mirrors the active leg by making the same motions 180 degrees out of phase. This tail-like use of the idle leg reduces the pitching motions of the body.

After a brief review of previous work on biped locomotion, we review the algorithms used to control one-legged hopping machines and describe the modifications needed for bipedal running. Then we describe the biped apparatus used for laboratory experiments and present data that characterize the machine's operation. We close with a discussion of how the biped running algorithms have been extended to allow more advanced bipedal behavior, including fast running, running on rough terrain, and simple gymnastic maneuvers.

Background

Kato and his colleagues built an early computer controlled biped (Ogo et al. 1980). Their biped had ten hydraulically powered degrees of freedom that moved two large feet. The first version of their machine was statically stable, moving along a preplanned trajectory that kept the center of mass of the body located over the base of support provided by the grounded foot. Each step took several seconds.

A later version of Kato's machine transferred support from one foot to the other during a dynamic tipping phase (Kato et al. 1983). This machine was statically stable most of the time. Once during each step, however, the machine slowly leaned forward until the center of mass moved forward past the front edge of the supporting foot. The machine then tipped forward onto the other foot, which was positioned so that it would catch the machine and passively return the system to static equilibrium. An inverted pendulum model of the system was used to determine where to place the catching foot.

This approach was an interesting way to achieve dynamic behavior. The system was not dynamic in the sense of reacting at run-time to the progress of the motion. Instead, an off-line analysis of the dynamics of the system specified how to position the catching foot statically to get run-time dynamic behavior. Knowledge of dynamics of the system was *compiled*, if you will, into a simple run-time strategy.

Miura and Shimoyama (1984) built the first walking machine that balanced actively. It

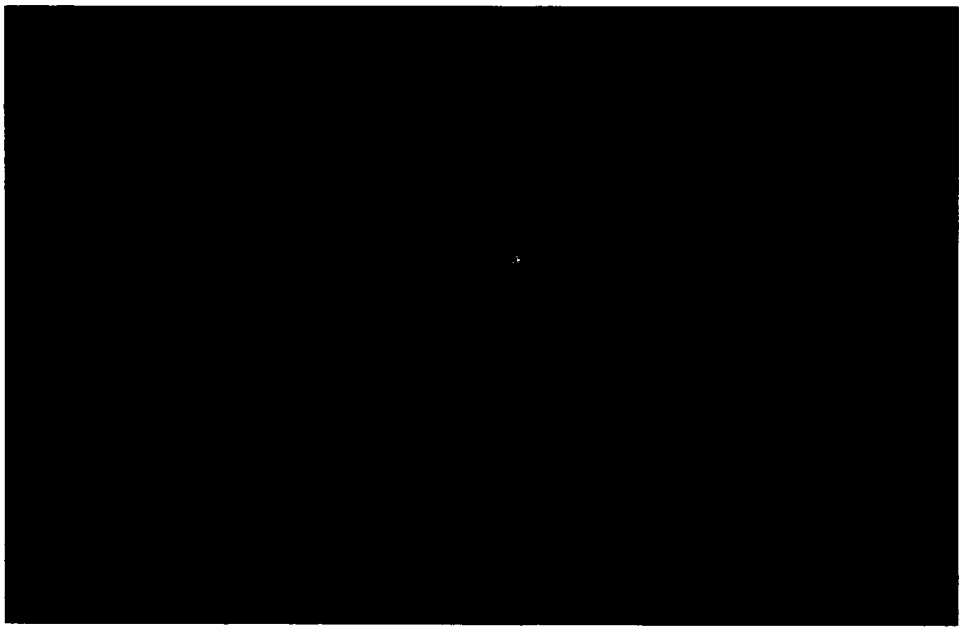

Figure 2–1: Photograph of the planar biped. Light sources were attached to the feet and the center of the body. The dashed line is a flashing light source on leg 1, which is the leg farther from the camera. The biped ran from left to right in the darkened laboratory. The control computer triggered the flash when the machine was directly in front of the camera. The trajectory of the light sources illustrates the bouncing motion of the machine.

adjusted its motions in response to changes in the dynamic state of the system. Their stilt biped, Biper 3, was patterned after a human walking on stilts, with each foot providing only a point of support. The machine had three actuators. One actuator moved one of the legs sideways, one actuator moved the other leg sideways, and a third actuator separated the legs fore and aft. Sensors in each foot detected ground contact and measured the angle of the leg with respect to the ground.

The control for Biper 3 was also derived from the inverted pendulum model of tipping during single support. Unlike the Kato machine, this biped adjusted the placement of each foot in response to the ongoing behavior of the system as measured by the sensors. Separate mechanisms controlled tipping in the forward and sideways directions. In each direction, placement of the foot was adjusted in response to the actual and desired tipping motion. Since the legs could not shorten, the machine lifted each leg by rocking onto the other leg. The machine rocked from one foot to the other, while the airborne foot was repositioned according to the algorithm. Because of the stiff legs, the machine looked like Charlie Chaplin when it walked.

The many theoretical studies of biped locomotion can be characterized by the techniques used to reduce the order of the model and to make the problem tractable. For example, Gubina, Hemami, and McGhee (1974) assumed a massless leg. Vukobratovic and Stepanenko (1973) added extra constraints to the motion of their biped model to resolve

the indeterminacies that occur when both feet are on the ground. Furusho and Masubuchi (1987) assumed that the ankle joint of the support leg was passive.

Matsuoka (1979; 1980) was the first to build a machine that ran with periods of ballistic flight. He formulated a model consisting of a body and one massless leg and derived a time-optimal state feedback controller that provided stability for hopping in place and for hopping with translation. To test this controller, Matsuoka built a planar one-legged hopping machine that operated in low gravity by lying on a table inclined 10° from the horizontal. The machine hopped about once per second and balanced as it traveled back and forth on the table.

2.3 Review of Hopping on One Leg

Raibert and his colleagues built planar and three-dimensional one-legged hopping machines that hopped in place, traveled along simple paths, jumped over obstacles, and maintained balance when disturbed mechanically (Raibert and Brown 1984; Raibert, Brown, and Chepponis 1984; Raibert 1986). These machines used a simple control system that had independent controllers for hopping height, forward speed, and body attitude. The purpose of their experiments was to explore the role of balance in legged locomotion, while avoiding the issues of gait and inter-leg coordination. In this section we give a brief description of the one-legged hopping algorithms because they provide the basis for our approach to biped locomotion.

Each one-legged hopping machine had a rigid body and a springy telescoping leg that pivoted with respect to the body at a hinge-type hip joint. One actuator exerted torque between the leg and the body and a second actuator acted along the axis of the leg, in series with a spring in the leg.

The task of controlling the hopping machines is decomposed into three parts. One part sustains the machine's bouncing motion, the second part regulates the angle of the body, and the third part stabilizes the forward running speed. A summary of the control is as follows:

- *Hopping Height*—Hopping is a resonant bouncing motion of the spring-mass system formed by the springy leg and the mass of the body. A leg actuator excites the motion by thrusting during stance. The hopping converges to a height for which the mechanical losses occurring throughout the hopping cycle balance the energy added during thrust.
- *Body Attitude*—The control system regulates the angle of the body by applying torques to the body during stance. Vertical loading on the foot keeps it from slipping when the hip actuators apply torque. A linear servo moves the body toward its nominal angle whenever the foot is on the ground:

$$\tau = -k_p(\phi - \phi_d) - k_v(\dot{\phi}) \tag{2.1}$$

  where τ is the hip torque, ϕ is the angle of the body, ϕ_d is the desired angle of the body, $\dot{\phi}$ is the angular rate of the body, and k_p, k_v are gains.
- *Forward Running Speed*—During each flight phase, the control system positions the foot to control the acceleration of the body during the next stance phase. When the control

system places the foot in the center of the distance the body travels during stance, the forward speed is the same at liftoff as it is at touchdown. We call this position of the foot the *neutral point.* When the control system displaces the foot from the neutral point, the body accelerates, with the magnitude and direction of acceleration proportional to the magnitude and direction of the displacement, as shown in figure 2–2. The control system displaces the foot from the neutral point by a distance proportional to the difference between the actual speed and the desired speed. The control system computes the desired foot position as:

$$x_{fh,d} = \frac{\dot{x}T_s}{2} + k_{\dot{x}}(\dot{x} - \dot{x}_d) \tag{2.2}$$

where $x_{fh,d}$ is the forward displacement of the foot from the projection of the center of gravity, $\dot{x}$ is the forward speed, $\dot{x}_d$ is the desired forward speed, T_s is the predicted duration of the next support period, and $k_{\dot{x}}$ is a gain. The first term of equation 2.2 is an estimate of the neutral point and the second term is a correction for the error in forward speed. The duration of the next support period is predicted to be the same as the measured duration of the previous support period. Once the control system finds $x_{fh,d}$, a kinematic transformation determines the hip angle that will position the foot as specified, and a linear servo drives the hip actuator. Figure 2–3 describes the kinematic transformation for the planar biped.

The control system uses a cyclic state machine to keep track of the behavior of the mechanism as it hops. The state machine specifies which of the three controllers operates during each phase of the hopping cycle. These algorithms stabilized the hopping of both a two-dimensional one-legged machine that was mechanically constrained to operate in a plane, and a three-dimensional one-legged machine that traveled freely about the laboratory. More detailed accounts of the control algorithms used for the one-legged machines and of the experimental results can be found in the references.

2.4 Bipedal Running Is Like Hopping

Running bipeds typically use only one leg for support at a time. During running, there is a strict alternation between support phases, during which one or the other leg supports the body by pushing downward on the ground, and flight phases, during which no legs touch the ground. During stance, we call the leg providing support the *active leg,* and the other leg the *idle leg.* During flight, we call the leg that will next provide support the active leg, and the leg that just left the ground the idle leg. The two legs exchange roles at liftoff.

We argue that the active leg can be controlled using the algorithms developed for the one-legged machines. If the idle leg is kept immobile with respect to the body, then the dynamics of bipedal running are the same as the dynamics of one-legged hopping. Because the biped uses just one leg for support at a time, the vertical thrust delivered by the active leg can be calculated using the algorithm that the one-legged system used. The torque exerted between the active leg and the body to keep the body level can also be calculated

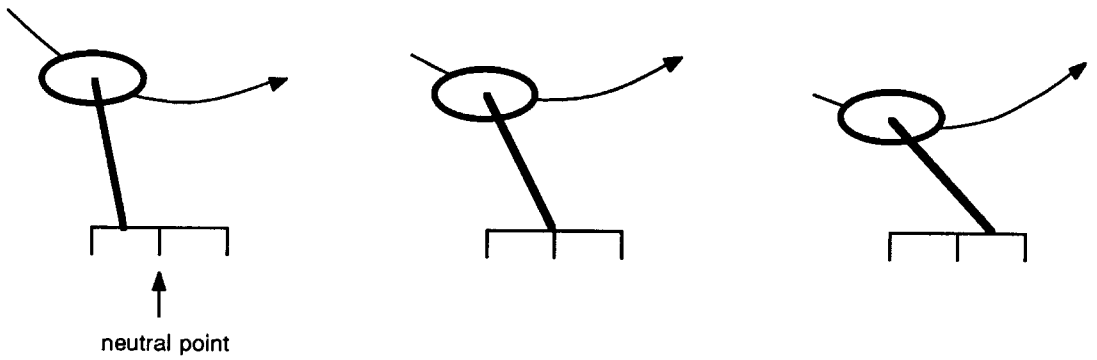

Figure 2–2: Displacement of the foot from the neutral point accelerates the body by skewing the symmetry of the body's trajectory. When the foot is placed closer to the hip than the neutral point, the body accelerates forward during stance and the forward speed at liftoff is higher than the forward speed at touchdown (left). When the foot is placed further from the hip than the neutral point, the body accelerates backward during stance and the forward speed at liftoff is slower than the forward speed at touchdown (right). Horizontal lines under each figure indicate the distance the body travels during stance, and the curved lines indicate the path of the body.

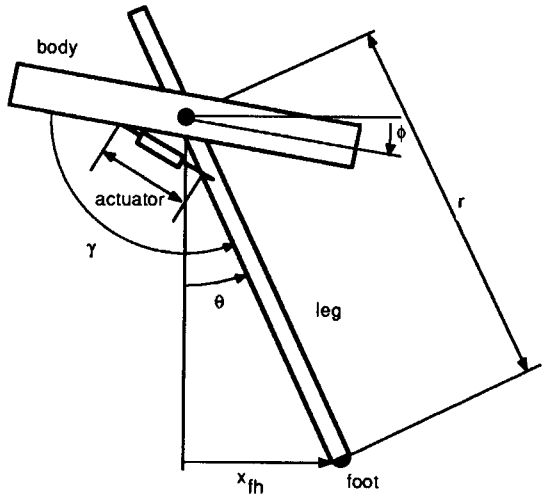

Figure 2–3: Kinematics of planar two-legged running machine. The length of the leg is ℓ, the angle between the leg and vertical is θ and the pitch angle of the body is ϕ. The control system has computed $x_{fh,d}$ according to equation 2.2. The required leg angle is $\theta_d = \arcsin(\ell/x_{fh,d})$, and the desired hip angle is $\gamma_d = \theta_d - \phi$. The hip linkage of our biped uses a linear hydraulic actuator, the desired position of which is $w_d = \sqrt{c^2 + d^2 - 2cd\cos(\gamma_d - \alpha - \beta + \pi/2)} - w_0$. The parameters are $a = 0.3194\,\mathrm{m}$, $b = 0.0032\,\mathrm{m}$, $e = 0.0439\,\mathrm{m}$, $f = 0.0062\,\mathrm{m}$, and $w_0 = 0.316\,\mathrm{m}$. The hip actuator servo law is $\tau = k_w(w_d - w) + k_{\dot{w}}\dot{w}$.

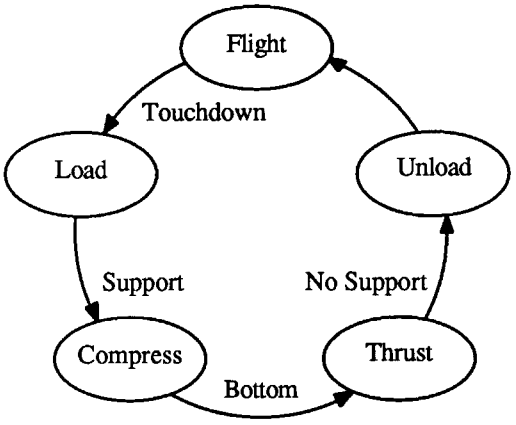

Figure 2–4: State machine for planar one-legged hopping machine. The five states are shown along with the events that trigger the state transitions.

using the one-leg algorithm. Finally, because just one of the biped's legs is placed on the ground at a time, the algorithm for calculating the placement of the active leg can be the same as that used by one-legged systems. Thus the control system for a biped can use the same three algorithms for controlling hopping height, body attitude, and forward running speed as were used by the control system for a one-legged hopping machine.

Despite these similarities, there are several differences in the control of one- and two-legged running. One difference is that a two-legged system needs the ability to shorten and lengthen its legs substantially. The idle leg must shorten so that it does not strike the ground while the active leg is compressed during stance, and it must lengthen again in preparation for providing support, soon after it becomes the active leg. The mechanical design of the leg must allow these motions.

Another difference is in the sequence of states that occur during running. The state machine for a biped must keep track of which leg is active and which is idle, and switch between them at appropriate times. The composite state machine shown in figure 2–5 performs this function. It is essentially two copies of the state machine used for the one-legged systems, joined together so that the legs take turns providing support. At liftoff, the legs switch roles with the idle leg becoming active and the active leg becoming idle.

These two changes extend the one-legged control algorithms for bipedal running. A third modification of the algorithms, called mirroring, improves stability and reduces pitching of the body. Mirroring causes the hip motion of the idle leg to follow the hip motion of the active leg, but with opposite sign. This control strategy allows the net angular momentum of the system to remain small when the legs sweep back and forth, and reduces the disturbance to body attitude.

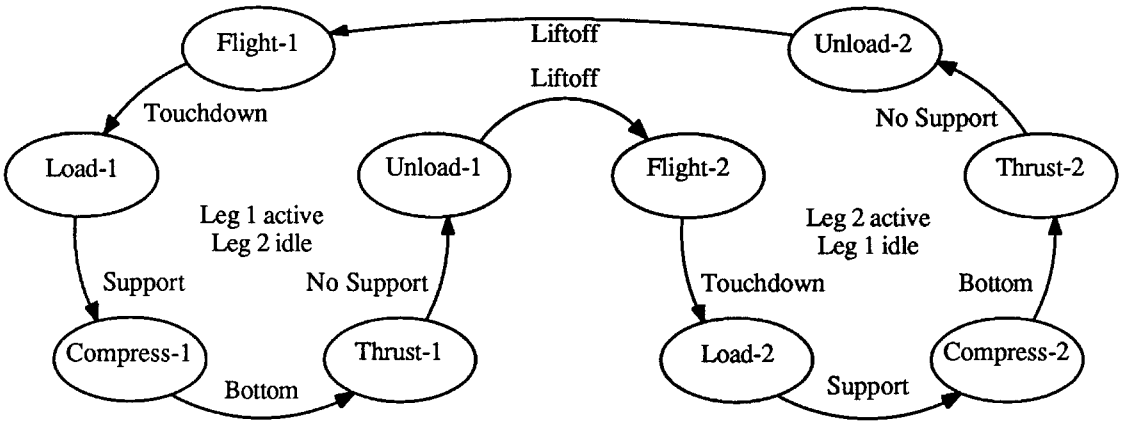

State	Trigger Event	Actions
FLIGHT	Active leg leaves ground (liftoff)	Interchange active and idle legs Lengthen active leg for landing Position active leg for landing Shorten idle leg Mirror angle of active hip with idle hip
LOADING	Active leg touches ground (touchdown)	Zero active hip torque Keep idle leg short Mirror angle of active hip with idle hip
COMPRESSION	Active leg air spring shortens (support)	Servo pitch with active hip Keep idle leg short Mirror angle of active hip with idle hip
THRUST	Active leg air spring lengthens (bottom)	Extend active leg Servo pitch with active hip Keep idle leg short Mirror angle of active hip with idle hip
UNLOADING	Active leg air spring approaches full length (no support)	Shorten active leg Zero hip torques active leg Keep idle leg short Mirror angle of active hip with idle hip

Figure 2–5: Finite state machine that coordinates two-legged running. The state shown in the left column is entered when the event listed in the center column occurs. The controller advances through the states in the sequence indicated by the arrows. The LOADING and UNLOADING states occur when the foot is on the ground, but the leg spring is not compressed. To avoid skidding the foot along the ground, no hip torque is applied in these states.

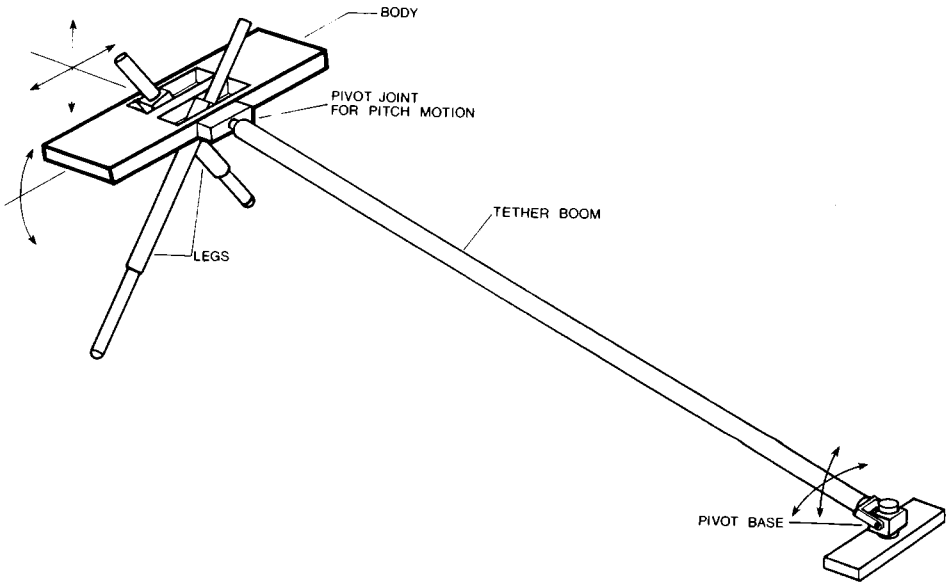

Figure 2–6: Planar biped running machine used for experiments. The body is an aluminum frame, on which are mounted hip actuators and computer interface electronics. Each hip has a low friction hydraulic actuator that positions the leg fore and aft. An actuator within each leg changes its length, while an air spring makes the leg springy in the axial direction. Figure 2–7 shows the leg in greater detail. Sensors measure the lengths of the legs, the positions and velocities of the hip actuators, pressures in the leg air springs, contact between the feet and the floor, and the pitch angle of the body. An umbilical cable connects the machine to hydraulic, pneumatic, and electrical power supplies, and to the control computer, all of which are located nearby in the laboratory. The arrangement of body, legs, hips, and actuators provides a means to control the position of the feet with respect to the body, to generate an axial thrust with each leg, and to provide hip torques during running. The tether boom constrains the machine to motion in two dimensions, fore and aft, up and down and rotation in the plane, and it provides a means of sensing body pitch angle and vertical and horizontal position in the room.

2.5 Planar Biped Experiments

We built a planar two-legged running machine to test the control of bipedal running using the one-leg algorithms. The machine, shown in figure 2–1, has two telescoping legs connected to the body by pivot joints at the hips. A hydraulic actuator exerts a torque about each hip, between the leg and the body. A hydraulic actuator within each leg works in series with a pneumatic spring. Together, they change the length of the leg and make the leg compliant along its long axis.

A tether boom mechanically constrains the machine to move on the surface of a large sphere. Locally, the machine can move fore and aft, up and down, and pitch nose up or nose down. Figures 2–6 and 2–7 show the details of the planar biped machine, and figure 2–8 indicates the motion permitted by the tether boom. The machine has a total of nine degrees of freedom, described by table 2–1. The appendix gives the physical parameters of the machine.

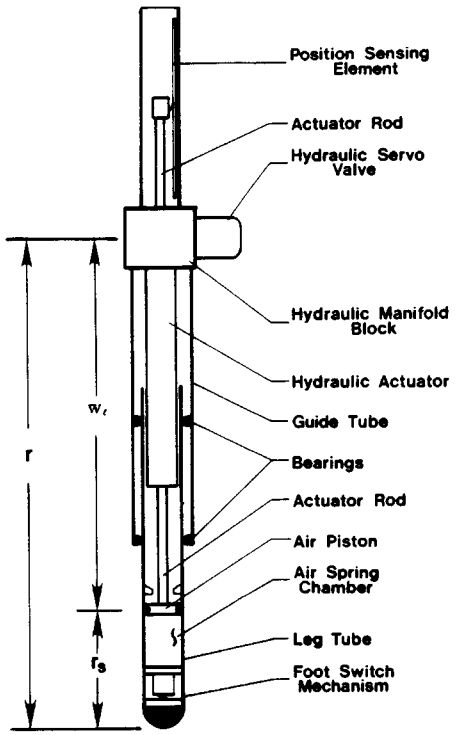

Figure 2–7: Diagram of leg used in running machine. A hydraulic actuator acts in series with an air spring. The hydraulic actuator is used to drive resonant bouncing motion of the machine and to retract the leg during flight. It also acts in conjunction with the air spring to determine the axial force the leg exerts on the ground. Sensors measure hydraulic actuator length, overall leg length, air pressure in the spring, and loading on the foot.

Constrained by its tether boom, the biped runs in a circle in the laboratory. It steps alternately on each foot as it bounces rhythmically up and down. Figure 2–1 shows the paths of the feet and the vertical bouncing motion of the body. The top graph of figure 2–9 shows the vertical motion of the biped as it ran with an alternating gait. The two legs operated 180° out of phase, as shown by the middle graph. During each support phase the leg spring first compressed and then extended, as shown in the bottom graph.

A bipedal running machine has more opportunities to regulate the angular momentum of the body than does a machine with only one leg. During flight, a machine hopping on one leg must swing its leg forward to position it for the next support phase. The hip torques that swing the leg forward also pitch the body forward, so the body accumulates a pitch error that must be corrected during the stance phase.

A machine with two legs can both swing its legs and keep its body level while conserving angular momentum. It does so by moving the two legs with equal and opposite motions, so that the hip torques exerted on the body to move one leg cancel the hip torques exerted on the body to move the other leg. We call this action *mirroring*, because the motion of the idle leg mirrors the motion of the active leg. Mirroring is reminiscent of the way that a kangaroo reduces the rotation of its body by moving its tail in the opposite direction

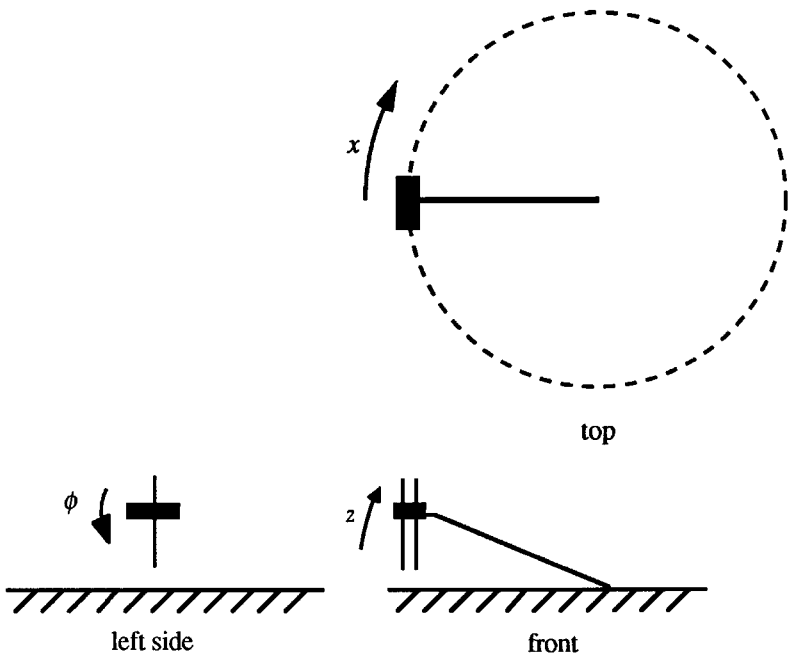

Figure 2–8: A boom constrains the biped's motion to the surface of a sphere. The boom pivots at its base, allowing the machine to travel on a circle and to jump up and down. There is also a pivot joint at the machine end of the boom, which allows the biped to rotate about its pitch axis. These three degrees of freedom allow the machine to move fore and aft, up and down, and to rotate in the plane.

Planar Biped Degrees of Freedom

degree of freedom	range of motion
horizontal position, x	0–16 m
vertical position, z	0.4–1.4 m
pitch, ϕ	$\pm 180°$
leg lengths, ℓ_1, ℓ_2	0.44–0.67 m
leg actuator positions, h_1, h_2	0.00–0.23 m
hip actuator positions, w_1, w_2	± 0.025 m

Table 2–1. The planar biped has nine degrees of freedom. A potentiometer senses the position along each degree of freedom. The length of each leg spring is determined by the difference between the total leg length and the position of the leg actuator: $s = \ell - h - 0.338\,\text{m}$.

from the motion of its legs. Mirroring does not totally eliminate disturbances to the body, because the two legs do not have the same length all the time, so their moments of inertia are not always equal.

The effect of mirroring the legs is illustrated in figure 2–10. For this experiment, the planar biped hopped on one leg, with the idle leg servoed to a fixed angle with respect to the body. After the time indicated by the vertical dashed line, the hip angle of the idle leg

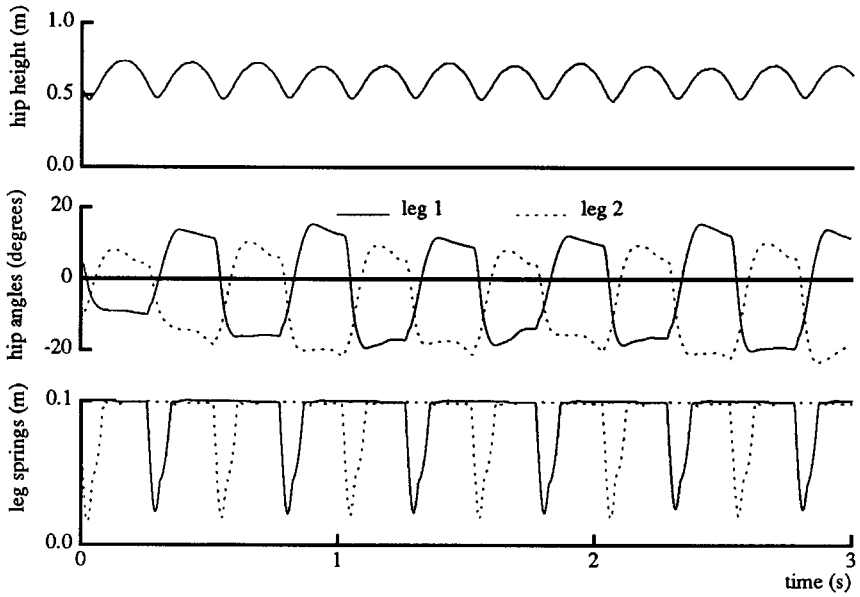

Figure 2–9: Running data for the planar biped. The top curve shows the height of the hip above the floor. The middle curve shows the angles of the two legs with respect to the body in the fore-aft plane. The legs oscillate 180° out of phase and at half the frequency of the bouncing motion. The bottom curve shows compression of the air springs as the legs are used for support in alternation. (Data file B85.226.14)

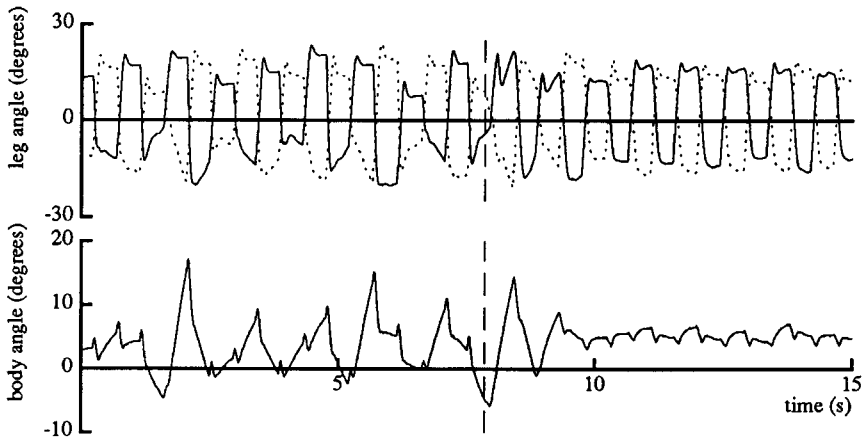

Figure 2–10: A control algorithm that kept the leg angles equal and opposite reduced the amplitude of the oscillations in body attitude. The top graph shows the angle of each leg with respect to the axis of symmetry of the body. The vertical line marks a switch from an algorithm that moved the legs independently to one that ensured that the leg angles were mirror images. The axis of symmetry was a line passing through the hip joint perpendicular to the body. The bottom graph shows that mirroring reduced the oscillations in body angle from about 20° peak-to-peak to about 6° peak-to-peak. In this experiment the planar biped was running about 2.5 m/s. (Data file B87.325.3)

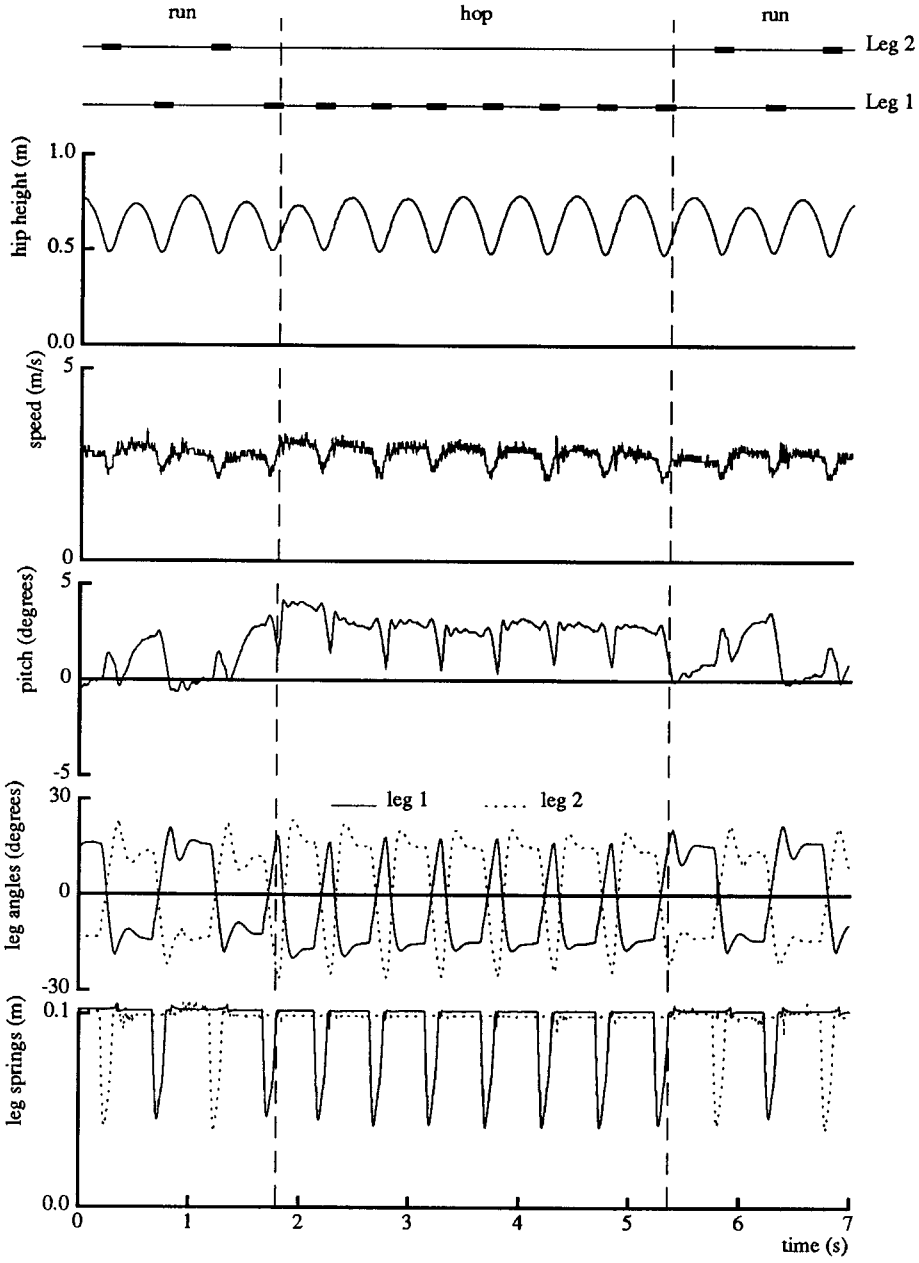

Figure 2–11: Gait transitions. The planar biped switched from two-legged running to one-legged hopping and back to two-legged running. The gait transitions did not affect the forward speed or vertical bouncing. The biped had a slightly greater pitch angle during hopping than during running. The top plot shows the pattern of footfalls during the run, with the bold line indicating ground contact. The vertical dashed lines mark the gait transitions. (Data file B89.123.2)

was servoed to the negative of the hip angle of the active leg. This mirroring of the legs reduced the maximum pitch oscillations of the body by about a factor of two.

The planar biped can run with the alternating gait described above, it can run by hopping on one leg, and it can switch between the two gaits. It runs with a hopping gait by making one leg active all the time, keeping the other leg idle. The bouncing motion of the machine is unchanged when running on one leg and, if mirroring is turned on, the idle leg acts like a tail. It is easy to do a transition from one gait to the other by switching between state machines at the beginning of a flight phase. Figure 2–11 shows data recorded as the biped switched from two-legged running to one-legged hopping and back again, as it traveled forward at 2.8 m/s.

2.6 Fast Running, Rough Terrain, and Gymnastics

We have used the bipedal locomotion algorithms just described as the basis for other legged behaviors. We have done experiments in which the planar biped ran at high speed, traveled over simple forms of rough terrain, and did gymnastic maneuvers. In each case we started with the algorithms described earlier, and either modified them or used them as a substrate upon which to build additional layers of control.

In the course of studying the limits of running speed in legged locomotion, Koechling made the planar biped run fast (Koechling and Raibert, 1988; Koechling 1989). In the fastest experiment, the machine traveled at 5.9 m/s (13.1 mph) for over 40 m. To achieve top speed, the legs of the planar biped were lengthened by 0.18 m, the control algorithms for body attitude were modified to compensate for the pressure/flow characteristics of the hip actuators, and the leg springs were made about twice their normal stiffness. Aside from these changes, the control algorithms for high-speed running were same as the algorithms described earlier.

Hodgins (1988, 1989) studied how an actively balanced legged system could adjust the length of each of its steps without losing balance. The ability to adjust step length is an important component of traveling on rough terrain. She found that the control system could adjust the length of each step by manipulating the duration of the stance phase, the duration of the flight phase, or the forward running speed. In the course of her experiments, Hodgins programmed the planar biped to step on particular spots, to jump over obstacles, and to run up and down a short flight of stairs.

To study the production of discrete maneuvers and to have some extra fun, we made the planar biped do a forward flip (Hodgins and Raibert, 1987).

To perform a flip, the biped machine runs forward, brings the legs together and thrusts with both legs to jump high, exerts a large hip torque to pitch the body forward, shortens the legs to tuck once airborne, untucks in time to land on the feet, and then continues running. To develop this behavior, we modified the algorithms that operate during three steps of otherwise normal running.

2.7 Summary

There is a class of gaits for which only one foot touches the ground at a time and each stance phase is followed by a flight phase. A biped executing such a gait can be controlled with algorithms developed for one-legged hopping machines. One of the two legs is designated the active leg, which is used to adjust hopping height, body attitude, and forward speed. The other leg is designated the idle leg, which is kept short to clear the ground and made to mirror the sweeping motions of the active leg. A state machine synchronizes the actions of the control computer to the behavior of the running machine, and selects which leg will be active on each step.

We have demonstrated the feasibility of this approach with a planar two-legged running machine that operates in the laboratory. It runs with an alternating gait, a one-legged hopping gait, and it can switch between gaits. The planar biped and the basic control algorithms have also been used to investigate the limitations of fast running, the control of step length for rough terrain, and simple robot gymnastics.

2.8 References

J. Furusho, M. Masubuchi, 1987. Control of a dynamical biped locomotion system for steady walking, in *Study on Mechanisms and Control of Bipeds*, H. Miura, I. Shimoyama (eds.) Tokyo: University of Tokyo, 116–127.

F. Gubina, H. Hemami, R.B. McGhee, 1974. On the dynamic stability of biped locomotion, *IEEE Trans. Biomedical Engineering* BME-21:102–108.

J. Hodgins, 1988. Legged robots on rough terrain: experiments in adjusting step length, in *Proceedings of the IEEE International Conference on Robotics and Automation* Philadelphia.

J. Hodgins, 1989. *Legged Robots on Rough Terrain: Experiments in Adjusting Step Length*, Ph.D Thesis, Computer Science, Carnegie Mellon University, Pittsburgh, Pennsylvania.

J. Hodgins, M. H. Raibert, 1987. Biped gymnastics, in *Robotics Research: The Fourth International Symposium*, B. Bolles, B. Roth (eds.), Cambridge, Mass.: MIT Press.

T. Kato, A. Takanishi, H. Jishikawa, I. Kato, 1983 The realization of the quasi-dynamic walking by the biped walking machine, In *Theory and Practice of Robots and Manipulators, Proceedings of RoManSy'81*, A. Morecki, G. Bianchi, K. Kedzior (eds.), Warsaw: Polish Scientific Publishers, 341–351.

J. Koechling, 1989. *The Limits of Running Speed: Experiments with a Legged Robot.* Ph.D Thesis, Mechanical Engineering Department, Carnegie Mellon University, Pittsburgh, Pennsylvania.

J. Koechling, M. Raibert, 1988. How fast can a legged robot run? in K. Youcef-Toumi and H. Kazerooni, (eds.), *Symposium in Robotics, DSC-Vol. 11.* American Society of Mechanical Engineers.

K. Matsuoka, 1979. A model of repetitive hopping movements in man, in: *Proceedings of Fifth World Congress on Theory of Machines and Mechanisms*, International Federation for Information Processing.

K. Matsuoka, 1980. A mechanical model of repetitive hopping movements, *Biomechanisms* 5:251–258.

H. Miura, I. Shimoyama, 1984. Dynamic walk of a biped, *International Journal of Robotics Research* 3(*2*):60–74.

K. Ogo, A. Ganse, I. Kato, 1980. Dynamic walking of biped walking machine aiming at completion of steady walking, in *Third Symposium on Theory and Practice of Robots and Manipulators*, A. Morecki, G. Bianchi, K. Kedzior (eds.). Amsterdam: Elsevier Scientific Publishing Co.

M. H. Raibert, *Legged Robots That Balance*, 1986. Cambridge, Mass.: MIT Press.

M. H. Raibert, H. B. Brown, Jr., 1984. Experiments in balance with a 2D one-legged hopping machine, *ASME Journal of Dynamic Systems, Measurement, and Control* 106:*1,* 75–81.

M. H. Raibert, H. B. Brown, Jr., M. Chepponis, 1984. Experiments in balance with a 3D one-legged hopping machine. *International Journal of Robotics Research* 3:*2,* 75–92.

M. Vukobratovic, Y. Stepaneko, Y., 1973. Mathematical models of general anthropomorphic systems. *Mathematical Biosciences* 17:191–242.

2.9 Appendix: Physical Parameters of Planar Biped Running Machine

Body:		
length	0.75 m	(30 in)
width	0.23 m	(9 in)
mass	11.5 kg	(25 lb_m)
moment of inertia	0.4 kg-m^2	(1370 lb_m-in^2)
Leg:		
total mass	1.66 kg	(3.66 lb_m)
unsprung mass	0.29 kg	(0.64 lb_m)
moment of inertia	0.13 kg-m^2	(444 lb_m-in^2)
Hip actuator:		
Bore	0.01613 m	(0.625 in)
Rod diameter	0.00953 m	(0.375 in)
Area	1.27×10^{-4} m^2	(0.197 in^2)
Stroke	0.051 m	(2.0 in)
Hip sweep	± 0.52 radian	($\pm 30°$)
Maximum velocity	0.500 m/s	(19.7 in/s)
Maximum force	2630 N	(591 lbf)
Moment arm	0.0444 m	(1.75 in)
Maximum torque	117 N-m	(1030 in-lb_f)
Leg actuator:		
Bore	0.0127 m	(0.500 in)
Rod diameter	0.00953 m	(0.375 in)
Area	5.54×10^{-5} m^2	(0.0859 in^2)
Stroke	0.23 m	(9.0 in)
Maximum velocity	3.42 m/s	(11.21 ft/s)
Maximum force	1146 N	(258 lb)
Maximum leg length	0.67 m	(26.4 in)
Minimum leg length	0.44 m	(17.3 in)
Air spring:		
Bore	0.0286 cm	(1.125 in)
Area	6.42×10^{-4} m^2	(0.994 in^2)
Length	0.10 m	(4.0 in)
Hip spacing	0.090 m	(3.54 in)
Boom radius	2.54 m	(100 in)
Circle circumference	15.96 m	(628 in)
Computer	DEC VAX 11/785	

This empty page was substituted for a blank page in the original document.

Chapter 3

Adjusting Step Length for Rough Terrain Locomotion

Jessica K. Hodgins

3.1 Abstract

For a legged system to travel on rough terrain it must use the available footholds, even when they are isolated or occluded by obstacles. This paper addresses the task of adjusting the length of each step to place the feet on available footholds, in the context of a dynamic biped robot that actively balances itself as it runs. In order for the biped to use specific footholds, the control system must simultaneously satisfy the constraints for stability and the constraints dictated by the geometry of the terrain. We explored three methods for controlling step length that each adjusted a different parameter of the running cycle. The parameters were forward running speed, running height, and duration of ground contact. All three control methods were successful in manipulating step length, but the forward speed method provided accurate control of step length (average absolute error 0.07 m) and the widest range of step lengths (0.1 m and 1.1 m). In laboratory demonstrations, the biped used step length adjustment to place its feet on targets, leap over obstacles, and run up and down a short flight of stairs.

3.2 Introduction

Legged vehicles may someday travel on terrain that is too rough for wheeled and tracked vehicles of comparable size. To travel on rough terrain, legged vehicles will have to use the best footholds they can reach, even those which are isolated or occluded by obstacles. The problem of traveling over rough terrain includes many sub-problems, including terrain

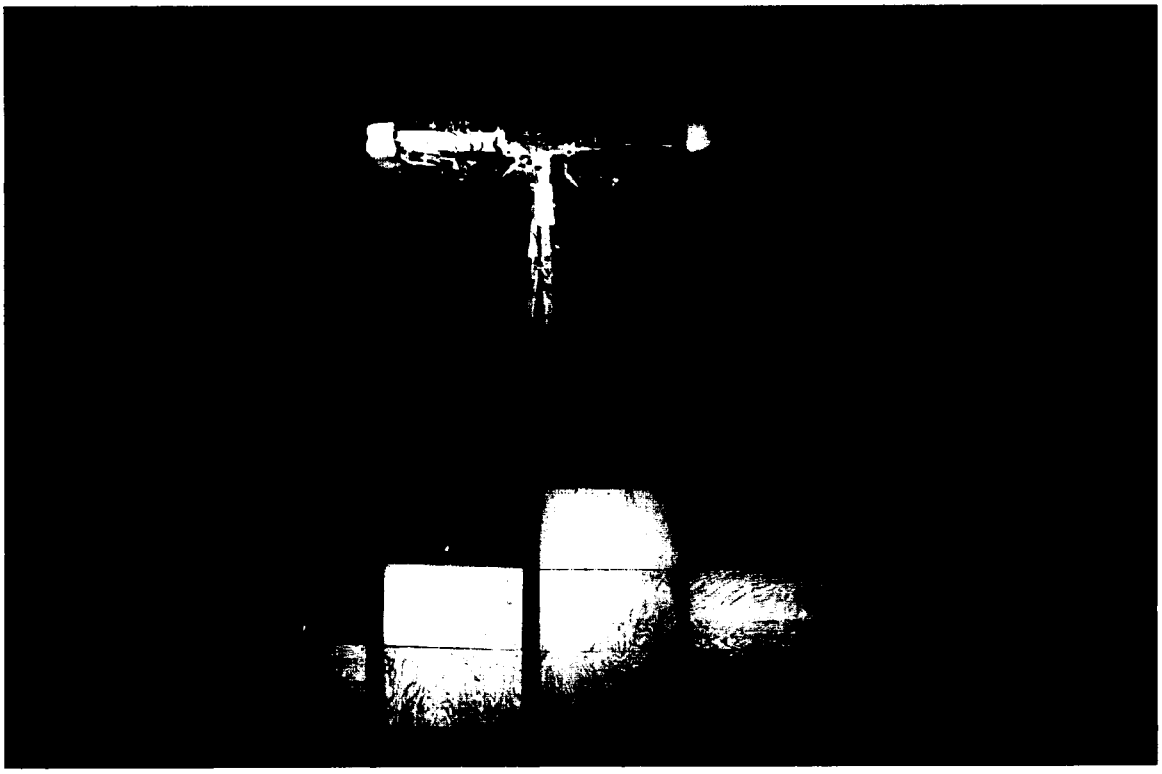

Figure 3–1: Photograph of the planar biped running up and down a flight of three stairs. The control system adjusts the length of the machine's steps so that the feet land approximately in the center of each stair. The machine is shown running from left to right at about 0.5 m/s. Light sources indicate the paths of the feet. Each step is 7 inches high and 12 inches deep.

sensing, path planning, selections of foothold, and adjustment of step length. This paper concentrates on the last of these problems, the need to adjust the length of each step so the feet are placed on chosen footholds.

We studied the control of step length in the context of systems that move dynamically. This problem is an interesting one because the act of positioning the feet with respect to available footholds interacts with the stability and general behavior of the system. Each placement of a foot on the ground causes the body to accelerate, influencing the system's forward speed and direction of travel. A system that controls placement of the feet must simultaneously satisfy the geometric constraints dictated by the locations of good footholds and the dynamic constraints for stability.

Once the problem of placing feet on chosen footholds is solved, a dynamic legged system should be able to traverse more difficult terrain than a static system of comparable size and reach. A dynamic system need not maintain support continuously in time, nor must there be a continuous path of closely spaced footholds to allow a gradual transfer of support from one support tripod to another. A dynamic system can use its flight phase to leap over regions that do not offer any good footholds. Generally, a dynamic system can use its kinetic energy to bridge from one foothold to another, and it does not require a broad base

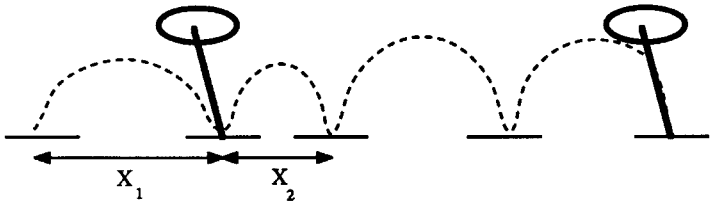

Figure 3–2: One-dimensional rough terrain consists of a series of footholds with uneven spacing in the direction of running. The footholds lie on a straight line at the intersection of the horizontal and sagittal planes. The legged system is constrained to move with three degrees of freedom in the sagittal plane. Three-dimensional rough terrain would include vertical and lateral variations in the spacing of footholds.

of support at each foothold. These potential advantages are obtained by dynamic legged systems at the expense of more difficulty in placing the feet on footholds. Foot placement is trivial for a statically stable system, once a reachable foothold has been chosen.

To study placement of feet on footholds in dynamic legged systems, we considered a special case of rough terrain locomotion in which the footholds are unevenly spaced on a straight line in the horizontal plane (figure 3–2). We used a planar biped running machine to evaluate three methods for controlling step length. One method adjusted the forward running speed of the system, while keeping the duration of the stance and flight phases constant. The second method adjusted the duration of the flight phase, while holding constant the forward running speed and duration of the stance phase. The third method for controlling step length adjusted the duration of the stance phase, while forward running speed and the duration of the flight phase were held constant. The various adjustments were made by varying the foot position, leg thrust, and leg stiffness on each step. The experiments showed that all three methods were able to provide changes in the step length while maintaining balance, but the forward speed method gave the widest range of adjustments with good accuracy.

In the next section of the paper we review previous work on rough terrain locomotion. Then we describe the planar biped machine used for the step length experiments and the details of the control methods studied. Data from the experiments are presented, along with a discussion of their relative precisions, strengths, and weaknesses. We close with demonstrations of placing a foot on a target, jumping over obstacles, and climbing stairs.

3.3 Background

Results from several fields provide background for this research. Studies of humans running on rough terrain suggest how machine locomotion might be achieved. Studies of traversing rough terrain with legged vehicles show how other researchers have approached the problem.

Lee, Lishman, and Thomson (1982) studied skilled human long jumpers, who must place their feet near the front edge of the takeoff board if they are to maximize their jump. A series of adjustments in step length permitted the jumpers to arrive at the takeoff board

with the toe very near the leading edge. They found that subjects manipulated the vertical impulse delivered to the ground by the legs. Vertical impulse, the integral of vertical force exerted on the ground during the stance phase, determines the duration of the flight phase, and, assuming constant running speed, it determines the length of each step. The use of vertical impulse to control step length is quite similar to the flight duration method for controlling step length that we report below.

Warren, Lee, and Young (1985) studied how runners adjust step length when required to place their feet on randomly positioned footholds on a treadmill. They were primarily interested in the use of vision for placing the feet on visible targets. They confirmed the long jump results, in that the subjects used vertical impulse to control step length, with nearly constant forward speed.

Patla, Robinson, Samways, and Armstrong (1989) explored the question of how step length is adjusted while running on flat, level terrain. In their experiments, human runners were required to adjust the length of one step between short, normal, and long, according to a signal from the experimenter. Both the length of the adjusted step and the timing of the signal were varied. The stance period just prior to the adjustment occurred when the foot was on a force platform, so the data included ground force information as well as ground contact times. The experimenters were able to determine which parameters were adjusted and how the choice of parameters was affected by timing of the signal. The results indicate that both horizontal and vertical impulse were adjusted to control step length and that the timing of the signal for adjustment affected the parameters used to perform the adjustment. For example, when the cue occurred late in the step, the adjustment was made during the flight phase.

Patla's conclusion that both horizontal and vertical impulse are used to control step length disagrees with Warren's conclusion that adjustments in vertical impulse are the primary technique for controlling step length. This discrepancy may result from different experimental designs: the subjects in Warren's experiment ran on a treadmill while Patla's subjects ran on the ground. The treadmill may have artificially constrained the runner's forward speed to be constant, whereas the overground runners could vary their forward speed freely.

Research in robotic legged locomotion on rough terrain has focused on the statically stable case, in which the legged system always has at least three feet on the ground and moves forward slowly. The work has concentrated on building a terrain map from sensor information, choosing suitable footholds, and reacting when the terrain does not match the map. Research has included extensive testing of algorithms in simulation as well as the study of physical machines in the laboratory and, more recently, in natural environments.

For statically stable locomotion, the difficult problem is not using a foothold or controlling step length, but deciding which locations on the terrain are suitable as footholds, allowing the legged system to maintain balance and continue walking. Researchers have addressed this problem by beginning with a desired motion trace for the body and using heuristic algorithms to select footholds along the motion trace. For instance, Okhotsimski and Platonov (1973, 1975) simulated a hexapod walking on three-dimensional poles and holes terrain. Information from a simulated range-finder was used to find feasible footholds

given knowledge about the machine's physical limitations. The simulated machine walked using the sequence of support polygons found by the foothold selection algorithms, with the additional constraint that the maximum force for any leg should be minimized and that the reaction force should be kept as close to the center of the friction cone as possible.

McGhee and Iswandhi (1979) also worked on the problem of choosing appropriate footholds for a six-legged walking machine, given a desired motion trace for the body and a model of the terrain. They proposed an algorithm for finding a sequence of acceptable footholds: legs closest to their kinematic limits in the direction of motion of the body were lifted and legs with the largest kinematic range in the direction of motion were placed first. These heuristics extended each support state forward and increased the probability that it would overlap with the next support state. Adaptability and avoidance of deadlock were emphasized over stability by maximizing the number of legs in the air. Computer simulation indicated that this heuristic approach generally found a sequence of appropriate footholds when the motion trace contained a large number of appropriate sequences.

Hirose (1984) developed hierarchical algorithms to control the terrain-adaptive gait of a statically stable quadruped, given a desired motion trace for the body. One level provided gait control, so that the machine tended to converge to a crab gait. The lowest level provided basic motion regulation, including such functions as controlling the pitch and height of the body and preventing collisions between the legs. Hirose demonstrated the feasibility of these algorithms through computer simulations. The simulated quadruped walked across terrain with holes, crossed a river, and made local modifications to the motion trace to avoid a large hole.

The first walking machines to walk on rough terrain used fixed patterns of gait generated by kinematic linkages (Morrison 1968; McGhee 1976). These systems had no sensors or feedback and could not adapt to variations in the terrain, but they sometimes walked successfully over obstacles.

The quadruped transporter built by Ralph Mosher and his colleagues at General Electric walked on rough terrain with a human providing control and sensing (Mosher 1968; Liston 1964; Liston 1970). The human drove the machine by making crawling motions with his arms and legs. A hydraulic force-reflecting master-slave servo caused the four legs of the vehicle to follow the motions of the operator, and provided force information from the legs of the vehicle back to the arms and legs of the operator. Despite the intense concentration required to drive the machine, Mosher was able to make it amble along at about 5 mph, climb a stack of railroad ties, and walk through an orange grove. These experiments showed that a legged machine could move effectively on rough terrain, provided it has excellent sensing and control systems, such as those provided by a human.

Hirose (1984) built a quadruped which used a set of reflexes to walk on rough terrain. One reflex pulled the foot back and lifted it if a touch sensor on the foot indicated that it had bumped into an obstacle as the foot moved forward. Another reflex caused support legs to push downward if a load cell in the foot indicated that it was not bearing an adequate vertical load. A third reflex caused the relative altitude of the feet to be adjusted so the body remained level, as indicated by an oil-damped pendulum. Hirose's quadruped used these reflexes to climb up and down steps without a model of the terrain.

Okhotsimski and his co-workers continued their work on six-legged walkers by building a series of machines (Okhotsimski et al. 1977; Gurfinkel et al. 1981; Devjanin et al. 1983). The final machine in this series was a six-legged walker, 0.7 m long and weighing 10 kg. The legs were powered by electric motors. Pitch and roll information was provided by a vertical gyroscope. The machine could climb up onto a small ledge by raising its body and then placing each foot up on the ledge. Care was taken to keep the body level during climbing.

McGhee's group at the Ohio State University (OSU) built a hexapod walking machine (McGhee 1980). Like most legged vehicles, the OSU hexapod could use input from an operator to specify direction and speed of travel for walking on smooth terrain, but it could also position its feet on footholds selected by the operator on rough terrain (Ozguner, Tsai, and McGhee 1984, McGhee 1983). The operator pointed out footholds with a laser. The machine then used stereo cameras to locate the foothold in three dimensions, evaluated the foothold based on leg kinematic limits and vehicle stability, and placed a front foot on the foothold if it was acceptable. The two pairs of rear legs used these same footholds, and motion proceeded with a follow-the-leader gait.

Waldron and McGhee (1986) built a second hexapod at OSU, the ASV (adaptive suspension vehicle). This vehicle was much larger than the first—5.2 m long, 2.4 m wide, 3.0 m high—and weighed 2700 kg. An operator rode on board to provide general speed and direction inputs, while leg coordination and foothold selection were performed by the control computers. A range sensor provided terrain depth information for the 10 m in front of the vehicle. The OSU ASV was able to walk up and down grassy slopes, through a muddy cornfield, and it walked on railroad ties.

3.4 Experimental Apparatus

To study the control of step length, we used a planar, two-legged running machine for experiments. Figures 3–3 and 3–4 illustrate the design of the planar biped machine. It has two telescoping legs connected to the body by pivot joints that form hips. Each hip has a hydraulic actuator that positions the leg fore and aft. An actuator within each leg changes the leg length, while an air spring makes the leg springy in the axial direction. The leg actuator and spring act in series. The biped is constrained mechanically to move fore and aft (x), up and down (z), and to rotate about the pitch axis of the body (ϕ). Figure 3–5 shows the kinematics of the biped.

In a typical experiment, the planar biped travels around a circle with a running gait that uses one leg for support at a time. Each support phase is an elastic rebound, during which the mass of the running machine bounces off the spring in the leg. Between each pair of stance phases is a ballistic flight phase, during which linear and angular momentum are conserved. Every 6 ms the control computer collects data from the sensors, executes the control algorithms, sends outputs to the actuators, and records data for later analysis. The control system receives setpoints for the desired forward speed, hopping height, and stiffness of the leg springs from a control panel operated by a human driver, or from a predetermined sequence of set points stored in the control code.

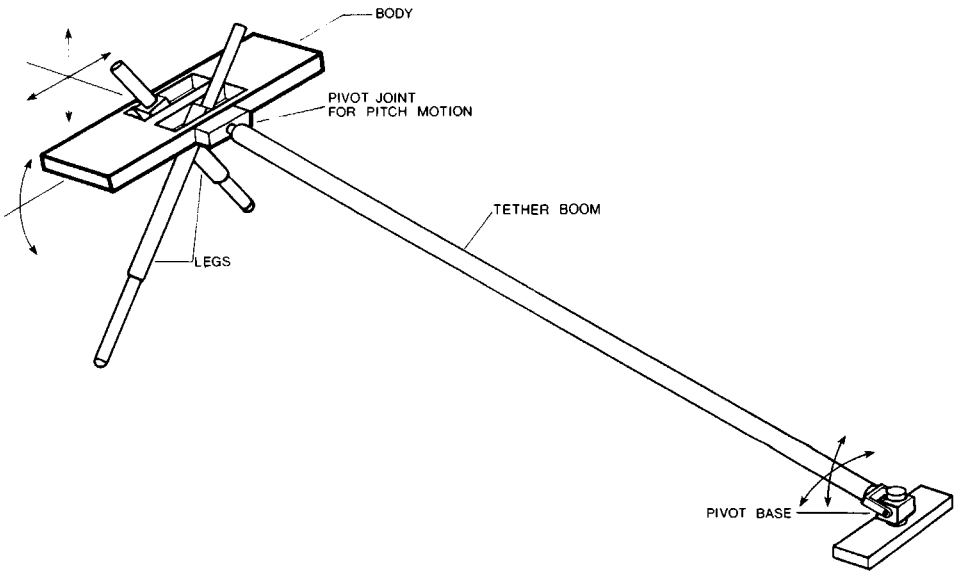

Figure 3–3: Diagram of planar, two-legged running machine used for experiments. The body is an aluminum frame on which are mounted hip actuators and computer interface electronics. Each hip has one low friction hydraulic actuator that positions the leg fore and aft. An actuator within each leg changes its length, and an air spring makes the leg springy in the axial direction. Sensors measure the lengths of the legs, the positions and velocities of the hip actuators, pressures in the air springs, contact between the feet and the floor, and the pitch angle of the body. An umbilical cable connects the machine to hydraulic, pneumatic, and electrical power supplies, and to the control computer, all of which are located nearby in the laboratory. The arrangement of body, legs, hips, and actuators provides a means to control the position of the feet with respect to the body, to generate an axial thrust with each leg, and to provide hip torques during running. A tether boom constrains the machine to move fore and aft, up and down, and to rotate about the pitch axis. The tether boom also provides a means of sensing body pitch angle and vertical and horizontal position in the room. The biped pivots freely with respect to the tether boom about the pitch axis.

To develop the control algorithms used for adjusting step length, we modified a set of control programs used previously to make the planar biped run. The approach in the previous algorithms was to decompose the control into three parts. One part regulated the amplitude of the machine's bouncing motion, the second part maintained the body in an upright posture, and the third part controlled the forward running speed. Experiments with these algorithms showed that they were adequate for running in place, running fast (13 mph), switching gaits between hopping and running, and performing simple gymnastic maneuvers (Hodgins, Koechling, & Raibert 1986; Koechling & Raibert 1988; Hodgins and Raibert 1987). These control algorithms adjusted running speed, hopping height, and maintained the body in a level posture, but they did not specify the length of the step nor the locations on the ground where the feet were to be placed. We developed algorithms for adjusting step length by extending these previous algorithms.

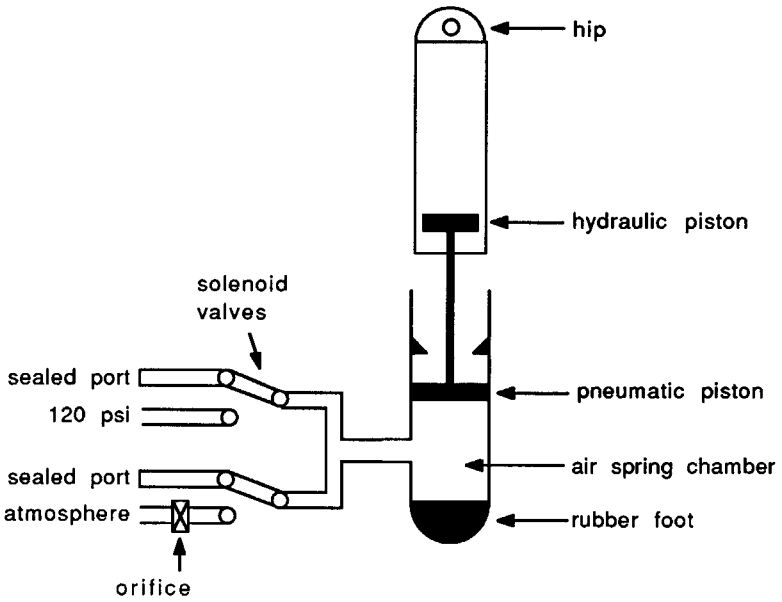

Figure 3–4: Schematic of the leg used in the planar biped machine. A hydraulic actuator acts in series with a pneumatic spring. The hydraulic actuator drives the vertical bouncing motion of the machine, and retracts the leg during flight. Two-way solenoid valves regulate the flow of air to the chambers of the spring and seal off the chambers during the stance phase. The foot is a rubber hemisphere with a 3 cm diameter. Sensors measure hydraulic actuator length, overall leg length, pressure in the pneumatic spring, and contact between the foot and the ground.

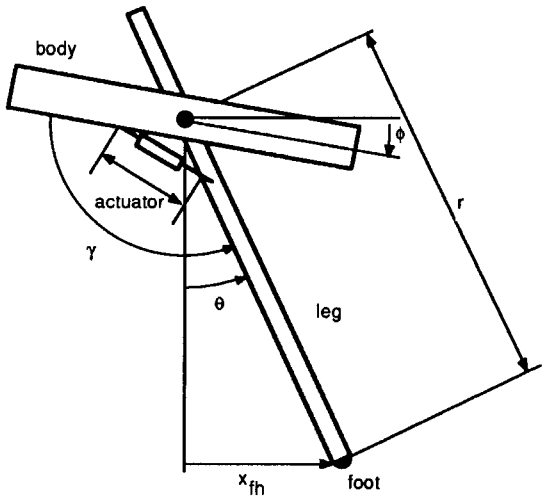

Figure 3–5: Kinematics of planar two-legged running machine. The length of the leg is r, the angle between the leg and vertical is θ and the pitch angle of the body is ϕ. $\theta = \gamma - \phi - 90$. The foot position relative to the hip, x_{fh}, is equal to $r \sin\theta$. The kinematics for the second leg are similar except that the hip actuator is attached to the other side of the body.

3.5 Control of Step Length

The length of a step is the distance between two successive footholds, as illustrated in figure 3–6.† It is the distance traveled during the stance phase plus the distance traveled during the flight phase:

$$L_{step} = \dot{x}_s T_s + \dot{x}_f T_f, \tag{3.1}$$

where $\dot{x}_s$ and $\dot{x}_f$ are the forward running speeds during the stance and flight phases, and T_s and T_f are the durations of the stance and flight phases. The distance traveled by the body during a given period is the product of the duration of the period and the forward speed. Therefore, variations in the duration of the flight phase, duration of the stance phase, or in the forward running speed will each influence the step length. These observations suggest three methods for controlling step length while maintaining balanced running:

- *Forward Speed Method*—For given durations of the stance and flight phases, forward running speed determines step length. The control system manipulates the forward running speed by positioning the foot to accelerate or decelerate the system on each step. The control system can position the foot to cause zero, positive, or negative net acceleration during the next stance phase, as shown in figure 3–7. The forward position of the foot at touchdown is specified by

$$x_{fh} = \frac{T_s \dot{x}_s}{2} + k_{\dot{x}}(\dot{x}_f - \dot{x}_d), \tag{3.2}$$

  where T_s is expected duration of the next stance phase, $\dot{x}_s$ is the expected forward speed during the stance phase, $\dot{x}_f$ is the present forward speed (during flight), $\dot{x}_d$ is the desired forward speed for the next flight phase, and $k_{\dot{x}}$ is an empirically determined gain. For the experiments described in this paper, we estimated the forward running speed during the next stance phase to be

$$\dot{x}_s = \frac{k(\dot{x}_f + \dot{x}_d)}{2}. \tag{3.3}$$

  This estimate takes into account that the forward running speed will change from its current value to the desired value during the stance phase and that there is a normal pattern of deceleration and acceleration that occurs during each step. More details of the forward speed control are given in Raibert (1986) and Hodgins (1989).
- *Flight Duration Method*—With constant forward speed, the duration of the flight phase determines the distance traveled during flight. The duration of the flight phase is determined by the vertical energy of the system when the foot leaves the ground and the difference between the altitude of the body at liftoff and touchdown. If the altitude of the body is the same at touchdown and liftoff, the duration of the flight phase is

$$T_f = \frac{2\dot{z}_{lo}}{g}, \tag{3.4}$$

† In the biomechanics literature, "step length" refers to the distance traveled by the body while the foot is on the ground, but that is not the definition used in this paper.

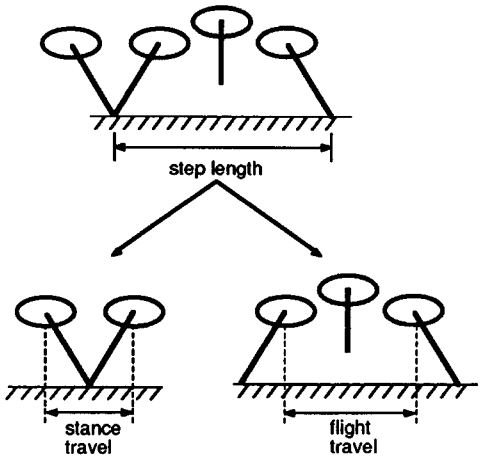

Figure 3–6: The step length is the distance traveled during the stance phase plus the distance traveled during the flight phase. The length of a step can be modified by changing the forward speed, duration of the stance phase, or duration of the flight phase.

where $\dot{z}_{lo}$ is the vertical velocity at liftoff and g is the acceleration of gravity.

At the peak of the flight phase, all vertical energy takes the form of potential energy of elevation, and the altitude of the body indicates the duration of the flight phase. Therefore, if we assume no energy sources or sinks, the measure of energy at any time during the stance phase predicts the duration of the flight phase. The control system adjusts the vertical energy throughout stance by modulating the thrust delivered by the leg actuator. This thrust makes up for mechanical losses and produces the desired changes in the duration of the flight phase from one step to the next.

The vertical energy of the system at liftoff is

$$E = \frac{1}{2} m \dot{z}_{lo}^2 + mgz_{lo}, \tag{3.5}$$

where z_{lo} is the vertical altitude of the body at liftoff and m is the mass of the system. The control system manipulates the thrust delivered by the leg during stance so that the energy at liftoff results in the correct flight duration. Combining (3.4) and (3.5) we obtain an equation for the desired vertical energy as a function of the desired flight duration:

$$E = \left(z_{lo} + \frac{gT_f^2}{8} \right) mg. \tag{3.6}$$

- *Stance Duration Method*—The distance the body travels during the stance phase is the product of the average forward running speed and the duration of the stance phase. The duration of the stance phase is determined, to first order, by the spring-mass oscillator formed by the system mass bouncing on the stiffness of the leg. The duration of the stance phase is approximately one half cycle of the natural oscillation, $T_s \approx \pi/\omega_0$, where ω_0 is the natural frequency of the system. The natural frequency is approximately $\sqrt{k/m}$, where k is the stiffness of a linear approximation to the leg air spring and m is the mass supported by the leg spring, (upper leg, body, and other leg).

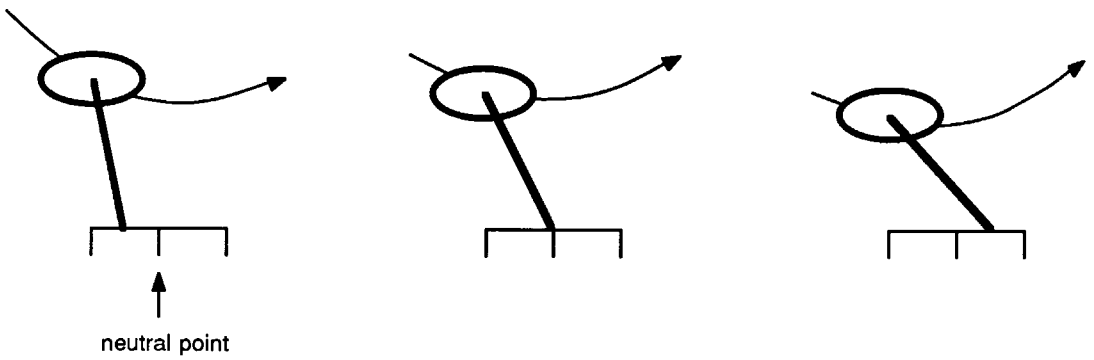

Figure 3–7: Controlling forward speed. Center) When the foot is placed in front of the hip one-half the distance the body will travel while the foot is on the ground, the forward speed will remain unchanged. We call that location the *neutral point.* Left) When the foot is displaced backward from the neutral point, the system accelerates forward. Right) Displacing the foot forward from the neutral point causes the system to decelerate. See Raibert (1986) for details.

The control system manipulates the stiffness of the leg by controlling the resting air pressure in the leg spring during the flight phase. Data from experiments with the running machine were used to find an empirical relationship between the resting pressure of the air spring and the duration of the stance phase. Higher pressures cause the spring to be stiffer and reduce the duration of the stance phase. This relationship is observed to be independent of vertical velocity at touchdown and of forward speed, except when the spring is very soft. The control system manipulates the stance duration to determine the distance traveled during the stance phase and, thereby, to control the step length.

The three methods for controlling step length are illustrated in figure 3–8. Each method adjusts one parameter of the running cycle to produce the desired step length, leaving the other two parameters unchanged. The best control of step length will probably be achieved by combining the three methods to adjust several parameters at once. However, in order to learn more about each method, we measured behavior while adjusting just one parameter at a time.

We performed two experiments for each step length control method. In the first experiment, the control system specified a pattern of desired values for the adjusted parameter while specifying fixed nominal desired values for the two unadjusted parameters. The purpose of this experiment was to measure the accuracy with which the adjusted parameter—forward speed, flight duration, or stance duration—could be controlled. In the second experiment, the control system specified a pattern of desired step lengths. A desired value for the adjusted parameter was determined on each step based on the desired step length and the nominal values used for the unadjusted parameters. The purpose of this experiment was to measure the precision with which the step lengths could be controlled. Precise control of step length requires that the unadjusted parameters do not vary in reaction to manipulations of the adjusted parameter. For instance, when the foot is positioned to control forward speed, the action must not disturb the duration of the stance or flight phases.

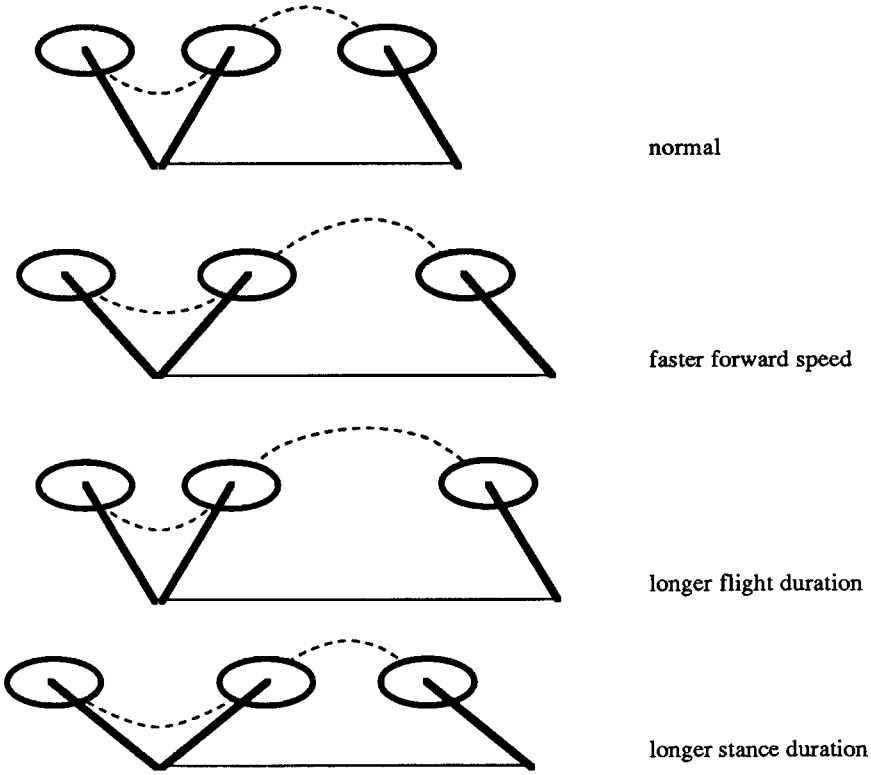

Figure 3–8: Three methods for controlling step length. The top drawing portrays a normal step. The others show longer steps produced by adjusting one of the parameters of the step. The second drawing has increased forward speed, the third an extended flight phase, and the fourth an extended stance phase. In each case, increasing one of the parameters of the step produces a longer step length.

3.6 Results

To measure the precision of control for the adjusted parameters, the control system specified a pattern of desired variations for the adjusted parameter, while specifying fixed nominal values for the two unadjusted parameters. The nominal values were approximately $T_{f,nom} = 0.4\,\text{s}$, $T_{s,nom} = 0.15\,\text{s}$, and $\dot{x}_{nom} = 1.1\,\text{m/s}$. These nominal values provided an operating point about which all manipulations were made. The results are given in figure 3–9 for all three methods. Figure 3–9A plots the pattern of desired forward speeds (solid line) and the forward speed that was actually achieved on each step (dots). The forward speed ranged between 0.25 m/s and 2.0 m/s, with an average absolute error of 0.06 m/s, or 5% of the nominal forward running speed. Figure 3–9B plots the results of a similar experiment for flight duration. Flight durations varied between 0.2 s and 0.5 s. The average absolute error in flight duration was 0.03 s, or 5% of the nominal flight duration. Figure 3–9C plots the results for the control of stance duration. The desired stance durations varied between 0.1 s and 0.2 s. The average absolute error was 0.005 s, or 1% of the nominal stance duration.

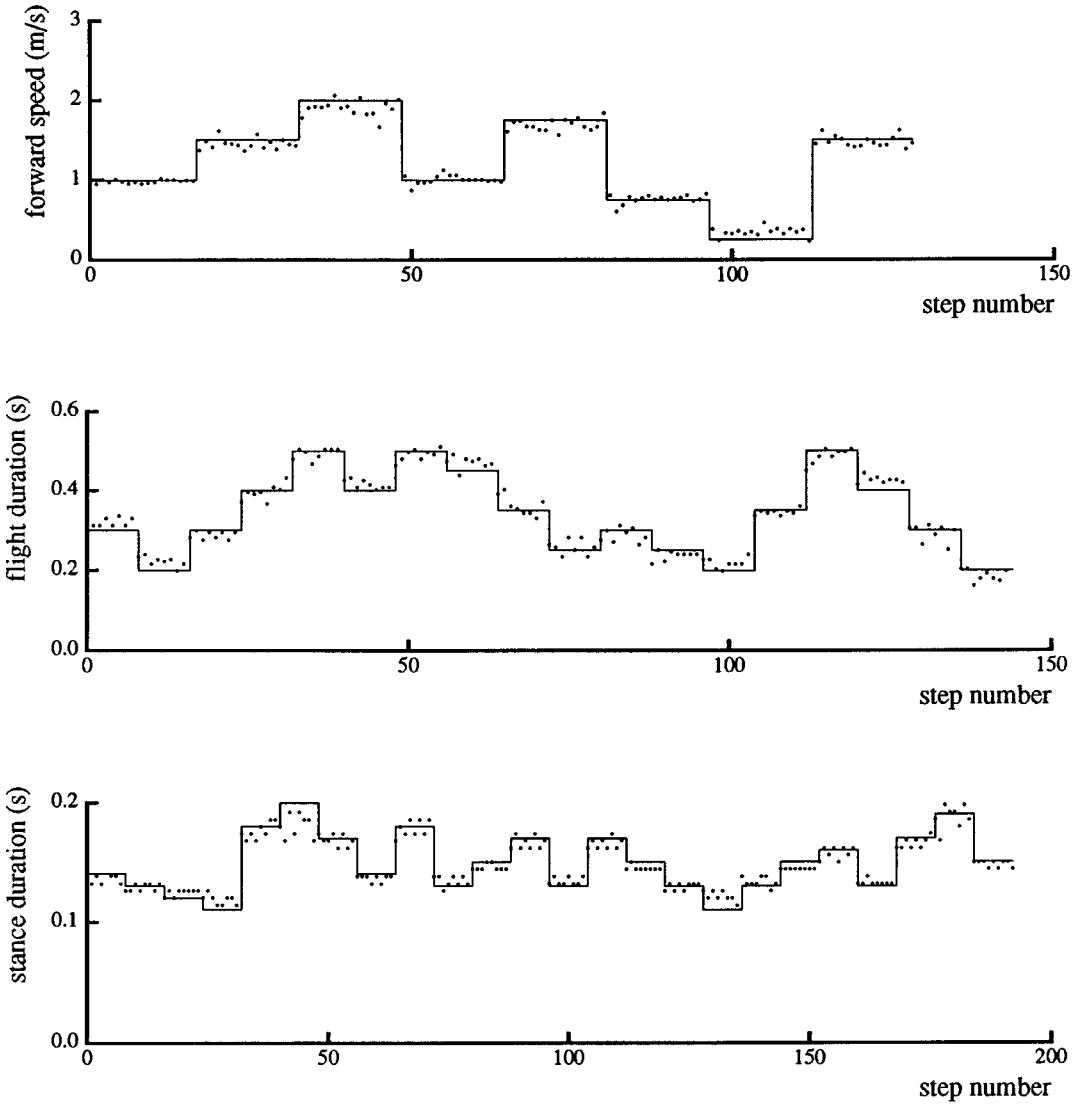

Figure 3–9: Data showing the control of the adjusted parameters. In each experiment two of the three parameters were held constant at nominal values while the third was adjusted according to a stored pattern of desired values. The solid lines show the desired values for the adjusted parameter and the dots represent the value that was actually generated on each step. (Top) Control of forward running speed. The biped ran for sixteen steps at each desired forward speed. Then the desired speed was changed to the next value in the pattern. The average absolute error in forward speed was 0.06 m/s. The nominal values were $T_s = 0.14$ s and $T_f = 0.47$ s. (Middle) Control of the duration of the flight phase. The average absolute error in flight duration was 0.03 s. $\dot{x} = 1.2$ m/s, $T_s = 0.15$ s. (Bottom) Control of the duration of the stance phase. The average absolute error in stance duration was 0.005 s. $\dot{x} = 1.0$ m/s, $T_f = 0.38$ s. (B87.248.4, B88.336.12, B88.243.4)

To measure the control of step length, the control system specified a pattern of desired step lengths. Figure 3–10 shows the results for each of the three methods. For the forward speed method, step lengths varied between 0.1 m and 1.1 m, with an average absolute error of 0.07 m, or 12% of the nominal step length, (which was 0.6 m = $\dot{x}_{nom}(T_{f,nom} + T_{s,nom})$). Figure 3–10B plots data for the flight duration method. The average absolute error in step length was 0.07 m, 12% of nominal. Figure 3–10C plots data for the stance duration method. The average absolute error in step length was 0.03 m, 5% of the nominal step length. The error measurements for each method were made by including only those step lengths that were within the range obtainable by the method.

The data in figure 3–10 illustrate several characteristics of the three methods for step length control. First, the error in step length depended on the magnitude of the step length. For example, the step length error obtained by the forward speed method was larger for longer steps than for shorter steps. The control of forward speed was less accurate at higher speeds, as indicated by an increased step length error for longer steps. Second, each of the methods had a saturation point, beyond which increases in desired step length were not matched by increases in achieved step length. Such saturation is clear in figure 3–10B, where step length did not increase beyond about 0.6 m. These saturation limits are not absolute, in that they depend on the choice of nominal control parameter values. For example, if the nominal forward speed were doubled, then the maximum step length for the flight duration method would double to about 1.2 m.

The performance of the three methods for controlling step length relied on maintaining two of the parameters constant at nominal values while the third was adjusted. When either of the nominal parameters varied, step length was not well controlled. Figure 3–10C shows a nearly square pattern of dots, indicating that the error in step length was approximately equal to the range of possible step lengths. The error in step length was caused by deviations of forward speed from the nominal value in response to adjustments of stance duration. These data show that good control of the adjusted parameter does not ensure accurate control of step length: good step length control requires that the unadjusted parameters be controlled to their nominal value.

The three methods for controlling step length can be compared in terms of accuracy and range. Accuracy is a measure which reflects the error between the desired and actual step length. Range is the difference between the minimum and maximum possible step length. The accuracy of a method determines the size of a foothold the legged system could use successfully. If a legged system were to use a foothold 0.1 m long and 1.0 m away, then it would have to take a step of 1.05 m with an error of less than ± 0.05 m. Otherwise it would not land on the foothold.

Good accuracy does not guarantee that a method will be successful in controlling step length. The controller must also be able to vary step length over a wide range. For example, if a system were running with a step length of 1 m but there was not a good foothold 1 m ahead, then it would have to take a shorter or longer step to avoid stepping on the undesirable region of the terrain. If the undesirable region were large, the required adjustment might be substantial.

Table 3–1 gives the minimum and maximum step lengths obtained with each method.

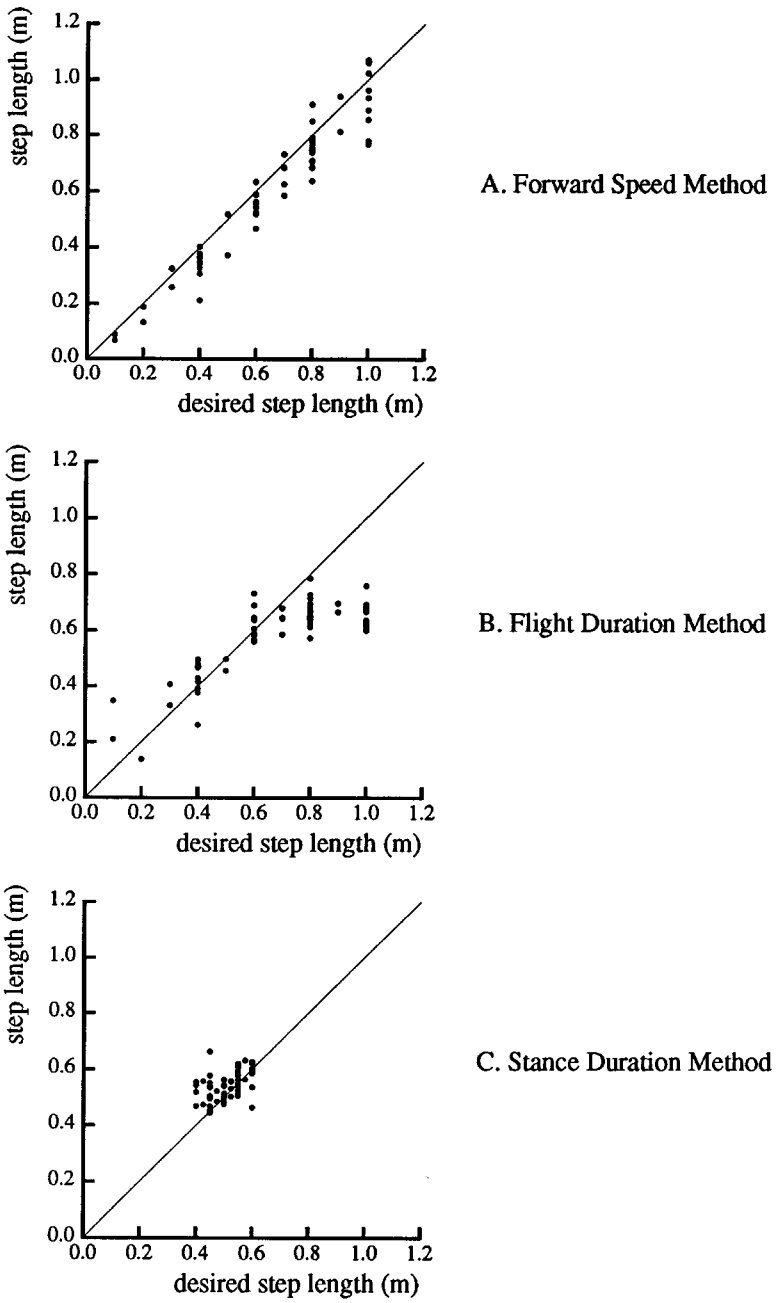

Figure 3–10: Scatter plot of actual step length against desired step length for each method. In each experiment the machine ran forward using one of the three methods to follow a pattern of desired step lengths. (Top) Forward speed method. The desired step lengths ranged between 0.1 m and 1.0 m. The average absolute error in step length was 0.07 m. Nominal values were $T_f = 0.4$ s and $T_s = 0.15$ s for this experiment. (Middle) Flight duration method. The pattern of desired step lengths was the same as that used in the forward speed method experiment. The average absolute error in step length was 0.07 m when the desired step length was within the range of step lengths possible through adjustments in flight duration with the given forward speed and stance duration. $\dot{x} = 1.1$ m/s, $T_s = 0.15$ s. (Bottom) Stance duration method. The desired step lengths ranged between 0.4 m and 0.6 m. The average absolute error in step length was 0.03 m when the desired step length was within the range of step lengths possible with adjustments in stance duration with the given forward speed and flight duration. $\dot{x} = 1.1$ m/s, $T_f = 0.33$ s. (B.88.102.0, B88.106.10, and B.88.265.7)

Control Method	Step Length			Error in Step Length	
	minimum	maximum	range	mean	standard deviation
forward speed	0.00 m	1.10 m	1.10 m	0.05 m	0.07 m
flight duration	0.32 m	0.72 m	0.40 m	−0.04 m	0.09 m
stance duration	0.55 m	0.66 m	0.11 m	−0.01 m	0.04 m

Table 3–1. Maximum and minimum values for the step lengths produced by each method, and the mean and standard deviation of the error in step length for each method.

Adjusting forward speed produced variation in step length that was twice as large as obtained manipulating flight duration, and more than ten times the variation obtained manipulating stance duration. The range of each method was affected by the range of the adjusted parameter, as well as the nominal values selected for the two unadjusted parameters. The range of any of the methods could be manipulated by changing the nominal values of the three parameters. The nominal values used for the experiments were chosen to be in the middle of the range for each parameter and provided an operating point where all three variables are well controlled.

Table 3–1 also gives the mean and standard deviation of the error in step length for each method. Forward speed and flight duration were tested using the same pattern of desired step lengths, but the error calculations included only those step lengths that were within the range of the method. A smaller range of desired step lengths was used to test the stance duration method, so that more data points would lie within the achievable range of the method. Manipulating stance duration provided the most accurate control, with a mean of −0.01 m and a standard deviation of 0.04 m. Manipulating forward speed and flight duration provided less accurate control of step length, but for a much larger range of step lengths.

How might the three methods for adjusting step length be combined? One approach would be to allocate the change in step length between adjustments in forward speed and flight duration in proportion to the range of each method. For the planar biped, two-thirds of the change in step length would be produced by adjustments in forward speed and one-third by adjustments in flight duration. To improve accuracy, the change in step length could be allocated so that each parameter was near the center of its working volume or was in the area of its working volume where control is most accurate.

In principle, the range and accuracy of the control of step length could be improved when methods are combined. For example, increasing both the flight duration and the forward speed to their maximum values would produce a longer step than increasing only one. Accuracy might also be improved if a desired change in step length were divided among the three parameters in an appropriate fashion.

Range and accuracy are not the only criteria for choosing a method for controlling step length. The demands of the task may determine which methods are feasible. For example, a long jumper might want to avoid controlling step length through adjustments in forward

Control Method	Error at Target		
	# of trials	mean	standard deviation
random foot placements	none	0.000 m	0.320 m
forward speed	21	−0.004 m	0.023 m
flight duration	20	−0.051 m	0.046 m
forward speed + direct placement	25	0.001 m	0.004 m
flight duration + direct placement	25	0.000 m	0.005 m

Table 3–2. Mean and standard deviation of the error in placing the left foot on a target. The machine began adjusting step length about 5 m before reaching the target. Only the error in step length on the target step was included in the calculated error. The first line of the table shows the expected mean and standard deviation at the target with no control operational, assuming a uniform distribution of foot placements.

speed if those adjustments would reduce the forward speed at the takeoff board and the length of the subsequent jump. Similarly, the flight duration of the steps preceding a vertical jump may affect the height of the jump. As these examples illustrate, the control system may want to vary the method for controlling step length depending on the constraints of the rough terrain task.

3.7 Demonstrations

Step on Target

Using the three methods to adjust the length of its steps, the planar biped ran on simple rough terrain. One task was to place a particular foot on a target foothold. This task is similar to the one faced by a long jumper who must step accurately on the takeoff board to obtain the longest possible jump. To perform this task the biped began adjusting its step length about 5 m before it reached the target foothold. With no control of step length, the error would have been uniformly distributed with a range of plus or minus the step length (±0.55 m) and the standard deviation of the error would be 0.32 m. Using the forward speed method for adjusting step length the mean and standard deviation of the error in foot placement were −0.004 m and 0.023 m. Data for the flight duration method are given in Table 3–2. The non-zero mean was the result of a systematic error in the control of flight duration and therefore in the control of step length. This error could be eliminated by adding an offset to the control algorithms.

Direct Placement

One might ask what would happen if the control system temporarily ignored the need for balance, and placed the foot exactly on the chosen foothold. We call this approach "direct placement." Direct placement could be expected to place the foot precisely on target footholds, but at the expense of stability whenever there was a substantial discrepancy between the locations of the target foothold and the balance foothold, the foothold that would provide balance. The system might recover its balance on subsequent steps if the discrepancy were small, but tip over entirely if the discrepancy were large.

If one of the three methods for controlling step length described earlier were used to move the balance foothold close to the desired terrain foothold, then direct placement might be used to placed the foot precisely on the desired terrain foothold. The separation between the balance foothold and the actual placement would be small enough for the system to regain its balance on subsequent steps.

We tested direct foot placement in conjunction with the forward speed and flight duration methods. In both cases, foot placement errors were essentially eliminated, as shown in Table 3–2. Whatever disturbances direct placement caused to the stability of the system in these experiments were generally not visible to us when we watched the biped perform this task.

Despite the success of direct placement in these demonstrations, direct placement fails when the task involves a long series of precisely specified footholds. In that case, the disturbances caused by direct placement generally accumulate on each step, making balance more and more difficult to maintain.

Leap Over Obstacle

The biped leapt over obstacles by adjusting the length of its steps as it approach the obstacle. The approach was much like the place-foot-on-target demonstration just described. The control system adjusted step length on the approach to align the machine appropriately with the obstacle prior to the leap. When it reached the target takeoff point, the biped jumped as high as it could and shortened its legs to increase clearance. The machine has jumped over a rectangular obstacle 0.36 m high and 0.32 m long on fifteen consecutive attempts. It has also jumped through a hoop.

Climb Stairs

The biped has run up and down a flight of three stairs, as shown in figure 3–1. As the machine approached the stairs, the forward speed method was used to place a foot on a target foothold just below the first step. During the climb up and down the stairs, the control system used the forward speed method to match step lengths to the stair tread depth and it manipulated flight duration to account for stair riser heights. The precision of step length control was degraded during stair climbing, due to the changing altitudes of the footholds. The reduced vertical velocity at touchdown during the descent of the stairs

caused the duration of the stance phase and the forward running speed to decrease more than was expected, and this error resulted in shorter steps than expected. Despite these limitations, the machine usually climbed the stairs successfully and on one occasion it ran up and down the stairs on seven consecutive trials.

3.8 Summary

A legged system must control the length of its steps if it is to use isolated footholds on rough terrain. This paper explores three methods for controlling step length in the context of dynamic legged systems. Each method adjusts a parameter of the running cycle, leaving the others set to nominal values. The parameters were forward running speed, running height, and duration of ground contact.

We measured the performance of each method for controlling step length. The forward speed method produced the widest range of step lengths. The flight duration method produced steps with about half the range of the forward speed method. The stance duration method produced step lengths with a tenth the range produced by the forward speed method. When each method was tested with a pattern of desired step lengths that fell entirely within its range, the stance duration method produced the highest accuracy. The forward speed method provided the best combination of wide range and the high accuracy.

It remains to factor out the degree to which these results are affected by the particular characteristics of the experimental apparatus, and other elements of the implementation.

3.9 References

Devjanin, E. A., Gurfinkel, V. S., Gurfinkel, E. V., Kartashev, V. A., Lensky, A. V., Shneider, A. Yu., Sktilman, L. G. 1983. The six-legged walking robot capable of terrain adaptation. *Mechanisms and Machine Theory* 18:257–260.

Gurfinkel, V. S., Gurfinkel, E. V., Shneider, A. Yu., Devjanin, E. A., Lensky, A. V., Shtilman, L. G. 1981. Walking robot with supervisory control. *Mechanism and Machine Theory* 16:31–36.

Hirose, S. 1984. A study of design and control of a quadruped walking vehicle. *International J. Robotics Research* 3:113–133.

Hodgins, J. K. 1989. *Legged Robots on Rough Terrain: Experiments in Adjusting Step Length*, Ph.D Thesis, Computer Science, Carnegie Mellon University, Pittsburgh, Pennsylvania.

Hodgins, J., Koechling, J., Raibert, M. H. 1986. Running Experiments with a Planar Biped. In *Robotics Research: The Third International Symposium*, O. Faugeras, G. Giralt (eds.). (MIT Press, Cambridge).

Hodgins, J., Raibert, M. H, 1987. Biped gymnastics, in *Robotics Research: The Fourth International Symposium*, B. Bolles, B. Roth (eds.), Cambridge, Mass.: MIT Press.

Koechling, J, Raibert, M, 1988. How fast can a legged robot run? in K. Youcef-Toumi and H. Kazerooni, (eds.), *Symposium in Robotics, DSC-Vol. 11.* American Society of Mechanical Engineers.

Lee, D. N., Lishman, J. R., Thomson, J. A. 1982. Regulation of gait in long jumping. *J. Experimental Psychology* 3:448–459.

Liston, R. A. 1964. Walking machine. *Journal of Terramechanics* 3:18–31.

Liston, R. A. 1970. Increasing vehicle agility by legs: The quadruped transporter. Presented at *38th National Meeting of the Operations Research Society of America.*

McGhee, R. B. 1976. Robot locomotion. In *Neural Control of Locomotion*, R. N. Herman, S. Grillner, P. S. Stein, D. G. Stuart (eds.). (Plenum Press: New York, NY).

McGhee, R. B. 1980. Robot locomotion with active terrain accommodation. In *Proceedings of National Science Foundation Robotics Research Workshop*, University of Rhode Island.

McGhee, R. B. 1983. Vehicular legged locomotion. In *Advances in Automation and Robotics*, G. N. Saridis (ed.). (JAI Press)

McGhee, R. B., Iswandhi, G. I. 1979. Adaptive locomotion of a multilegged robot over rough terrain. *IEEE Trans. Systems, Man, and Cybernetics* SMC-9:176–182.

Morrison, R. A. 1968. Iron mule train. In *Proceedings of Off-Road Mobility Research Symposium.* International Society for Terrain Vehicle Systems, Washington, D.C., 381–400.

Mosher, R. S. 1968. Test and evaluation of a versatile walking truck. In *Proceedings of Off-Road Mobility Research Symposium*, International Society for Terrain Vehicle Systems, Washington, D.C., 359–379.

Okhotsimski, D. E., Gurfinkel, V. S., Devyanin, E. A., Platonov, A. K. 1977. Integrated walking robot development. In *Conference on Cybernetic Models of the Human Neuromuscular System.* Engineering Foundation.

Okhotsimski, D. E., Platonov, A. K. 1973. Control algorithm of the walker climbing over obstacles. In *International Joint Conference on Artificial Intelligence*, Stanford, CA.

Okhotsimski, D. E., Platonov, A. K. 1975. Perceptive robot moving in 3D world. In *Proceedings of the IV International Joint Conference on Artificial Intelligence.* Tbilisi, USSR, 3–8 Sept. 1975.

Ozguner, F., Tsai, S. J., McGhee, R. B. 1984. An approach to the use of terrain-preview information in rough-terrain locomotion by a hexapod walking machine. *International J. Robotics Research* 3:134–146.

Patla, A.E., Robinson, C., Samways, M., Armstrong, C.J. 1989. Visual control of step length during overground locomotion: task-specific modulation of the locomotor synergy. *Journal of Experimental Psychology*, 15(3).

Raibert, M. H. 1986. *Legged Robots That Balance* (MIT Press: Cambridge Mass.)

Waldron, K. J., McGhee, R. B. 1986. The adaptive suspension vehicle. *IEEE Control Systems Magazine.* 6(6):7–12.

Warren, W. H., Jr., Lee, D. N., Young, D. S. 1985. Visual control of step length during running over irregular terrain. *Journal of Experimental Psychology: Human Perception and Performance.* 12(3):259-266.

This empty page was substituted for a blank page in the original document.

Chapter 4

How Fast Can a Legged Robot Run?

Jeff Koechling

4.1 Abstract

Several parameters can limit the running speed of a legged system. Among them are the strength, length, and stiffness of the legs, the range of joint motion, and the actuator force-velocity characteristics. We have explored how varying these parameters affects top running speed. We developed a dependency tree that suggests that a robot should have long, strong, stiff legs, and actuators with high peak velocity in order to run fast. We have also proposed three ways to improve the control of body attitude in high speed running: keeping hip motions symmetric, compensating for actuator characteristics, and accelerating the hip joint in anticipation of touchdown. In laboratory experiments a planar two-legged robot has reached a top speed of 5.9 m/s (13 mph).

4.2 Introduction

"How fast can it go?" Since time immemorial, people have staged races to compare the speed of people, animals, or vehicles. Speed excites people, often because it is the focus of a competition, and sometimes because of the danger or novelty of going fast. Speed is also an easily understood measure of performance. It summarizes the capabilities of a complex system with a single number that says something about an athlete's prowess, an animal's likelihood of survival, or a vehicle's utility.

Three things limit the speed of a vehicle: the power available to overcome drag, the ability of the structure to withstand loads, and the stability of the motion in the face of disturbances. As the system accelerates it encounters a limit of power, strength, or stability

that establishes its maximum speed. If the limitation is power, then at maximum speed the drag force cancels the thrust force, leaving no thrust to accelerate the system. If the limitation is strength, then at maximum speed the loading on some component equals its strength, and any increase in speed would cause it to break. If the limitation is stability, then at the maximum speed some equilibrating mechanisms is at its stability limit, and at any higher speed the system would tumble out of control. Most vehicles are designed so that their speed is limited by power, rather than by structure or stability, since a simple inability to accelerate is preferable to structural failure or loss of control.

How fast a legged system can run depends on its design, and on how it is controlled. The important parts of the design are the legs and the hips. To run fast, the legs should be long, strong, springy, and stiff, and the hips should be able to rotate rapidly and through a large angle. The control system must coordinate the actions of the legs and hips so as to regulate the momentum of the system in the horizontal, vertical, and rotational directions. The principles of symmetry, modeling, and anticipation help the control system to regulate rotation of the body.

Running speed is the product of step length and step frequency. The simple prescription for fast running is to take long steps, and to take them quickly. Step length depends on leg length and hip joint range of motion, while stepping rate depends on leg stiffness, leg strength, and hip rotation rate.

Leg length — Long legs allow long steps, so legs should be long for fast running. The distance that a legged system can move forward while its foot is on the ground is proportional to how long its legs are. Mass, moment of inertia, and strength all depend on leg length, and there is a limit to how big a leg can be and still be strong enough to support its own weight and the inertial forces required to move it.

Hip joint rotation — The distance that a legged system can travel forward during a bounce depends not only on the leg length, but also on the range of motion of the hip joint. The hip joint limits how far the leg can pivot during stance without disturbing the attitude of the body.

Hip rotation rate — Hip rotation rate can directly limit running speed. During stance, a legged system is like a polar manipulator. The foot remains fixed on the ground, and the leg length and hip angle determine the position of the body with respect to the foot. The hip position, plus the rate of extension of the leg and the rate of rotation of the hip joint determine the velocity of the body. The faster the hip joint can rotate, the faster the body can advance during stance.

Leg stiffness — A running system alternately bounces off of the ground and flies through the air. For the system to bounce, the legs must be springy. During each bounce against the ground, ground contact forces reverse the vertical momentum of the system. As the legs compress during stance, they build up force, and the vertical component of that force reverses the vertical momentum of the system. The stiffer the springs are, the faster the forces build up and the more quickly the system bounces.

Leg strength — The total impulse required to reverse the vertical momentum of the body is the integral of the contact force over the duration of the bounce. The legs must be strong enough to transmit the ground reaction force to the body without breaking or

buckling. The shorter the bounce, the larger the contact forces must be. Thus, the stronger the legs are, the faster the system can bounce off of the ground without damaging the legs.

Symmetric leg motions — By moving its two legs symmetrically, a biped minimizes how much its body attitude deviates from the nominal angle. If the hip joints are at the center of gravity of the body, then the only disturbances to the body attitude are caused by hip torques. Equal and opposite motions of the hip joints ensure that the hip torques cancel out, and thus do not disturb the body attitude.

Actuator velocity compensation — During stance, the hip of the stance leg is pushed forward by the body, causing the hip to rotate at a rate proportional to running speed. Velocity dependent torques in the hip joints should be compensated so that the body is not rotated forward with the leg.

Ground speed matching — When the leg touches down, an impulsive contact force brings the unsprung mass of the foot to rest. At high speeds, this impulse is not aligned with the axis of the stance leg, so it tends to rotate the leg. The impulse happens very quickly, faster than the hip joint can respond, so some torque is transmitted to the body, which also begins to rotate. If the control system anticipates the touchdown, and accelerates the hip joint before impact, then the impulse is aligned with the axis of the leg. In this case the hip joint does not transmit any torque to the body.

Taken together, symmetric leg motions, actuator velocity compensation, and ground speed matching substantially reduce body attitude disturbances associated with running fast.

In the following section we review relevant previous studies. Then we develop a dependency tree that expresses the speed of a running system in terms of its physical parameters. Finally, we present laboratory experiments suggested by the analysis.

4.3 Background

The study of running is interdisciplinary. Some areas of research that provide results helpful in understanding running speed are:

- Studies of running animals
- Creation of artificial legged systems (robots)
- Investigation of the performance of vehicles in general

Biologists have studied innumerable aspects of running animals, including their structure, the motions and forces that occur during running, and the energy consumed for different speeds and gaits. Robots and vehicles that travel on legs provide a way to study walking and running in simple, easily instrumented systems, without the complexity inherent to biological systems. Research into the performance of boats, aircraft, and land vehicles is relevant to studying running speed, because the task of locomotion and the physical principles of support, balance, and progress are common to all vehicles.

4.3.1 Biomechanical Research

Scaling

Biologists have proposed various similarity models to describe how the shape, structure, and motions of an animal depend on its size. Similarity models either describe measurements gathered from animals that are similar in arrangement but vary in size, or they describe the way that such measurements should vary in order to keep some quantity the same at all sizes.

Similarity models apply to all mechanisms, not just biological ones. A mechanism design only works over a limited range of sizes. Typically, at a very small size the ratio of viscous forces to inertial forces increases and the resultant damping prevents the mechanism from operating. At a very large size, gravitational forces become dominant and exceed the strength of the materials.

Hill (1950) concluded that speed is independent of size for animals of similar design. An animal makes movements that are proportional to its size, but at a frequency that is inversely proportional to its size. For geometrically similar animals, the differences cancel out, so top speed is the same regardless of size. Hill introduced the idea of physiological time, saying that animals live on a time scale proportional to body size. Thus large animals live longer than small animals, their hearts beat more slowly, and they take more time for each running step. Hill also noted that for large animals, a greater portion of skeletal and muscular strength is required to support the animal's weight than for small animals.

McMahon (1975) compared and discussed three scaling laws: geometric similarity, elastic similarity, and static stress similarity. Geometrically similarity preserves shape across scale, as all linear dimensions change with the same scale factor. Elastic similarity preserves resistance to column buckling. For columns of different size to have the same safety factor against buckling, long columns must be relatively thicker than short columns. The scale factor for the diameter of elastically similar columns is 3/2 the scale factor for length. Static stress similarity preserves resistance to bending failure in simply supported beams bearing their own weight. In this case, the scale factor for diameter is twice the scale factor for length.

McMahon presented a variety of evidence that the design of animals is in accordance with elastic similarity. In particular, the running speed of animals is proportional to body weight raised to the 1/4 power, as predicted by elastic similarity. Geometric similarity predicts an exponent of zero, and static stress similarity predicts an exponent of 2/5. Table 4–1 includes a few predictions of the three similarity models.

Alexander (1988) found that animals weighing over 20 kg scale according to elastic similarity, while the dimensions of smaller animals obey geometric similarity. Alexander also describes an extension of geometric similarity called dynamic similarity. For geometric similarity, animals of different sizes undergo a uniform scaling of linear dimensions. For dynamic similarity, the scaling of linear dimensions is accompanied by uniform scaling of time and force. Thus, dynamic similarity specifies not only the change in shape of animals

Comparison of Three Similarity Models

	geometric similarity	elastic similarity	static stress similarity
length, ℓ	$\ell \propto W^{1/3}$	$\ell \propto W^{1/4}$	$\ell \propto W^{1/5}$
diameter, d	$d \propto W^{1/3}$	$d \propto W^{3/8}$	$d \propto W^{2/5}$
surface area, S	$S \propto W^{2/3}$	$S \propto W^{5/8}$	$S \propto W^{3/5}$
cross sectional area, A	$s \propto W^{2/3}$	$A \propto W^{3/4}$	$A \propto W^{4/5}$
natural frequency, ω	$\omega \propto W^{-1/3}$	$\omega \propto W^{-1/8}$	$\omega \propto W^{0}$
speed, V	$V \propto W^{0}$	$V \propto W^{1/8}$	$V \propto W^{2/5}$

Table 4–1. Three similarity principles predict different variations in shape and speed as a function of body weight, W. The table is adapted from a paper by McMahon (1985), who cites examples of animal measurements that match the elastic similarity model.

at different sizes, but also changes in their motions. Alexander proposes that the scale factor for forces be the cube of the scale factor for length, and that the scale factor for time be the square root of the scale factor for length. These scale factors work for motions characterized by gravitational and inertial forces. However, Alexander points out that if both elastic and gravitational forces are important it is impossible to maintain strict dynamic similarity.

Energetics

The power required for running increases with speed. The environment opposes motion with drag forces, dissipating power equal to the product of the forward speed and the drag force. Drag forces remain constant or increase with running speed. For example, the gravitational drag caused by climbing a hill is independent of speed, while aerodynamic drag increases as the square of running speed.

Several investigators have measured the oxygen consumption of running animals. Consumed oxygen produces metabolic energy at a rate of $1\,\text{ml}\,O_2 = 20.1\,\text{J}$. The rate of oxygen consumption indicates the metabolic power produced by the animal, some of which is used to overcome the resistance of the environment, some of which is dissipated in muscle inefficiency, and some of which is used to maintain the animal's basal metabolism.

The rate of metabolic energy consumption increases with running speed. Taylor, Heglund, and Maloiy (1982) report that the energy consumed during running is:

$$\dot{E}_{\text{metab}}/M_b = 10.7 M_b^{-0.316} v_g + 6.03 M_b^{-0.303} \tag{4.1}$$

where E_{metab} is the metabolic energy consumed in watts, M_b is the body mass in kg, and v_g is the running speed in m/s. The equation is based on measurements from 60 species of animals, ranging in size from 0.0072 kg pygmy mice to 254 kg zebu cattle. It indicates that energy consumption increases linearly with running speed, and that the rate of increase is smaller for large animals than for small animals.

Dawson and Taylor (1973) studied the energetic cost of locomotion in kangaroos. They found that over a range of speeds from 2 m/s to 6 m/s, hopping frequency and energy consumption remain nearly constant, and the stride length increases in proportion to the

speed. This is in contrast to the linear increase in energy consumption with speed indicated by equation 4.1. Dawson and Taylor attributed the constant consumption of energy with increasing speed to increased storage and recovery of elastic energy, particularly in the kangaroo's large Achilles tendon.

Alexander and Vernon (1975) measured the ground forces exerted by hopping kangaroos using force plates, and combined the measurements with film records of the motion to determine the fluctuations of energy during hopping. They calculated that elastic storage of energy in the kangaroo's Achilles tendon reduced the energetic cost of hopping by 40%. Alexander and Vernon also noted that the kangaroo's tail rotates in the opposite direction from the legs, in a way that reduces the angular motions of the body. Large sheets of elastic tendon along the tail contribute to its oscillation.

McMahon and Greene (1978, 1979) considered not only the compliance of a runner's legs, but the compliance of the ground as well. Their model predicted that top running speed would be slightly greater on a compliant track than on a rigid surface. The model predicted that the fastest running would be on a track four times as stiff as the runner's legs. McMahon and Greene built such a track at Harvard University, and observed the predicted 2% increase in running speed, along with a decrease in injuries. This study points out the importance of the environment in determining the top speed of a running system.

Hoyt and Taylor (1985) studied the energetics of horses walking, trotting and galloping. For each gait they found one speed that provided the best energy efficiency, and if allowed to move freely, a horse always chose a speed and gait that corresponded to a local maximum in efficiency.

4.3.2 Robotic research

There are very few artificial systems that walk or run. Walking and running require dynamic stability, meaning that the system moves continuously in order to keep the average point of support beneath the center of gravity. Table 4–2 lists the number of legs, leg length, and speed of several legged robots. Keep in mind that none of these systems was designed for speed. Each was designed to study some aspect of the control of locomotion.

Huang and Waldron (1987) derived the relationship between weight and maximum speed for a hexapod vehicle crawling with a particular gait. By assuming that the distribution of forces among the support legs was a linear function of the forward and lateral position of the legs, and requiring the vehicle to remain in static equilibrium, they determined the proportion of the vehicle's weight on each leg as a function of speed. By limiting the force on the most heavily loaded leg to the maximum safe load they computed the tradeoff between speed and payload.

4.3.3 Vehicular Research

Gabrielli and von Kármán (1950) studied the cost of locomotion at different speeds. They gathered data on the gross weight, installed power, and maximum speed of many land vehicles, ships, boats, aircraft and animals. For each vehicle they computed the *specific*

Legged Robots and Vehicles

Machine	Leg Length	Speed	
	m	m/s	mph
6 legs			
OSU Hexapod (McGhee)	0.8	0.3	0.7
USSR Hexapod (Gurfinkle)	0.35	0.1	0.2
SSA Hexapod (Sutherland)	1.0	0.14	0.3
ODEX (Odetics)	1.3	0.5	1.1
ASV (Waldron)	1.90	2.2	5
4 legs			
PV II (Hirose)	0.87	0.5	1.1
Quadruped (Raibert)	0.66	3	6.7
2 legs			
WL10-RD (Kato)	0.96	0.23	0.51
Biper-3 (Miura)	0.20	0.02	0.04
MEG-2 (Funabashi)	0.48	0.5	1.1
Kenkyaku (Furusho)	0.72	0.8	1.8
Planar Biped (Koechling)	0.80	5.9	13.1

Table 4–2. These are a few of the machines and vehicles that have been used to study the control of legged locomotion. None of the machines was explicitly designed for high speed. All of the leg lengths and speeds are approximate.

resistance, which is the ratio of power to the product of weight and velocity: $\epsilon = P/WV$. This nondimensional quantity is a measure of the energetic cost of locomotion. Gabrielli and von Kármán's data indicate that any particular means of locomotion is only energy efficient over a narrow range of speeds, and that in general small, fast vehicles are less efficient than large, slow vehicles. For example, a merchant ship has a specific resistance of about 0.003 at a speed of 6 m/s, while a jet fighter plane has a specific resistance of 0.3 at a speed of 300 m/s.

The graphs of specific resistance as a function of speed show a limiting line, a minimum specific resistance that increases with speed. This line represents an efficiency limit imposed by aerodynamic or hydrodynamic drag. Single vehicles of sufficient size should have specific resistances below the limit, because specific resistance decreases with vehicle size. Railroad trains achieve a greater energetic efficiency because the aerodynamic drag is smaller for the train than for the individual cars, and because the power is supplied by a few large, efficient engines. Gabrielli and von Kármán point out that the size of the vehicles that can be built is limited by the strength to weight ratio of the available construction materials.

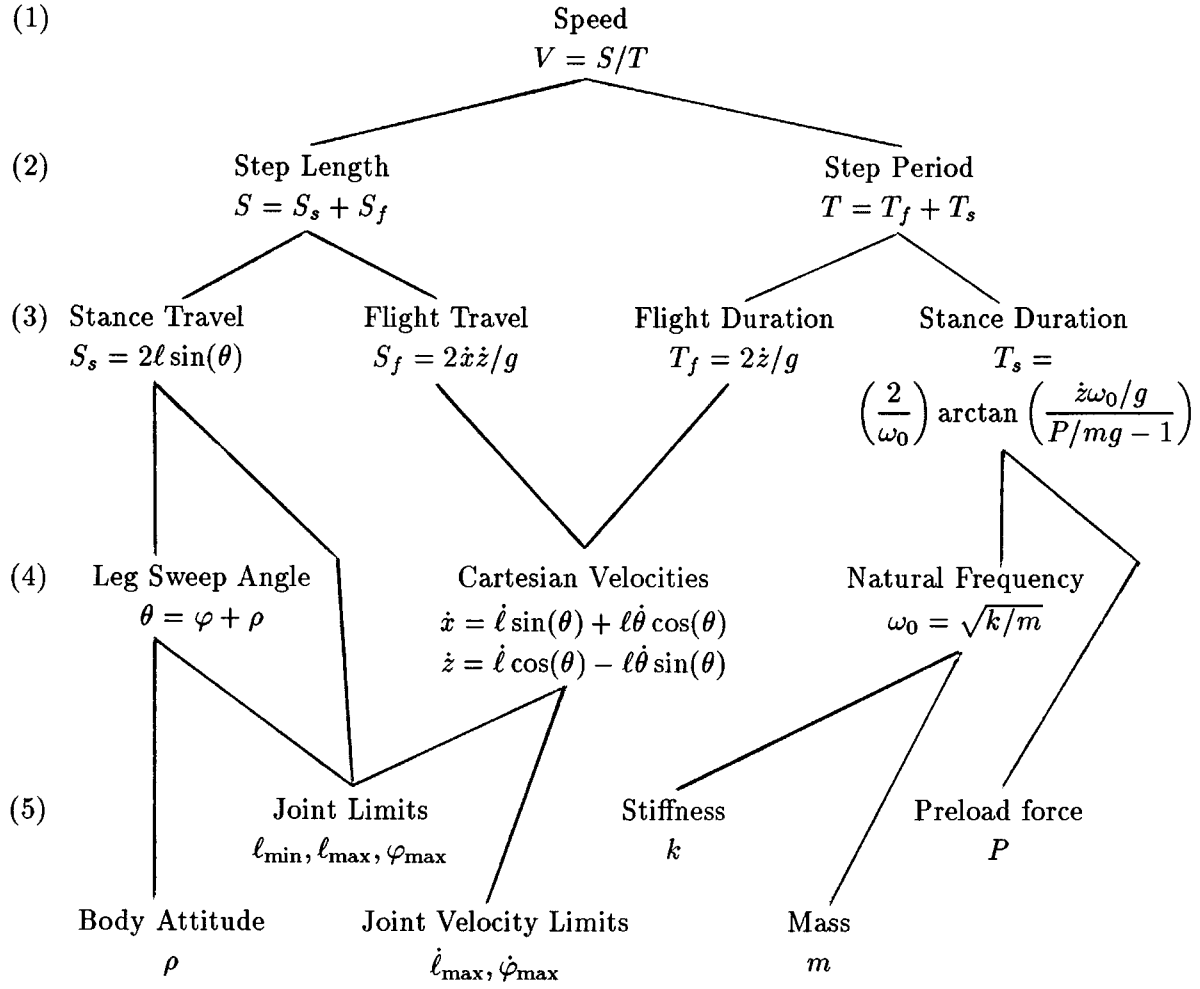

Figure 4–1: A tree indicating some of the ways the running speed of a legged system depends upon parameters of the mechanism. The top of the tree represents speed, a measure of performance. The intermediate rows represent characteristics of the running motion, and the bottom row represents the parameters of the mechanism. The state variables of the system are the leg length, the rate of leg extension, the leg angle, and the rate of leg rotation. The operating point is described by the state at the moment of liftoff: ℓ, $\dot{\ell}$, θ, and $\dot{\theta}$. The horizontal and vertical components of liftoff velocity are $\dot{x}$ and $\dot{z}$. If the steps are symmetric and the pitch angle of the body is uniformly zero, then the operating point completely characterizes the motion. Steps are symmetric if the horizontal velocity and the leg length are the same at touchdown as at liftoff, and the vertical velocity and the leg angle change signs from touchdown to liftoff. The coordinate system is shown by figure 4–2.

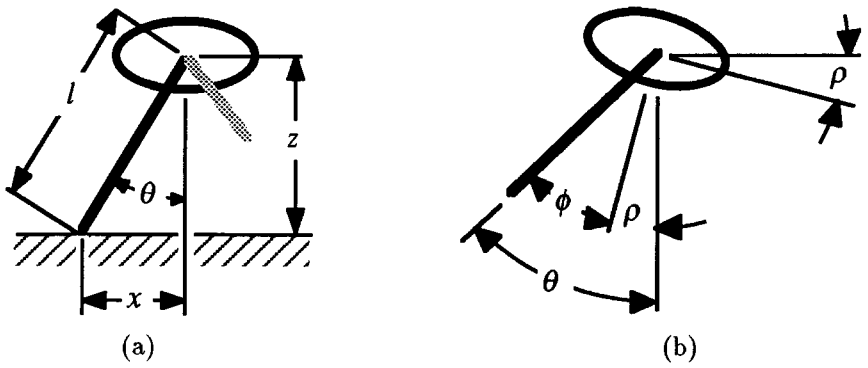

(a) (b)

Figure 4–2: (a) The horizontal and vertical distances from the foot to the hip are determined by the leg length and leg angle: $x = \ell \sin(\theta)$, $z = \ell \cos(\theta)$. During stance the foot is motionless, so the derivatives of the hip coordinates give the horizontal and vertical velocity with respect to the ground: $\dot{x} = \dot{\ell} \sin(\theta) + \ell\dot{\theta} \cos(\theta)$, $\dot{z} = \dot{\ell} \cos(\theta) - \ell\dot{\theta} \sin(\theta)$. (b) The leg angle is the sum of the leg angle with respect to the body, and angle of the body with respect to the ground: $\theta = \phi + \rho$. The three angles, θ, ϕ, and ρ are measured clockwise from the nominal position, in which the leg is vertical and the body horizontal.

4.4 The Dependency Tree

One way to impose structure on the relationship between the physical parameters of a mechanism and how fast it can run is to build a dependency tree, as shown in figure 4–1. The top of the tree is running speed. The branches are formed by expressing running speed as the ratio of step length to step period, and successively refining those quantities to simpler characteristics of the running motion. The leaf nodes are parameters of the links, joints, and actuators. Body attitude is an exception; it is determined by how well the control system corrects disturbances.

The equations in figure 4–1 embody several assumptions, which are explicitly stated in the paragraphs below. The resulting analysis accurately represents the kinematics of the mechanism, but it uses simplified dynamics, and says nothing about energetics. It leads to tractable expressions for running speed that qualitatively predict how parameter variations affect speed.

Speed

The first row of the dependency tree in figure 4–1 is the definition of running speed (V), which is the ratio of the forward progress on each step (S) to the time required to complete that step (T):

$$V = S/T. \tag{4.2}$$

To increase its speed, a running system must take longer steps, more frequent steps, or both. In bipedal running, stance and flight proceed in strict alternation, and a step consists of exactly one stance and one flight. Figure 4–3 shows that the distance traveled during

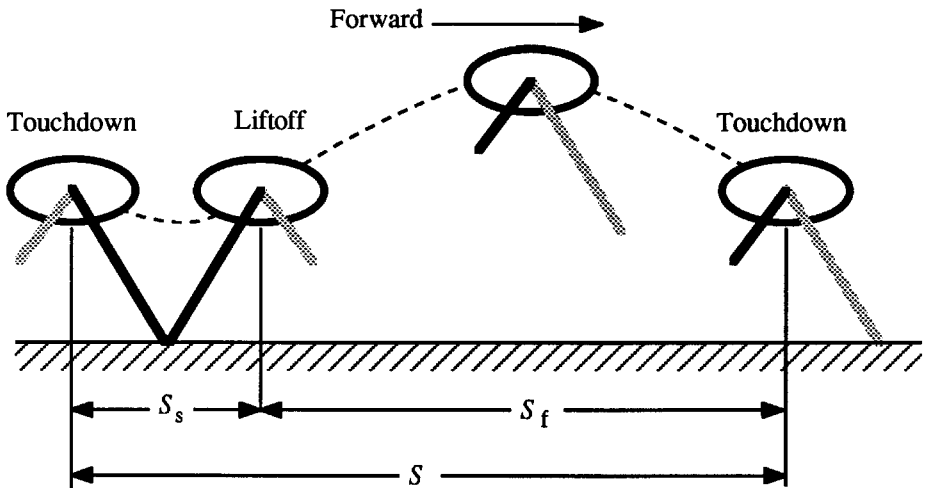

Figure 4–3: Step length (S) is the sum of the forward progress of the hip during stance (S_s) and the forward progress of the hip during flight (S_f).

one step is the sum of the distance traveled during stance (S_s) and the distance traveled during flight (S_f):

$$S = S_s + S_f. \tag{4.3}$$

Likewise, the time required for a step is the sum of the stance duration (T_s) and the flight duration (T_f):

$$T = T_s + T_f. \tag{4.4}$$

These definitions make up the second row of the tree.

In the third row of the tree, the dynamics of the system come into play. In the stance phase, the system resembles both a mass bouncing on a spring and an inverted pendulum pivoting over its fulcrum, as shown in figure 4–4. The dynamics are much simpler during flight, when the system approximates a rigid ballistic projectile rising and falling under the influence of gravity.

Stance

The leftmost and rightmost nodes of row three describe the stance duration and the stance travel. The stance travel is the forward progress of the body during stance, and is a function of the leg lengths and leg angles at the beginning and end of the stance phase, as shown in figure 4–5. For symmetric steps, the leg length and leg rotation rate are the same at touchdown and at liftoff, while the leg extension rate and the leg angle have opposite signs at touchdown and at liftoff. Under the assumption of symmetry, the distance traveled during stance is:

$$S_s = 2\ell \sin(\theta), \tag{4.5}$$

where θ and ℓ represent the leg angle and leg length at liftoff.

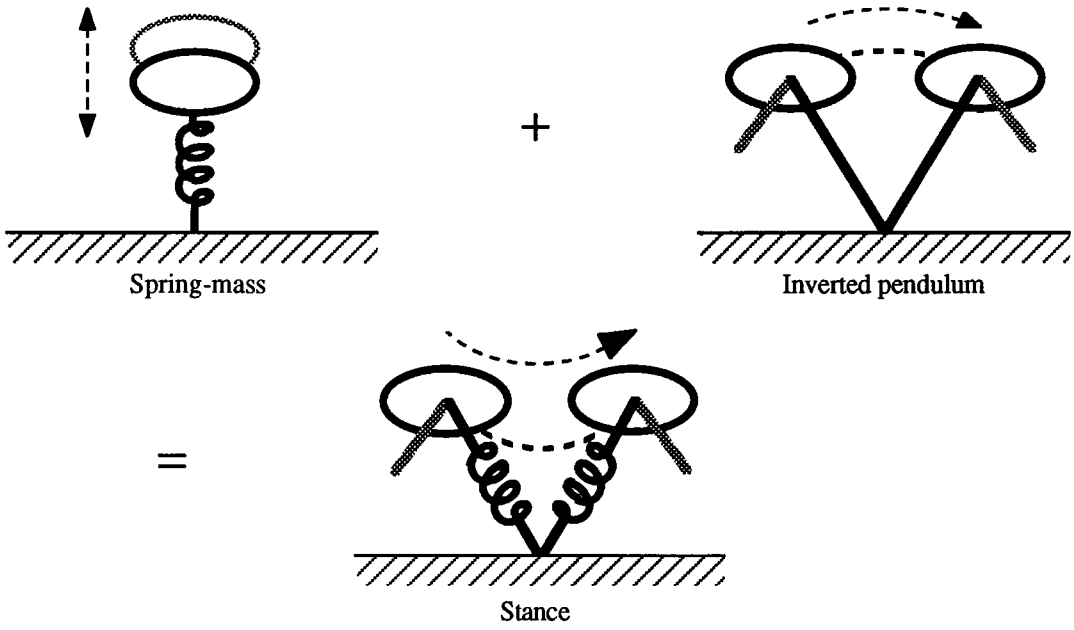

Figure 4–4: The motion of a running system during stance results from the interaction of two simpler motions. The vertical motion is predominantly the bouncing motion of a spring-mass oscillator. The forward travel results from the tipping motion of an inverted pendulum that moves first toward and then away from the unstable equilibrium point. Forward speed decreases during the first half of stance, because some of the horizontal kinetic energy is temporarily stored in the leg spring. During the second half of stance, the spring releases energy and the system speeds back up.

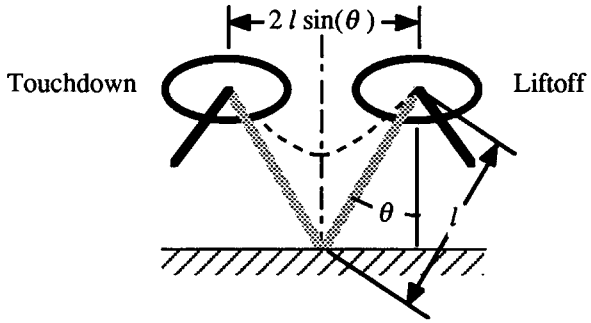

Figure 4–5: The distance traveled during stance is a function of the leg length and hip angle at the beginning and end of stance. If the motion is symmetric, so that the state at liftoff is a mirror image of the state at touchdown, the distance traveled is $2\ell\sin(\theta)$. The system in the figure is moving from left to right, touching down with the foot in front of the hip and lifting off with the foot behind the hip.

The motion during stance is described by a pair of coupled second-order non-linear differential equations. The stance duration can be computed by integrating these equations forward in time from the moment of touchdown until the moment of liftoff. We know of no

closed form expression for the stance duration as a function of the mechanism parameters and the state of the system at touchdown. In order to proceed with the analysis, we pretend that the horizontal and vertical motion of the system are decoupled, and that the stance duration is determined only by the vertical motion.

For the simple case of a mass bouncing vertically on a linear spring, McMahon (1986) showed that the time required to rebound from the ground depends on a parameter he called the Groucho number. Modifying McMahon's formula to take the leg spring mechanical stops into account gives an expression for the stance duration:

$$T_s = \begin{cases} (2/\omega_0)\left[\pi - \arctan\left(N'_G\right)\right], & \text{if } N'_G > 0 \quad (P < mg); \\ \dfrac{\pi}{\omega_0}, & \text{if } N'_G = \infty \quad (P = mg); \\ (2/\omega_0)\arctan\left(N'_G\right), & \text{if } N_G < 0 \quad (P > mg). \end{cases} \tag{4.6}$$

where

N'_G	is a modified Groucho Number ($N'_G = \frac{\dot{z}\omega_0/g}{P/mg-1}$),
ω_0	is the natural frequency of the spring-mass system ($\sqrt{k/m}$),
$\dot{z}$	is the vertical velocity at liftoff,
g	is the acceleration of gravity
k	is the leg stiffness,
m	is the body mass,
P	is the preload force.

The entry for stance duration in figure 4–1 is the third case of equation 4.6, where the preload force exceeds the weight of the system.

Equation 4.6 gives the stance duration of a system bouncing in place on a linear spring. Increasing the leg stiffness, the preload force, or the vertical velocity shortens the stance duration, whereas increasing the mass or the acceleration of gravity lengthens the stance duration. The behavior is qualitatively similar for the more complex case of a nonlinear spring and the leg pivoting about the foot. In the nonlinear case, equation 4.6 can be used to predict stance duration by assuming, computing, or measuring a value for the natural frequency. The natural frequency depends on the effective vertical stiffness, which depends on the sweep angle and impact velocity as well as on the stiffness of the leg.

Flight

The two nodes in the middle of row three of figure 4–1 describe the flight travel and the flight duration. The formulas give the duration of flight and forward progress of a rigid body that has an initial velocity $(\dot{x}, \dot{z})$ and is accelerated only by gravity (g). The formulas thus ignore changes in the location of the center of gravity due to the motions of the legs, and accelerations due to aerodynamic drag. The rigid body assumption leads to simple expressions for the flight duration and the flight travel:

$$T_f = 2\dot{z}/g \tag{4.7}$$

$$S_f = 2\dot{z}\dot{x}/g. \tag{4.8}$$

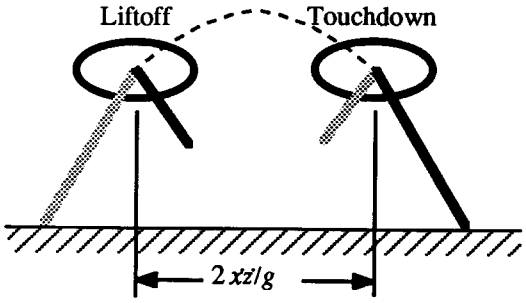

Figure 4–6: The distance traveled during flight is determined by the liftoff velocity $(\dot{x}, \dot{z})$. For symmetric steps, in which the height of the body above the ground is the same at touchdown as at liftoff, the duration of flight is $2\dot{z}_{lo}/g$. The forward progress during flight is $2\dot{z}\dot{x}/g$. The system in the figure is moving from left to right, lifting off from the foot behind the hip and landing on the foot in front of the hip.

The third row of figure 4–1 divides running speed into four quantities: stance travel, stance duration, flight travel, and flight duration. These four quantities depend on the quantities in row four, which are functions of the operating point, and on the parameters in row five, which characterize the mechanism. The behavior in stance depends on the mass of the system, the stiffness and preload of the leg spring, the length and angle of the leg at liftoff, and the regulation of body attitude. The behavior in flight depends on the joint positions and velocities at liftoff. The following sections discuss the dependencies on operating point and mechanism parameters in more detail.

Stance Travel

The system travels a distance $S_s = 2\ell \sin(\theta)$ during stance. The motion during stance depends on the leg length and leg angle at touchdown, which are chosen by the control system to make the motion during stance symmetric and thus maintain a constant forward speed. The higher the speed, the farther forward the foot must be ahead of the hip at touchdown. The design of the leg limits the leg length, and the design of the hip joint limits the angle of the leg with respect to the body.

The leg angle is limited by the angle of the leg with respect to the body, and by the angle of the body with respect to the ground. We call the angle of the body with respect to the ground the pitch of the body. With the body in its nominal orientation, the range of leg angles permitted by the hip joint is symmetric about vertical, allowing the leg to swing equally far forward and backward. Deviations of the body from its nominal orientation reduce either the distance that the leg can reach forward for touchdown or the distance that it can reach back before liftoff. Either case reduces top speed by reducing the travel that can be achieved during stance.

If the body rotates away from its nominal pitch angle, the travel of the foot with respect to the hip is asymmetric. If the body is pitched forward, the distance that the foot can reach ahead at touchdown is reduced. During flight, the control system positions the foot

in front of the hip by a distance that is proportional to running speed. Reducing the foot travel ahead of the hip reduces the maximum stable running speed, regardless of how much foot travel is gained behind the hip. If the body rotates backward, the foot can reach farther ahead of the hip for touchdown. However, the hip joint then reaches its limit of rearward travel before the end of stance, abruptly pitching the body forward.

Stance Duration

The duration of stance is $T_s = (2/\omega_0)\arctan\left(\frac{\dot{z}\omega_0/g}{P/mg-1}\right)$. The expression is based on the assumption that the stance duration is determined by the vertical motion of the system independent of the horizontal motion. Other plausible expressions for the stance duration might be derived from the strength of the leg, from the decrease in forward speed during stance, and from the velocity and acceleration limitations of the hip joints. For figure 4–1, we chose the representation based on stiffness, because leg stiffness *determines* stance duration, while leg strength and hip joint properties might *limit* stance duration. The stance duration must be long enough that the forces do not break the leg, and that the hip joint has time to move from the touchdown angle. The stance duration must be long enough, or the speed slow enough, that the hip joint does not exceed its maximum angle of rotation.

Flight Travel and Flight Duration

During flight the center of gravity of the system moves along a parabolic trajectory determined by the velocity at liftoff and the acceleration of gravity. The liftoff velocity depends on the leg length, leg extension rate, leg angle and leg rotation rate. It has magnitude $\sqrt{\ell^2\dot{\theta}^2 + \dot{\ell}^2}$ and direction $\arctan(\dot{\ell}/\ell\dot{\theta}) - \theta$. The magnitude is independent of the leg angle. The horizontal and vertical components are:

$$\dot{x} = \dot{\ell}\sin(\theta) + \ell\dot{\theta}\cos(\theta) \tag{4.9}$$

$$\dot{z} = \dot{\ell}\cos(\theta) - \ell\dot{\theta}\sin(\theta). \tag{4.10}$$

Speed Equations

Combining the formulas in figure 4–1 yields a single equation that expresses running speed as a function of operating point and mechanism parameters. The top row of the tree defines running speed as $V = S/T$. Breaking up the step length and step period expands the definition to:

$$V = \frac{S_f + S_s}{T_f + T_s}. \tag{4.11}$$

Incorporating the definitions of stance travel, flight travel, flight duration, and stance duration gives:

$$V = \frac{\dot{x}\dot{z} + g\ell\sin\theta}{\dot{z} + (g/\omega_0)\arctan\left(\frac{\dot{z}\omega_0/g}{P/mg-1}\right)}. \tag{4.12}$$

Finally, replacing the Cartesian components of liftoff velocity according to equations 4.9 and 4.10, gives an equation for running speed in terms of the state variables $(\ell, \dot{\ell}, \theta, \dot{\theta})$ at liftoff and the parameters (ω_0, P, m, g):

$$V(\ell, \dot{\ell}, \theta, \dot{\theta}, \omega_0, P, m, g) \tag{4.13}$$
$$= \frac{(\dot{\ell}^2 - \ell^2\dot{\theta}^2)\sin(2\theta) + 2\ell\dot{\ell}\dot{\theta}\cos(2\theta) + 2g\ell\sin(\theta)}{2\dot{\ell}\cos(\theta) - 2\ell\dot{\theta}\sin(\theta) + (2g/\omega_0)\arctan\left\{\left(\frac{\omega_0/g}{P/mg-1}\right)\left[\dot{\ell}\cos(\theta) - \ell\dot{\theta}\sin(\theta)\right]\right\}}.$$

The extent of the state space is determined by mechanism parameters that describe maximum excursions and velocities of the joints. The construction of the leg establishes minimum and maximum leg lengths, and the rate of change of leg length is less than some maximum. If the pitch angle is always zero, then the leg angle and leg rotation rate are limited by the maximum excursion and velocity of the hip joint. At liftoff the leg angle, leg rotation rate, and leg extension rate are all positive:

$$\begin{aligned} \ell_{\min} \leq \ell &\leq \ell_{\max} \\ 0 \leq \dot{\ell} &\leq \dot{\ell}_{\max} \\ 0 \leq \theta &\leq \varphi_{\max} < \pi/2 \\ 0 \leq \dot{\theta} &\leq \dot{\varphi}_{\max}. \end{aligned} \tag{4.14}$$

The operating point, which is the state at liftoff, lies in this restricted region of the state space.

Summary of the Dependency Tree

The top of the dependency tree shown in figure 4–1 is a performance measure, running speed. The intermediate rows are characteristics of the running motion:

- step rate
- step length
- flight duration
- stance duration
- stance travel
- flight travel
- leg sweep angle
- horizontal and vertical velocity at liftoff
- natural frequency

At the bottom of the tree are the parameters of the physical mechanism that determine running speed:

- body attitude
- leg length
- hip position
- leg extension rate

- hip rotation rate
- leg spring preload force
- leg stiffness
- mass

The formulas in the dependency tree are based on the following assumptions:

- There is no air drag, so the speed during flight is constant.
- The center of gravity is fixed with respect to the body, so the mechanism moves like a rigid body during flight.
- The motion during stance is symmetric:

$$\begin{array}{llll} \ell_{td} = \ell_{lo} & \theta_{td} = -\theta_{lo} & x_{td} = -x_{lo} & z_{td} = z_{lo} \\ \dot{\ell}_{td} = -\dot{\ell}_{lo} & \dot{\theta}_{td} = \dot{\theta}_{lo} & \dot{x}_{td} = \dot{x}_{lo} & \dot{z}_{td} = -\dot{z}_{lo} \end{array}$$

This structure provides a framework for studying how running speed depends on the operating point and on the physical mechanism parameters.

The dependency tree provides a model of running speed. Although it incorporates several simplifying assumptions, it provides more intuition about how running speed depends on mechanism parameters than more complex models would. In particular, dynamic simulations would predict the results of experiments, but they have too many parameters to offer much insight to the problem. The dependency tree models running with a small number of parameters, and shows qualitatively how each affects speed.

4.5 Experiments

We have experimented with the planar biped to study how the design and control of a legged system affect its top running speed. The planar biped runs faster with long legs than with short legs, and faster with stiff leg springs than with soft leg springs. Experimenting with the biped has made it clear that there are speed dependent disturbances to body attitude, and that fast running requires that the control system reject or correct those disturbances. The biped's power dissipation increases with running speed, but the increase is small compared with the power required just to run in place.

How Fast Running Differs from Slow Running

Figure 4–7show the motions of the legs and body as the biped ran forward at a constant speeds of 1, 3, and 5 m/s, respectively. Table 4–3 lists the properties of a typical step at each speed. Compared to running slowly, running fast was characterized by longer and more frequent steps, higher frequency oscillations of leg length, leg angle, and body attitude, smaller and more frequent vertical oscillations of the body, and larger angular motions of the legs.

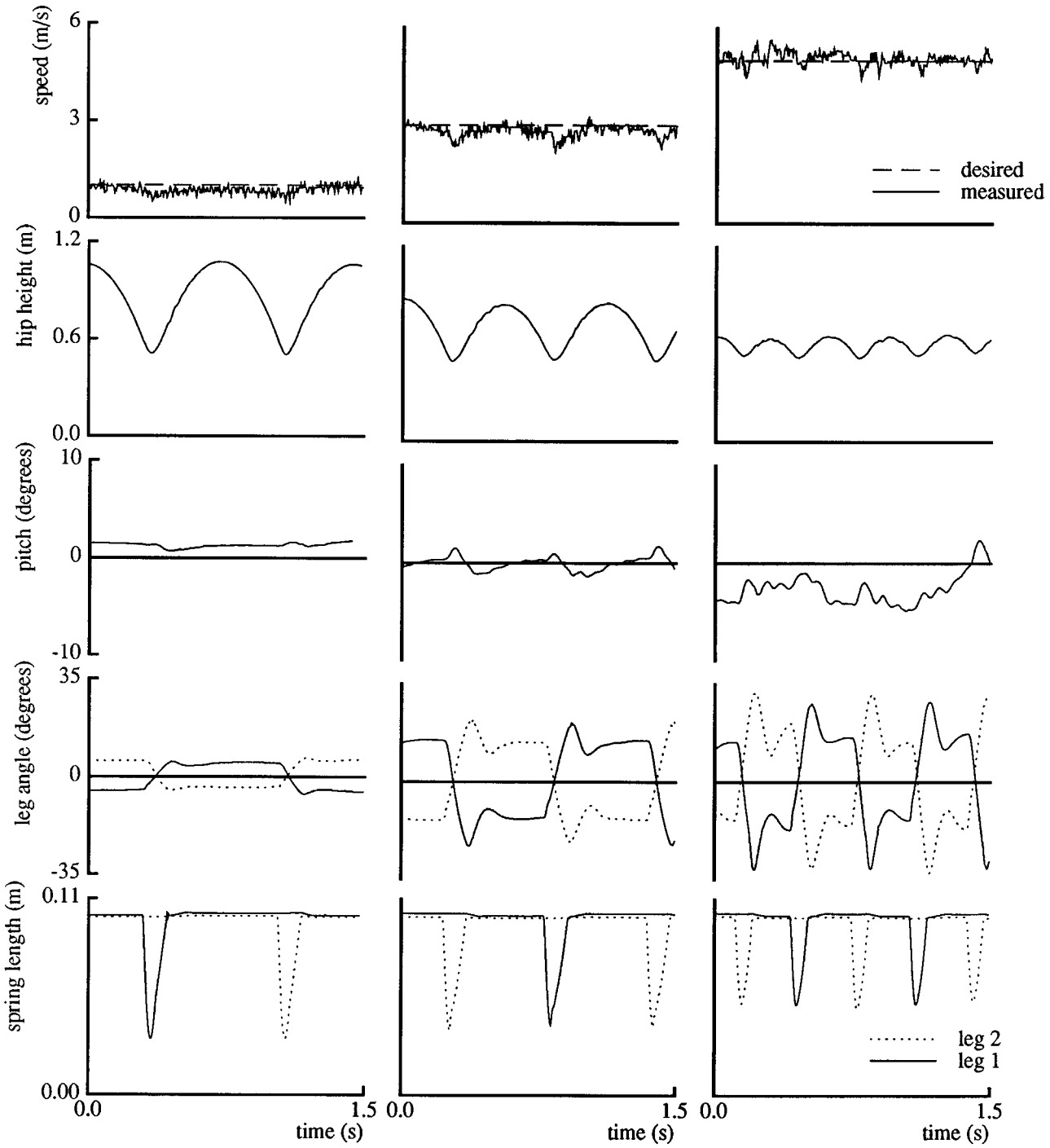

Figure 4–7: The planar biped ran forward at 1, 3, and 5 m/s. The top three graphs show the forward speed, hip height, and pitch angle of the body. The fourth graph shows the equal and opposite motions of the two legs as they sweep back and forth. The bottom graph shows how the two leg springs compressed as the biped bounced alternately on the two feet. As running speed increased, the frequency of stepping and leg angle excursion increased, and the compression of the legs during the bounce decreased. (Data files B88.241.4, B88.241.3, B88.241.1)

Step Parameters at 1, 3, 5 m/s			
commanded speed (m/s)	1.0	3.0	5.0
observed speed (m/s)	0.90	2.92	4.99
stance duration (s)	0.128	0.128	0.088
flight duration (s)	0.588	0.392	0.320
step period (s)	0.716	0.520	0.320
stance travel (m)	0.10	0.34	0.43
flight travel (m)	0.55	1.18	1.17
step length (m)	0.65	1.52	1.60
leg length (m)			
touchdown	0.595	0.595	0.591
liftoff	0.666	0.658	0.620
leg angle w.r.t vertical (°)			
touchdown	-2.2	-11.1	-19.5
liftoff	7.4	21.9	25.2
body angle w.r.t horizontal (°)			
touchdown	1.3	0.0	-4.1
liftoff	1.3	-0.2	-2.5
vertical velocity (m/s)			
touchdown	-2.95	-2.38	-1.60
liftoff	3.00	2.12	1.54
horizontal velocity (m/s)			
touchdown	0.75	2.58	5.02
liftoff	0.86	2.97	4.97
data file	B88.241.4	B88.241.3	B88.241.1

Table 4–3. Each column of data is for a typical step on leg two of the planar biped while it was running at constant speed. Increasing speed was accompanied by longer steps and shorter step periods, as shown by these data. During these experiments, the air pressure in the leg springs was 90 psi and the thrust algorithm extended the leg actuator as quickly as possible during stance.

4.6 Leg Length

The longer a legged system's legs are, the faster it can run. Figure 4–8 shows the results of nine experiments with the planar biped, each with a different leg length. During flight, the control system servoed the active leg to the the indicated length. During stance, the leg actuator extended, so the leg was longer at liftoff than it was at touchdown. During each experimental run, I used a joystick to increase the desired running speed, attempting to find the highest speed at which the biped would run without losing its balance. The reported speed for each run is the highest average speed for one lap of the 16 m running track.

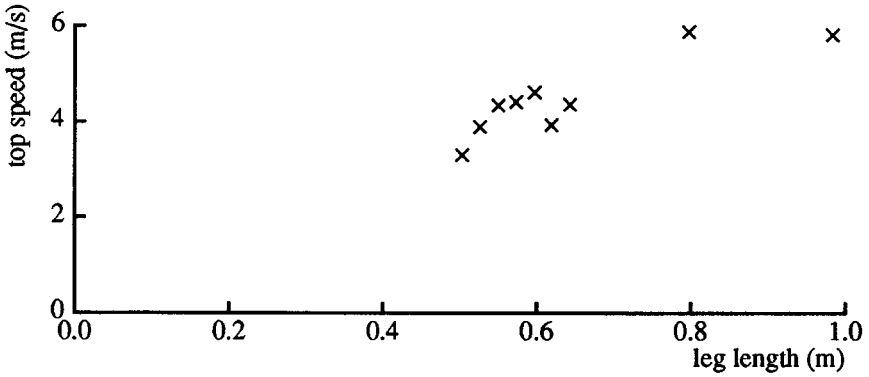

Figure 4–8: The longer the legs, the faster the planar biped ran. The planar biped ran nine times, each time with a different leg length. During flight, the control system adjusted the length of the leg. In each run, the experimenter raised the forward running speed to the highest value that could be maintained without the biped losing its balance. The listed speed is the average for a complete circuit around the 16 m circular track. Initially the range of possible leg lengths was 0.50 m to 0.65 m. Longer leg lengths were obtained by adding stilts to the end of the biped's legs. A 0.191 m stilt gave a leg length of 0.844 m, and a 0.391 m stilt gave a leg length of 1.005 m. During the experiments with the stilts, the leg actuator extended as fast as possible during stance, rather than trying to extend 0.021 m as in the other experiments. With a leg length of 0.844 m, the biped ran 5.9 m/s (13.1 mph), the highest speed ever recorded.

The control system could select leg lengths between 0.50 m and 0.65 m by adjusting the leg actuator. For longer leg lengths, the biped's legs were extended with stilts and joined to the bottom of the legs. The feet were moved to the bottom of the stilts. A 0.191 m stilt gave a leg length of 0.844 m, and a 0.391 m stilt gave a leg length of 1.005 m. Figure 4–8 shows that the top running speed of the biped increased with increasing leg length, but may flatten out above 0.8 m.

The increasing leg length of the biped was not accompanied by other changes specified by any principle of geometric or elastic similarity. No dimension other than leg length changed. Since the diameter of the legs did not change, the strength of the legs remained the same, and the factor of safety against structural failure got smaller as the legs got longer. Figure 4–9 shows one of the consequences. After several running experiments at the longest leg length, one of the stilts broke where it was attached to the leg. The bending force on the leg had torn the stilt where it was fastened to the leg.

The leg springs did not get any longer when the legs got longer, and that may have caused a problem. If the body were to move horizontally during stance, then the leg length when the leg was vertical would be $\ell \cos(\theta)$, where ℓ and θ are the leg length and leg angle at touchdown. So when the leg was vertical, the leg spring would be deflected at least $\ell[1 - \cos(\theta)]$ from its length at touchdown. The actual deflection of the spring would be greater, since the path of the body is concave upward, so that the hip is always lower in the middle of stance than at touchdown or liftoff. The air springs on the biped have a maximum deflection of less than 0.10 m. For a leg angle of 25°, a leg length of 0.66 m would require the spring to deflect at least 0.06 m, but for a leg length of 0.98 m, the required deflection

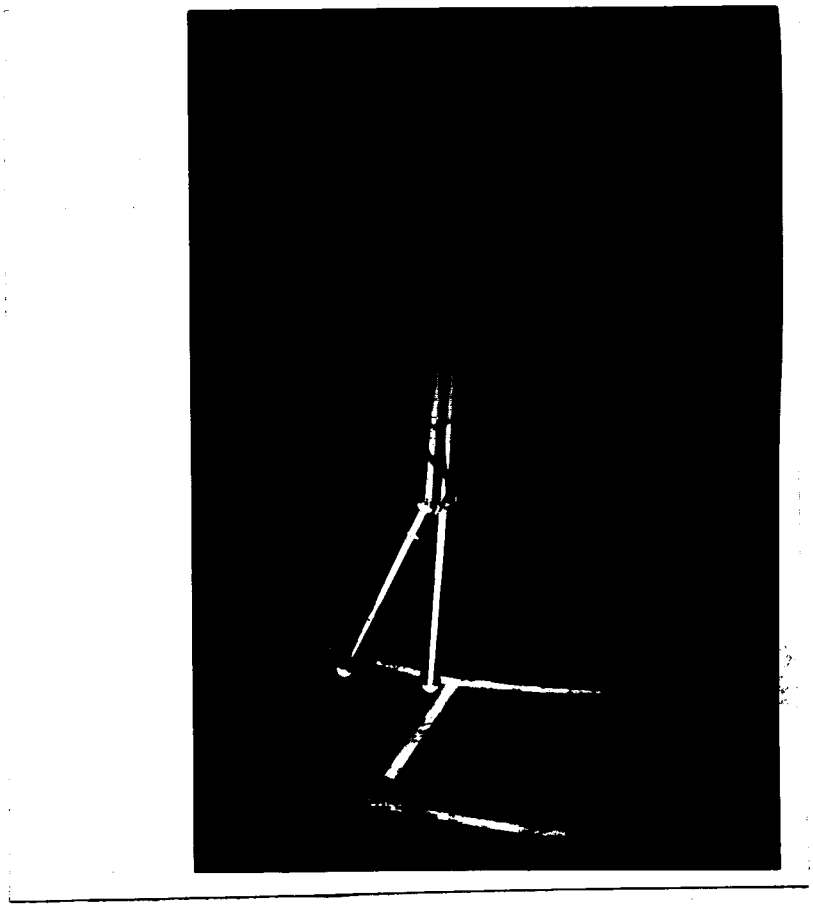

Figure 4–9: One of the long stilts broke after several running experiments. The wall of the tubing tore where it was screwed onto the plug that joined the stilt to the leg tube. Long legs are more vulnerable to buckling failure than short legs.

would be more than 0.09 m. The limit on leg spring deflection probably prevented the biped from using its full hip travel when it was running with the long stilts.

When the long stilts were on the machine, the hip servo position gain had to be reduced to keep the servo from oscillating. Lengthening the legs increased their moment of inertia and their flexibility, both of which lowered the natural frequency of the first mode of vibration of the leg. Lowering the position gain softened the servo so that it did not excite the vibration of the leg.

The planar biped runs faster with long legs than with short legs. The broken stilt and the need to soften the hip servo point out some of the problems that accompany increasing leg length.

4.7 Leg Stiffness

The stiffer the leg springs are, the faster a legged system can run. Figure 4–10 shows the results of eight experimental runs with the planar biped, each at a different leg stiffness. Before each experimental run, I set the indicated pressure with the regulator that supplies air to the pneumatic leg springs. During the runs, I used a joystick to gradually increase the desired running speed to find the highest speed at which the biped would run without losing its balance. The reported speed for each run is the highest average speed for one lap of the 16 m circumference running track. The reported stance duration is the average of the stance durations observed during the fastest lap.

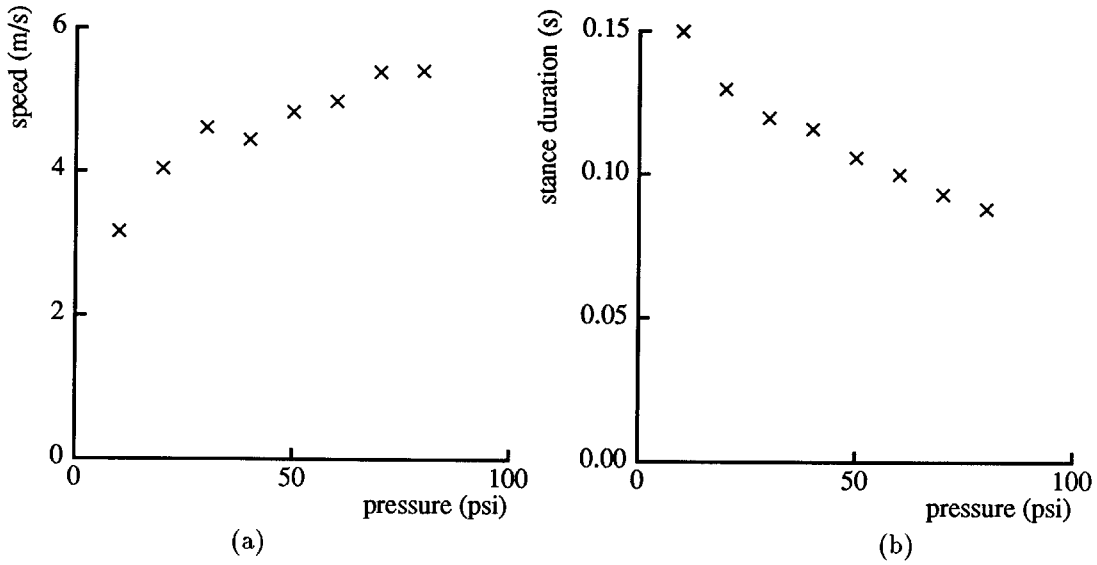

Figure 4–10: These plots show the variation of top running speed (a) and of stance duration (b) as a function of the air pressure in the leg springs. Each point represents the average stance duration or forward speed over the fastest lap at the given air pressure. To generate the data the planar biped ran eight times, each with a different air pressure in the leg springs. In each run, the experimenter raised the forward running speed to the highest value that could be maintained without the biped losing its balance. The reported forward speed, stance duration, and vertical landing velocity are average values for a complete circuit around the 16 m circular running track. During these runs, the leg length at touchdown was 0.623 m, and the thrust algorithm extended the leg actuator as rapidly as possible during stance.

The leg stiffness of the planar biped depends on how much air is in the leg springs. An air line leads from the spring chamber to a regulator that maintains the desired pressure in the line. A check valve isolates the spring chamber when pressure inside is higher than the pressure in the line. If air leaks out of the spring while it is compressed, then when the spring extends the pressure inside drops below the pressure in the air line. In this case the check valve opens, restoring the spring pressure to the desired value. The higher the air

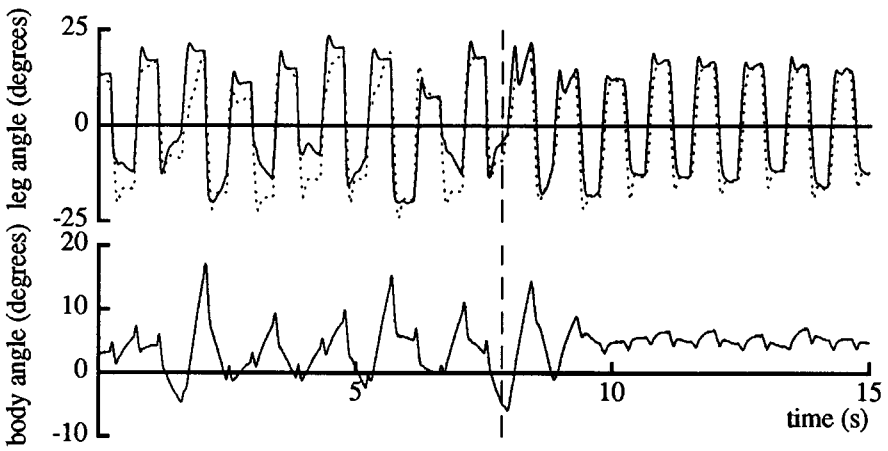

Figure 4–11: A control algorithm that kept the leg angles equal and opposite reduced the the amplitude of the oscillations in body attitude. The top graph shows the angle of each leg with respect to the axis of symmetry of the body. The sign of the angle of leg 2 is reversed so that when the leg angles are symmetric the lines are on top of one another. The vertical line marks a switch from an algorithm that moved the legs independently to one that ensured that the leg angles were mirror images. The axis of symmetry was a line passing through the hip joint perpendicular to the body. The bottom graph shows that changing the leg positioning algorithm reduced the oscillations in body angle from about 20° peak-to-peak to about 6° peak-to-peak. In this experiment the planar biped was running about 2.5 m/s (5.6 mph). (Data file B87.325.3)

pressure, the more air there is inside of the leg spring. Higher air pressure increases both the stiffness and the preload force of the spring.

Figure 4–10 shows that the biped ran faster and took steps with shorter stance duration when it was running with high leg spring air pressure than when it was running with low leg spring air pressure. The stiffness of the legs, and thus the natural frequency of the bouncing motion increased with the pressure.

4.8 Body Attitude

Body attitude is important to top running speed because of the limited range of motion of the hip joints. If the body tips forward during flight, the hip joint limit prevents the foot from reaching as far forward for landing as it can with a level body. The distance that the foot needs to reach forward for landing is proportional to running speed, so forward tipping of the body reduces the top running speed. If the body tips backward during stance, the hip joint limit prevents the foot from reaching as far backward as it can with a level body. In this case, the hip may reach the joint limit before the leg leaves the ground, causing a sudden forward pitching of the body. Top running speed requires good control of body attitude so the hip joint can sweep through its full range of motion during stance. If there were no kinematic limits to hip angle, then body attitude would not affect running speed.

Mirroring

Hip torques that position the legs also rotate the body. The control system can minimize disturbances to the body attitude by ensuring that the two legs move at the same time and in opposite directions. During stance, while the support leg sweeps backward, the other leg swings forward. During flight, while one is positioned for landing, the other leg makes compensating motions to reduce the torques on the body. This mirroring action substantially reduces the variation in body attitude that occurs when each leg is moved independently.

Figure 4–11 shows the result of an experiment comparing two different algorithms for moving the idle leg. At the time marked by the vertical dotted line, the control system switched algorithms. Before that time, the legs were positioned independently, and afterwards they were positioned according to the mirroring algorithm. The mirroring algorithm reduced the oscillations in pitch angle, from about 20° peak-to-peak to about 6° peak-to-peak.

When the two legs were being positioned independently, the algorithm was as follows: during stance, the stance leg was swept back by the forward motion of the body, and by hip torques selected by the body attitude control servo. A leg angle servo moved the swing leg forward into position for the next touchdown. During flight, leg angle servos positioned the leg that would touch down next for landing, and servoed the leg that had just lifted off to the angle it had at liftoff. The leg angle servos were as stiff as possible, in order to minimize steady state error. The swing leg moved forward very quickly and stopped at the desired position well before the end of stance. After liftoff, the leg that had just left the ground was still rotating, so the servo applied torques to stop the rotation and move the leg back to the position it had at liftoff. These torques disturbed the body attitude.

The mirroring algorithm servoed the idle leg so that its hip angle was equal and opposite to that of the active leg. During stance, the support leg was active, and swept back as the body moved forward. The swing leg was idle, and moved forward at the same rate as the support leg moved back. During flight, the leg that would next touch down was active, and was positioned for landing as usual. The leg that had just lifted off was idle, and made motions symmetric to the active leg. Compared with the independent positioning algorithm, mirroring caused the swing leg to advance more slowly, which reduced the disturbance to body attitude. During flight, mirroring caused the reaction torques generated by positioning one leg to be canceled by torques from moving the other leg.

Sweep Compensation

The hip actuators on the planar biped have internal damping that causes a velocity dependent discrepancy between the commanded force and the delivered force. When the biped runs fast, it leans forward until the body attitude servo commands enough force to overcome the actuator damping. Explicitly compensating for the velocity dependent forces reduces the tendency to lean forward.

Figure 4–12 shows the body angle during an experimental run in which the control

system gradually increased the running speed from zero to 4 m/s. The graphs show that the average body angle increased as running speed increased.

When the biped runs in place, the hips barely move. When it runs forward, each hip rotates one way as the leg sweeps back during stance and the other way as the leg swings forward in preparation for the next step. These hip joint velocities are proportional to running speed. Each biped hip actuator behaves like a torque source in parallel with a damper. For a given input signal, the actuators produce less force when they are moving quickly than when they are moving slowly. The damping forces are proportional to hip rotation rate, which is proportional to running speed.

The hip torque to overcome the actuator damping comes from the body attitude servo. During stance, the servo applies torques proportional to the angle and angular velocity of the body. The angle stabilizes when the body has leaned forward enough that the attitude servo generates a correcting torque equal to the torque caused by the actuator damping force. Because the force is proportional to running speed, the body leans farther forward as the biped runs faster.

Compensating for the velocity dependent torques reduces the lean of the body. Figure 4–13 shows the body angle during an experimental run in which the body attitude servo added negative damping to the hip actuators by feeding back a signal proportional to the actuator velocity. The signal to the servovalve was:

$$\tau = k_\rho \rho + k_{\dot\rho} \dot\rho + k_{\dot w} \dot w, \tag{4.15}$$

where ρ and $\dot\rho$ are the pitch angle and the pitch rate, $\dot w$ is the hip actuator velocity, and k_ρ, and $k_{\dot\rho}$ are the position and velocity gains that control pitch, and $k_{\dot w}$ is the inverse damping coefficient. The modification reduced the body angle offset from about 7° to about 3°. The same result might have been obtained by adding an integral term to the body attitude servo.

4.9 Power Dissipation

The planar biped dissipates slightly more power when it runs fast than when it runs slowly. Figure 4–14 shows the power dissipated during an experimental run in which the control system gradually increased the running speed from zero to 4 m/s. The peak power was nearly constant, increasing very slightly at 4 m/s. The average power increased gradually as running speed increased. The instantaneous power shown is the product of the supply pressure measured by a sensor on the robot, and the total flow computed from the actuator velocities. The flow computation included an estimate of the flow that leaked through the servovalves, which does not appear in the actuator velocities. The estimated leakage was about 39 cc/s, which at a system pressure of 3000 psi corresponds to 0.8 kW. The hydraulic pump maintained a nearly constant pressure, so the power was proportional to the flow.

A 7.5 kW motor drives the hydraulic pump. The peak instantaneous power of 6.6 kW probably exceeds what the pump can deliver. However, the 5 gal hydraulic accumulator, the compliance of the hydraulic hoses, and the inertia of the oil all filter out flow transients,

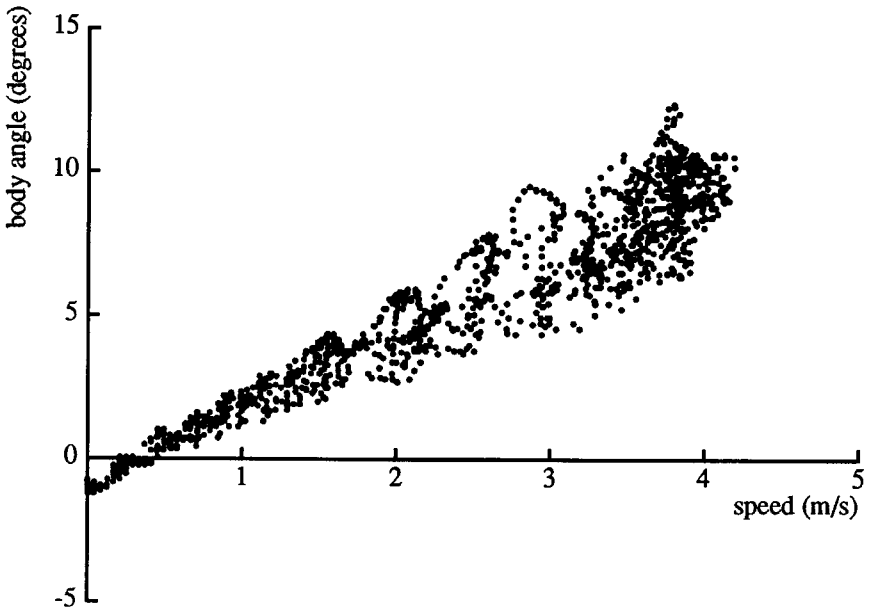

Figure 4–12: The planar biped leans forward when it runs fast. The graph shows body angle plotted as a function of running speed. The body angle oscillated during each step. As the running speed increased, the peak-to-peak amplitude increased with a slope of about 2.0 °s/m. Similarly, the average body angle increased with a slope of about 2.2 °s/m. At 4 m/s the offset was 7 ° and the peak-to-peak amplitude was 5 °. (Data file B89.6.2)

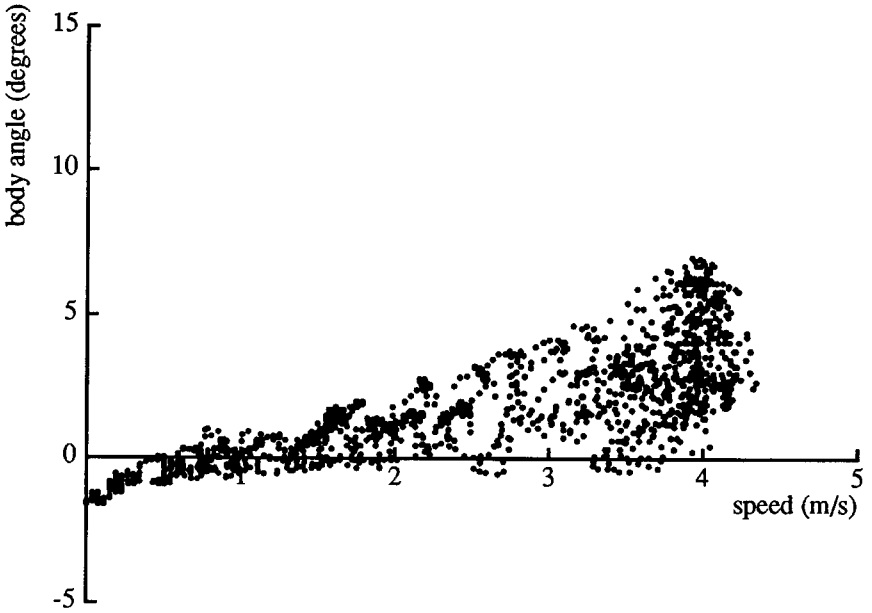

Figure 4–13: Compensating for velocity dependent forces in the hip actuators reduced the average body angle, but did not reduce the amplitude of oscillation. As in figure 4–12, the body angle took on an offset and an oscillation as the running speed increased. Sweep compensation reduced the average body angle but not the amplitude of the oscillations. The increase in offset was about 1.5 °s/m. At 4 m/s the offset was about 3 ° and the peak-to-peak amplitude was about 6 °. (Data file B89.16.3)

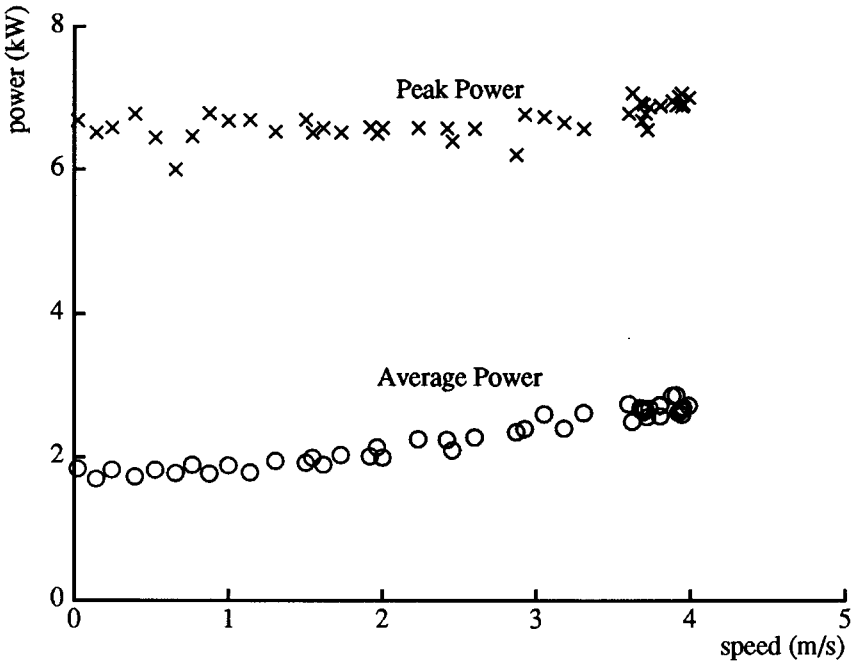

Figure 4–14: The planar biped dissipates slightly more energy to run fast than it does to run slowly. The top two graphs show the instantaneous power and the running speed as the biped accelerated from rest to 4 m/s. The bottom graph shows power plotted as a function of running speed. The crosses show the peak instantaneous power on each step, and the circles show the average power for each step. The peak power was a nearly constant 6.6 kW, increasing very slightly at speeds of about 4 m/s. The average power increased gradually, from 1.8 kW for hopping in place, to 2.7 kW for running 4 m/s. (Data file B89.16.3)

so the pump never has to deliver the peak power. The average power dissipation was less than 3 kW, which is well within the capacity of the pump and motor. The biped's running speed is not currently limited by the available power.

We measured the power dissipation during a pair of experiments in which the planar biped ran using two different gaits. In the first experiment, the biped ran with its usual alternating two-legged gait. In the second experiment, it ran by hopping on one leg. The second leg stayed short, and moved back and forth to compensate for the reaction torques of the active leg.

The biped ran at about the same speed with both gaits, but dissipated less energy when it ran on only one leg. It ran 5.3 m/s on two legs, and dissipated 3.5 kW, with instantaneous peaks of 7.2 kW. On one leg, it ran 5.4 m/s, dissipated 2.9 kW, with instantaneous peaks of 6.0 kW.

Running on one leg required the legs to sweep back and forth twice as frequently as they did in two-legged running, so the hip actuators dissipated more power. On the other hand, running on one leg meant that the other leg never had to change length. The leg actuator has a large area and a long stroke, so moving it causes a large flow that dissipates a lot of power without doing any work. Keeping one leg short and not moving its actuator saved more than enough energy to compensate for the increased dissipation of the hip actuators.

The biped's hydraulic system is very inefficient for applying small forces at high velocities. The pump supplies oil at constant pressure, so the power supplied is proportional to the flow of oil. To apply a small force, an actuator throttles the oil down to a lower pressure, dissipating energy. That the biped dissipated less power running on one leg than running on two is an artifact of the constant pressure hydraulic system.

4.10 Summary

The running speed of a legged system depends upon the frequency and length of its steps. The time required for a step can be reduced by stiffening the legs, and the step length can be increased by lengthening the legs. If body attitude is not well controlled, the limited range of motion of the hips limits the length of the steps.

Experiments with the planar biped showed that it runs faster with stiff legs than with soft legs, and that it runs faster with long legs than with short legs. To get it to run fast, the control system reduces variation of body attitude by moving the legs symmetrically, and by compensating for velocity dependent hip actuator forces. The biped's power dissipation is well within the capacity of its power supply.

During its fastest run the planar biped ran 5.9 m/s (13.1 mph) on long, stiff legs. The leg length at landing was 0.844 m, and the air spring pressure was 85 psi. The control system moved the legs symmetrically, and compensated for hip actuator damping forces.

4.11 References

R. McN. Alexander, V. A. Langman, and A. S. Jayes. 1977. Fast locomotion of some African ungulates. *J. Zoology, (London)* 183:291–300.

R. McN. Alexander and A. Vernon. 1975. The mechanics of hopping by kangaroos (Macropodidas). *J. Zoology (London)* 177:265–303.

R. McN. Alexander. 1988. *Elastic Mechanisms in Animal Movement.* Cambridge: Cambridge University Press.

T. J. Dawson and C. R. Taylor. 1973. Energetic cost of locomotion in kangaroos. *Nature* 246:313–314.

J. Furusho, M. Masubuchi. 1987. Control of a dynamical biped locomotion system for steady walking. In H. Miura, I. Shimoyama, editors, *Study on Mechanisms and Control of Bipeds*, Tokyo: University of Tokyo, 116–127.

G. Gabrielli and T. H. von Kármán. 1950. What price speed? *Mechanical Engineering* 72:775–781.

V. S. Gurfinkel, E. V. Gurfinkel, A. Yu. Shneider, E. A. Devjanin, A. V. Lensky, L. G. Shitilman. 1981. Walking robot with supervisory control. *Mechanism and Machine Theory* 16:31–36.

A. V. Hill. 1950. The dimensions of animals and their muscular dynamics. *Science Progress* 38:209–230.

S. Hirose. 1984. A study of design and control of a quadruped walking vehicle. *International J. Robotics Research* 3:113–133.

D. F. Hoyt and C. R. Taylor. 1981. Gait and the energetics of locomotion in horses. *Nature* 292:239–240.

M. Huang and K. J. Waldron. 1987. Relationship between payload and speed in legged locomotion. In *Proceedings of Conference on Robotics and Automation*, IEEE, Raleigh, NC. 533-538.

T. Kato, A. Takanishi, H. Jishikawa, I. Kato. 1983. The realization of the quasi-dynamic walking by the biped walking machine. In A. Morecki, G. Bianchi, K. Kedzior, editors, *Theory and Practice of Robots and Manipulators, Proceedings of RoManSy'81*, Warsaw: Polish Scientific Publishers. 341–351.

T. A. McMahon. 1975. Using body size to understand the structural design of animals: quadrupedal locomotion. *J. Appl. Physiol.* 39:619–627.

T. A. McMahon and P. R. Greene. 1978. Fast running tracks. *Scientific American* 239:148–163.

T. A. McMahon and P. R. Greene. 1979. The influence of track compliance on running. *J. Biomechanics* 12:893–904.

T. A. McMahon. 1985. The role of compliance in mammalian running gaits. *J. Exp. Biol.* 115:263–282.

T. A. McMahon, G. Valiant, and E. C. Frederick. 1986. Groucho running. *J. Appl. Physiol.* 62:2326–2337.

H. Miura, I. Shimoyama. 1984. Dynamic walk of a biped. *International J. Robotics Research* 3:60–74.

M. H. Raibert. 1986. *Legged Robots That Balance.* MIT Press.

I. E. Sutherland, M. K. Ullner. 1984. Footprints in the asphalt. *International J. Robotics Research* 3:29–36.

M. Russel. 1983. ODEX I: The first functionoid. *Robotic Age.* 5(5):12–18.

C. R. Taylor, N. C. Heglund, and G. M. O. Maloiy. 1982. Energetics and mechanics of terrestrial locomotion: I. Metabolic energy consumption as a function of speed and body size in birds and mammals. *J. exp Biol.*. 97:1-21.

K. J. Waldron, V. J. Vohnout, A. Pery, and R. B. McGhee. 1984. Configuration design of the adaptive suspension vehicle. *International J. Robotics Research* 3:37–48.

This empty page was substituted for a blank page in the original document.

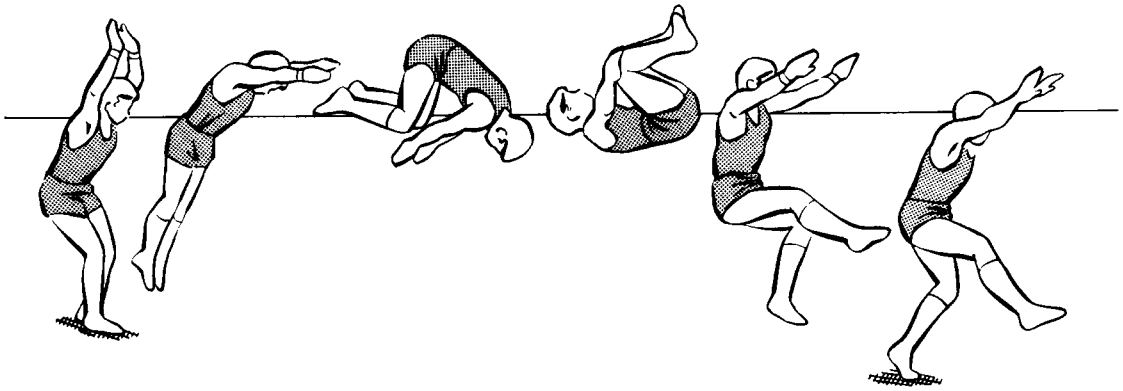

Figure 5–1: Forward flip as performed by a human gymnast. Drawings reprinted from Tonry (1983).

to do a flip in the laboratory. To perform the flip the biped machine runs forward, thrusts with both legs to jump while pitching the body forward, shortens the legs to tuck once airborne, untucks in time to land on the feet, and then continues running. To develop this program of action, we modified three steps in an otherwise normal sequence of steps. At particular points during the three steps the control system initiated the actions required for the maneuver, such as bringing the legs together, tucking the legs, etc. The timing and pattern of some actions, like accelerating the body about the pitch axis, were provided by prespecified parameters. In most cases, the algorithms normally used to control running speed, balance, and body attitude remained in effect, provided they did not interfere with producing the maneuver. Figure 5–2 is a photograph of the biped taken during a successful flip.

We studied the flip because it exemplifies a class of maneuvers that have significant dynamic content and incorporate extended ballistic phases. The high-jump and baseball pitch are additional examples. The control system responsible for such maneuvers must take action in anticipation of the ballistic phase, because linear and angular momentum can not be manipulated once the ballistic phase begins. This situation increases the need for an overall plan or strategy for producing the maneuver. A strategy can establish initial conditions for the ballistic phase that will result in the desired ballistic behavior by arranging the events that lead up to the ballistic phase.

In implementing the flip we have begun to test the *motor tape model*, a concept of how animals might produce, store, and modify patterned movement. The motor tape model likens the issuing of neural commands to the playing of a multi-channel tape recorder, with output signals connected directly to actuators (Evarts et al. 1970). We wanted to develop the motor tape model, and to see if such a mechanism could be used to produce maneuvers. Although we did not use a pure implementation of the motor tape model, we found that prespecified patterns of actuator output signals could be used to produce flips with a good degree of reliability, when used in conjunction with more conventional algorithms that provided attitude control and balance. Finally, we found working on flips to be lots of fun.

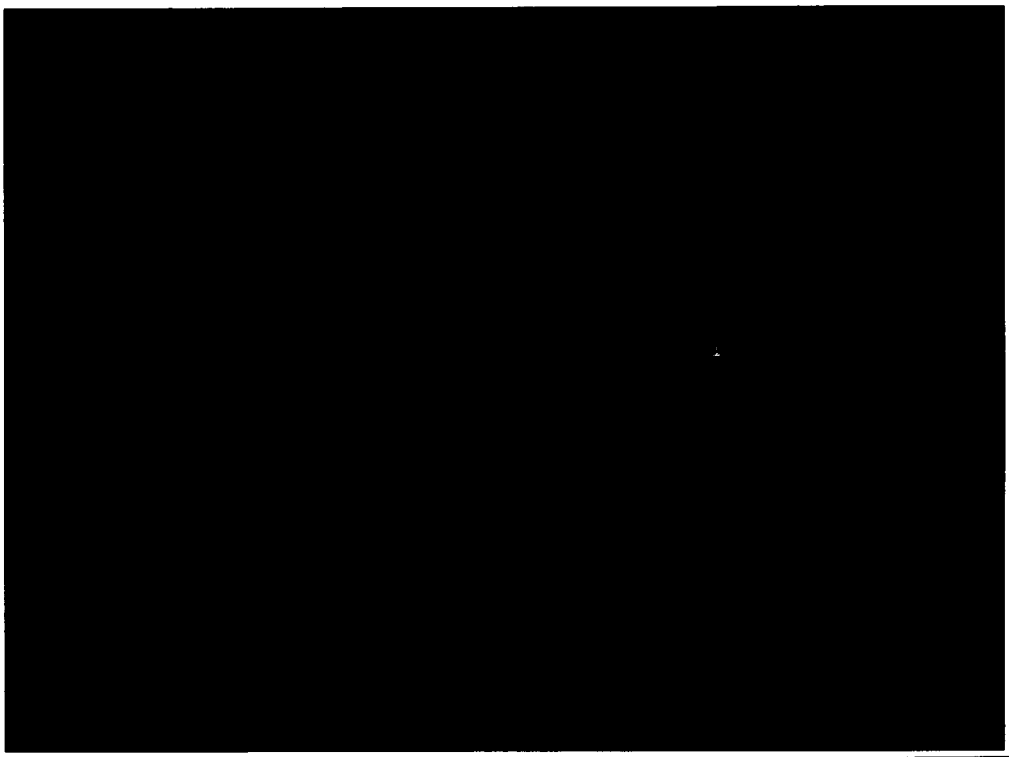

Figure 5–2: Photograph of planar biped doing a flip. Lines indicate the path of a foot and the flashes are synchronized with liftoff, the highest altitude of the body during flight, and touchdown. The machine was running from right to left.

5.3 Mechanics of the Flip

The planar biped running machine used for the project is shown in figure 5–3. It has two telescoping legs connected to a body by pivot joints that form hips. Each hip has a hydraulic actuator that positions the leg fore and aft. A hydraulic actuator within each leg acts along the leg axis to change the length of the leg, while an air spring makes the leg compliant in the axial direction. The overall motion of the biped is constrained to a plane by a tether mechanism that allows it to move fore and aft, up and down, and to rotate about the pitch axis. The biped running machine is described more fully in Hodgins, Koechling, and Raibert (1985).

A flip is a maneuver in which the body and legs rotate through one or more full rotations during the flight phase. The control must ensure that the system neither over-rotates nor under-rotates. A basic equation governing the behavior of the body during the flight phase of a flip is

$$n\pi = \frac{\dot{\phi}\dot{z}}{g}, \tag{5.1}$$

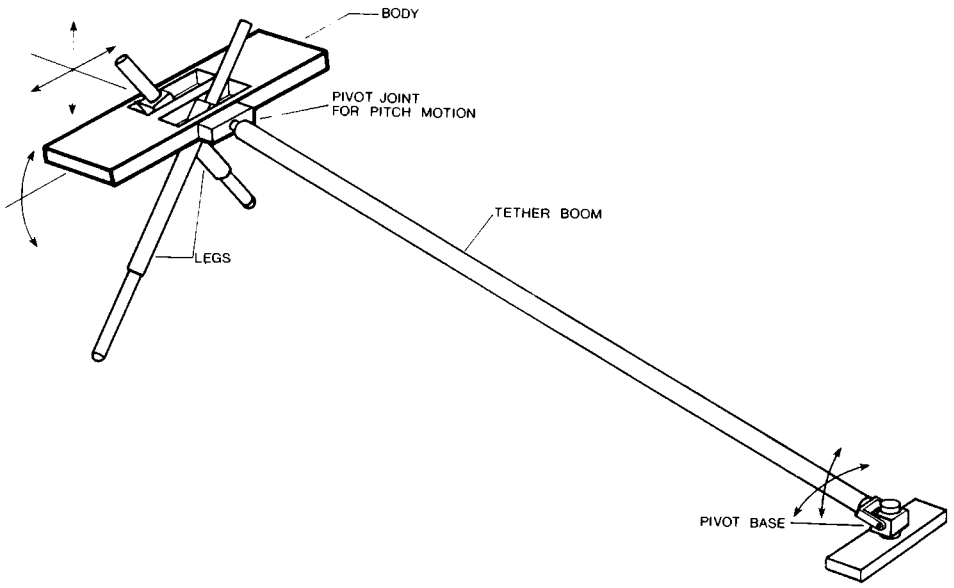

Figure 5–3: Diagram of planar biped used for experiments. The machine travels by running on a 2.5 m radius circle on the laboratory floor. The body is an aluminum frame on which are mounted actuators, hydraulic accumulators, and computer interface electronics. The hip is driven fore and aft by two low-friction hydraulic actuators. Actuators within the legs change the leg lengths and air springs make the legs springy in the axial direction. Onboard accumulators on the hydraulic supply and return lines increase the instantaneous actuator rate. Sensors on the machine measure the lengths of the legs and air springs, the positions and velocities of the hydraulic hip actuators, and contact between each foot and the floor. A tether mechanism constrains the body to move with three degrees of freedom—fore and aft, up and down, and pitch rotation. Sensors on the tether mechanism measure vertical displacement of the body, forward displacement, and pitch rotation. The tether also supports an umbilical cable that carries hydraulic connections, electrical power, and a connection to the control computer. See Hodgins, Koechling, and Raibert (1985) for more details.

where

- n is the number of full pitch rotations of the body,
- $\dot{\phi}$ is the pitch rate of the body,
- $\dot{z}$ is the vertical velocity of the body at the beginning of the flight phase, and
- g is the acceleration of gravity.

Equation (5.1) relates the vertical velocity of the body to its angular velocity. For n full rotations of the body during the flight phase, the rate of body pitch rotation $\dot{\phi}$, times the duration of the flight phase $2\dot{z}/g$, equals the angular displacement of the body $2n\pi$.

Equation (5.1) relies on several simplifying assumptions. We assume that the legs do not swing with respect to the body during the flight phase, so $\dot{\phi}$ represents the angular rates of both the body and the legs. We further assume that the pitch angle of the body is zero at both liftoff and touchdown, that the altitude of the body is the same at liftoff as it is at touchdown, and that there is negligible rotational friction from the pivot at the end of the boom or wind resistance and, therefore, constant angular momentum during flight.

For (1) we also assume the pitch rate of the system is constant during the flip. Actually, angular rate may change even though angular momentum is constant. For instance, humans reduce their moment of inertia to increase their rotation rate by tucking the arms and legs in close to their bodies. Tucking reduces the moment of inertia by concentrating the masses nearer to the center of mass of the system than when untucked. The ice skater's spin is a dramatic demonstration of this phenomena.

If the angular rate and moment of inertia of the system in the untucked configuration are $\dot{\phi}_1$ and J_1, and the moment of inertia in the tucked configuration is J_2, then conservation of angular momentum requires the angular rate in the tucked configuration to be $\dot{\phi}_2 = (J_1/J_2)\dot{\phi}_1$. The planar biped tucks† by shortening its legs to minimum length during the flight phase. To justify the assumption of constant angular rate during the flip, we further assume that the system tucks instantaneously just after the feet leave the ground, liftoff, and that it untucks instantaneously just before the feet touch the ground, touchdown. This simplification results in constant pitch rate during the flight phase of a flip. Later in the paper we relax this assumption by considering the case of slower tucking and untucking.

Frohlich (1979; 1980) points out in his elegant papers on the physics of diving that a system with several masses can change orientation and angular rate without any angular momentum. This is done by windmilling the arms, peddling the legs, or folding the joints of the body in one sequence and unfolding the body in another sequence. Such configuration effects are not considered here.

Flip Strategies

Equation (5.1) shows a direct trade-off between the pitch rate and vertical rate of the body at liftoff. If the control system increases the vertical rate at liftoff, then a lower pitch rate is needed to rotate the body around in time for landing, and vice versa. The values at liftoff are important because the ballistic nature of the task makes liftoff the last moment the control system can affect either the linear or angular momentum until the next landing. The vertical velocity of the body determines the altitude and the duration of the flight phase, whereas the angular rate determines how far around the body will rotate during that time. The control system must ensure that the system does not over-rotate or under-rotate if it is to continue balanced running. This trade-off between vertical velocity and angular velocity suggests three strategies for producing a flip.

One strategy is to maximize the vertical velocity while adjusting the body pitch rate to provide the correct amount of rotation in the available time. Gymnastics coaches seem to teach this strategy to humans learning the forward flip. The second strategy is to maximize the body pitch rate while adjusting the vertical velocity to produce a flight phase that takes the correct amount of time. The third strategy is to compromise on both angular

† In describing the actions of the biped running machine we use the terminology of gymnastics. When the biped *tucks* it reduces its moment of inertia by shortening its legs. When it *throws* the body a hip torque is applied that increases the body's rotation rate. In using gymnastic terminology we do not mean to suggest too strong an analogy between the planar biped and a human. The human versions of each of these actions and the human's physical system itself are substantially richer and more elaborate than the planar biped versions we describe here. Moreover, we may find that the suggested functional analogies are not correct.

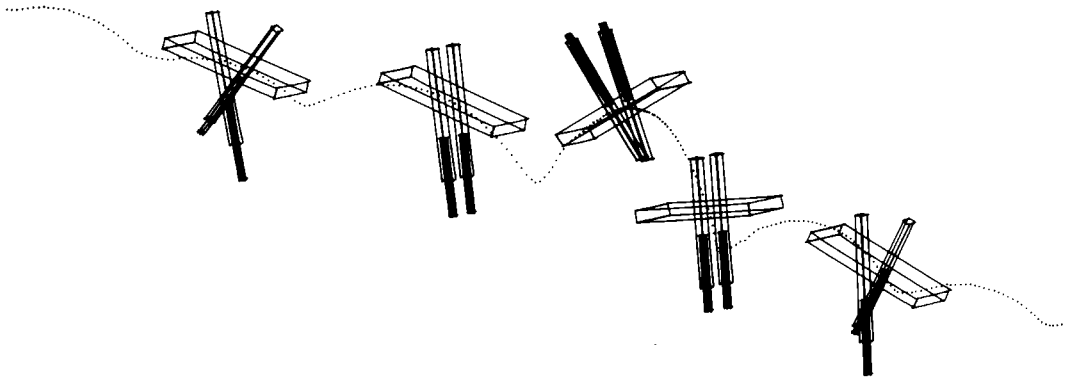

Figure 5–4: Drawing of planar biped doing a forward flip. The machine was running from left to right. 1) Approach with normal alternating gait, 2) hurdle step to gain altitude and bring the legs together for double support, 3) the body has accelerated forward to initiate the flip and the legs have shortened to increase pitch rate, 4) landing step reduces pitch rate and vertical rate, and 5) resume normal alternating gait. The body configurations are from data recorded from the physical biped during a flip. The dots indicate the path of the center of mass at 12 ms intervals.

and vertical rates, perhaps by introducing an additional constraint on the maneuver or an optimization criterion. The control system we implemented uses the first of these three strategies—maximize flight duration and adjust pitch rate accordingly.

Angular Rate During Flip

Because a system doing a flip can have nonzero body pitch angle at both the beginning and end of the flight phase, the total required rotation of the body may deviate from the nominal one revolution that was used in (5.1). When the liftoff and touchdown pitch angles have the right sign—nose down at liftoff and nose up at touchdown—the distance the body must rotate is reduced. Equation (5.1) can be modified to incorporate this reduction in the required rotation angle, $\Delta\phi$. Another correction to (5.1) is required because the legs do not maintain a fixed orientation with respect to the body during flight. At liftoff the body has rotated into a nose down orientation, so the legs are near their extreme forward position with respect to the body. See figure 5–4. During the flip the legs are rotated forward over the top to place them near the back end of their travel. This rotation of the legs and conservation of angular momentum causes backward rotation of the body. We use the notation that when a leg is of length r its moment of inertia is given by $J_l(r)$. If we assume the legs reorient through an angle $\Delta\theta$ with respect to the body, that reorientation takes place when each leg has minimum length r_{min}, and that the body has moment of inertia J_b, then reorientation adds $2\Delta\theta J_l(r_{min})/J_b$ to the required rotation of the body. Modifying (5.1) to account for these factors, the basic flip equation becomes

$$\frac{\Delta\phi_{total}}{2} = n\pi + \frac{\phi_{td} - \phi_{lo}}{2} + \frac{\Delta\theta J_l(r_{min})}{J_b} = \frac{\dot{\phi}\dot{z}}{g}. \tag{5.2}$$

Parameter	Symbol	Value
Body mass	m_b	11.45 kg
Body moment of inertia	J_b	0.40 kg-m^2
Upper leg mass	m_{l1}	1.055 kg
Upper leg moment of inertia at COM	J_{l1}	0.0204 kg-m^2
Distance from hip to upper leg COM	r_1	0.0838 m
Lower leg mass	m_{l2}	0.608 kg
Lower leg moment of inertia at COM	J_{l2}	0.0237 kg-m^2
Distance from foot to lower leg COM	r_2	0.317 m
Min leg length	r_{min}	0.44 m
Max leg length	r_{max}	0.67 m
Min leg moment of inertia about hip	$J_l(r_{min})$	0.062 kg-m^2
Max leg moment of inertia about hip	$J_l(r_{max})$	0.126 kg-m^2

Table 5–1: Physical parameters of planar biped.

where ϕ_{lo} and ϕ_{td} are the body pitch angles at liftoff and touchdown, assuming positive values for nose down body pitch angle.

To compute the angular rate during the flip, we need to know the angular momentum of the system. The angular momentum of the system is the sum of the angular momenta of the body and legs. To simplify the analysis we make the approximation that the center of mass of the system remains located at the hip throughout all maneuvers.

The angular momentum of the legs at liftoff is a function of the configuration at liftoff and the forward and vertical speeds. During normal running the net angular momentum of the legs is small because the legs sweep out of phase—one moves forward while the other moves backward. In a flip, however, the legs move together as they sweep backward during stance, giving them substantial angular momentum. The planar biped has telescoping legs as shown in figure 5–3. Calculation of angular momentum for such legs is simple because the orientation and angular rate for all parts of the leg are determined by the hip-foot axis. The angular velocity of the stance leg is

$$\dot{\theta} = \frac{\dot{z}_f x_f - \dot{x}_f z_f}{x_f^2 + z_f^2}, \tag{5.3}$$

where x_f is the forward position of the foot with respect to the center of mass and z_f is the altitude of the foot with respect to the center of mass. The forward and vertical position of the center of mass are x and z. During stance when the foot is stationary on the ground $\dot{x}_f = -\dot{x}$ and $\dot{z}_f = -\dot{z}$. The kinematics of the planar biped are given in figure 5–5. The angular momentum of each leg at liftoff is

$$H_l = \dot{\theta} J_l(r), \tag{5.4}$$

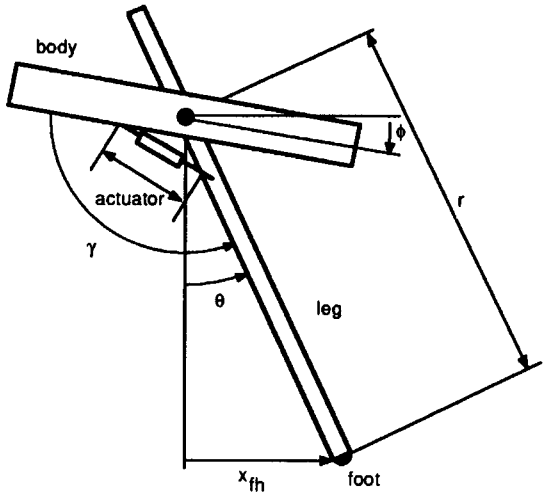

Figure 5–5: Kinematics of planar two-legged running machine. The length of the leg is r, the angle between the leg and vertical is θ and the pitch angle of the body is ϕ. $\theta = \gamma - \phi - 90$. The foot position relative to the hip, $x_{fh} = r \sin\theta$. The kinematics for the second leg are similar except that the hip actuator is attached to the other side of the body.

where the moment of inertia of each leg about the hip is

$$J_l(r) = J_{l1} + m_{l1} r_1^2 + J_{l2} + m_{l2}(r - r_2)^2. \tag{5.5}$$

J_{l1}, J_{l2}, m_{l1}, m_{l2}, r_1, and r_2 are physical parameters of the leg and are given in table 5–1. The angular momentum of the body is just $\dot{\phi} J_b$.

The pitch rate of the system once airborne can be found by equating the angular momentum just before liftoff and just after the tuck. If the legs have length r_{lo} just before liftoff, then the angular momentum of the system is

$$\dot{\phi}(J_b + 2J_l(r_{min})) = \dot{\phi}_{lo} J_b + 2\dot{\theta}_{lo} J_l(r_{lo}). \tag{5.6}$$

If the legs shorten immediately after liftoff to length r_{min} and do not swing with respect to the body, then the pitch rate after the tuck is

$$\dot{\phi} = \frac{\dot{\phi}_{lo} J_b + 2\dot{\theta}_{lo} J_l(r_{lo})}{J_b + 2J_l(r_{min})}. \tag{5.7}$$

Equation (5.7) provides a means of predicting the angular rate of the body during the flight phase, given the state of the system just before liftoff.

5.4 Control

To control flips we start with normal biped running and the control algorithms described in Hodgins, Koechling, and Raibert (1986). Briefly, the control system used for normal biped

Step	Action
Approach	Run forward at 2.5 m/s with alternating gait
Hurdle	Hop with maximum thrust Prepare to land on two legs Extend legs further forward than normal
Flip	Jump with maximum thrust Pitch body forward with large hip torque Shorten legs once airborne Lengthen and position both legs for landing
Landing	Hop with small or negative thrust Return pitch rate to zero and restore posture
Following	Resume running with alternating gait

Table 5–2: Summary of actions taken by the planar biped to do a flip.

running positions the legs during flight to regulate the forward running speed, thrusts axially with the stance leg to drive the up-and-down bouncing motion of the body, and exerts hip torque between the stance leg and the body to keep the body level. Using these algorithms the machine runs with an alternating gait that uses each leg for support, one at a time, with a flight phase separating each stance phase. The control actions needed for the flip are superimposed upon the normal running behavior produced by this set of control algorithms.

Three steps of the normal running sequence are modified to perform a flip. The three modified steps are the *hurdle step*, *flip step*, and *landing step*. The hurdle step is used to prepare for the maneuver by developing extra hopping height and by making a transition from the normal running gait that uses the legs in alternation, to the double support needed for the flip. The flip step uses both legs together to power the jump, and accelerates the body about the pitch axis for the actual rotating maneuver. The landing step dissipates the high angular and vertical rates and returns the system to the alternating gait. The activities that take place in these three steps are summarized in table 5–2, with additional detail given in the appendix. We now describe these three steps and how the control system uses them to generate a flip.

Maximum Jump Altitude

Earlier we suggested three possible strategies for establishing the trade-off between pitch velocity and vertical velocity. We decided to control the flip using the first strategy, which attempts to achieve a maximum vertical velocity and an intermediate pitch rate. The rationale for this decision was that it would be easier to remove excess vertical energy with a hard landing than it would be to remove excess angular energy. The large hip torque needed to remove angular energy might demand more traction than would be available, and we were unsure of the ability of the pitch control servo to correct large rate errors.

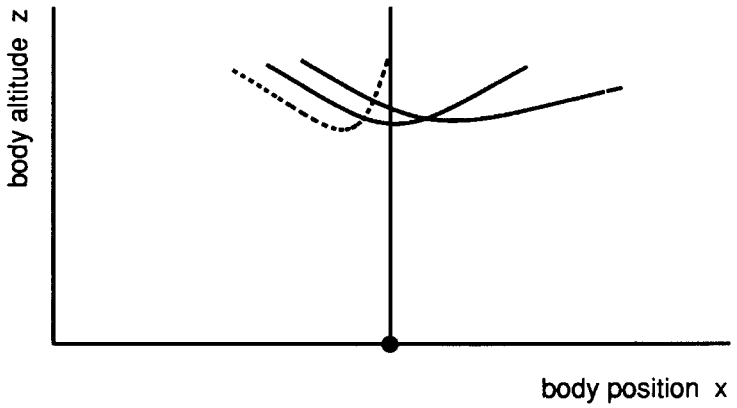

Figure 5–6: Trajectory of body for various foot positions. During normal running the foot is positioned so that the forward velocity of the body is the same at the end of the stance phase as it was at the beginning of the stance phase (solid line). During a flip the foot is extended forward to transfer some of the forward kinetic energy into vertical kinetic energy, thereby increasing the altitude of the flip and the time available to rotate the body (dotted line). It is also possible to convert vertical velocity into forward velocity, a procedure that can be used upon landing after the flip. For each trajectory shown in the plot, the foot is located at the solid circle (•). Adapted from Stentz (1983).

To get maximum altitude during the flip the control program does three things. It jumps high on the hurdle step to increase the vertical energy in the system, it converts forward speed into vertical speed by placing the foot further forward than normal on the landing just before the flip, and it delivers maximum thrust during the flip step.

The control system delivers maximum thrust to the leg on the hurdle step to increase the altitude that will be reached during the next flight phase. Since the legs are springy, they absorb a portion of the system's vertical energy on landing and then return the absorbed energy to help power the next flight. A hurdle step with increased altitude will result in a flip step with increased altitude as well. Gymnastics coaches for humans generally do not recommend a high hurdle step (George 1980).

Maximum thrust is developed during the hurdle step by setting the hydraulic servovalve that extends the leg to its maximum value as soon as the stance phase begins. On a normal step, thrust is delayed to the middle of stance, but thrusting throughout all of stance provides more time for the leg actuator to compress the leg spring and accelerate the body upward.

The second thing the control program does to maximize altitude is to convert some of the forward kinetic energy into vertical kinetic energy. This is done by extending the legs further forward than normal just before the stance phase of the flip step. In normal running, the control system positions the foot to leave the forward and vertical speeds of the body unchanged from one step to the next. The foot position that achieves this result is called the *neutral point* (Raibert 1986a). When the control system places the foot forward of the neutral point, the forward speed declines and the vertical speed increases as shown in figure 5–6.

If the foot were positioned to change the forward speed from $\dot{x}_a$ to $\dot{x}_b$ and if there were no mechanical losses in the leg, then the vertical velocity would increase from $\dot{z}_a$ to $\dot{z}_b = \sqrt{\dot{x}_a^2 - \dot{x}_b^2 + \dot{z}_a^2}$ and the duration of flight would increase by $2(\sqrt{\dot{x}_a^2 - \dot{x}_b^2 + \dot{z}_a^2} - \dot{z}_a)/g$. On a typical flip, $\dot{x}_a = 2.5$ m/s and $\dot{x}_b = 1.5$ m/s, so the flight phase could increase by 0.2 seconds if the leg were lossless. We have not measured how much this actually increases flight duration.

The third method of increasing altitude for the flip is to deliver maximum thrust on the flip step itself. During this step there are two legs in support, both of which thrust with maximum hydraulic servovalve settings from the beginning of the stance phase to the end.

Figure 5–7 shows data recorded from the sensors and actuators of the planar biped as it performed a forward flip. Examining these data, we find that an approach at 2.5 m/s, a hurdle step, and a two-legged jump resulted in a vertical velocity at liftoff of 3.4 m/s, an altitude of 1.04 m, and a flight time of about 0.67 s.

The description so far has centered on maximizing the duration of flight. Assuming this method produces a consistent duration of flight from one flip to the next, the task that remains is to provide one full rotation of the body in the time available. The next section addresses this task.

Desired Body Rotation

We implemented a simple control program for providing the correct amount of pitch rotation. The human operator chooses a running speed that gives the legs a certain angular momentum, the hip actuator throws the body to give it angular momentum, and once airborne, the legs shorten into a tuck to increase the angular pitch rate.

The angular momentum of the body is $\dot{\phi} J_b$. The body is given angular momentum by exerting a large nose-down pitch torque about the hip during the final part of the stance phase, just before the flip. This is called throwing the body. When a gymnast throws, he or she typically uses the arms, head, and trunk. The planar biped has no head or arms, so it is restricted to throwing the body. The control system uses two parameters to regulate how much throw the body is given. One parameter is the magnitude of pitch torque. The other parameter is a threshold for the pitch rate—when the pitch rate exceeds this value, the control system turns off the pitch torque. The actual pitch rate exceeds the threshold value by some amount, which we have found to be repeatable.

It is undesirable for the body to over-travel the limited motion of the hip joint during the period of throw. If the body runs out of travel and hits the mechanical stop before liftoff, the collision and resulting ground forces dissipate the angular momentum of the body. To avoid this the control system initiates the throw early enough so that the pitch rate reaches the threshold value at approximately the same time the feet leave the ground at the end of stance. The control system uses a third parameter to specify this delay.

Acceptable values for these three parameters—the delay for initiation of pitch torque, the magnitude of pitch torque, and the threshold pitch rate to terminate pitch torque—were determined empirically through a series of attempted flips. We started with zero delay, maximum pitch torque, and a very large pitch rate threshold. After about 20 attempts with

manual adjustment after each, we arrived at values that provided acceptable rotational behavior for a flip.

When the body reaches its peak altitude during the flight phase of the flip, the control system swings the legs part way forward to center the hip joints. As the body approaches the floor, the control system lengthens the legs to untuck for landing and orients the legs to position the feet. The vertical altitude of the body at which the control system begins to lengthen and orient the legs is specified by another parameter, which was adjusted manually throughout the course of attempting several flips. The leg orientation on landing is calculated as in normal running, where the goal is to provide balance and to control forward running speed.

For the flip shown in figure 5–7, the biped approaches with a forward running speed of about 2.5 m/s. After 36 ms of the stance phase of the flip step the control system sets the hip servovalve output signals to 85% of maximum. The hip servovalve is turned off when $\dot{\phi} = 7.85\,\text{rad/s}$ (450 deg/s). At liftoff the body has developed angular momentum $H_b = 3.9\,\text{kg-m}^2/\text{s}$ and each of the two legs has angular momentum $H_l = 0.42\,\text{kg-m}^2/\text{s}$. The total angular momentum at liftoff is $H = 4.7\,\text{kg-m}^2/\text{s}$. Once the system tucks, the total moment of inertia is $J = 0.52\,\text{kg-m}^2$ and the rotation rate is $\dot{\phi} = 9.97\,\text{rad/s}$ (571 deg/s). Equation (5.2) suggests a pitch rate of 9.92 rad/s for the measured values $\phi_{lo} = -0.40\,\text{rad}$, $\phi_{td} = 0.10\,\text{rad}$, and $\Delta\theta = 0.33\,\text{rad}$.

Once the system lands after the flip, the control system must eliminate the large vertical and angular energies that were needed for the flip. The control system reduces the vertical energy in two ways. It returns the desired forward running speed to the value used before the flip, converting some of the vertical kinetic energy back into forward kinetic energy. This accelerates the system forward while reducing the height of the next hop. The control program also specifies a smaller than usual leg thrust to absorb some of the vertical energy.

To return the body pitch angle and pitch rate to their normal values the control program exerts hip torques between both legs and the body using a linear PD servo:

$$\tau = -k_p(\phi - \phi_d) - k_v(\dot{\phi}), \tag{5.8}$$

where

τ	is the hip torque and
ϕ	is the pitch angle of the body,
ϕ_d	is the desired pitch angle of the body (level),
$\dot{\phi}$	is the pitch rate of the body, and
k_p, k_v	are gains.

This servo is the same mechanism that is used to maintain the body posture in normal running. After the landing step, the control program switches back to an alternating gait with the control algorithms for normal running.

Aerials

The front aerial is a variant of the flip. It differs from the flip in that the performer takes off from one leg rather than two, the legs are spread during the pitch rotation rather than

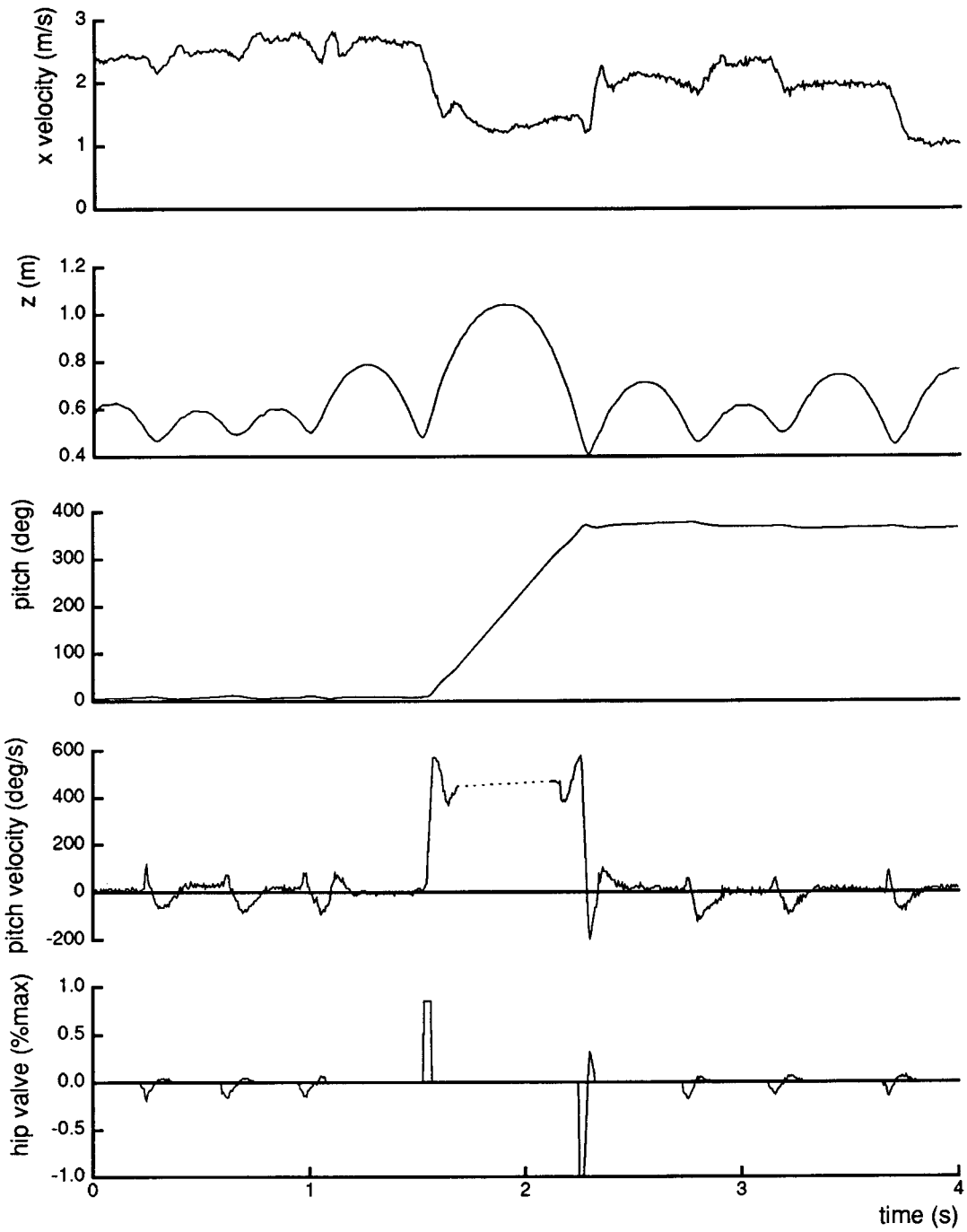

Figure 5–7: Data recorded during a biped flip. The top two curves show that forward speed is converted into vertical motion. The second graph shows that the flip step is the highest in the sequence. The bottom curves of pitch velocity and hip torque illustrate the inherent symmetry in the flip. Data recorded at 6 ms, the cycle time of the control system. (Data file TL.157.6)

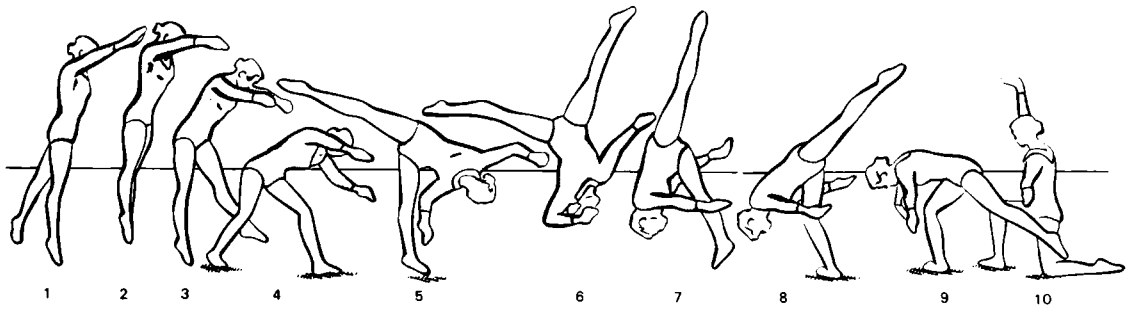

Figure 5–8: Aerial as performed by a human gymnast. Drawings reprinted from Tonry (1983).

kept together, and the landing takes place on one leg. See figure 5–8. For humans, an aerial is a variant of the cartwheel, except that the hands do not touch the ground. The aerial is considerably easier than a flip for humans, because humans can spread the legs a large amount to reduce the amount of body rotation needed during the flight phase.

For the biped, the aerial is more difficult than the flip. Just one leg is used to power the flight phase, so the duration of flight for an aerial is about 80% of that for a flip, 0.55 s vs. 0.67 s. The reduced flight time makes it difficult to get adequate rotation during the time available in the flight phase. On the other hand, there is no need to swing the legs forward during the flight phase, because the angles between the legs and the body at liftoff are already correct for landing. This reduces the amount the system has to rotate during flight by about 0.10 rad as compared to a flip.

The planar biped control program for aerials differs from that for the flip in only one important characteristic; both the body and the swing leg are thrown to develop angular momentum about the pitch axis. Because the legs move in opposite directions during the approach for an aerial, the net angular momentum of the legs is small. The stance leg sweeps backward while the swing leg sweeps forward. The control program throws the swing leg along with the body to increase the contribution of the legs to the angular momentum of the system. See figure 5–9. The procedure for throwing the body is the same as for the flip, but with just one hip actuator exerting torque. Examining the data shown in figure 5–10, we find that the leg thrown has angular momentum just before liftoff of $H_l = 0.6\,\text{kg-m}^2$. At that time the angular momentum for the stance leg is $H_l = 0.2\,\text{kg-m}^2$, for the body is $H_b = 3.7\,\text{kg-m}^2$, and for the total system is $H_{aerial} = 4.5\,\text{kg-m}^2$. The total is slightly less than for the flip $H_{flip} = 4.7\,\text{kg-m}^2$.

The planar biped executes aerials using the control sequence outlined in table 5–3. Data for one aerial are shown in figure 5–10. The machine has performed aerials successfully many times. In every case, however, the time available for rotation was so short that the control system could not orient the landing leg to properly position the foot for best stability on landing. The system kept its balance on landing, but with a noticeable reduction in forward running speed after the maneuver, as can be seen in the top curve of figure 5–10.

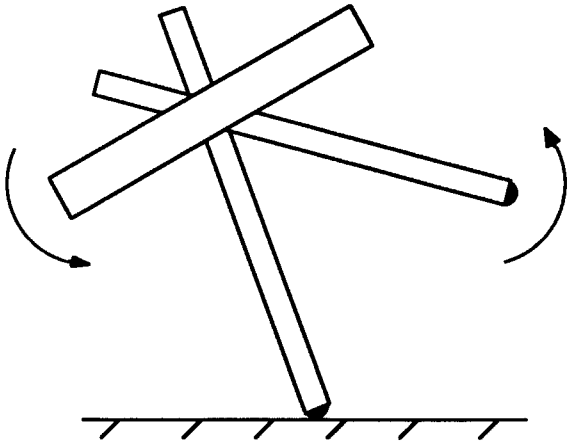

Figure 5–9: To develop angular momentum in the aerial the control system accelerates both the body and the swing leg in the same direction during the final part of the stance phase.

Step	Action
Approach	Run forward at 2.5 m/s with alternating gait
Hurdle	Hop with maximum thrust Extend leg further forward than normal
Aerial	Hop with maximum thrust Swing free leg backward Pitch body forward with large hip torque Shorten legs once airborne Lengthen and position forward leg for landing
Landing	Hop with small or negative thrust Return pitch rate to zero and restore posture
Following	Resume running with normal alternating gait

Table 5–3: Summary of actions taken by the planar biped to do an aerial.

Adjusting Pitch Rate During Flight

The control system we implemented for the biped flip makes no attempt to adjust pitch rate once the system is airborne. It keeps the legs tucked during most of the flight phase, resulting in constant moment of inertia and constant angular rate. The amount of rotation during the flight phase is a function of the system's state at liftoff.

It should be possible to control a flip more precisely by manipulating the rate of rotation during the flight phase. Because angular momentum must be conserved during the flight phase, the control system could manipulate the rate of rotation by changing the length

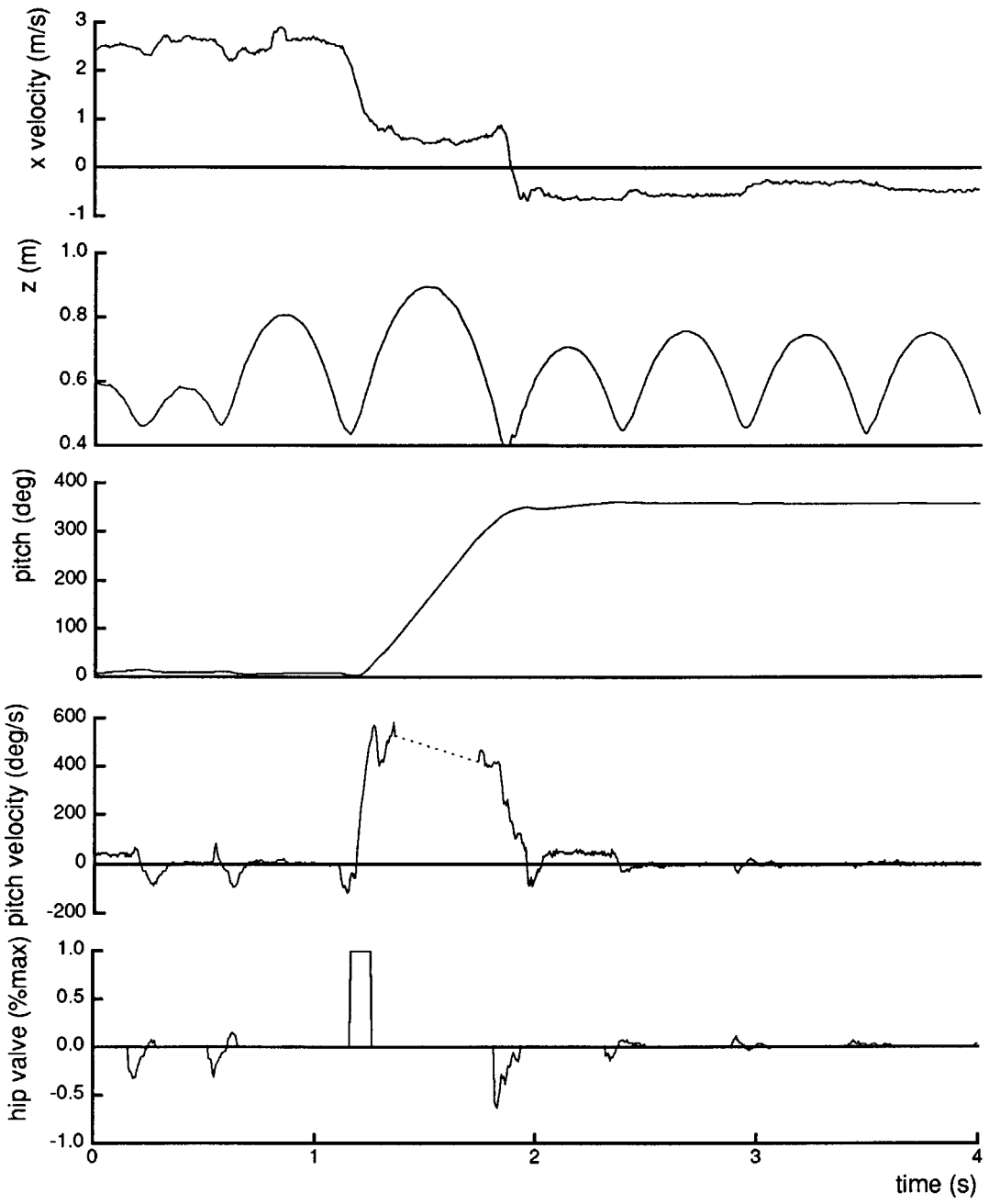

Figure 5–10: Data recorded during a biped aerial. The top curve of x velocity shows how the forward speed is converted to vertical motion, and how after the aerial the foot is not positioned well enough for the machine to continue traveling forward although it does continue running. The second graph shows that the aerial step is the highest in the sequence, although the difference between the hurdle step and the aerial step is not as dramatic as it was for the flip. (Data file TL.194.3)

and moment of inertia of the legs. To synchronize foot contact with full body rotation, the control system could measure the vertical position and rate of the body and rotational progress of the flip to determine the moment to untuck the legs.

A simplified model assumes that the legs lengthen instantaneously, resulting in just two rates of rotation. If $2J_l(r_{min}) + J_b$ is the moment of inertia of the system with the legs short and $2J_l(r_{max}) + J_b$ is the moment of inertia with the legs long, then to synchronize full rotation with the moment of landing the legs should lengthen when

$$\Delta\phi = \dot{\phi}\left(\frac{2J_l(r_{min}) + J_b}{2J_l(r_{max}) + J_b}\right)\left(\frac{\dot{z} + \sqrt{\dot{z}^2 + 2g(z - z_{td})}}{g}\right) \tag{5.9}$$

where

- $\Delta\phi$ is the remaining rotation required before landing,
- $\dot{\phi}$ is the angular rate of the body with the legs short,
- z is the vertical position of the body,
- z_{td} is the expected vertical position of the body at touch-down, and
- $\dot{z}$ is the vertical velocity.

The control system could evaluate (5.9) throughout the flight phase of the flip to determine when the legs should lengthen to reduce the rotation rate.

Equation (5.9) depends on the ability to lengthen the legs in zero time. For the planar biped, the maximum rate at which the legs can lengthen is determined by the maximum rate at which oil can flow through the hydraulic servovalves, which is a system constant. Equation (5.9) can be modified to accommodate such a fixed rate of leg lengthening.

We start by determining how far the body rotates when the legs are lengthened at a fixed rate. Suppose the legs change length from r_a to r_b at a fixed rate $\dot{r}_k$. Define t_a and t_b so that $r(t_a) = r_a$ and $r(t_b) = r_b$. If the pitch rate is initially $\dot{\phi}_a = \dot{\phi}(t_a)$, then the angular rate during leg lengthening is a function of leg length

$$\dot{\phi}(t) = \dot{\phi}_a\left(\frac{2J_l(r_a) + J_b}{2J_l(r) + J_b}\right). \tag{5.10}$$

Substituting for $r = r_a + (t - t_a)\dot{r}_k$ and integrating we determine how much ϕ changes during lengthening

$$\begin{aligned}\Delta\phi' &= \int_{t_a}^{t_b} \frac{\dot{\phi}_{lo}(2J_l(r_b) + J_b)}{2J_l(r_a + (t - t_a)\dot{r}_k) + J_b} dt \\ &= \frac{a}{\dot{r}_k b}\left\{\arctan\left(\frac{r_b - r_2}{b}\right) - \arctan\left(\frac{r_a - r_2}{b}\right)\right\},\end{aligned} \tag{5.11}$$

where $J_l(r)$ is defined in (5.5), r_2 and m_{l2} are constants defined in table 5–1, and

$$a = -\frac{\dot{\phi}_{lo}(J_b + 2J_l(r_b))}{2m_{l2}}$$

$$b = \sqrt{(r_b - r_2)^2 - \frac{J_b + 2J_l(r_b)}{2m_{l2}}}.$$

We can now solve for the state of the system to begin untucking at constant rate. If the legs are length r_a during the tucked part of a flip, then they should lengthen to r_b at rate $\dot{r}_k$ when

$$\Delta\phi = \dot{\phi}\left(\frac{2J_l(r_a) + J_b}{2J_l(r_b) + J_b}\right)\left(\frac{\dot{z} + \sqrt{\dot{z}^2 + 2g(z - z_{td})}}{g} - t_b + t_a\right) + \frac{a}{\dot{r}_k b}\left\{\arctan\left(\frac{r_b - r_2}{b}\right) - \arctan\left(\frac{r_a - r_2}{b}\right)\right\}. \tag{5.12}$$

5.5 Discussion

Symmetry of the Flip

The locomotion algorithms that are normally used to generate running in the planar biped are based on a principle of control called *running symmetry* (Raibert 1986b). This principle was useful in the design phase of the biped flip. The basic idea of symmetry is that a legged system will travel in steady state when the accelerations it experiences have odd symmetry during each stride. Odd functions integrate to zero over appropriate limits, resulting in no net change in running speed or in posture. For a legged system to run with symmetry throughout a series of steps, the vertical and angular velocities of the body must be coordinated during the flight phases. In normal running the constraint is

$$\frac{\phi}{\dot{\phi}} = \frac{\dot{z}}{g} \tag{5.13}$$

assuming constant angular rate during flight. An implication of (5.13) is that the pitch angle of the body at the end of the flight phase is equal and opposite to the pitch angle at the beginning of the flight phase $\phi_{td} = -\phi_{lo}$. Despite temporary but radical departures from the steady state, the flip and aerial conform to these symmetries.

For flips and aerials (5.13) becomes

$$\frac{\phi + n\pi}{\dot{\phi}} = \frac{\dot{z}}{g}, \tag{5.14}$$

which is related to (5.1) and (5.2). Equation (5.14) implies the same constraint as does (5.13), but with n additional full rotations of the body during flight. See figure 5–11. Reorientation of the legs with respect to the body during flight is ignored here, but the nonzero pitch angles at liftoff and touchdown are included. The torque exerted at the hip

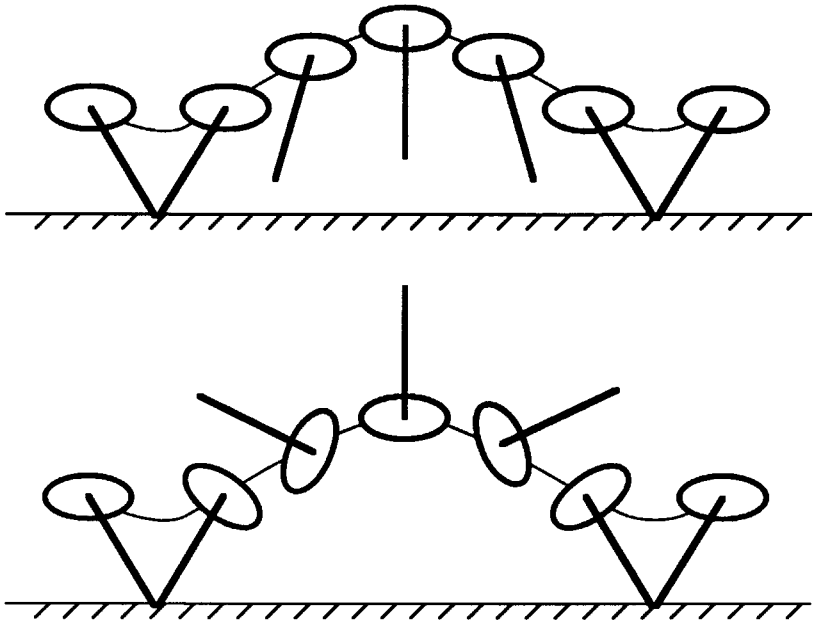

Figure 5–11: Diagram of symmetric behavior during the flight phase for a normal step and for a flip. In both cases the forward displacement and pitch angle of the body are described by odd functions of time, and the altitude of the body is described by an even function of time.

to accelerate the body about the pitch axis to start the flip forms a symmetric pair with the torque exerted at the hip to decelerate the body upon landing—they exhibit the odd actuator symmetry characterized in the theory. The bottom curves in figures 5–7 and 5–10 illustrate this symmetry.

Recognition that flips, too, should conform to symmetry helped us to reason through the design of the flip control programs and to generalize our understanding of symmetry. For instance, at first we worried about getting adequate traction after the flip to dissipate the large angular momentum. Symmetry considerations permitted us to see that if there were adequate traction at liftoff to generate the angular momentum in the first place, then there should be adequate traction at touchdown to dissipate the angular momentum. A similar consideration was useful in reasoning about the vertical motion.

Open-loop Control

The flip and aerial belong to a class of movements that are dynamic and ballistic. Other members of the class are those that occur in tumbling, diving, and high jumping. These movements are dynamic in that speed and kinetic energy are significant factors in their production. The movements are ballistic in that there are intervals during which the actuators cease to have any direct influence on the key variables of the task. For instance, during the flight phase of a flip no actuator can change the altitude, vertical rate, or an-

gular momentum of the system. In contrast, for the task of making a manipulator move along a trajectory, there is a separate motor to drive the motion of each joint directly and continuously.

Another attribute of these tasks is that outside disturbance plays a relatively minor role. The environment for the movement is essentially unchanging during and between movements, changing only slightly from one repetition to the next. If the initial conditions are precisely established and if the same forces are exerted by each actuator on each repetition, then the behavior repeats in nearly identical form time after time. Sensing and feedback are important in executing such tasks, but in a less direct role than the inner loop of a high bandwidth servomechanism. At the same time, prespecified feedforward control signals can play a more important role in such behavior.

The approach we have taken to control flips and aerials relies on the repeatability of the system, on constancy of the environment, and on repeatably establishing the initial conditions for the movement. These features allow the use of a rather inflexible open-loop actuation pattern to produce the behavior. For instance, to accelerate the pitch rotation of the body the control system waits 36 ms after the start of the flip step, sets the output signal for the hip servovalves to 85% of maximum, waits until the pitch rate reaches 7.85 rad/s, and then turns the hip servovalves off. This control is not devoid of feedback, however, feedback is used sparingly. It uses the pitch rate to determine when to stop throwing the body, and it uses the underlying running pattern to synchronize each flip action to the behavior of the machine.

The control system we implemented for flips is somewhat like a multichannel tape recorder, with the output signal from each channel wired directly to one actuator. To begin a movement the control system establishes the initial conditions for the movement and "it presses the play button" on the tape recorder. In the biological context, this model of motor control has been called the *motor tape* (Evarts et al. 1971). It is thought that under certain circumstances the nervous system may produce patterned behavior, not through sensors and high-gain feedback loops, but by issuing sequences of open-loop commands that go directly to the muscles. In the pure form of the model, commands would be issued independent of progress in executing the movement. One can also imagine learning complicated patterns of motion by editing short segments of motor tape together. It is not known whether the motor tape accurately models biological motor mechanisms.

The flip implementation described in this paper does not embody a pure form of the motor tape model. The implementation is like the motor tape in that it uses sequences of motor commands that are issued directly to the actuators, without a local servo. The magnitude of actuator signals for thrust in the hurdle and flip steps and the throw delay and magnitude are specified in this manner. The flip control system is unlike the motor tape in that the timing of control actions is synchronized to events in the locomotion cycle, and thereby, to the progress of the movement. For example, the maximum vertical thrust does not begin until the normal locomotion control algorithm has entered stance. The starting time and magnitude of hip torque for pitch acceleration are determined with a fixed sequence like the motor tape, but hip torque is terminated when pitch rate reaches a desired value. One could obtain a more systematic study of the motor tape model by comparing

maneuvers produced by several implementations: a pure motor tape implementation of a maneuver, a trajectory servoed implementation, and an intermediate implementation like the one described here.

The use of feedforward without high bandwidth feedback is not new. It is used to send spacecraft to the moon, Mars, and beyond. At a predetermined moment the engines ignite for a predetermined period to take the craft out of Earth orbit and send it toward the remote rendezvous. In space travel there is no attempt to adjust thrust continuously throughout the trip to stay exactly on course with precisely the desired speed, because such an approach would require far too much energy. Occasional adjustments are made instead.

There are two characteristics of space travel that make this approach feasible. First, unexpected external disturbances are minimal. Second, variability in the actuators and internal mechanism is small. These conditions imply that for the same initial conditions and the same actuator output signals, the actual behavior of the system is very nearly the expected behavior and that behavior of the system will reliably repeat on successive executions. These conditions apply to the maneuvers described in this paper.

Where do the Feedforward Control Signals Come From?

Given a task and strategy, the feedforward signal needed to accomplish the task must be found. The feedforward signal can be found using analytical or empirical techniques. The analytical technique is to calculate the feedforward signal from models of the mechanism and the task. For instance, to calculate the feedforward signals for the biped flip described earlier, one might:

1. model the running machine, including its springy legs, hydraulic actuators, and hydraulic power supply, to calculate the maximum attainable vertical velocity of the body.
2. find the appropriate pitch rate using equation (5.2).
3. calculate the forward running speed and the pitch rate of the body required before liftoff using a model of the body and legs.
4. calculate the hip torque needed during stance to develop the desired pitch rate using a model of the body and legs.
5. calculate the output signal that will provide the desired torque using a model of the actuator.

Once again, this approach clearly depends on an a priori specification of the general form of the solution, the strategy. In the case of a flip, the strategy includes the decision to maximize flight time and to adjust body pitch rate accordingly, as well as many other details.

The empirical approach to finding the feedforward signals uses data obtained by attempting to perform the task—learning. Rather than use a model of the system to determine the maximum attainable vertical velocity, the physical system itself is used to make the measurement. Output is applied, the behavior is measured, and the output is ad-

justed accordingly. The nature of such adjustment and the effectiveness of the results is a long-standing problem.

For both of these approaches, the analytic and the empirical, there is the separate question of what role humans or other outside agents play in the process, as opposed to an automated process. A human could go through the steps described to calculate the control signal from the model, or the control system itself could incorporate these calculations for control. For the empirical approach, a human can look at the results of attempts to do a maneuver and adjust the output for the next try, as we did for the flip and aerial, or the control system could make the adjustment. In the experiments reported in this paper the empirical approach was used and all adjustments were made by humans.

Formulating Strategies

We have described the specific control used to make the biped running machine do forward flips and aerials. The essential features of the approach are a strategy for executing the flip and a set of low-level actions and parameters that implement the strategy. The strategy we chose is based on several decisions:

- Maximize time of flight, with pitch rate adjusted accordingly.
- Extend the legs forward on the flip step to convert forward speed into vertical speed.
- Adjust the start of pitching torque to synchronize the end of hip travel with liftoff.
- Shorten the legs during flight to increase pitch rate.
- Reduce thrust to absorb vertical energy on landing.
- Use normal attitude control algorithm to absorb angular energy on landing.

Each of these decisions was made by humans based on knowledge of the mechanics of the problem and intuition. It is not difficult to imagine that future control systems may be able to formulate strategies such as these automatically. Such systems will embody a model of the mechanical system to be controlled, a working knowledge of the physics that govern behavior of the model, and an ability to reason. Heuristics and optimizations may be important. The need for techniques that bridge the gap between the task level of a motor act and the actuator control level is a deep and important problem.

If strategies for performance of a task were found automatically, optimal behavior might be easier to find. A given strategy for performing a particular task may not be the only or the best strategy, and it may be difficult to know if a better strategy exists. Richard Fosbury demonstrated this point in 1968 when he introduced a previously unknown form for doing the high jump, the *Fosbury Flop*, in which the jumper goes over face-up rather than face down. Fosbury won an Olympic gold medal in 1968, and Dwight Stones used the Fosbury Flop to set a new high jump world record of $7'7\frac{1}{4}''$ in 1974 (Doherty 1976). Strategy design is crucial for executing maneuvers. Automated techniques may some day permit us to find all possible strategies for a task, and to identify the best possible solution.

5.6 References

Doherty, J. K. 1976. *Track and Field Omnibook* Los Altos, CA: Tafnews Press.

Evarts, E. V., Bizzi, E., Burk, R. E., Delong, M., Thach, W. T., Jr. 1971. Central control of movement. *Neurosciences Research Progress Bulletin* 9.

Frohlich, C. 1979. Do springboard divers violate angular momentum conservation? *American Journal of Physics* 47:583–592.

Frohlich, C. 1980. The physics of somersaulting and twisting. *Scientific American* 242:154–164.

George, G. S. 1980. *Biomechanics of Women's Gymnastics* Englewood Cliffs, NJ: Prentice-Hall Inc.

Hodgins, J., Koechling, J., Raibert, M. H. 1986. Running experiments with a planar biped. *Third International Symposium on Robotics Research*, Cambridge: MIT Press, pp.349–355.

Raibert, M. H. 1986a. *Legged Robots That Balance* Cambridge: MIT Press.

Raibert, M. H., 1986b. Running with symmetry. *Int. J. of Robotics Research* 5(4):3-19.

Stentz, A. 1983. Behavior during stance. *Dynamically Stable Legged Locomotion—Third Annual Report*, M. H. Raibert et al. CMU-RI-TR-83-20. Pittsburgh, PA: Robotics Institute, Carnegie-Mellon University, pp. 106–110.

Tonry, D. 1983. *Tumbling* New York: Harper & Row.

5.7 Appendix A: Details of Control Sequence for Flip

State	Trigger Event	Action	Flip Action
Approach			
LOADING 110	Leg 1 touches ground	Hold leg 1 at landing length Zero hip torque leg 1 Keep leg 2 short Don't move hip 2	
COMPRESSION 120	Leg 1 air spring shortened	Hold leg 1 at landing length Erect body with hip 1 Keep leg 2 short Position leg 2 for landing	
THRUST 130	Leg 1 air spring lengthening	Extend leg 1 Erect body with hip 1 Keep leg 2 short Position leg 2 for landing	
UNLOADING 140	Leg 1 air spring near full length	Shorten leg 1 Zero hip torque leg 1 Keep leg 2 short Position leg 2 for landing	
FLIGHT 150	Leg 1 not touching ground	Shorten leg 1 Don't move hip 1 Lengthen leg 2 for landing Position leg 2 for landing	
Hurdle Step			
LOADING 1210	Leg 2 touches ground	Keep leg 1 short Don't move hip 1 Hold leg 2 at landing length Zero hip torque leg 2	
COMPRESSION 1220	Leg 2 air spring shortened	Keep leg 1 short Position leg 1 for landing † Erect body with hip 2	Reduce desired speed Max thrust: leg 2
THRUST 1230	Leg 2 air spring lengthening	Keep leg 1 short Position leg 1 for landing Erect body with hip 2	Max thrust: leg 2
UNLOADING 1240	Leg 2 air spring near full length	Keep leg 1 short Position leg 1 for landing Shorten leg 2 Zero hip torque leg 2	
FLIGHT 1250	Leg 2 not touching ground	Lengthen both legs for landing Position both legs for landing	

—Continued—

† Expected T_s is adjusted by a factor of $1/\sqrt{2}$ to account for two legs in support during the flip step.

State	Trigger Event	Action	Flip Action
Flip Step			
LOADING 2110	Both legs touch ground	Hold both legs at landing length	
			Zero both hip torques
COMPRESSION 2120	Both air springs shortened		Max thrust: both legs Zero both hip torques
THRUST 2130	Compression + delay (36 ms)		Max thrust: both legs Exert large pitch torque: both legs (85% of max)
THRUST 2131	Pitch velocity > desired pitch velocity (7.85 rad/s)		Max thrust: both legs Zero both hip torques
UNLOADING 2140	Both air springs near full length	Shorten both legs Zero both hip torques	
FLIGHT A 2150	Both legs not touching ground		Shorten both legs Don't move either hip
FLIGHT B 2151	Vertical velocity zero		Keep both legs short Center both hips
FLIGHT C 2152	Body altitude < threshold (.7 m)	Lengthen both legs for landing Position both legs for landing †	
Landing Step			
LOADING 3210	Both legs touch ground	Hold both legs at landing length Zero both hip torques	
COMPRESSION 3220	Both air springs shortened	Keep both legs at landing length Erect body: both hips	
THRUST 3230	Both air springs lengthening	Erect body: both hips	Reduced thrust: both legs
UNLOADING 3240	Both air springs near full length	Shorten both legs Zero both hip torques	
Resume normal running			

† Expected T_s is adjusted by a factor of $1/\sqrt{2}$ to account for two legs in support during the flip step.

5.8 Appendix B: Details of Control Sequence for Aerial

State	Trigger Event	Action	Aerial Action
Approach			
LOADING 110	Leg 1 touches ground	Hold leg 1 at landing length Zero hip torque leg 1 Keep leg 2 short Don't move hip 2	
COMPRESSION 120	Leg 1 air spring shortened	Hold leg 1 at landing length Erect body with hip 1 Keep leg 2 short Position leg 2 for landing	
THRUST 130	Leg 1 air spring lengthening	Extend leg 1 Erect body with hip 1 Keep leg 2 short Position leg 2 for landing	
UNLOADING 140	Leg 1 air spring near full length	Shorten leg 1 Zero hip torque leg 1 Keep leg 2 short Position leg 2 for landing	
FLIGHT 150	Leg 1 not touching ground	Shorten leg 1 Don't move hip 1 Lengthen leg 2 for landing Position leg 2 for landing	
Hurdle Step			
LOADING 1210	Leg 2 touches ground	Keep leg 1 short Don't move hip 1 Hold leg 2 at landing length Zero hip torque leg 2	
COMPRESSION 1220	Leg 2 air spring shortened	Keep leg 1 short Position leg 1 for landing Erect body with hip 2	Reduce desired speed Maximum thrust: leg 2
THRUST 1230	Leg 2 air spring lengthening	Keep leg 1 short Position leg 1 for landing Erect body with hip 2	Maximum thrust: leg 2
UNLOADING 1240	Leg 2 air spring near full length	Keep leg 1 short Position leg 1 for landing Shorten leg 2 Zero hip torque leg 2	
FLIGHT 1250	Leg 2 not touching ground	Lengthen both legs for landing Position both legs for landing	

—Continued—

State	Trigger Event	Action	Aerial Action
Aerial Step			
LOADING 2110	Leg 1 touches ground	Hold leg 1 at landing length Zero hip torque leg 1 Keep leg 2 short Don't move hip 2	
COMPRESSION 2120	Leg 1 air spring shortened	Keep leg 2 short	Maximum thrust: leg 1 Zero hip torque leg 1 Don't move hip 2
THRUST 2130	Compression + delay (36 ms)	Keep leg 2 short	Maximum thrust: leg 1 Exert large pitch torque: leg 1 (85% of maximum) Swing leg 2 backward
THRUST 2131	Pitch velocity > desired pitch velocity (7.85 rad/s)	Keep leg 2 short	Maximum thrust: leg 1 Zero hip torque: leg 1 Swing leg 2 backward
UNLOADING 2140	Leg 1 air spring near full length	Shorten leg 1 Zero hip torque leg 1 Keep leg 2 short	Swing leg 2 backwards
FLIGHT A 2150	Leg 1 not touching ground	Shorten leg 1 Don't move hip 1 Lengthen leg 2 for landing Position leg 2 for landing	
FLIGHT B 2151	Body altitude < threshold (.7 m)	Keep leg 1 short Don't move hip 1 Lengthen leg 2 for landing Position leg 2 for landing	
Landing Step			
LOADING 3210	Leg 2 touches ground	Keep leg 1 short Don't move hip 1 Hold leg 2 at landing length Zero hip torque leg 2	
COMPRESSION 3220	Leg 2 air spring shortened	Keep leg 1 short Position leg 1 for landing Erect body with hip 2 Hold leg 2 at landing length	
THRUST 3230	Leg 2 air spring lengthening	Keep leg 1 short Position leg 1 for landing Erect body with hip 2	Reduced thrust: leg 2
UNLOADING 3240	Leg 2 air spring near full length	Keep leg 1 short Position leg 1 for landing Shorten leg 2 Zero hip torque leg 2	
Resume normal running			

This empty page was substituted for a blank page in the original document.

Chapter 6

Quadruped Trotting, Pacing, and Bounding

Marc H. Raibert

6.1 Abstract

This chapter explores the quadruped running gaits that use the legs in pairs: the trot (diagonal pairs), the pace (lateral pairs), and the bound (front and rear pairs). Rather than study these gaits in quadruped animals, we studied them in a quadruped robot. We found that each of the gaits that use the legs in pairs can be transformed into a common underlying gait, a *virtual biped gait.* Once transformed, a single set of control algorithms produce all three gaits, with modest parameter variations between them. The control algorithms manipulated rebound height, running speed, and body attitude, while a low-level mechanism coordinated the behavior of the legs in each pair. The approach was tested with laboratory experiments on a four-legged robot. Data are presented that show the details of the running motion for the three gaits and for transitions from one gait to another. Estimates of the energetic cost of locomotion in the quadruped machine for each of the gaits are given in an appendix.

6.2 Introduction

Running animals have control systems that allow them to propel the body in the desired direction at the desired speed, while stabilizing the attitude and altitude. Unfortunately, the control of running is difficult to study directly in animals because of the richness of the biomechanics and of the nervous system involved.

Rather than attempt to study the control of running in animals, we explored the con-

trol of running in a legged robot. Programs executing on a digital computer were used to sense and actuate the behavior of the four-legged running machine shown in figure 6–1. During each experiment the control computer acquired data from the machine's sensors, accepted commands from a human operator, performed calculations according to control algorithms, and issued commands to the machine's actuators. In many cases the quadruped machine exhibited behavior that we describe as running, including trotting, pacing, bounding, pronking, and transitions between these gaits.

A specific goal of this work was to see if control algorithms used previously for one- and two-legged running robots could be generalized for four-legged running. A more general goal was to understand quadruped running as a problem in dynamic balance and control, and to evaluate the effectiveness of various algorithms. A third goal was to explore the interplay between the mechanical elements of a system that moves and the information processing elements that guide and stabilize the movement: How might they both contribute to the motions needed for locomotion?

The following section describes the approach we took to controlling the behavior of a quadruped machine to make it trot, pace, and bound. Subsequent sections describe the implementation that was used to test the control algorithms and present data collected from the machine during experiments. Generally, algorithms for one-legged hopping were found to generalize for four-legged running, with the addition of a low-level leg coordination mechanism.

6.3 Approach

We considered the three simplest quadruped running gaits, the trot, the pace, and the bound. These gaits are simple in that the legs are used in pairs. In trotting the legs work in diagonal pairs: the left front and right rear legs (LF-RR), strike the ground at the same time, leave the ground at the same time, and swing in phase with one another about their hips.† After a flight phase during which no feet touch the ground, the other diagonal pair (RF-LR) provides support. Pacing uses the legs in lateral pairs (LF-LR and RF-RR), and bounding uses the front legs as a pair (LF-RF) and the rear legs as a pair (RF-RR). We restrict attention to running, so all three gaits involve a strict alternation between support phases and flight phases. Figure 6–2 shows gait diagrams for the three quadruped running gaits that use the legs in pairs, the *pair gaits.* Good descriptions of the pair gaits have been available for over a hundred years (Marey 1874, Muybridge 1957/1899).

The control task is to propel the body in the desired direction at the desired rate, to keep the body in a level posture, and to regulate the vertical rebounding motions of the body. In previous work, we studied these same problems in the context of one-legged hopping machines (Raibert 1986a). The control for one-legged hopping was made simple by decomposing the algorithms into separate parts that regulated the body's hopping height, forward running speed, and attitude:

† No distinction is made in this chapter between hips and shoulders.

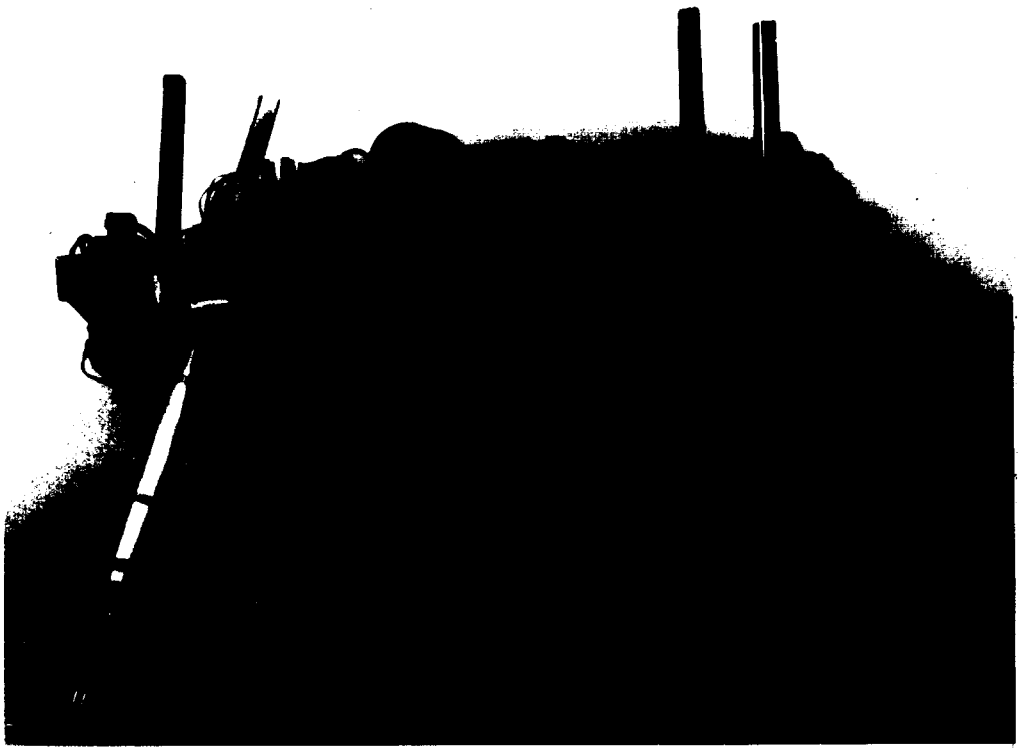

Figure 6–1: Photograph of quadruped running machine used for experiments.

- *Hopping Height*—The control system used leg thrust during the stance phase to excite and modulate spring-mass oscillations of the springy leg and body.
- *Forward Running Speed*—The control system positioned the feet during the flight phase to influence the accelerations of the body that would occur during the next stance phase. Symmetry was used to simplify the dynamics (Raibert 1986b).
- *Body Attitude*—The control system kept the body level by exerting torques about the hip axes during the stance phase.

These algorithms for one-legged hopping were adapted for control of systems that run on two legs by recognizing that bipeds typically run with just one leg active at a time—to first order, the swing leg can be thought of as idle. The algorithms that specified leg thrust, leg placement, and hip torque for one-legged hopping were used to specify these same parameters for the active leg of the biped. Experiments with one- and two-legged systems showed that the three-part algorithms could provide balance and control for running in place, traversing simple paths, running fast (13 mph), switching gaits between hopping and running, climbing stairs, and performing simple gymnastic maneuvers (Raibert 1986a; Hodgins, Koechling, & Raibert 1986; Koechling & Raibert 1988, Hodgins 1989).

To generalize the one-leg control algorithms a step further, to the case of quadruped running, we invoke the concept of the *virtual leg.* The virtual leg was first introduced by

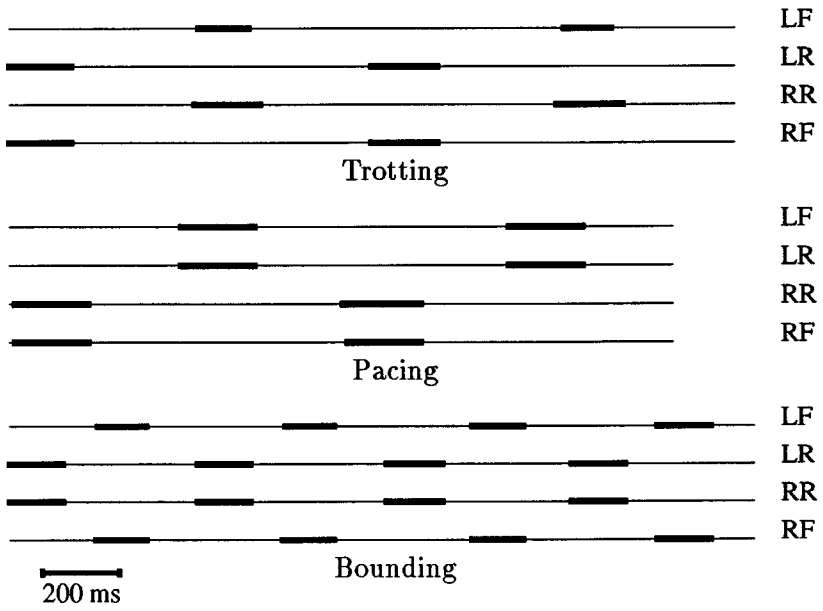

Figure 6–2: Pair gaits. Gait diagrams showing the pattern of leg use for the trot, pace, and bound, as executed by the quadruped robot in experiments. Each of these gaits use the legs in pairs. The bars indicate periods of ground contact, as measured by load switches in the feet. (Trotting data Q87.335.3, pacing data Q87.142.4, bounding data Q87.167.1.)

Sutherland to simplify the design of a one-ton six-legged walking machine that carried a human driver (Sutherland and Ullner 1984). Sutherland designed a hydraulic circuit that coupled the load-bearing behavior of two legs to act as though they were just one leg. This arrangement simplified control of the legs.

Generally, the virtual leg is a construct that allows several separate legs to be represented by fewer virtual legs. For instance, the virtual leg shown at the top right of figure 6–3 represents the two physical legs shown at the top left. So long as the two physical legs exert equal forces on the ground, equal torques at their hips, and their feet have equal horizontal displacements from their hips, then their behavior is precisely equivalent to the behavior of the virtual leg (Raibert, Chepponis, & Brown 1986).

The value of this approach is that it lets us reduce the quadruped pair gaits to equivalent *virtual biped gaits.* Figure 6–3 shows the correspondences between each of the pair gaits and an equivalent virtual biped gait. The control techniques used earlier for bipeds can then be used to control the virtual biped gaits in quadrupeds. We have already shown that bipeds can be controlled as though they use just one leg at a time, and that the three-part hopping algorithms are effective. What remains is to provide a low-level mechanism that coordinates the behavior of the physical legs so that the virtual leg and the physical legs have mechanically equivalent effects on the behavior of the body. This approach allows us to transform trotting, pacing, and bounding into a common underlying gait, the virtual biped gait.

In order to implement a control system based on the virtual leg concept, rules are needed for transforming the desired behavior of the virtual leg into the prescribed behavior

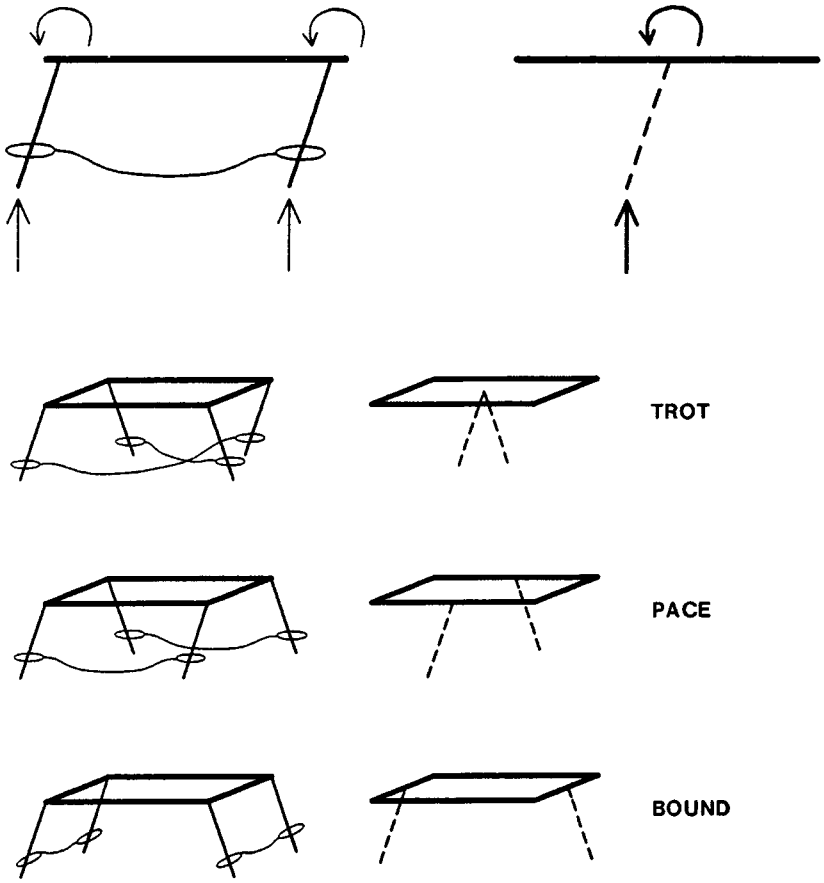

Figure 6–3: Virtual legs. When two legs are coordinated to act in unison, they can be represented by a functionally equivalent *virtual leg.* The virtual leg and the original pair of physical legs both exert the same forces and moments on the body, so they both result in the same behavior. When each pair of legs is replaced by a virtual leg, the trot, the pace, and the bound are transformed into virtual equivalent biped gaits. One virtual leg is used for support at a time. Sutherland first introduced the concept of the virtual leg to simplify the design of a six-legged walking machine (Sutherland and Ullner 1984).

of two physical legs.

- The legs should each exert axial thrust equal to half the axial thrust specified for the virtual leg.
- The hips should each exert a torque between the leg and body equal to half the hip torque specified for the virtual leg.
- The feet should strike the ground in unison and leave the ground in unison.
- The forward position of the feet with respect to their hips should equal the desired forward position of the virtual foot with respect to the virtual hip.

These rules eliminate degrees of freedom in the system, so they can be thought of as constraints or synergies. They allow the control system to map the desired system behavior into specific commands for each actuator of each leg.

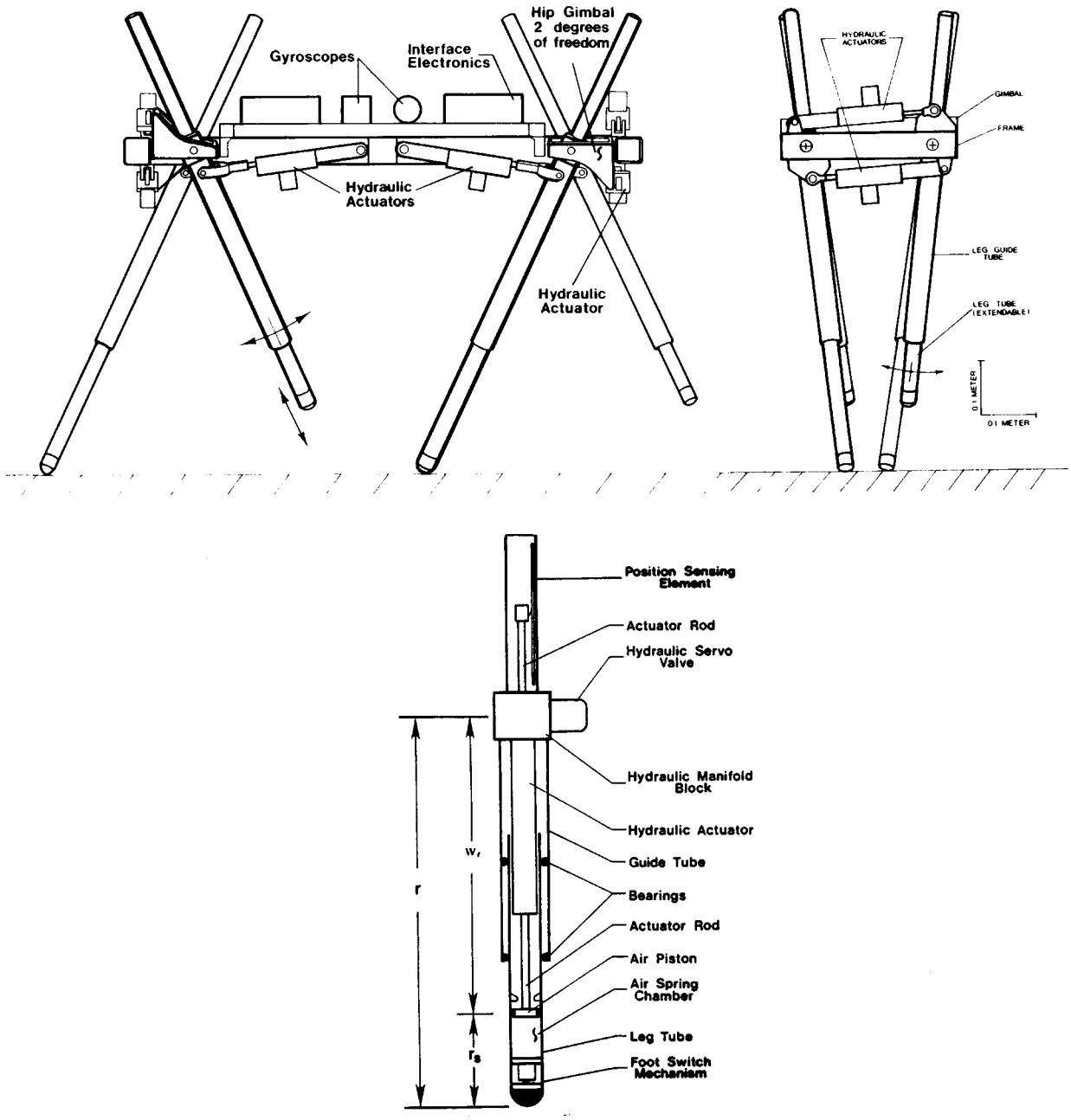

Figure 6–4: Diagram of quadruped running machine used for experiments. The body is an aluminum frame, on which are mounted legs, hip actuators, gyroscopes, and computer interface electronics. Each hip has two low friction hydraulic actuators that position the leg fore and aft, and sideways. Sensors measure the position, velocity, and force of the hydraulic hip actuators, hydraulic leg length, overall leg length, leg spring length, contact between the feet and the floor, and the pitch, roll, and yaw orientations of the body. An umbilical cable connects the machine to hydraulic, pneumatic, and electrical power supplies, and to the control computer (VAX/785), all of which are located nearby in the laboratory. The arrangement of spring in series with position source in each leg was motivated by simple muscle models. Physical parameters of the quadruped machine are given in table 6–1.

Parameter	Metric Units	English Units
Overall length	1.05 m	41.2 in
Overall height	0.95 m	37.5 in
Overall width	0.35 m	13.8 in
Hip height (max)	0.668 m	26.31 in
Hip spacing (x)†	0.776 m	30.56 in
Hip spacing (y)	0.239 m	9.40 in
Leg sweep angle (x)	± 0.565 rad	±32.4°
Leg sweep angle (y)	± 0.384 rad	±22.0°
Leg stroke (hydraulic)	0.229 m	9.0 in
Leg stroke (spring)	0.102 m	4.0 in
Body mass	25.2 kg	55.4 lb
Body moment of inertia (x)	0.257 kg-m^2	880 lb-in^2
Body moment of inertia (y)	1.60 kg-m^2	5470 lb-in^2
Body moment of inertia (z)	1.86 kg-m^2	6340 lb-in^2
Leg mass, total each	1.40 kg	3.08 lb
Leg mass, unsprung	0.286 kg	0.63 lbm
Leg moment of inertia (about hip)	0.14 kg-m^2	480 lb-in^2
Leg spring stiffness @20 psi (fully extended)	2100 N/m	12 lbf/in
Hip torque, @3000 psi (x)	166 N-m	1474 in-lbf
Hip torque, @3000 psi (y)	116 N-m	1030 in-lbf
Leg thrust, @3000 psi	1147 N	258 lbf

† x—fore and aft, y—sideways, z—up and down.

Table 6–1: Physical parameters of quadruped running machine.

We have outlined an approach to quadruped running that separates the problem into two parts. At one level, the control system guides and stabilizes motions of the body. This can be done the same way for the body of a four-legged system as for the body of one- or two-legged systems. At a lower level, the control system coordinates the behavior of individual legs to make them work together according to the rules of the virtual leg. The coordination specifies the relative placement of the feet, the relative thrust the legs deliver to the ground, and the relative hip torque exerted between the legs and the body. The virtual leg specifies how the individual legs should be controlled to make their net behavior equivalent to the desired behavior of the virtual leg.

6.4 Algorithms for Trotting, Pacing, and Bounding

In order to evaluate the approach outlined in the last section, we did experiments with the machine shown in figures 6–1and 6–4. During experiments, a human operator communicated with the running machine through a control panel and joy stick connected to the control computer. Experiments typically started out with the machine running in place. The machine ran forward when the operator specified a desired speed and direction of travel. The machine either traveled the length of the laboratory, with someone running behind carrying the umbilical, or it ran on a large treadmill. During each experiment the control computer recorded data from the sensors and from the internal variables of the control algorithms, and saved them for later analysis.

We designed the control system for these experiments according to the outline of the previous section. The control system used the three-part algorithms to specify desired behavior for each virtual leg and it used the rules of the virtual leg to coordinate the behavior of the physical legs.

Three-Part Locomotion Algorithms

To control the forward running speed, the control system positioned the foot of the virtual leg with respect to the center of mass of the body during each flight phase:

$$x_{f,d} = \frac{\dot{x}T_s}{2} + k_{\dot{x}}(\dot{x} - \dot{x}_d) \tag{6.1}$$

$$y_{f,d} = \frac{\dot{y}T_s}{2} + k_{\dot{y}}(\dot{y} - \dot{y}_d) \tag{6.2}$$

where

$x_{f,d}$, $y_{f,d}$	is the desired displacement of the foot with respect to the projection of the center of mass,
$\dot{x}$, $\dot{y}$	is the forward running speed,
$\dot{x}_d$, $\dot{y}_d$	is the desired forward running speed,
T_s	is the duration of a support period, and
$k_{\dot{x}}$, $k_{\dot{y}}$	are gains.

The control system estimated the forward speed of the body, $(\dot{x}, \dot{y})$, using the assumption that the feet do not move with respect to the ground during the stance phase. Under this assumption, the backward motion of a foot with respect to the body is equal to the forward motion of the body with respect to the ground. Gyroscope and hip angle measurements were used together with kinematics to make this estimate. The control system assumed that the forward running speed did not change during flight. The control system measured the duration of each stance phase, T_s, and used the most recent value for control. A human operator used a two-axis joystick to specify the desired forward running speed $(\dot{x}_d, \dot{y}_d)$ during each experiment. See Raibert, Chepponis, and Brown (1986) for additional explanation and details of these control algorithms.

To control the pitch and roll attitude of the body during stance, the control system applied torques about the virtual hips, using linear servos:

$$u_x = -k_{p,x}(\phi_P - \phi_{P,d}) - k_{v,x}(\dot{\phi}_P) - k_{f,x}(f_x) - k_{\dot{\gamma}}(\dot{\gamma}_d) \tag{6.3}$$

$$u_y = -k_{p,y}(\phi_R - \phi_{R,d}) - k_{v,y}(\dot{\phi}_R) - k_{f,y}(f_y) \tag{6.4}$$

where

u_x, u_y	are the servovalve output signals for the hip actuators,
ϕ_P, ϕ_R	are the pitch and roll angles of the body,
$\dot{\gamma}_d$	is the desired hip rate of the actuator,
f_x, f_y	are the forces measured in the hip actuators, and
k_p, k_v, k_f, $k_{\dot{\gamma}}$	are gains.

Hip actuator forces were included in the attitude control to help stabilize the under-damped modes caused by the lateral compliance of the foot pads.

During fast forward running, the fore-aft hip actuators must move with substantial velocity if the body is to remain level with the foot stationary. An ideal torque control system would generate these high actuator rates as an outcome of body attitude control, without explicitly programming them. In the quadruped we obtained a more nearly ideal response by adding a term to the hip actuator output signal that was proportional to the desired actuator rate. The desired actuator rate was determined from the desired forward running speed, the measured pitch rate of the body, and the kinematics of the mechanism. The resulting term is the last term on the right hand side of equation (6.3).

To control the vertical thrusting motion, the control system adjusted the hydraulic length of the virtual leg throughout the running cycle. When a virtual leg was in the swing phase, the desired hydraulic length was shortened, to L_1, to keep the feet from touching the ground. This kept the virtual leg out of the way. When a virtual leg was preparing for landing or compressing under load of the body, the desired hydraulic length was set to the intermediate value L_2. During the second part of the stance phase, when the virtual leg delivered a thrust to the body, the desired hydraulic length was increased to L_3. The operator specified L_1, L_2, and L_3 from the control panel, with $L_1 < L_2 < L_3$.

Implementation of Virtual Legs

In order to make the legs work together in pairs, the control system coordinated positioning of the feet, synchronized ground contact, and equalized axial leg thrust. Because of symmetry in the geometry of the quadruped machine, the desired position of the virtual foot with respect to the virtual hip could be used as the desired position of the physical feet with respect to the physical hips:

$$x_{h,i,d} = x_{h,j,d} = x_{f,d} \tag{6.5}$$

$$y_{h,i,d} = y_{h,j,d} = y_{f,d} \tag{6.6}$$

where

$x_{h,i,d}$, $y_{h,i,d}$	is the desired displacement of the ith foot with respect to the

projection of the ith hip,
$x_{f,d}$, $y_{f,d}$ is the desired displacement of the virtual foot with respect to the projection of the virtual hip,
i, j are indices of two physical legs that form one virtual leg.

Once the desired foot displacements were known, transformations based on the kinematics of the legs, hips, and actuators were used to find actuator lengths that positioned the feet as desired. These transformations took into account the pitch and roll orientations of the body and the lengths of the legs.

To synchronize the instant of ground contact for the two legs forming a virtual leg, the control system servoed the leg lengths during flight, so that both feet had the same altitude above the ground. This adjustment affected only the difference in leg lengths, while L_2 determined the average leg length. Pitch and roll measurements made from onboard gyroscopes and a kinematic calculation were required to perform these adjustments.

To equalize the axial forces the legs delivered to the ground during stance, the control system differentially servoed the lengths of the leg hydraulic actuators:

$$w_{\ell,i,d} = w_{\ell,i} + \frac{r_{s,i} - r_{s,j}}{2} \tag{6.7}$$

where

$w_{\ell,i}$ is the hydraulic length of the ith leg,
$w_{\ell,i,d}$ is the desired hydraulic length of the ith leg, and
$r_{s,i}$ is the air spring length of the ith leg.

This differential adjustment forced the air springs to assume equal lengths and therefore to generate equal axial force. Once again, values for L_2 and L_3 determined the average length of the hydraulic actuators.

Yaw Control

The algorithms used to control the quadruped, as stated so far, do not control the yaw orientation of the body. A torque about the yaw axis was generated by manipulating the position of the feet at touchdown. Foot position was selected so the axial load on the two legs in contact with the ground exerted a couple on the body about the yaw axis. The feet were positioned on a circle centered at the vertical projection of the center of mass. The forward speed calculation specified the average foot position with respect to the projection of the center of mass, but this leaves two degrees of freedom unspecified: the distance between the feet that form the virtual leg and the yaw orientation of the line passing through the feet. The distance between the feet is irrelevant here, but the control system manipulated the orientation of the line connecting the feet to generate yaw torque on the system.

If the system were to run in place and each foot were placed directly under its hip, no torque would be exerted about the yaw axis. In this case the orientation of the line connecting the feet, viewed from above, would be the same as the orientation of the line connecting the hips. See figure 6–5. If the feet were positioned to rotated the line connecting the feet about the center of mass, then the axial thrust of each leg would have a component

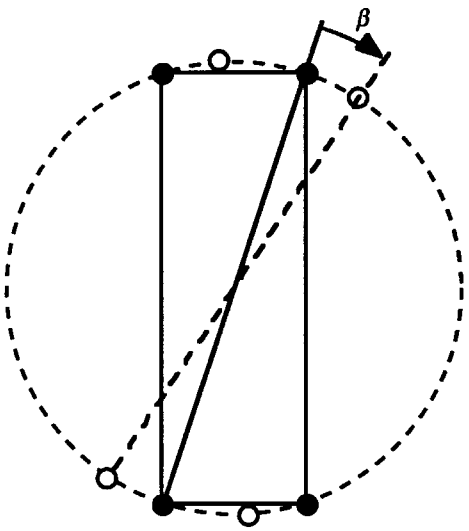

Figure 6–5: Control of turning about the yaw axis. The diagram shows the quadruped viewed from above, indicating how the placement of the feet can be used to generate a torque about the yaw axis. The torque is proportional to the angle between the line through the hips and the line through the feet. The filled circles indicate the location of the hips. The open circles indicate the placement of the feet. β is the angle that determines the turning moment. The foot placement shown in the figure would cause the machine to turn counter-clockwise.

about the yaw axis of the system. The resulting couple was used to manipulate the yaw orientation of the quadruped, without disturbing the average position of the feet.

To control yaw in the experiments, foot placement was used to generate a yaw moment. The operator specified the desired yaw rate with a lever on the control panel. The angle between the line connecting the hips and the line connecting the feet, β, was manipulated as follows:

$$\beta = k_1 \dot{\phi}_{Y,d} + k_2 \dot{\phi}_Y \tag{6.8}$$

where

$\dot{\phi}_Y$	is the yaw angle of the body with respect to room coordinates,
$\dot{\phi}_{Y,d}$	is the desired yaw angle of the body, and
k_1, k_2	are gains.

The yaw rate that appears in (6.8) is not the instantaneous yaw rate, but an average taken for an entire stride. Use of the average yaw rate over the stride permits there to be variations in yaw rate within the stride, without interfering with the control of the machine's facing direction.

Augmenting (6.1) and (6.2) above to include turning we have:

$$x_{f,d,i} = \frac{\dot{x}T_s}{2} + k_{\dot{x}}(\dot{x} - \dot{x}_d) + D\cos(\beta + \beta_{0,i}) \tag{6.9}$$

$$y_{f,d,i} = \frac{\dot{y}T_s}{2} + k_{\dot{y}}(\dot{y} - \dot{y}_d) + D\sin(\beta + \beta_{0,i}) \tag{6.10}$$

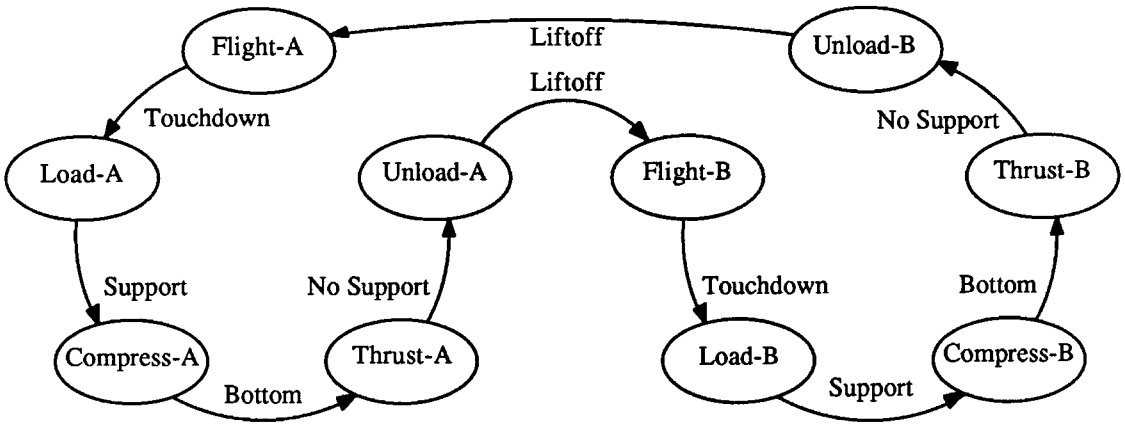

Figure 6–6: Diagram of finite state machine used to synchronize the control programs to the behavior of the quadruped. Virtual leg $\mathbf{B}_\ell$ swings forward while virtual leg $\mathbf{A}_\ell$ provides support, and vice versa. State transitions are determined by events related to the support leg. See table 6–2 for details.

where

i	indicates the physical leg,
β_0, i	is $\arctan(W/L)$ for $i = 1,3$ and $-\arctan(W/L)$ for $i = 2,4$,
D	$= \sqrt{(W^2/2 + L^2/2)}$

Once these calculations for controlling vertical bouncing, forward speed, body attitude, and turning were performed and the desired actuator lengths were known, twelve linear servos acted on the hydraulic actuators to position the hips and leg lengths

$$u_i = -k_p(w_i - w_{i,d}) - k_v(\dot{w}_i) \tag{6.11}$$

where

u_i	is the servovalve output signal for the ith actuator,
w_i, $w_{i,d}$, $\dot{w}_i$	are the position, desired position, and velocity of the ith actuator,
k_p, k_v	are position and velocity gains.

Sequencing

In addition to providing control functions for the body and legs, quadruped locomotion required a mechanism to sequence the use of the legs. The sequencing mechanism selected which leg would next provide support so that it could move to a forward position for landing, and it assigned the thrust and attitude control functions to the leg currently providing support. The sequencing mechanism shortened the idle legs to keep them out of the way of the ground until they once again become active.

State	Trigger Event	Action
1 LOADING $\mathbf{A}_\ell$	$\mathbf{A}_\ell$ touches ground	Equalize axial force $\mathbf{A}_\ell$ Zero hip torque $\mathbf{A}_\ell$ Shorten $\mathbf{B}_\ell$ Don't move hip $\mathbf{B}_\ell$
2 COMPRESSION $\mathbf{A}_\ell$	$\mathbf{A}_\ell$ air springs shortened	Equalize axial force $\mathbf{A}_\ell$ Erect body with hip $\mathbf{A}_\ell$ Shorten $\mathbf{B}_\ell$ Position $\mathbf{B}_\ell$ for landing
3 THRUST $\mathbf{A}_\ell$	$\mathbf{A}_\ell$ air springs lengthening	Extend $\mathbf{A}_\ell$, equalizing force Erect body with hip $\mathbf{A}_\ell$ Keep $\mathbf{B}_\ell$ short Position $\mathbf{B}_\ell$ for landing
4 UNLOADING $\mathbf{A}_\ell$	$\mathbf{A}_\ell$ air springs near full length	Shorten $\mathbf{A}_\ell$, equalizing force Zero hip torques $\mathbf{A}_\ell$ Keep $\mathbf{B}_\ell$ short Position $\mathbf{B}_\ell$ for landing
5 FLIGHT $\mathbf{A}_\ell$	$\mathbf{A}_\ell$ not touching ground	Shorten $\mathbf{A}_\ell$ Don't move hip $\mathbf{A}_\ell$ Lengthen $\mathbf{B}_\ell$ for landing Position $\mathbf{B}_\ell$ for landing
States 6–10 repeat states 1–5, with $\mathbf{A}_\ell$ and $\mathbf{B}_\ell$ reversed.		

Table 6–2: Finite state sequence used to synchronized the control algorithms to the behavior of the quadruped machine. The state shown in the left column is entered when the event listed in the center column occurs. States advance sequentially during normal running. $\mathbf{A}_\ell$ refers to the virtual leg made up of physical legs LF and RR for trotting, LF and LR for pacing, and LF and RF for bounding. $\mathbf{B}_\ell$ refers to the virtual leg made up of physical legs RF and LR for trotting, RF and RR for pacing, and LR and RR for bounding. During states 1–5, $\mathbf{A}_\ell$ is the support leg and $\mathbf{B}_\ell$ is the swing leg. During states 6–10, $\mathbf{B}_\ell$ is the support leg and $\mathbf{A}_\ell$ is the swing leg.

The control system used a finite state machine throughout the running cycle to perform this sequencing task, and to synchronize the actions of the control algorithms to the behavior of the machine. It kept track of the legs and assigned the three control functions to the appropriate virtual leg at the appropriate time. The finite state machine traversed ten states during each stride. Each state prescribed a set of sensor conditions that triggered transition into the state, and a set of control actions to be taken during the state. The state transitions synchronized the various control functions—vertical thrust, attitude control, and foot placement—to the ongoing behavior of the running machine. Figure 6–6 and table 6–2 give the details of the state machine as implemented.

Differences in Algorithms for Trotting, Pacing, and Bounding

To a large degree, the control program used to produce trotting is the same as the program used to produce pacing and bounding. Of course, the identity of the legs forming each pair varied among the gaits. In addition, several parameters were adjusted individually to producing each gait.

The *track* parameter, the nominal horizontal separation of the feet, was normally set equal to the hip spacing (0.23 m) for trotting and bounding. For pacing, the track parameter was reduced to 0.09 m. This value of the track parameter brought the feet closer to the midline, which reduced the roll motion of the body during the stance phase.

During the stance phase, the legs lengthened from L_2 to L_3 to drive the body upward. The amount the legs lengthened was about the same for trotting and pacing, but was larger by about 0.03 m for bounding. This difference was required because the thrust delivered by the legs caused the body to pitch during bounding, and the loading on the legs was reduced. To provide the same vertical acceleration required greater leg extension.

The most important variation in how the gaits were implemented concerns pitch control during bounding. We found that bounding did not require active control of the pitch attitude. The observed pitch oscillation was passively stabilized by the mechanical system. In previous work we found that passively stable pitch oscillations occurred in computer simulations of a planar model with two separated legs (Murphy and Raibert 1985). In the bounding experiments reported here, the hip actuators were used to position the legs during the flight phase and to servo the hips to zero force during stance. They were not programmed to respond to errors in the pitch attitude of the body. Earlier implementations of bounding used the pitch control algorithms that were used for trotting and pacing, but data from those runs have not been included in this chapter. Stability about the roll axis was controlled actively for all three pair gaits.

6.5 Results

Data recorded during trotting experiments are shown in figures 6–7 and 6–8. In trotting, the legs are used for support in diagonal pairs. The synchronization of foot impacts was controlled to within 12 ms in most cases, and equalization of pressure in the leg spring was controlled to a few psi, with transients reaching 70 psi briefly. The vertical bouncing motion of the body was regular and smooth.

Regulation of forward running speed was not perfect, as shown in figure 6–8. Only a rough relationship existed between the desired and actual running speeds. The errors in speed were due to known limitations of the velocity control algorithm. Hodgins (1989) describes improvements to the velocity control algorithm that reduce forward speed control errors to about ± 0.1 m/s, when tested with a planar biped running machine. During forward trotting the inclination of the body about the pitch axis, ϕ_P, deviated from the desired value by up to 8°. The magnitude and sign of this error were generally related to the forward running speed. The control system kept error about the roll axis within $\pm 5°$ in these experiments.

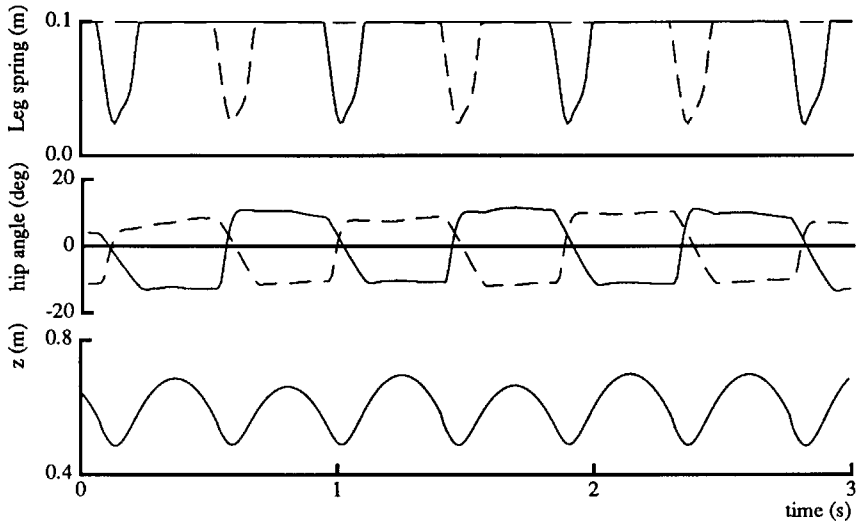

Figure 6–7: The vertical bouncing motion. These data show the bouncing motion that underlies quadruped running. The data were recorded during trotting, for the left front and rear legs (LF shown solid, LR shown dashed). The top curve shows the compression of the air springs. The middle curve shows the the hip joint motions for the same two legs. The bottom curve shows the altitude of the body above the floor, as estimated by the control system from internal joint sensors, data from the gyroscopes, and a rigid body model. (Data file Q86.343.5.)

Data recorded during pacing are shown in figure 6–9. The behavior was similar to trotting, except for an oscillation about the roll axis of the body of about $\pm 5°$, and a small amount of lateral motion. Roll and lateral motions were both expected because the center of mass was not located over the the virtual hips, as it was for trotting. During pacing the lateral position of the feet were biased so as to bring them near the center line. This was done by including a *track* term in equation 6.6, that was adjusted manually. For the data shown in the figure, the nominal lateral foot separation was set to 0.1 m with the lateral hip separation fixed at 0.239 m. The machine paced with both larger and smaller lateral foot separations. We were not successful in making the machine pace with the feet on the center line because of leg and foot collisions.

Data for bounding are shown in figure 6–10. Bounding was characterized by large oscillations about the body pitch axis. These oscillations can be predicted from the large forward and rearward displacements of the virtual hips from the center of mass. The data show a pitch oscillation of $\pm 18°$, with little body rotation about the roll or yaw axes. Vertical displacement of the center of mass was about 0.05 m in bounding, as compared to about 0.2 m for trotting and pacing. Angular motion of the body was the primary factor that lifted and placed the legs in bounding, while vertical motion of the body was the primary factor in trotting and pacing.

Two Separate State Machines for Bounding and Pronking

The state machine shown in figure 6–6 was used to generate trotting, pacing, and bound-

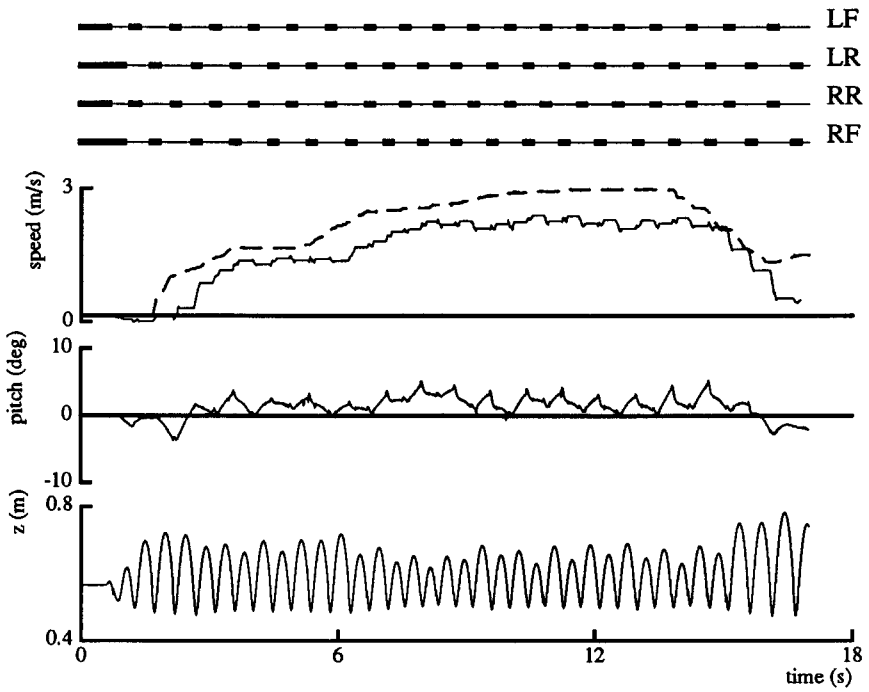

Figure 6–8: Forward running. The machine stood on four legs until an operator initiated running by pressing a button. The operator used a joystick to specify the desired running speed (shown dashed) and direction. There was about a 0.3 m/s steady state discrepancy between the desired and measured forward running speed. The body tipped in the direction of running, as shown by the plot of pitch angle. Positive pitch indicates nose down. When the operator reduced desired forward running speed at about 15 s, some of the forward energy was converted into vertical motion, as shown in the plot of z. (Data file Q86.343.5.)

ing. For bounding we also experimented with a variation of the control system that used a separate state machine for each virtual leg, as shown in figure 6–11. In this implementation the legs were paired as before, but the behavior of the front virtual leg (LF-RF) was tracked and controlled by one state machine, and the behavior of the rear virtual leg (LR-RR) was tracked and controlled by an entirely separate state machine. No explicit action was taken to synchronize the front and rear virtual legs.

Using separate state machines for the front and rear virtual legs, the system was observed to stablize in either of two gaits, pronking or bounding. In pronking, the system hopped on all four legs at once, with the pitch angle of the body nearly level and zero phase lag between the behavior of the front and rear virtual legs. The left half of figure 6–12 shows the quadruped pronking. In pronking the system rejected phase disturbances by returning itself to synchronous use of all four legs. There was nothing explicit in the control system to provide this synchronization.†

Using separate state machines, it was also possible for the quadruped machine to stabi-

† Control about the roll axis during pronking was marginally stable, which made extensive testing of this gait difficult. Roll stability was poor because the combined moments of inertia of the four legs about the roll axis was large compared to the moment of inertia of the body. In this case, the algorithm that stabilized lateral translation (equation 6.6) disturbed the roll posture of the body.

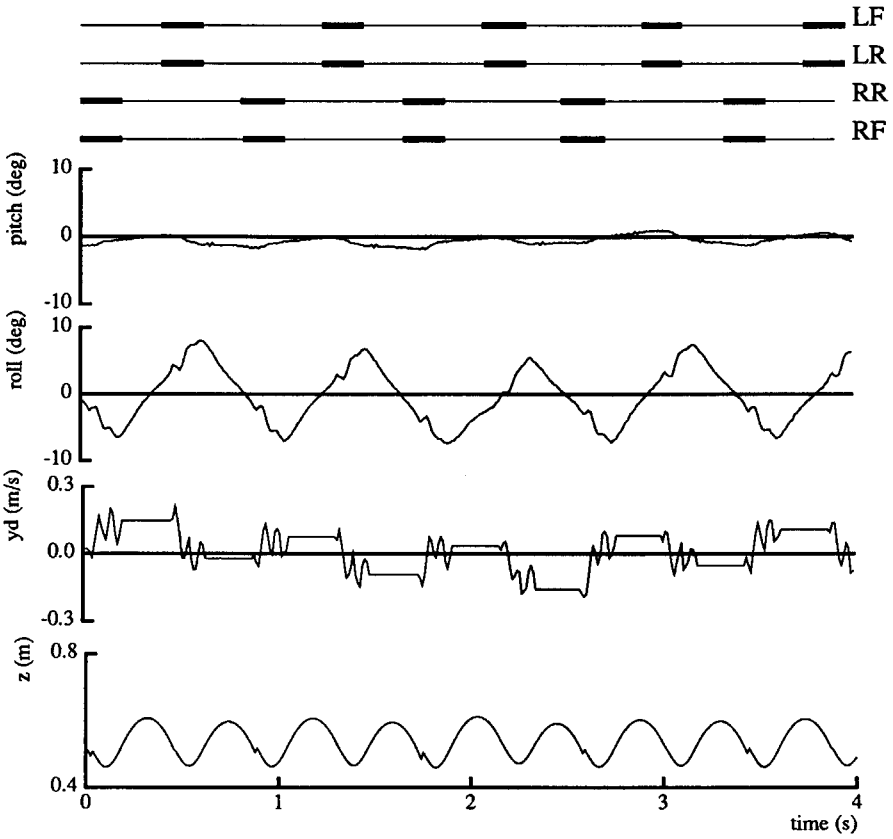

Figure 6–9: Pacing. Data recorded as the quadruped paced in place. The roll oscillation and lateral translation were characteristic of pacing. Neither trotting nor pacing involve much pitching of the body. For pacing, the nominal lateral spacing of the feet, the track, was set to 0.09 m. This value is less than the hip spacing, which is 0.239 m. The discontinuities in the data for z were due to errors in estimating the vertical velocity of the body when the feet leave the ground and to disturbances introduced by the umbilical. (Data file Q87.142.4.)

lize in a bounding gait, with 180° phase between the behavior of the front and rear virtual legs. Data recorded during bounding using separate state machines are plotted in figure 6–13. They are difficult to distinguish from the other bounding data. In this experiment the machine started bounding in place, accelerated up to 3.0 m/s, then stopped as it approached the end of the running area. When the quadruped bounded in place with separate state machines, the phase relationship between front and rear legs was stable at 180°. When the quadruped traveled forward, the phase shifted to reduce the duration of extended flight phases (the ones occurring after the rear legs provide support) and increased the duration of the gathered flight phases (the ones occurring after the front legs provide support). This phenomenon can be seen in figure 6–13.

To initiate bounding with separate state machines, an *inhibition* function was implemented, as shown in figure 6–11. Inhibition was used to artificially desynchronize the front and rear state machines by permitting only one of the them to enter the thrust state at

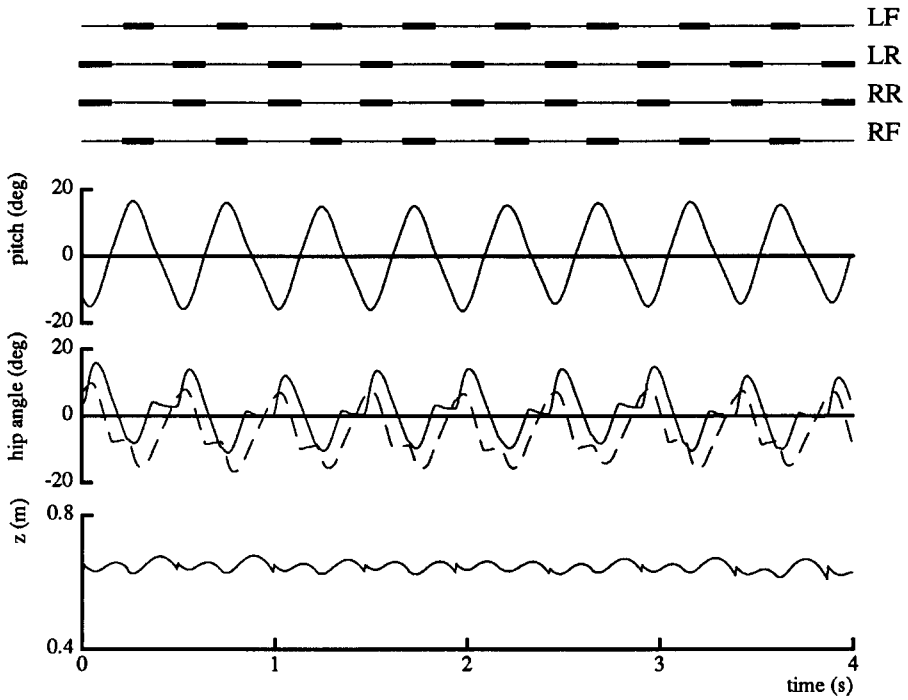

Figure 6–10: Bounding. Bounding was characterized by large pitching motions of the body. Vertical motion of the center of mass was less than for trotting and pacing, even with greater leg thrust. For bounding, the nominal longitudinal spacing of the feet, the base, was set to 0.776 m, equal to the longitudinal hip spacing. (Data file Q87.167.1.)

a time. With just one virtual leg thrusting at a time, a large pitch moment and pitching motion of the body was generated. This served to introduce a phase difference between the front and rear virtual legs, which eventually stabilized at 180°. The transition from pronk to bound using inhibition is shown in figure 6–13.

Gait Transitions

In previous work we demonstrated that the planar biped could switch between an alternating gait and a hopping gait (Hodgins, Koechling, & Raibert, 1986). The approach was to execute the switch, or gait transition, during the flight phase, when the two gaits are nearly indistinguishable.

The quadruped presents a richer set of gait transition possibilities, as well as more complicated transitions. For instance, there are six different transitions possible among trotting, pacing, and bounding. During the flight phase these gaits differ with respect to the characteristic body motion. In trotting, the body is level during the flight phase. In pacing, the pitch angle of the body is level, but the roll angle of the body oscillates. In bounding the roll angle of the body is level, but the pitch angle undergoes oscillations of nearly $\pm 20°$.

One approach to achieving quadruped gait transitions designates a transition step, during which the control system generates the moment required to adjust the attitude

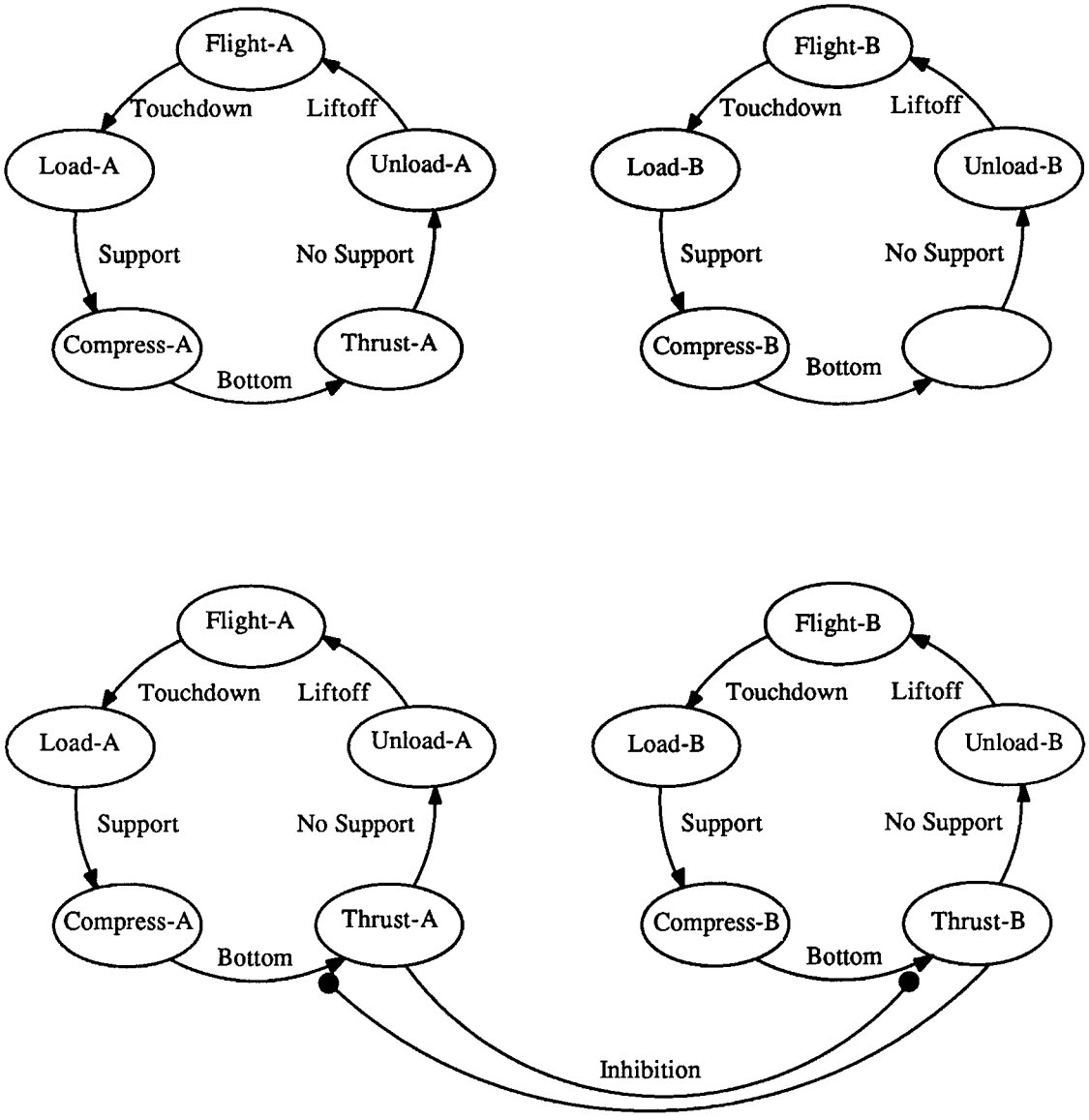

Figure 6–11: Independent state machines assigned to the virtual legs for bounding. Top) One state machine tracks the behavior of the front virtual leg while a second state machine tracks the behavior of the rear virtual leg. The phase relationship between the behavior of the two virtual legs is not specified by the state machine, but results from mechanical and dynamic coupling in the system. Bottom) When inhibition is enabled, it prevents both virtual legs from thrusting at the same time. It prevents one state machine from entering the thrust state if the other state machine is already in the thrust state. The unequal thrust caused by inhibition induces pitching of the body, and thereby desynchronizes the two state machines.

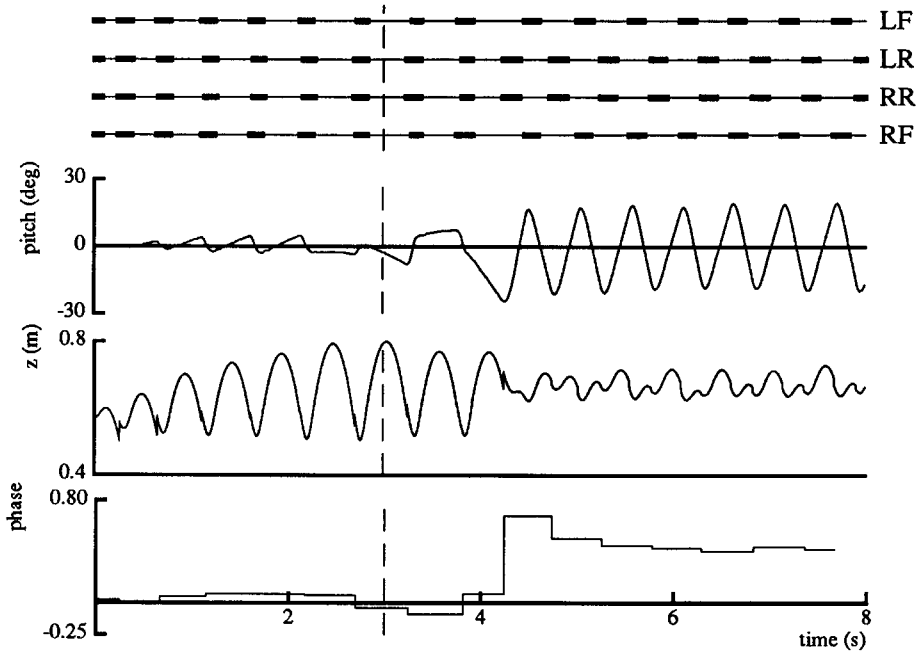

Figure 6–12: Pronk and bound. The machine started out pronking. During each stance phase, the pitch angle of the body returned to nearly level, which synchronized the front and rear virtual legs and their state machines. The machine began to bound when the operator enabled inhibition after 3 s, indicated by vertical dashed line. Inhibition acted during two steps: from $t = 3.31$ to 3.40 s the front virtual leg was prevented from thrusting, and from $t = 3.84$ to 3.93 s the rear virtual leg was prevented from thrusting. Phase shifted at the pronk to bound transition. Phase was calculated as the time difference between the front and rear virtual legs striking the ground, normalized by the period of a stride for the front virtual leg. (Data file Q89.188.9.)

motion of the body. For instance, a transition from trotting to bounding would introduce a pitching moment during the transition step, by differentially thrusting with the front and rear support legs. A transition from pacing to trotting would require a moment that eliminated body roll.

So far, we have used this approach on the pitch axis but not the roll axis. Roll axis oscillations are small enough to ignore. We have implemented gait transitions from trotting to pacing, trotting to bounding, and pacing to trotting. Data from two of these transitions are shown in figure 6–14. Transitions between trotting and pacing were typically quite smooth, with little disruption of the motion. For transitions to bounding, several steps were frequently required before the pitching motion of the body stabilized.

All gait transitions were done while the quadruped ran in place or traveled at low speed. We have not written programs that attempt transitions from bounding to trotting or bounding to pacing. Such transitions will require algorithms for leg thrust that bring the pitch motion to zero rate and to an approximately level body angle. We also have not experimented with high speed gait transitions.

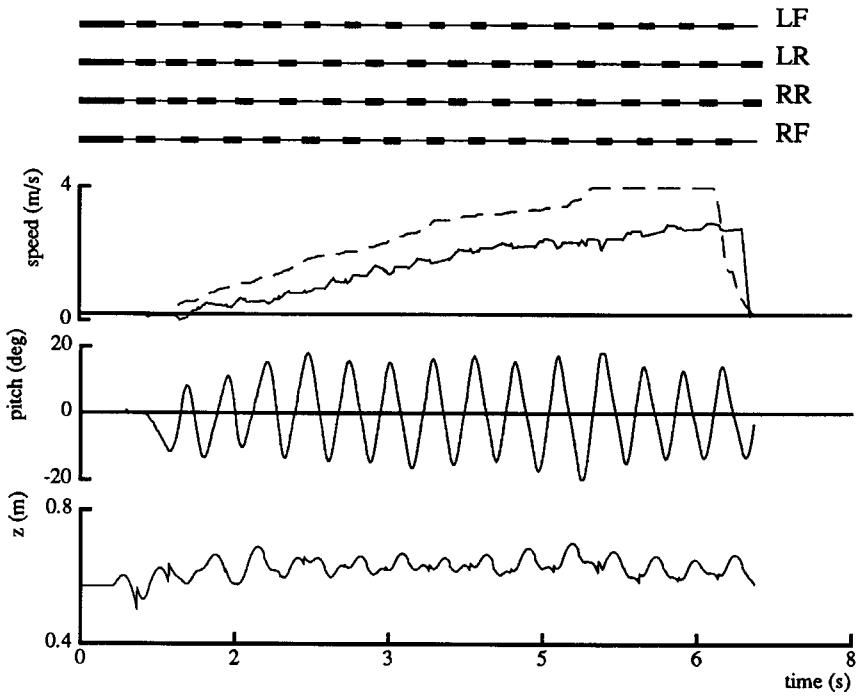

Figure 6–13: Bounding with independent state machines for front and rear virtual legs. The machine started bounding in place, accelerateed up to 3 m/s, and stopped abruptly just before reaching the end of the laboratory. Once again, there is a substantial discrepancy between the desired forward running speed (shown dashed) and the measured running speed. As the machine increased speed, the phase relationship between front and rear ground impacts shifted away from 180°. (Data file Q87.196.4.)

6.6 Discussion

Displacements of the Virtual Legs

In trotting, the points half way between the physical legs of each pair, the virtual hips, were both located under the center of mass of the body. Therefore, when each foot was positioned with respect to its hip, the virtual foot was positioned with respect to the center of mass, as specified by the one-leg algorithms.

In pacing and bounding, however, the center of the hips are displaced from the center of mass. In pacing, the virtual hips are displaced laterally from the center of mass by half the body width, or 0.119 m. In bounding, the virtual hips are displaced longitudinally from the center of mass by half the body length, or 0.388 m. As a result of these displacements, the control for bounding and pacing did not place the feet as required by the one-leg control algorithms: there were placement errors that alternated in sign on each step. These errors were responsible for the characteristic roll motions observed in pacing, and the characteristic pitching motion observed in bounding. Because the displacements alternate in sign on each step, there was a symmetry to the resulting accelerations that balanced out over an entire

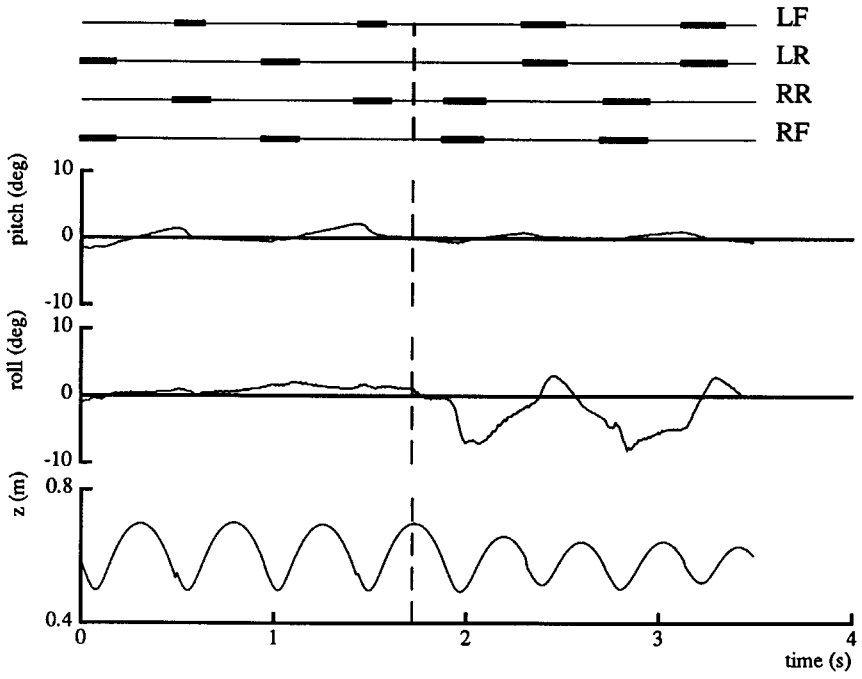

Trot to Pace

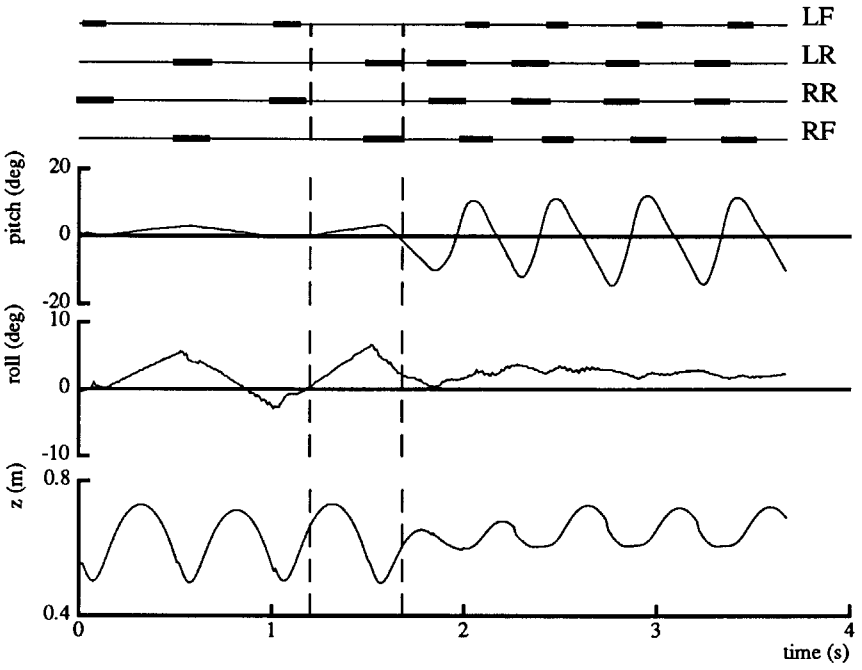

Trot to Bound

Figure 6–14: Gait transition: Top) Data recorded during a transition from trotting to pacing. The transition occurred during a flight phase, as indicated by the vertical dashed line. There was little disruption of the running motion. Forward running speed was essentially zero. Bottom) The transition from trotting to bounding took several steps to stabilize. The vertical dashed lines bracket the transition step, which induced pitching of the body. ((Data file Q87.335.3 and Q88.2.3.)

stride. Symmetries of this sort are described in (Raibert 1986b).

It is possible to eliminate these displacements by specifying fixed offsets for each virtual leg. *Track* and *base* parameters can be used for this purpose. For instance, the displacement was reduced to 0.05 m for pacing. Despite the theoretical possibility of eliminating these displacements entirely, there are practical limitations. One limitation comes from the range of motion of the legs. In bounding, the front legs can not reach far enough backward to be placed under the center of mass, nor can the rear legs reach far enough forward. A second limitation concerns foot collisions. If the feet were placed on the centerline in either pacing or bounding, it would be difficult to keep the legs from colliding. Of course, there are animals that do not suffer from either of these limitations.

An Alternative Method for Controlling Yaw

There is an alternative method for controlling yaw and turning to the one that was implemented. It is possible to manipulate the pitch and roll hip torques exerted during the stance phase to achieve a corrective torque about the yaw axis. The sum of the pitch and roll torques exerted on the body by the hips was determined by the virtual leg calculation. However, the difference in hip pitch and roll torques is free to be used to control yaw.

If the hips were separated W laterally, L longitudinally, and the legs were length R, then the yaw torque would be

$$\tau_Y = \frac{L}{2R}(\tau_{R,i} - \tau_{R,j}) + \frac{W}{2R}(\tau_{P,i} - \tau_{P,j}). \tag{6.12}$$

where $\tau_{R,i}$ is the roll hip torque exerted by leg i, and $\tau_{P,i}$ is the pitch hip torque exerted by leg i. Pure yaw torque would be obtained without internal forces in the closed chain when

$$\tau_{P,i} = -\tau_{P,j} \tag{6.13}$$

$$\tau_{R,i} = -\tau_{R,j} \tag{6.14}$$

$$W\tau_R = L\tau_P \tag{6.15}$$

This manipulation would leave the sum of the pitch hip torques available for controlling the body pitch angle, and the sum of the roll hip torques available for controlling the body roll angle. This method could be used in conjunction with the previous method of influencing yaw described earlier, with this one exerting torques during stance and the other positioning the feet during flight. This method has not been implemented.

Force-Equalizing Virtual Legs

A consequence of coordinating the legs of a pair so that they exert equal forces on the ground is the loss of passive stability that a pair of legs might otherwise provide. An ordinary table resists tipping when unevenly loaded because the legs near the load generate more supporting force than the legs that are far from the load. If a table had force-equalizing legs, then an uneven load would cause the legs near the load to shorten, the legs remote from the load to lengthen, and the surface to tip. This force-equalized behavior should be expected, since it is precisely the behavior of a table with just one leg located in the middle.

The experiments reported in this chapter showed that an approach which discards passive stability of the legs is workable. It leaves us with a design philosophy problem: On the one hand, the force-equalizing virtual leg permitted relatively sophisticated behavior with a simple implementation. On the other hand, a well-engineered control system should take advantage of the intrinsic mechanical stability of the mechanism. That approach would ultimately lead to the most efficient system, both in terms of energy and control.

Despite these limitations, it is entirely possible that four-legged animals use force equalization when they trot, pace, or bound. One might find out by measuring the axial forces that develop in the legs of running quadrupeds, perhaps using sets of force platforms. The experiment would disturb one of the feet during stance by shifting the support surface upward or downward. If force equalization were in effect, the difference in axial leg force would not be affected by the manipulation. Exact force equalization is unlikely to be found, because the distribution of mass in animals' bodies is skewed by the asymmetric placement of their heads and the unequal lengths of the fore and hind legs. One might find an asymmetry in force equalization comparable to the skewness of body mass distribution.

Gait Selection

This chapter presents data for three quadruped gaits and describes rudimentary techniques for switching between gaits. It is silent, however, on the question of how to choose which gait to use. In animals, energetic cost seems to be an important factor in selecting a gait. Animals change gait as they change speed, apparently to minimize the cost of transportation (Hoyt & Taylor 1981). The geometry of animals may also enter into gait selection. At low running speeds, for instance, long-legged animals use a pace rather than a trot, presumably to avoid interference between the front and rear legs on each side (Hildebrand 1960). Other factors, such as the range of leg motion and leg stiffness may also be important. Despite these potential factors, the experiments reported here do not suggest good criteria for selecting one gait over another.

This chapter refers to the pair gaits as "simple" gaits. They are simple because of the regular alternation between flight phases and double support phases, and because all the legs move the same way. Less simple quadruped gaits are the canter and gallop, which mix flight phases with single, double, and triple support periods. The key problem for the less simple gaits is how more than one leg can work together to rebound the body, without making them either synchronous or entirely disjoint in their motion, and without giving up the strain energy absorbed by the legs.

One way to approach these less simple gaits might be to generalize the virtual leg concept to apply to the behavior of physical legs that act in sequence, but overlapped in time. One might separate each support phase into the subintervals during which a fixed number of legs provides support. Then the entire support phase might be represented by a sequence of virtual support phases. For a rotary gallop the sequence of phases would be (1) right rear, (2) right rear and left rear, (3) left rear, (4) left rear and left front, (5) left front, (6) left front and right front, and (7) right front. Again, the key difficulty is to find a mechanism that can mediate the smooth exchange of support from one leg to another, without disrupting the bouncing motion of the body.

Relevance to Animals

There is no reason to assume that the mechanisms and algorithms studied in the context of legged robots are the same as those used by animals. However, experience implementing an artificial system that performs a task like the one an animal performs can provide a better appreciation of the task, and perhaps insights into strengths and weaknesses of various approaches. Specific control algorithms can also be used as initial hypotheses that are detailed, concrete, and testable in animals.

One could argue that robots have certain advantages over animals, when it comes to being the subject of motor behavior experiments. One important advantage is the experimenter's knowledge of the intended function of all components in the system. The control system architecture, control method, and implementation details are all known when the behavioral data are examined. This knowledge provides an important tool in interpreting observed behavior. Another advantage to studying robots comes from the experimenter's freedom to simplify and instrument the system. One can design a system with just enough complexity to be interesting, but no more. It is usually feasible to make direct measurements of important variables.

Robots also have disadvantages. The primary disadvantage is that the quality and richness of their behavior does not compare well to that of animals. Also, it is possible to study a form of animal behavior when little is known about it, whereas robots are useful only when knowledge is already quite advanced. Bootstrapping is required before there is any behavior to study at all, and then it is usually impoverished when compared to animal behavior. Finally, for those interested in the specific details of how an animal performs a task, rather than in the nature of the task performed, the study of robots may provide only indirect clues.

6.7 Summary

- We describe control algorithms for quadruped trotting, pacing, and bounding. The high-level part of the control performs three tasks: it regulates the vertical bouncing motion, stabilizes the forward running speed, and keeps the body level. The high-level algorithms are like those used previously to control one-legged hopping machines. The low-level part of the control system coordinates the behavior of legs by manipulating the relative placement of the feet on the ground, the relative forces the legs of a pair exert on the ground, and the net hip torque the legs exert on the body.
- Experiments with a four-legged running machine verify the general approach outlined in the chapter. The control system used the one-legged algorithms, a finite state machine, and virtual legs to make it run with trotting, pacing and bounding gaits.
- Gait transitions from trotting to pacing and from pacing to trotting were accomplished at low forward speed by switching from one gait to the other during the flight phase. Transitions from trotting to bounding were accomplished by introducing an adjustment step, during which differential thrust of the fore and hind legs gave the body a pitch moment.

- Estimates of power dissipation show that the quadruped dissipates about 1.5 kw (2 hp) standing still, about 2.6 kw (3.5 hp) hopping in place, and about 3.1 kw (4.2 hp) while running at a speed of 2.5 m/s.

6.8 References

Hildebrand, M. 1960. How animals run. *Scientific American* 148–157.

Hodgins, J.K., 1989. *Legged Robots on Rough Terrain: Experiments in Adjusting Stride*, PhD Thesis, Computer Science, Carnegie-Mellon University.

Hodgins, J., Koechling, J., Raibert, M. H. 1986. Running experiments with a planar biped. *Third International Symposium on Robotics Research*, G. Giralt, M. Ghallab (eds.). Cambridge: MIT Press.

Hoyt, D. F., Taylor, C. R. 1981. Gait and the energetics of locomotion in horses. *Nature* 292:239–240.

Koechling, J. and Raibert, M. 1988. How fast can a legged robot run? In: *Symposium in Robotics, DSC-Vol. 11*, K. Youcef-Toumi, H. Kazerooni (eds.). (American Society of Mechanical Engineers, New York).

Marey, E. J. 1874. *Animal Mechanism: A Treatise on Terrestrial and Aerial Locomotion.* New York: Appleton.

McGhee, R. B. 1980. Robot locomotion with active terrain accommodation. In *Proceedings of National Science Foundation Robotics Research Workshop*, University of Rhode Island.

McGhee, R. B., Frank, A. A. 1968. On the stability properties of quadruped creeping gaits. *Mathematical Biosciences* 3:331–351.

Murphy, K. N., Raibert, M. H. 1985. Trotting and bounding in a planar two-legged model. In *Theory and Practice of Robots and Manipulators, Proceedings of RoManSy'84*, A. Morecki, G. Bianchi, K. Kedzior (eds.). Cambridge: MIT Press, 411–420.

Muybridge, E., *Animals in Motion*, (Dover Publications, New York), First Published in 1899, Chapman and Hall, Ltd., London, 1957.

Raibert, M. H. 1986a. *Legged Robots That Balance* (MIT Press, Cambridge).

Raibert, M. H. 1986b. Symmetry in running. *Science,* 231:1292–1294.

Raibert, M. H., Chepponis, M., Brown, H. B. Jr. 1986. Running on four legs as though they were one. *IEEE J. Robotics and Automation*, 2:70–82.

Sutherland, I. E., Ullner, M. K. , Footprints in the asphalt. *International Journal of Robotics Research* 3:*2,* 29–36, 1984.

6.9 Appendix: Power Dissipated by Quadruped

An important parameter of any vehicle is its power dissipation. The quadruped running machine is by no means a vehicle, but we have estimated the hydraulic power it dissipates during its various modes of operation. Hydraulic power dissipation can be estimated by taking the product of the oil flow times the system pressure. For the quadruped, the hydraulic pump maintained system pressure at a constant 3000 psi. Oil flow was the sum of leakage flows and the volume displaced during actuator motion.

	Power Dissipation (kw/hp)			
Gait	0.0 m/s	1.0 m/s	2.0 m/s	2.5 m/s
Trot	2.4/3.2	2.8/3.7	3.0/4.0	3.4/4.5
Pace	2.5/3.4	2.6/3.5	-	-
Bound	2.8/3.7	2.8/3.8	3.0/4.0	3.1/4.2

Table 6–3: Power dissipation in the quadruped during trotting, pacing, and bounding. Each value includes the 2 hp leakage loss measured during standing. All measurements made with supply pressure of 3000 psi.

To estimate leakage flow, we measured the total flow through the system with the quadruped standing in place. In this condition, there was leakage flow through the flapper stage of the servovalves and through the clearance seals of the actuator pistons and rods. Leakage flow was measured by running the low pressure return line into a bucket for 30 seconds, and weighing the collected oil. We found that the quadruped consumed about 2 hp in leakage power when standing still.

To estimate flow when running, we integrated the absolute value of each actuator's velocity, and multiplied by the actuator area. The total flow was the sum of flows through all actuators plus the leakage flow. We have assumed that the leakage flow was about constant for standing and running.

Table 6–3 shows the power dissipation for the quadruped trotting, pacing, and bounding at several speeds. These data show that running speed accounted for about 30% of the total power dissipated, over the speed range of 0 to 2.5 m/s. A large fraction of the power was dissipated in lengthening and shortening the telescoping legs as they went in and out of service. These motions of the legs were essentially unloaded, and could be achieved at much lower power cost with a different leg mechanism design.

The quadruped running machine was not designed to operate with high energetic efficiency. Modest design changes could dramatically alter the power required to make the quadruped stand and run.

Chapter 7

Passive Dynamic Running

Clay M. Thompson and Marc H. Raibert

7.1 Abstract

Previous work has considered how springy legs can improve the efficiency of the vertical motions of running, making them into resonant spring-mass oscillations that recycle energy from one step to the next. This chapter considers how springy hips can be used to improve the efficiency of the legs' fore and aft swinging motions in running. We have studied a passive hopping machine model, composed of links, masses, and springs, but with no actuators. By tuning the mechanical parameters of the system and choosing appropriate initial conditions, we find reentrant trajectories for the system that coordinate the vertical body motions with the leg sweeping motions, and that accommodate ground interaction constraints. Data are presented from a computer simulation of the model.

7.2 Introduction

Running is a motion that combines a vertical oscillation of the body with a fore-aft oscillation of the legs. Previous work by us and by others has considered how elastic energy storage can be used to generate vertical motion of the body, without requiring a large expenditure of energy on each step. The body can bounce on springy legs during the stance phase, storing a portion of the kinetic energy as strain in the leg springs, and releasing it later to help power the next step. This approach is appealing because it offers energetically efficient vertical motions of the body, and contributes to simplified control. This approach is used by some legged robots (Raibert 1986) and by many animals (Alexander 1988).

In this chapter we consider how elastic energy storage might also be used to generate the fore-aft oscillations of the legs, without large energy expenditure. The goal is to avoid

losing the kinetic energy of the legs each time they reverse their fore-aft sweeping motion. The leg's kinetic energy increases with the square of running speed, so these losses are particularly severe at high running speeds. Our approach is to turn the legs into harmonic oscillators which approximate the motions needed for running. The legs can be made into harmonic oscillators by introducing torsional springs at the hip joints. The resulting leg oscillations move the foot backward with respect to the hip during the stance phase, and forward in preparation for the next step during the flight phase.

The objective of this study was to see if we could design a simple passive system that moved its legs with suitable trajectories for running. We implemented computer simulations of a planar one-legged model composed entirely of springs, masses, and linkages. The model is shown in Figure 7–1. We manipulated the running trajectories by tuning the natural frequency of the vertical bouncing motion to be a specific fraction of the natural frequency of the leg swinging oscillation, and by choosing initial conditions according to the running speed. We manipulated the parameters until phase plots of the variables indicated behavior that repeated on itself, one step after another. The observed running trajectories had a high degree of reentrance, with nearly no energy losses.

The systems we consider are passive in that they are made up of springs, links, and masses, with no actuators or other sources of external energy. In doing these studies we do not suggest that a physical legged system can operate passively for sustained periods of time. A source of energy is needed to make up for mechanical losses, some of which are unavoidable, and a source of control is needed to maintain the reentrant running trajectory. Once the passive part of the system is understood, it should be possible to introduce actuators and algorithms that provide energy and control. We expect physical legged systems that use this approach to have a *tuned gait*, for which the energy efficiency will be highest. At other gaits the system will perform with reduced efficiency, depending on how far the gait deviates from the tuned gait.

7.3 Background

Means for providing efficient fore-aft motion of the legs have been considered in previous work. Mochon and McMahon (1980, 1981) modeled the human leg as a compound pendulum. They showed that the behavior of the leg during the swing phase of human walking could be accomplished as a passive ballistic motion requiring no energy other than that delivered through forward motion of the hip. McGeer (1989a) built a nearly passive walking machine that used ballistic swing motions not too different from those modeled by Mochon and McMahon. His machine had two single-link pendulum legs and it used gravity to sustain the walking motion. More recently, McGeer (1989b) analyzed a two-legged passive dynamic running model and gave conditions for reentrant behavior and stability.

Ivan Sutherland discussed a *tuning fork* model of locomotion in 1983 (Sutherland 1983). He noticed that the motions of the tines of a tuning fork were somewhat like the leg motions used by animals during walking and running.

Alexander (1988) has studied the broad question of how springs are used in animal

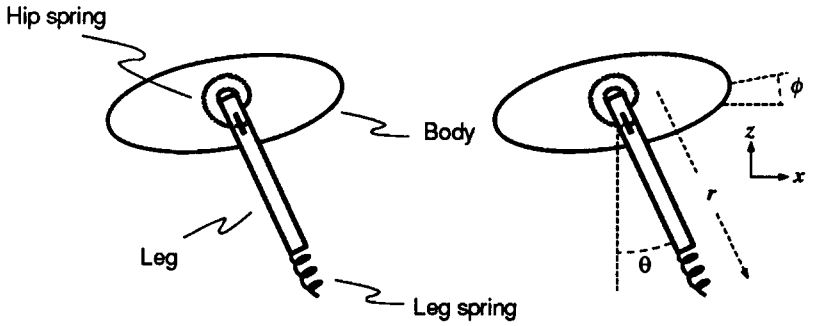

Figure 7–1: Diagram of planar one-legged model used in simulations.

locomotion. He has proposed that the aponeurosis, a sheet of tendon found in the backs of some quadrupeds, might act like a tension spring when the back is bent, with the vertebral column acting as a compression spring. These springs could reverse the direction of the legs during the gathered phase of galloping. He estimates that about half of the internal energy could be stored in the aponeurosis and vertebral column of a fast galloping deer (Alexander *et al.* 1985).

7.4 Models

To study passive dynamic running we used a computer simulation of a planar one-legged model. The model is shown in figure 7–1. The model has a body of mass m_b and moment of inertia J_b measured about the hip, and a leg of mass m_ℓ and moment of inertia J_ℓ, also measured about the hip. The model has two springs. The hip spring acts between the leg and the body, exerting torque about the hip axis. The hip spring has stiffness k_h. A leg spring acts along the leg axis, between the lower part of the leg and the support surface. The leg spring is massless, it exerts force only during the stance phase, and has stiffness k_ℓ.

There is a third spring that acts tangent to the leg axis. This spring, stiffness k_t, represents the combined lateral compliance of the foot and the ground. The constitutive relations for the leg and tangent springs determine the forces applied to the foot during contact. The equations of motion that describe the system are:

$$\ddot{x}(m_b + m_l) = F_x \tag{7.1}$$

$$\ddot{z}(m_b + m_l) = F_z - (m_b + m_l)g \tag{7.2}$$

$$\ddot{\phi}J_b = k_h(\theta - \phi) \tag{7.3}$$

$$\ddot{\theta}J_\ell = r(F_x \cos\theta + F_z \sin\theta) - k_h(\theta - \phi) \tag{7.4}$$

where $[x\ z\ \phi]$ are the position and orientation of the body in the plane, and $[F_x\ F_z]$ isthe ground force acting on the foot.

A variable-step Runge-Kutta routine was used to integrate the equations of motion to obtain behavior as a function of time. For each simulation, we chose initial conditions and adjusted parameters to get the desired reentrant behavior. In the following paragraphs we describe the behavior of the model when it runs, and the methods we used for choosing the parameters and initial conditions needed to obtain reentrant passive dynamic running.

Symbol	Description	Nominal Value
g	acceleration of gravity	$9.81\,\mathrm{m/sec^2}$
m_b	body mass	10.0 kg
J_b	body moment of inertia	$2.5\,\mathrm{kg \cdot m^2}$
r	leg length	
r_0	leg rest length	0.7 m
m_ℓ	leg mass	1.0 kg
J_ℓ	leg moment of inertia	$0.25\,\mathrm{kg \cdot m^2}$
k_h	hip spring constant	
k_ℓ	leg spring constant	
k_t	leg tangent spring constant	$k_\ell/10$
x	forward position of hip	
z	vertical position of hip	
θ_b	body pitch angle w.r.t horizontal	
θ_ℓ	leg angle w.r.t. vertical	
$\dot{z}_{lo}$	vertical liftoff velocity	
F_x	horizontal ground force	
F_z	vertical ground force	

Table 7–1: Parameters and variables names for one-legged passive model.

Vertical Bouncing

During flight, the center of mass of the system travels along a parabolic trajectory determined by the vertical position and velocity at liftoff

$$z(t) = z_{lo} + \dot{z}_{lo}t - \frac{gt^2}{2} \tag{7.5}$$

where z_{lo}, $\dot{z}_{lo}$ are the vertical position and velocity of the body at liftoff, and g is the acceleration of gravity. The peak altitude is

$$z_{max} = z_{lo} + \frac{\dot{z}_{lo}^2}{2g}. \tag{7.6}$$

The duration of the flight phase is

$$T_f = \sqrt{\frac{8z_{max}}{g}} = \frac{2\dot{z}_{lo}}{g}. \tag{7.7}$$

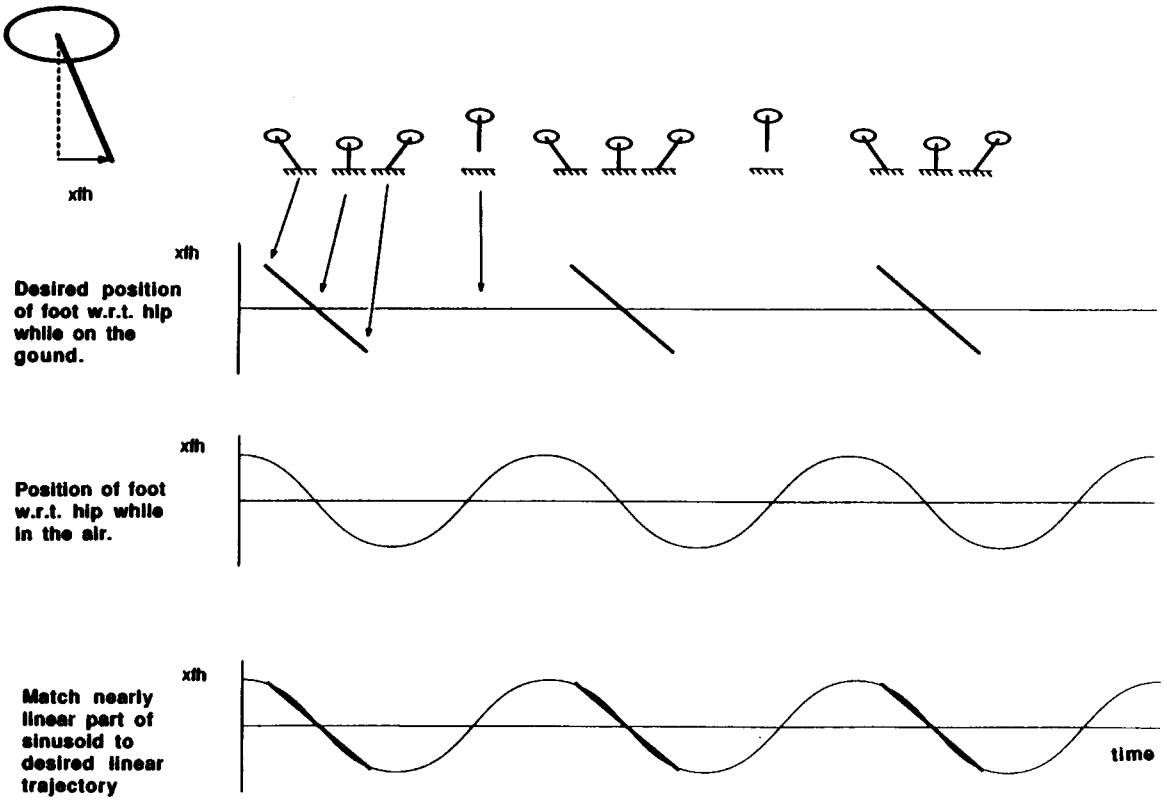

Figure 7–2: Harmonic oscillation of the hip moves foot approximately as desired for constant speed forward running. A) Plot of horizontal position of the foot with respect to the hip during the stance phase, for constant speed forward travel. B) Plot of horizontal position of foot with respect to the hip for harmonic hip oscillation, assuming a fixed leg length. C) Comparison of the two curves shows that harmonic hip motion would provide a good approximation to constant speed forward travel.

During stance, the vertical motion is a harmonic rebound determined by the system mass bouncing on the leg spring. The natural frequency of this rebound is

$$\omega_\ell = \sqrt{\frac{k_\ell}{m_b + m_\ell}}. \tag{7.8}$$

From McMahon and Cheng (1989) we know that the duration of the stance phase in vertical hopping is

$$T_s = \frac{2(\pi - \arctan(|\dot{z}_{lo}|\omega_\ell / g))}{\omega_\ell} \tag{7.9}$$

In this chapter we approximate the stance phase as one half cycle of the natural oscillation:

$$T_s \approx \frac{\pi}{\omega_\ell}. \tag{7.10}$$

This approximation is valid when the vertical velocity at touch down is large compared to g/ω_ℓ, or when the ratio of flight duration to stance duration is greater than 1. This analysis

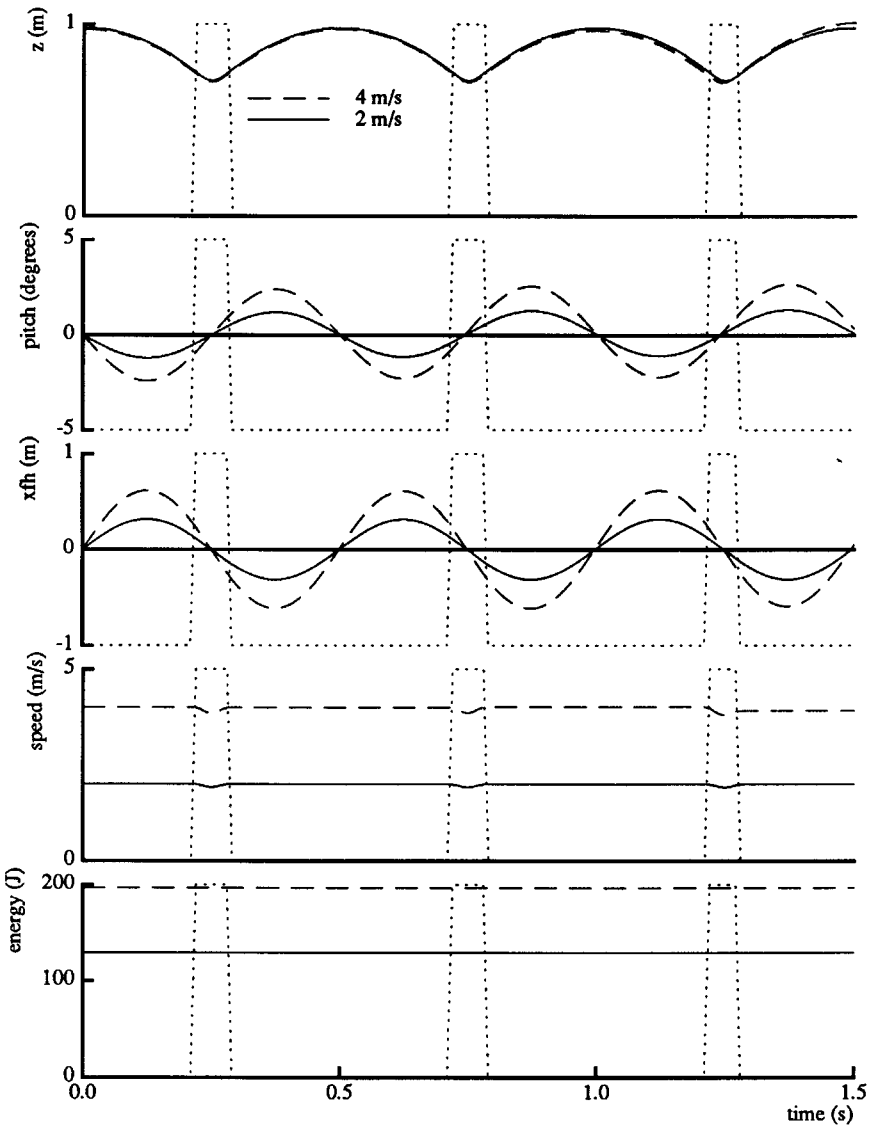

Figure 7–3: Passive dynamic running of planar one-legged hopper. Data are from computer simulations of model shown in figure 7–1a and described in table 7–1. Data are shown for running speeds of 2 and 4 m/s. Vertical dotted lines bracket the stance phase. Solid) $\dot{x} = 2\,\text{m/s}$, $k_h = 35.9\,\text{kg}\cdot\text{m}$, $k_\ell = 29{,}750\,\text{kg/m}$, $z_{max} = 0.98\,\text{m}$, $\dot{\theta}_0 = 2.67\,\text{rad/sec}$. Dashed) $\dot{x} = 4\,\text{m/s}$, $k_h = 35.9\,\text{kg}\cdot\text{m}$, $k_\ell = 25{,}500\,\text{kg/m}$, $z_{max} = 0.97\,\text{m}$, $\dot{\theta}_0 = 5.33\,\text{rad/sec}$.

of the vertical motion is strictly valid only for hopping in place, without forward travel and sweeping motions of the legs. Closed form solutions for the stance duration of non-vertical hopping are not known (McMahon and Cheng, 1989).

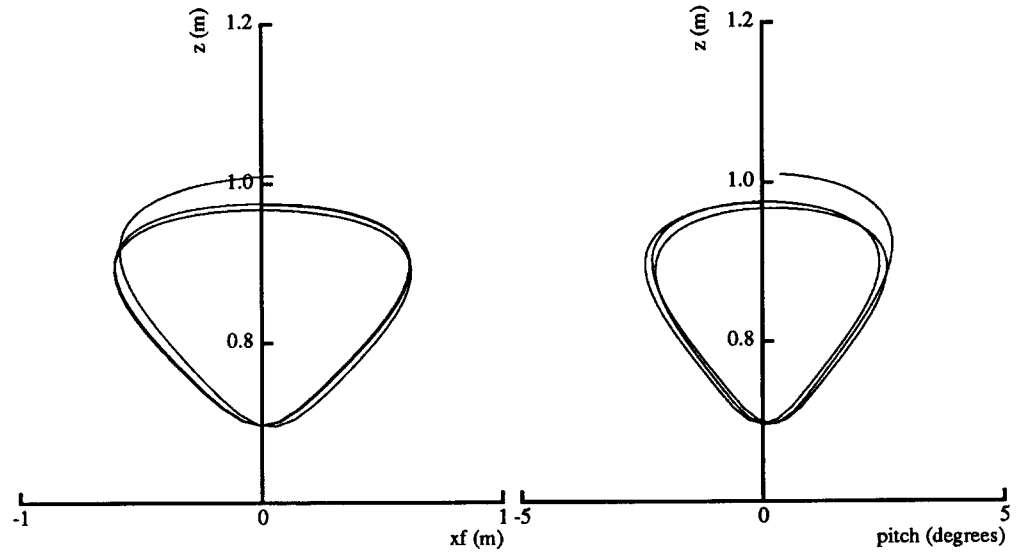

Figure 7–4: Data from figure 7–3 (4 m/s) replotted as one variable against another. If the behavior were perfectly reentrant, the plotted trajectories would perfectly superimpose. The outlying branches at the top of each plot indicate that after about three running cycles the behavior began to diverge from the reentrant trajectory. Both plots are for the same run of the one-legged model. $\dot{x} = 4\,\mathrm{m/s}$, $k_h = 35.9\,\mathrm{kg{\cdot}m}$, $k_\ell = 25{,}500\,\mathrm{kg/m}$, $z_{max} = 0.97\,\mathrm{m}$, $\dot{\theta}_0 = 5.33\,\mathrm{rad/sec}$.

Hip Oscillation

The natural frequency of the hip oscillation is given by

$$\omega_h = \sqrt{\frac{k_h}{J_{eff}}}, \tag{7.11}$$

where k_h is the hip spring constant and $J_{eff} = J_b J_\ell/(J_b + J_\ell)$ is the effective moment of inertia of the combined leg and body about the hip. The characteristic period of the hip oscillation is

$$T_h = \frac{2\pi}{\omega_h}. \tag{7.12}$$

The horizontal displacement of the foot from the hip is

$$x_f = r\sin(\theta_{max}\sin(\omega_h t)) \tag{7.13}$$

where r is leg length and θ_{max} is the amplitude of the hip oscillation. We have assumed that the hip spring is at rest when $\theta = \phi = 0$. This function, plotted in figure 7–2, is approximately linear in time for small values of time and θ_{max}.

7.5 Choosing Parameters for Passive Dynamic Running

Figure 7–2 plots foot motion for an ideal legged system traveling forward at constant speed. During the stance phase, the foot does not move with respect to the ground, so the velocity of

the foot with respect to the body is the negative of the body's forward velocity. Therefore, for forward travel at constant speed, foot position with respect to the body is a linear function of time. During the flight phase, the primary constraint on foot motion is that the foot be moved forward in time for the next stance phase.

Our basic approach to finding passive reentrant running trajectories is based on the fact that harmonic hip motion can generate foot motion that closely approximate the foot motion found in constant speed forward travel. Figure 7–2 shows a foot motion produced by a harmonic hip oscillation that was tuned to approximate the foot motion used in ideal constant speed travel. The approximation is based on the linearity of the *sin* function for small values of its argument.

The remainder of this section describes how we choose system parameters and initial conditions to find reentrant trajectories for the model. We assumed fixed values of body mass m_b, body moment of inertia J_b, leg mass m_ℓ, leg moment of inertia J_ℓ, and nominal leg length r_0. Given a desired running speed $\dot{x}_d$ and step period T_{step}, we choose the spring constant for the hip k_h, spring constant for the leg k_ℓ, initial leg pitch rate $\dot{\theta}_0$, initial body pitch rate $\dot{\phi}_0$, and initial body altitude z_{max}.

Hip spring constant k_h

The stiffness of the hip spring is chosen so the hip undergoes one complete oscillation during one complete step. The natural frequency of the hip oscillation is

$$\omega_h = \frac{2\pi}{T_{step}} = \sqrt{\frac{k_h}{J_{eff}}}. \tag{7.14}$$

From (7.14) we see that

$$k_h = (2\pi/T_{step})^2 J_{eff} \tag{7.15}$$

where T_{step} must be specified.

Leg spring constant k_ℓ

The stiffness of the leg spring is chosen to establish the duration of the stance phase as a fraction of the stride period. We define a duty factor ρ, which expresses the duration of the stance phase as a fraction of the step period

$$\rho = T_s/T_{step} = \frac{\omega_h}{2\omega_\ell}, \tag{7.16}$$

assuming the stance phase is one half cycle of leg spring oscillation. We choose a value for the duty factor to ensure that the stance phase occurs during the roughly linear portion of the foot's fore-aft travel. Small values of ρ give the best linearity, but result in larger peak leg forces and longer flight durations. We experimented with values of ρ between 0.125 and 0.35. A good value for ρ is 0.125, but the smaller the better.

Given the natural frequency of the hip and a value of ρ, the leg spring constant k_ℓ can be found

$$k_\ell = m(\frac{\pi}{\rho T_{step}})^2. \tag{7.17}$$

Because we do not have an exact expression for T_s, (7.17) gives a value for k_ℓ that only approximates the desired value for ρ. The desired value of ρ is obtained by adjusting k_ℓ iteratively on a series of trials.

Initial values for leg angular rate $\dot{\theta}_0$ and body angular rate $\dot{\phi}_0$

The amplitude of the hip oscillation and the speed of the foot as it moves back and forth are both determined by the initial value of the leg angular rotation rate, $\dot{\theta}_0$. This parameter is selected so the speed of the foot moving backward during the stance phase matches the desired forward speed of the body.

The simulation is begun by dropping the model from a specified height. Therefore, the initial state of the system is equivalent to the state at mid flight. The angular leg rate at mid flight equals the angular rate at mid stance, with a sign reversal. The angular leg rate is chosen so the backward foot velocity at mid stance is matched to the desired forward speed

$$\dot{\theta}_0 = \dot{x}_d / r. \tag{7.18}$$

From (7.18) and (7.13) we find the maximum leg angle $\theta_{max} = \dot{\theta}_0 / \omega_h$.

To maintain zero angular momentum during flight, the body and leg must counteroscillate, with rates and amplitudes inversely related to their moment of inertia

$$\frac{\dot{\phi}}{J_\ell} = -\frac{\dot{\theta}}{J_b}. \tag{7.19}$$

The initial value of body pitch rate is therefore $\dot{\phi}_0 = -(\dot{\theta}_0 J_\ell)/J_b$.

Initial value for vertical position of body, z_{max}

The duration of the flight phase is manipulated by choosing the initial altitude of the body. The duration of a step is $T_{step} = T_s + T_f$. We choose the parameters of the system so that $T_s = \rho T_{step}$, which gives a flight phase duration

$$T_f = (1 - \rho) T_{step}. \tag{7.20}$$

The initial altitude that provides the correct flight duration is

$$z_{max} = \frac{g}{8}(1 - \rho)^2 T_{step}^2 + \frac{r_0 \dot{\theta}_0}{\omega_h} \cos \frac{\omega_h T_s}{2}, \tag{7.21}$$

where the second term is the altitude of the body at touchdown. Examining (7.14) through (7.21), we see that three independent parameters are required to specify the passive dynamic running motion: T_{step}, ρ, and $\dot{x}$. Other parameters needed to specify the motion can be calculate from these three.

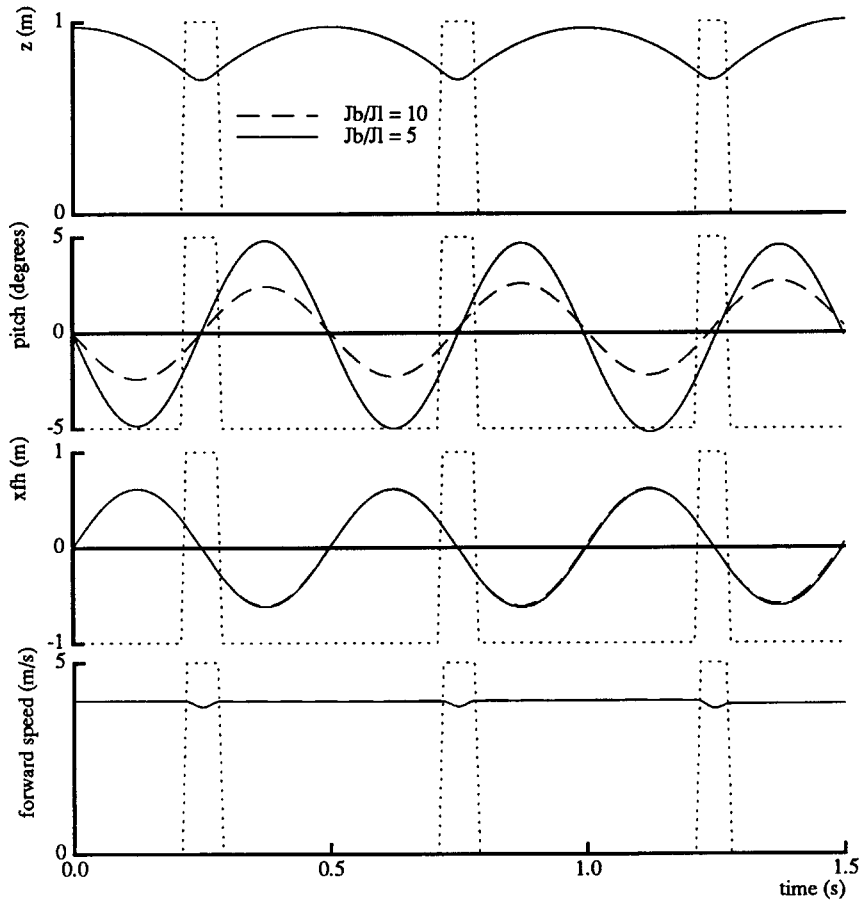

Figure 7–5: The ratio of body moment of inertia to leg moment of inertia determines the amount of body pitching. A larger body moment of inertia results in smaller body pitch amplitude. In all other respects, the two running motions are indistinguishable. $\dot{x} = 4\,\text{m/s}$, $k_h = 65.8\,\text{kg} \cdot \text{m}$, $k_\ell = 25{,}500\,\text{kg/m}$, $z_{max} = 0.97\,\text{m}$, $\dot{\theta}_0 = 5.33\,\text{rad/sec}$.

7.6 Results

Figures 7–3 and 7–4 show the results of a typical simulation of the model. The initial conditions used to generate the figures were determined from equations (7.5) – (7.21) as described above, and through a hand optimization process. During optimization, the leg spring constant was changed until we obtained the required stance duration and a reentrant running cycle.

Once the hip and leg spring stiffnesses are chosen, it is possible to manipulate the initial conditions to run at different speeds. Figure 7–3 includes data for two running speeds. The physical parameters of the model were the same for both running speeds, with adjustments made only in the initial conditions. This suggests that a single machine could run at a range of speeds, without requiring mechanical tuning.

Figure 7–5 shows data for simulations with two different ratios of leg moment of inertia to body moment of inertia. The magnitude and rate of body pitching are the only variables

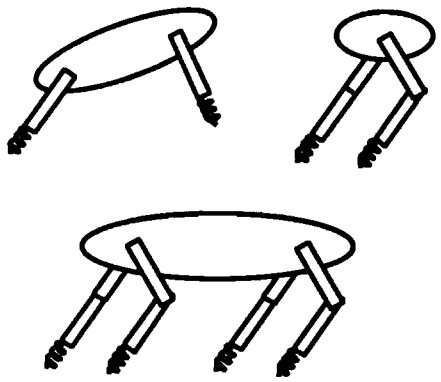

Figure 7–6: Models with compound pendulum legs and springy hips. The leg would fold during the swing phase, and pogo during the stance phase.

affected by this change. The behavior of all other variables remains unchanged.

The trajectories explored in this chapter represent unstable equilibria. Although the behavior is reentrant if the system is undisturbed, there is no mechanism to return the system to the passive trajectory if there is a disturbance that causes it to deviate. This effect is seen more clearly in figure 7–4, where the position of the foot with respect to the hip and pitch angle are plotted against altitude. These data show a gradual drift in the phase trajectory. If the trajectory were stable, it would return to an equilibrium limit cycle. A complete implementation of passive dynamic running would include a control mechanism to stabilize the oscillation and eliminate this sort of drift.

So far we have considered passive dynamic running in the context of a planar one-legged hopping machine with a telescoping leg. We have also considered a planar two-legged system with telescoping legs, as shown at the top left in figure 7–6. So far, we have found reentrant trajectories for this planar two-legged system when the legs are used in synchrony. We would like to find a passive bounding trajectory that uses the legs out of phase, but have not yet done so. We intend to study systems with compound pendulum legs, like those studied by Mochon and McMahon (1980) and shown in figure 7–6.

7.7 References

Alexander, R. McN. 1988. *Elastic Mechanisms in Animal Movement.* Cambridge: Cambridge University Press.

Alexander, R. McN., Dimery, N. J., Ker, R. F. 1985. Elastic structures in the back and their role in galloping in some mammals. *J. Zoology (London)* 207:466–482.

McGeer, T. 1989a. Powered flight, child's play, silly wheels and walking machines, *IEEE Conference on Robotics and Automation*, Phoenix.

McGeer, T., 1989b, Passive bipedal running, *Simon Fraser University Report CSS-IS TR 89-02.*

McMahon, T. A., Cheng, G. C., 1989, The mechanics of running: how does stiffness couple with speed?, Submitted to *Journal of Biomechanics.*

Mochon, S., McMahon, T. A. 1980. Ballistic walking. *J. Biomechanics* 13:49–57.

Mochon, S., McMahon, T. A. 1981. Ballistic walking: An improved model. *Mathematical Biosciences* 52:241–260.

Raibert, M. H. 1986. *Legged Robots That Balance* Cambridge: MIT Press.

Sutherland, I. E. 1983. *A Walking Robot.* Pittsburgh: The Marcian Chronicles, Inc.

Chapter 8

Articulated Leg

H. Benjamin Brown, Jr. and Woojin Lee

8.1 Abstract

Central to the design of a legged system is the mechanical design of the leg itself. Legs are the elements that exert forces on the body to propel the body forward for transport, to counteract gravitational loading, and to keep the body in an upright posture. Most legs designed for legged machines are intended to be rigid, yet animals have legs that deform substantially under load. Compliance in legs can improve efficiency, reduce maximum loading, and simplify control. We have built and tested a number of leg designs on machines having one, two and four legs. These designs use linear telescoping joints to change length and gas springs for axial compliance. This paper discusses a leg design that uses a rotary "ankle" joint for control of length and a fiberglass leafspring as the compliant element. We expect an articulated leg design to yield better performance, reliability, and simplicity. In this chapter, the pros and cons of the telescoping leg and the Monopod's present articulated leg are studied and an alternative improved leg design is considered. In addition, we discuss the design of a mechanism that constraints the motion of experimental legged systems to the plane.

8.2 Introduction

An intriguing characteristic of legs found in nature is their ability to deform elastically during running (Cavagna 1970). The elements primarily responsible for elastic deformation in animal legs are the muscles, tendons, and ligaments. Elastic deformation is used by biological systems to recover a portion of the energy expended during a stride, and to return that energy on the next stride. This can reduce the total cost of transport (Dawson and

Taylor 1973; Alexander and Vernon 1975; Cavagna et al. 1977; McMahon 1984). Another function of compliance in biological legs is to reduce the impact forces and peak loads that are experienced by the leg, the body, and the support surface. Finally, there is the possibility that the compliant character of biological limbs can simplify the control task performed by the nervous system.

In contrast to the compliance of legs found in nature, most legged robots have legs that are designed to be stiff. Because legged machines typically walk rather than run, there may be less need for compliant legs. For instance, locomotion can be energy efficient if the legs move the body in a purely horizontal motion with no actuators absorbing energy. Several legs have been designed according to this principle (Lucas 1894; Hirose and Umetani 1980; Waldron and Kinzel 1983). Impact forces may be kept small during walking by bringing each foot into contact with the ground at low relative speed. Small leg mass and low speed reduce the cost of accelerating the swing motion of the leg.

In this paper we follow nature's lead by concentrating on legs with elastic elements that deform during each stride. We have used such legs in machines that balance actively as they run. The functions of the elastic elements are to conserve energy associated with the bouncing motion, to reduce impact forces, and to simplify control.

Several possible leg configurations are described in figure 8–1. The Cartesian configuration using two linear joints is kinematically simple, but mechanically cumbersome. Most of the legs we have built have been of the polar configuration, having one rotary and one linear joint. Such legs are kinematically simple, and mechanically more elegant than the Cartesian arrangement. We are beginning to investigate articulated legs that use rotary joints. Articulated legs offer mechanical advantages, such as lower moment of inertia, less unsprung mass, larger range of motion, better ruggedness, and ease of construction. However, articulated legs also have added kinematic complexity and coupling between degrees of freedom. This coupling is evident from the fact that displacements of the two joints do not in general cause orthogonal displacements of the toe or hip.

Before describing the specific designs we have studied, we turn to a brief discussion of energy storage in elastic materials. For discussions of other important issues in leg design see (Hirose and Umetani 1980; Vohnout et al. 1983; Waldron and Kinzel 1983).

8.3 Mechanisms for Elastic Storage

Figure 8–2 shows the ratio of storable elastic energy to the mass of the material for several spring materials. Each material has properties that recommend it for use in leg springs, but each has drawbacks as well. Steel is an isotropic material that can easily be formed into shapes such as coils. However, steel springs have a relatively poor energy to mass ratio, about 140 J/kg. Fiberglass has about six times the energy capacity of steel, but because its fiber orientation is crucial, it is not so easily fashioned into a spring. Fiberglass is most readily used in bending as a leafspring or other beam shape.

Rubber and animal tendon have substantially higher energy capacities than steel, about 5000 J/kg. The value for animal tendon is based on Alexander's work with dogs (Alexander,

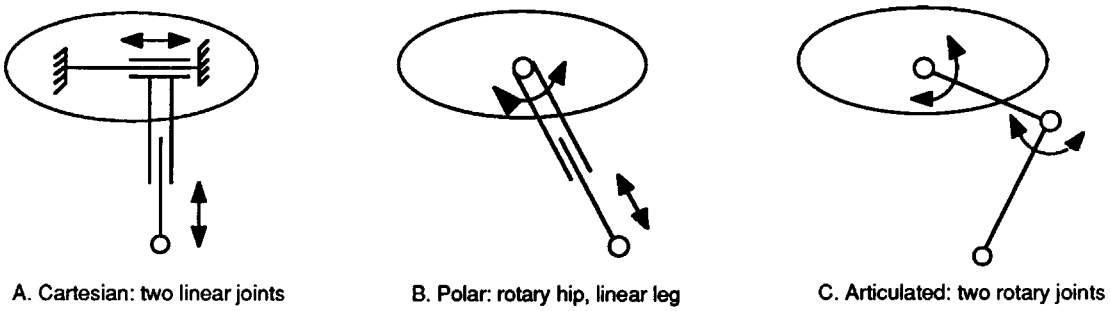

Figure 8–1: Three planar leg configurations: A) Cartesian: two orthogonal, linear joints produce independent motion. The upper joint may be troublesome because it must tolerate substantial torques while providing smooth sliding motion, and the entire mass of the leg must be accelerated in the fore/aft direction to obtain horizontal foot motion. B) Polar: rotary hip and telescoping leg provide motion in polar coordinates. The inertial loads associated with the fore/aft motion of the foot are smaller than for a Cartesian leg, because only the end of the leg moves at full foot speed. Cartesian and polar designs both require linear sliding joints, which are difficult to build with precision and resistance to side load. C) Articulated: two rotary joints avoid the friction, wear, and size disadvantages of linear joints. The drawback is the kinematic coupling of the two joints—a purely vertical or radial motion of the foot requires movement of both joints. This coupling necessitates larger ranges of joint travel than the polar leg to achieve the same foot motion, and it is difficult to resolve the springiness into the vertical direction without degrading the speed and precision of control in the horizontal direction.

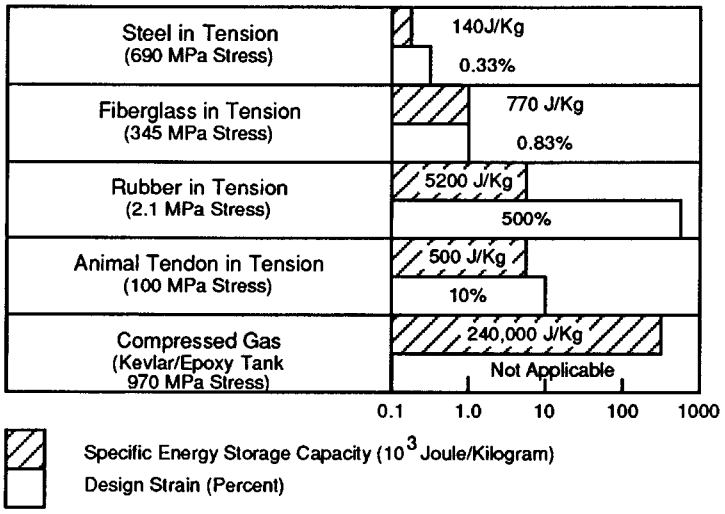

Figure 8–2: Strain energy per unit mass for various materials. The higher the value, the less mass of material needed for a given energy storage function. The strain, or relative elongation of the material, affects the design of the spring.

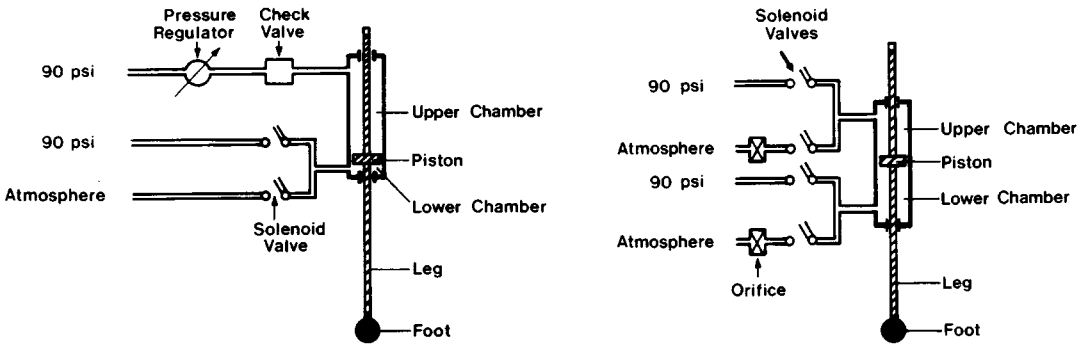

Figure 8–3: Pneumatic telescoping leg used in one-legged hopping machines. It consists of an air cylinder with a cushioned foot at one end of the rod. Electric solenoid valves control air flow to both chambers of the cylinder to extend and retract the leg, while trapped air makes the leg springy. Two pneumatic circuits were used. Left) *Top Control*—Air enters the top chamber to provide downward thrust on the foot during the support portion of the running cycle. The thrust is controlled by adjusting the pressure of the air in the top of the cylinder when the foot touches the ground. This circuit was used in a planar one-legged hopping machine (Raibert and Brown 1984). Right) *Bottom Control*—The control system adjusts thrust by regulating the pressure in the bottom chamber of the leg cylinder while a pressure regulator and check valve maintain a fixed charge of air in the top of the cylinder leg. The top chamber acts as a passive spring. To provide thrust, the control system exhausts air from the bottom chamber of the leg during support. Special quick-exhaust valves are used to dump air rapidly for maximum thrust. Bottom control is more efficient than top control because a smaller volume of air is exhausted on each cycle. This circuit was used in a three-dimensional one-legged hopping machine (Raibert et al. 1984). Sensors measured the length of the leg, the air pressure in both chambers of the air cylinder, the angle of the leg with respect to the body, and contact between the foot and the ground. The unsprung mass of the leg is 0.91 kg and moment of inertia about the hip is 0.11 kg-m^2.

1974). Because these materials can undergo large elastic strains they can provide usable deflections in pure tension. The 10% strain of the Achilles tendon of an animal is compatible with the short lever arm to which the tendon is attached behind the ankle joint. For example, Alexander's data for the dog indicate that its Achilles tendon is linked to the foot so that it undergoes about one-fourth the deflection of the toe. No material usable in human-made machines has been found with equivalent elastic properties. Rubber, because it strains about 50 times as much as animal tendon, cannot be used directly in a leg design like the dog's. Rubber is often used in the form of torsion springs and bushings that shear tangentially when loaded. Such torsion springs might be usable in rotary leg joints.

Gas compressed in a container with high specific strength has a very high energy capacity, about 240,000 J/kg. A usable gas spring requires a cylinder and piston or comparable hardware, however, which will likely weigh many times as much as an ideal container. Frictional and thermodynamic losses can be substantial. Still, gas springs may be used effectively if they are compatible with the overall design.

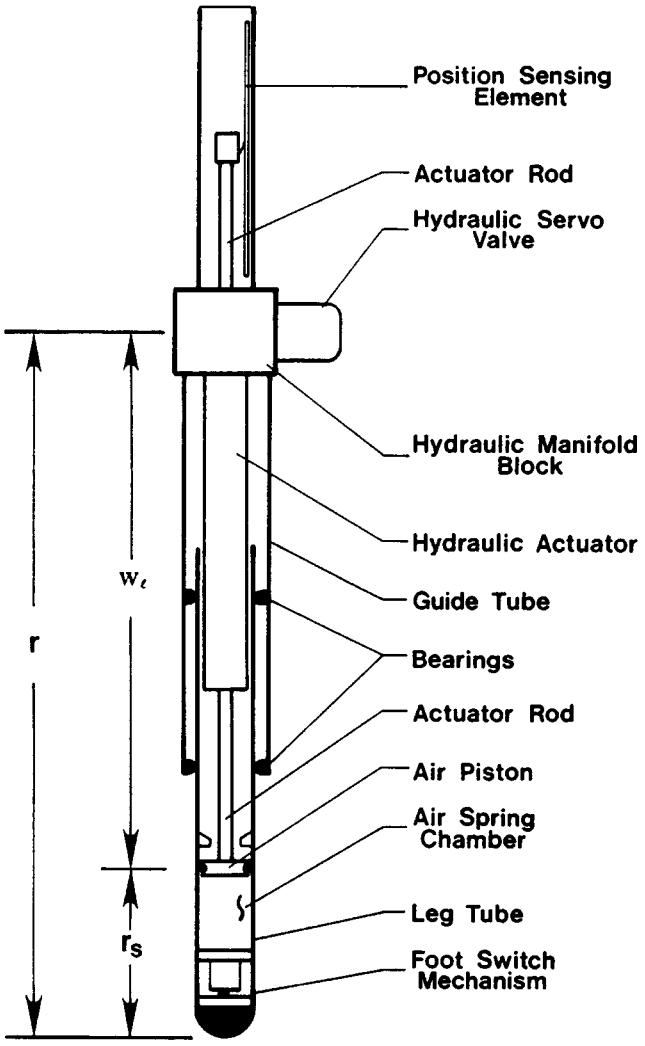

Figure 8–4: Hydraulic-pneumatic telescoping leg. See figure 8–5 for design details. A long-stroke hydraulic actuator provides controlled axial thrust and rapid retraction. An air chamber near the foot provides the spring. To reduce friction in the hydraulic actuator, all high-pressure seals are clearance seals (0.025 mm), with O-ring seals used to contain low-pressure leakage oil at the rods. Space between concentric cylinders provides paths for control and leakage flow to the lower end of the hydraulic actuator. The hydraulic actuator is servoed with a conventional high-bandwidth flow-control servo valve. The air cylinder forms the lower part of the leg and slides inside plastic guide buttons mounted in the upper leg tube. The foot includes a pneumatic check valve that allows makeup flow to the air spring, but prevents out-flow when the air spring is compressed. The hydraulic actuator has a 0.23 m travel and the air spring has a 0.10 m travel. At 17.5 MPa (2500 psi) hydraulic pressure, maximum thrust is about 950 N and maximum speed is about 2 m/s. The unsprung mass is 0.24 kg and moment of inertia of the leg about the hip is 0.13 kg-m^2. This leg design was used in a planar biped (Hodgins, Koechling, and Raibert 1986), and in a quadruped running machine (Raibert, Chepponis and Brown 1986).

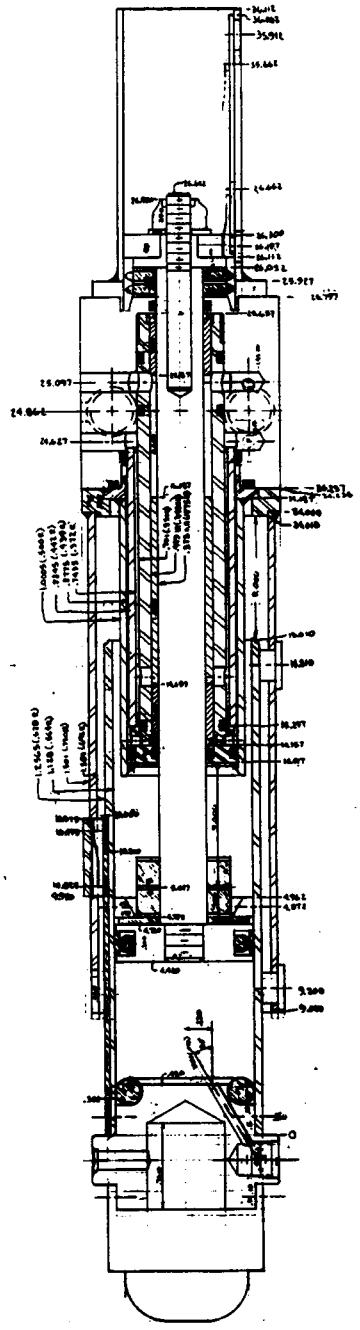

Figure 8–5: Engineering drawing of the hydraulic-pneumatic leg, showing details of the hydraulic actuator, air spring and position sensors. Leg is shown compacted in the axial direction.

8.4 Telescoping Legs

After initial attempts to use steel springs in compression, we turned to compressed gas as a mechanism for elastic energy storage in legs for running machines. A standard pneumatic cylinder with low friction seals formed the main structure of the leg in our first successful running machine. The cylinder was mounted to the body of the machine with a hinge-type hip joint, and a rubber bumper at the end of the piston rod served as a foot. A set of on-off pneumatic valves and the circuits shown in figure 8–3 provided thrust and retraction, and controlled the leg's springiness.

This pneumatic telescoping leg was used for a series of experiments on the control of machines that balanced actively as they ran (Raibert and Brown 1984; Raibert, Chepponis, and Brown 1984). One function of the spring used in these experiments was to recover part of the hopping energy during landing and return it during the subsequent upward acceleration. In an optimized design this could contribute to efficient locomotion. A second function was to provide a cushion for the upper leg and body. This cushion reduced the system's unsprung mass, the maximum loads produced by foot impacts with the ground, and the peak forces transmitted to the sprung part of the system. A third function of the spring was to simplify the control. The details of the vertical bouncing motion were determined largely by the passive oscillation of the body rebounding on the springy leg—the control system excited and modulated this oscillation but was not responsible for the details of the trajectory (Raibert 1986a).

To study running on several legs we needed a leg that could lengthen and shorten rapidly, and precisely control thrust. Rapid shortening was needed so that the recovery leg could have adequate ground clearance to swing forward while the stance leg was substantially compressed. The need to control thrust arises when coordinating the relative thrust delivered by a pair of legs that both provide support at the same time.

To satisfy these requirements—rapid retraction during recovery and precise control of thrust—we designed the leg shown in figures 8–4 and 8–5. It has a long-stroke hydraulic actuator that operates in series with a passive air spring. This leg has been used in a biped that runs and hops, and in a quadruped that trots (Hodgins, Koechling, and Raibert 1986; Raibert, Chepponis, and Brown 1986). Although this design has been used successfully in experiments, it has several limitations:

- The leg is relatively heavy.
- Seal leakage and friction during compression degrade the resilience of the air spring.
- The sliding joint is mechanically complex and bulky, and subject to wear and looseness.
- Measuring leg length requires a long, specially made sensor.
- Wires to the foot must go through slack cables that are vulnerable to a variety of hazards.
- The moment of inertia of the leg is substantially larger than desired.

These limitations have motivated us to explore articulated legs that use only rotary joints.

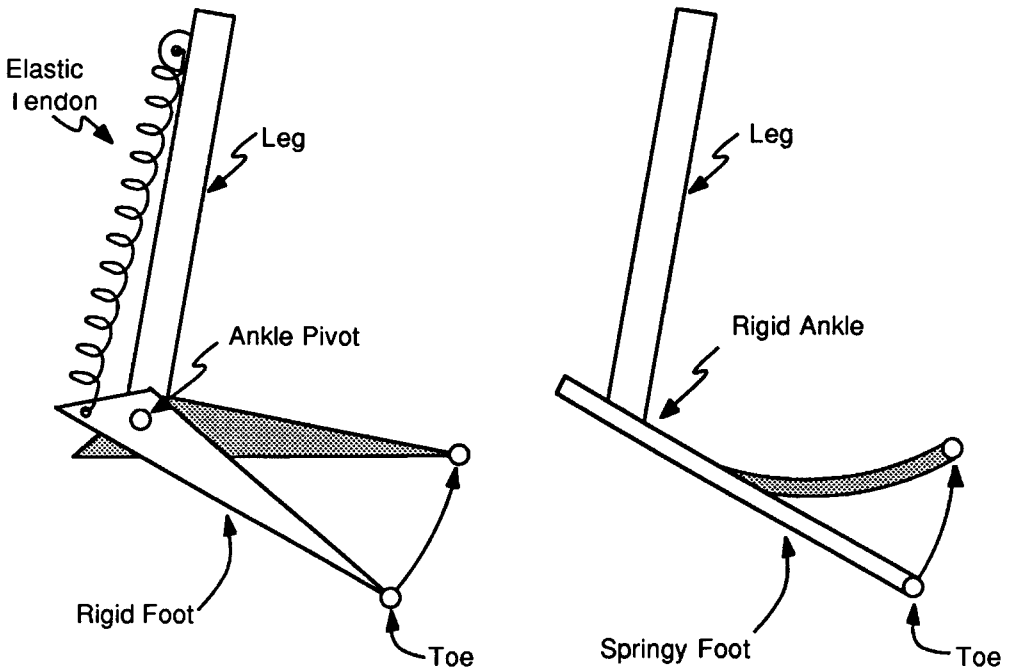

Figure 8–6: Articulated legs. Left) An anthropomorphic design uses a hinged, inflexible foot with a springy tendon. Right) Alternate design employs bending of an elastic foot to provide springiness.

8.5 Articulated Leg

A fundamental objective in the design of an articulated leg has been to provide compliance in the radial direction but not in the tangential direction. Such a leg would be functionally similar to the telescoping legs we have already built. As a first step, we considered two methods for incorporating springiness in the leg, as shown in figure 8–6. The somewhat anthropomorphic design shown on the left side of figure 8–6 incorporates a rotary ankle joint that connects a rigid foot to the leg. An elastic tendon acts through a lever behind the ankle to provide the needed downward force and compliance at the toe. A suitable tendon material for such a design has not been found.

The design shown on the right side of figure 8–6 employs a noncompliant tendon that acts on a leafspring foot. Energy can be stored in the bending of the foot. The design combines the structural and elastic functions into a single unit, minimizing mass. Because of the distributed nature of a leafspring, the effective unsprung mass is small. This results in low impact forces during running, minimizing energy losses.

To test the springy-foot concept we built the one-legged machine, or "monopod" shown in figure 8–7. This machine is constrained to operate in the plane by a tether mechanism that permits forward and vertical translation and pitch rotation. The foot is actuated about a rotary ankle joint by a linear hydraulic actuator that pulls on the foot through an inelastic tendon. This actuator is located at the hip to minimize the rotational inertia of the leg. A second hydraulic actuator drives the swing motion of the hip. The machine is designed to run on its toe, which is located below the center of mass of the machine when the leg

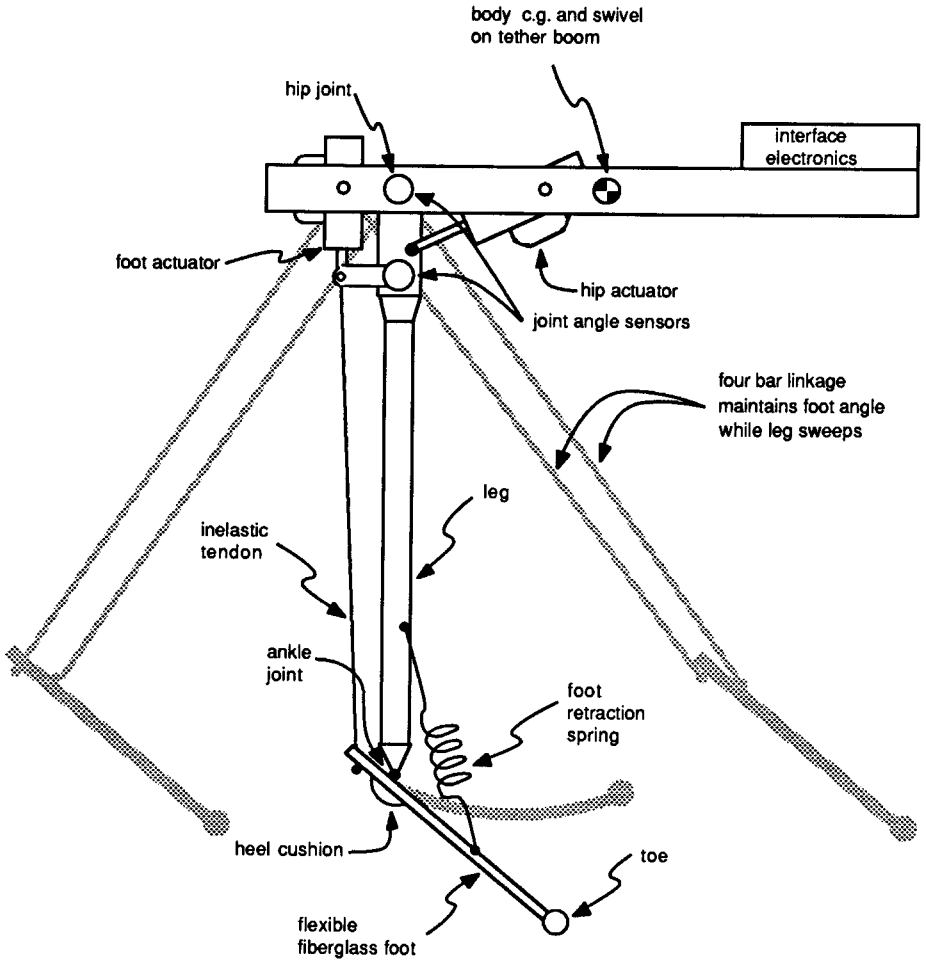

Figure 8–7: Diagram of monopod with articulated leg. The foot is a leafspring that deflects during hopping. The ankle is actuated through an inelastic tendon and hydraulic actuator mounted at the hip. A retraction spring attached to the foot maintains tension in the tendon. The linkage makes the foot angle with respect to the body nearly independent of the hip angle. Potentiometers measure the two joint positions and foot deflection. The leg is intended for planar operation. The unsprung mass is 0.063 kg and moment of inertia of the leg about the hip is 0.097 kg-m^2.

is vertical. The hip is offset from the center of mass by a distance roughly equal to the offset of the ankle with respect to the toe, so the leg is nominally vertical when the hip is centered. The four-bar linkage formed by the leg, heel lever, body, and tendon keeps the orientation of the foot with respect to the body nearly constant as the leg swings fore and aft. Appendix A gives the physical parameters for the machine. Appendix B describes in detail the kinematics of the machine.

The number of sensors used for control of the monopod is small. Rotary potentiometers measure the angles of the hip and ankle joints. A rotary potentiometer connected to

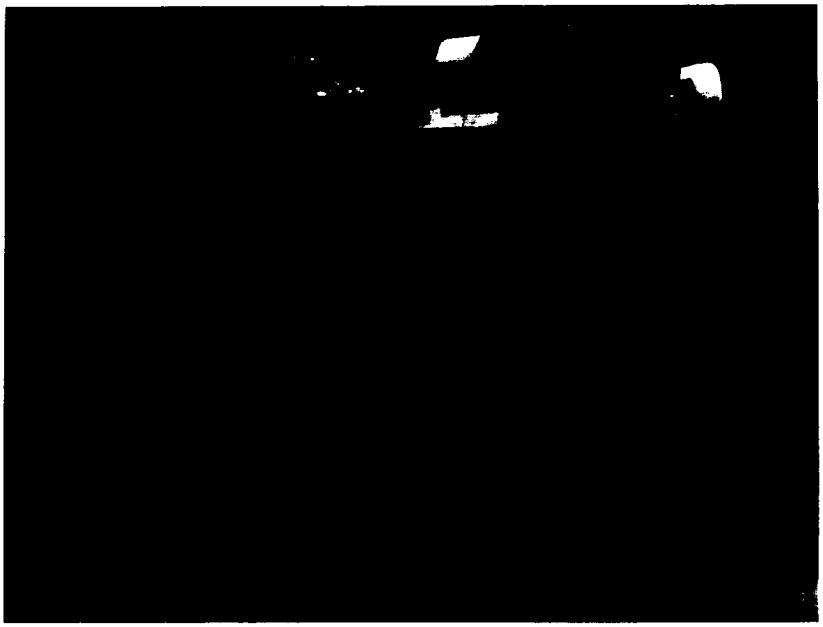

Figure 8–8: Photograph of the monopod. A long beam attached to the body allows mounting of weights to adjust location of the center of gravity and body moment of inertia. Metal tubing on frame carries hydraulic fluid which is fed through swivels to actuators. The aluminum arm and potentiometer on the foot are mounted to measure foot deflection.

the ankle and toe measures deflections of the foot and contact with the ground. Rotary potentiometers at the base of the tether boom measure the horizontal and vertical positions of the center of the machine.

The control system for the monopod uses the same three-part control decomposition that we have used many times in the past. Hopping height is controlled by shortening the tendon actuator during stance. This excites the spring-mass system formed by the springy foot and the body. The body's pitch attitude is controlled by applying hip torque during stance in proportion to body pitch angle and pitch rate errors. Forward speed is controlled by setting the position of the toe with respect to the body at touchdown. A number of features described later in this chapter have been incorporated to improve performance.

8.6 Monopod Experiments

The monopod is being used to evaluate mechanical designs, and to explore what impact an articulated leg has on the control of dynamic legged locomotion. In each experiment an operator starts the machine by aligning the body and leg, and then dropping the system from a few inches to start it bouncing. Then the operator manipulates a joystick to specify desired running speed. During these experiments the operator adjusts parameters to examine various aspects of the mechanical system or the control.

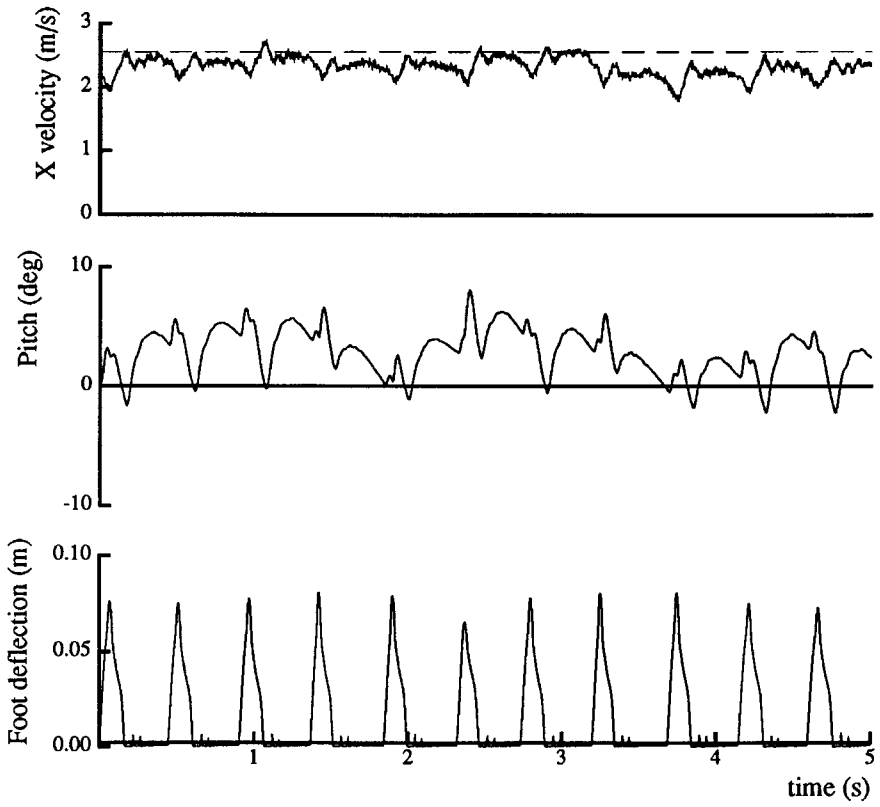

Figure 8–9: Running at constant speed. Periods of stance can be distinguished from the lower graph of foot deflection. The single peaks in foot deflection indicate the absence of heel impacts with ground. Positive spikes in pitch velocity show forward pitching when the toe strikes the ground. The top graph shows that forward running speed $\dot{x}$ is near the desired value, which is shown by the broken line. (Data file M.155.1)

Figure 8–9 shows data from one of the best runs the machine has made, with a maximum running speed of 2.3 m/s (5.1 mph) averaged over 16 m. The machine tracked the desired speed with an error of about 0.2 m/s at steady speed. The body's pitch angle error was kept below 5 deg, typically with a nose-down posture.

Early experiments were performed using 1500 psi hydraulic supply pressure, a relatively low value, to minimize the potential for damage to the machine. We found that this pressure was inadequate for the tendon actuator to maintain the foot's position under maximum loading during stance. This permitted the heel of the foot to collide with the ground. The 1500 psi of hydraulic pressure can produce only about 1100 N of tension in the tendon, while peak ground reaction forces are around 1600 N. Figure 8–10 shows this condition. The heel impact is shown by the disturbance in the foot deflection curve just after its peak. Comparison of the foot angle and its setpoint indicates that the actuator is being backdriven by the ground contact force. Impact of the heel causes a substantial disturbance in pitch, shown particularly in the pitch velocity signal, and results in severely nose-down running.

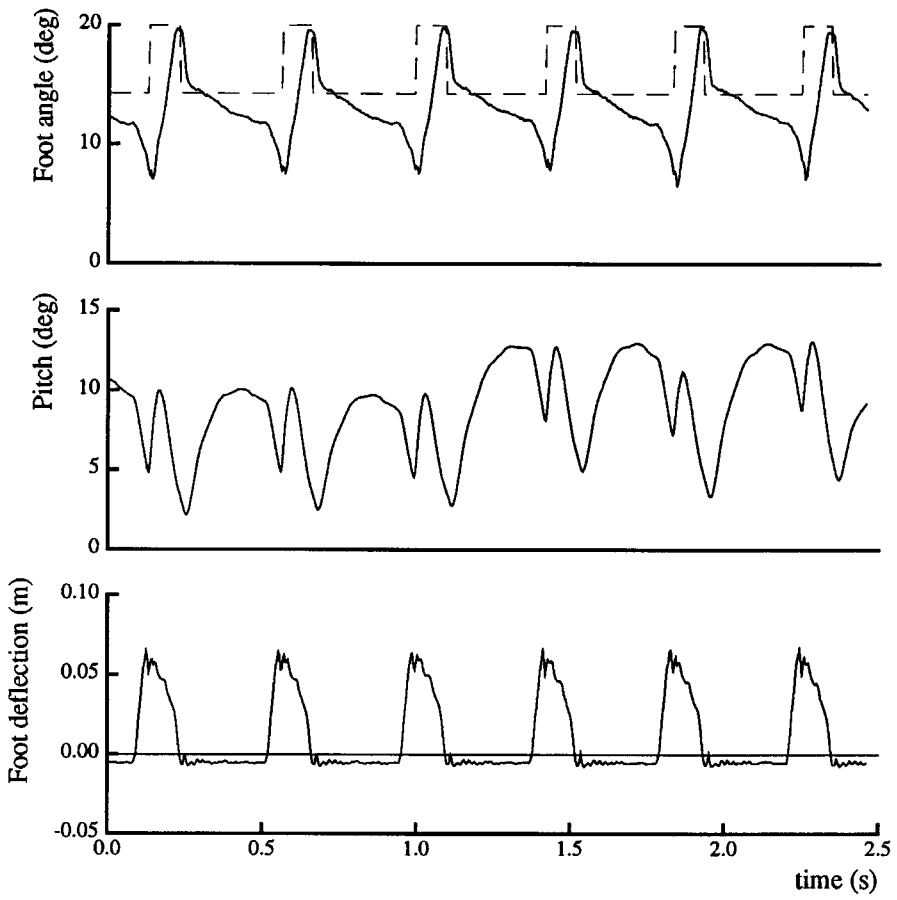

Figure 8–10: Running data for the monopod with the heel hitting the floor, 6 cycles. The disturbance in foot deflection just after the peak indicates impacting of the heel on the ground. The positive spikes in pitch velocity correspond to striking of the heel on the ground, which causes a substantial forward pitching moment. Graph of foot angle and setpoint (broken line) shows that the ground force is driving the foot away from the setpoint when foot deflection is large, due to inadequate actuator hydraulic pressure. Upward step in setpoint is where thrust begins. (Data file M.190.2)

Figure 8–11 shows data for a run with the hydraulic supply pressure set to 3000 psi. Whereas the heel no longer strikes the ground at 3000 psi, there are severe oscillations in thrust and body pitch, as explained below.

The control system delivers thrust during stance by moving the setpoint for the angle of the lever at the rear of the foot (θ_{heel}). This lengthens the zero point of the foot spring, adding energy to the system. The foot actuator is controlled during stance with a linear servo of the form

$$t = -k_p(\theta_{\text{heel}} - \theta_{\text{heelsp}}) - k_v\dot{\theta}_{\text{heel}} \tag{8.1}$$

where

t	is the signal to the hydraulic servo valve,
θ_{heelsp}	is the setpoint for the heel angle, one of two preselected positions,

$\dot{\theta}_{\text{heel}}$	is the time derivative of θ_{heel}, and
k_p and k_v	are position and velocity gains.

The data shown in figure 8–9 were produced using this servo.

At higher hydraulic supply pressures, the thrust servo oscillates as shown in figure 8–11. The oscillation results apparently from the relative loss of mechanical damping at the higher pressures and loads. We have been unable to solve the problem by simply reducing position gain or increasing the gain on the velocity signal, which is obtained by differentiation. One way to eliminate the oscillation is to control thrust with a timed signal of preselected magnitude, rather that with a position servo. In this scheme we control the timing and magnitude of the signal sent to the foot actuator during the stance period. This method reduces foot oscillations.

Increased hydraulic pressure has produced oscillations in the attitude control servo as well, as shown particularly by the pitch velocity graph in figure 8–11. These oscillations cause the machine to leave the ground with substantial, erratic pitch velocity. Because pitch velocity remains constant during flight, large errors in pitch position can accumulate before the next stance period. Further work is needed to determine how to damp these oscillations. The use of pitch acceleration feedback is one possibility being explored.

Several features have been added to the monopod control system to improve attitude control in general. To minimize the forward pitching that naturally occurs when the foot strikes the ground with the machine moving forward, the control system generates a signal to start sweeping the leg to match the relative ground speed just before the foot strikes the ground. This is done about 20 ms before contact. Time before touchdown is computed on the basis of vertical velocity, vertical height and the vertical component of leg length. This anticipatory leg sweep term reduces the attitude disturbance that occurs at touchdown. This same sweep term is incorporated into the pitch-control servo

$$t = -k_p\phi - k_v\dot{\phi} - k_{\text{sweep}}\dot{\theta}_{2\_nom} \tag{8.2}$$

where

t	is the signal to the hip actuator valve,
ϕ	is pitch angle,
$\dot{\phi}$	is pitch velocity,
$\dot{\theta}_{2\_nom}$	is the nominal leg sweep velocity based on the machine kinematics, and forward speed at touchdown, and
$k_p, k_v, k_{\text{sweep}}$	are gains.

The sweep gain, k_{sweep}, is determined by comparing the unloaded, steady-state, leg-sweep velocity with the corresponding signal to the hip servo valve. This additional term allows the leg's sweeping motion to proceed without errors in the body's pitch angle and pitch rate, and should reduce steady-state errors, or permit the use of lower attitude-control gains.

One advantage of the leafspring foot is that its unsprung mass is very low compared to that of the telescoping legs on previous machines. Unsprung mass is the mass whose kinetic energy is lost at touchdown. The bouncing efficiency of a machine, that is the fraction

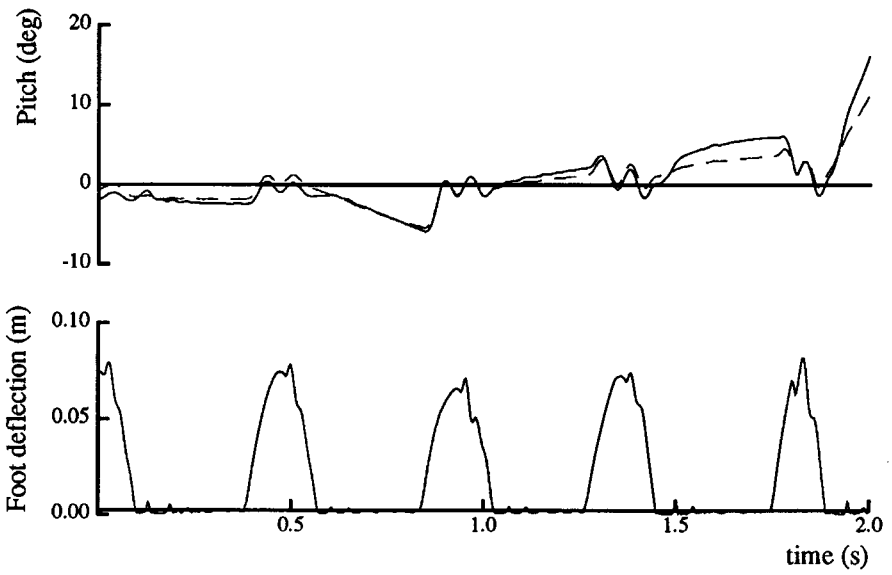

Figure 8–11: Oscillations in foot deflection and body pitch angle. Hydraulic supply pressure of 3000 psi results in oscillations in foot deflection and pitch. The pitch graph shows body pitch angle compared to the weighted average system pitch angle (body plus leg), shown by the dashed line. The average value goes through smaller pitch excursions than the body, as discussed in the text. (Data file M.225.2)

of the circulating energy recovered from one hopping cycle to the next, is limited by the unsprung mass, as given by

$$\eta_{\max} = (1 - \frac{M_{\text{un}}}{M_{\text{sys}}})^2 \tag{8.3}$$

where

$\eta_{\max}$ is the maximum theoretical bouncing efficiency,
M_{sys} is the mass of the whole system, and
M_{un} is the unsprung mass.

This equation accounts for the losses in kinetic energy of the system that occur at touchdown and lift-off. It ignores, of course, the energy needed for swinging the leg and for the various control functions, and frictional losses. Based on this equation and an unsprung-mass ratio of 0.008 for the monopod, we would expect a negligible loss (1.6%) in bouncing efficiency due to foot impacts. We tested the efficiency of the monopod's springy foot by measuring the behavior as the system bounced passively after being dropped from a height of several inches. The bouncing height and spring energy on successive bounces indicate an efficiency of about 0.67.

Mechanical Weaknesses

Several mechanical weaknesses have been found in the monopod design. Failure of the tendon, the "Achilles" tendon, has occurred on numerous occasions, usually at terminations

or bends in the cable. The original 1200 N (1.2 mm) aircraft cable (two strands in parallel) was replaced first by 1500 N cable, then by 2200 N cable, and finally by 1.4 mm dia. music wire having a breaking strength of around 3500 N, giving 7000 N strength for the two strands. Peak tension in the tendon, based on measured foot deflections, is around 1600 N for typical running. The fiberglass foot has broken and been replaced twice. Failures have resulted from shearing between the fiberglass laminations at the heel. The most recent prototype has been strengthened in this area. Strain gauges to measure foot deflection have failed repeatedly, due to delamination or breakage of the foil traces. Although the peak strains are high, about 1.2%, they are within specifications for the gauges and adhesives. A rotary potentiometer on the foot now provides deflection information. The leg tube has also failed twice, once near the hip, once near the ankle hinge. Both areas have been strengthened. We expect to expose other weaknesses as we push the machine toward better performance.

Discussion

A difficulty with the articulated legs is that deflection of the foot causes motion of the toe that is not along the axis of the leg. Assuming the toe is rigidly fixed to the ground during stance, the ankle will move along a path that is approximately circular, centered at the toe (figure 8–12, left). During vertical bouncing this causes the ankle and the lower part of the leg to have a horizontal component of motion. This kinematically induced horizontal motion increases with the foot's angle α with respect to the ground, and adds to the effective unsprung mass of the foot. It also requires an adjustment at the hip to avoid disturbing of the body attitude. A longer foot reduces α for the same vertical deflection, but at the expense of additional foot mass. Thus there is a tradeoff between a long foot that minimizes α and a short foot that minimizes mass. In principle one could compensate for this horizontal deflection by introducing an additional pair of leafsprings (figure 8–12, right). Properly designed, such a mechanism could deflect with a nearly vertical motion of the toe, although it might be difficult to build.

Because the tangential and radial motions of the toe depend on the positions of both the hip and ankle joints, there is heavy coupling between the sweeping motion of the hip and the thrusting motion of the ankle, particularly when the foot is steeply angled with respect to the leg. There are several possibilities for dealing with this interaction. One is to calculate a nominal correction for a standard bounce, and to adjust the hip's motion during stance accordingly. A second approach is to use a force servo on the pitch attitude control. The servo could use differential hydraulic pressure or an explicit measure of the hip actuator force output. Another approach would be to feed back the angular acceleration of the body for control. A fluid-inertia angular accelerometer that will be rugged and insensitive to cross-axis effects, is being developed for this purpose. We have not found suitable commercially available angular accelerometers.

The ratio of leg moment of inertia to body moment of inertia is a significant parameter in running. During ideal one-legged running, the body and leg counteroscillate so that the total angular momentum of the system remains zero. On previous one-legged machines, the leg moments of inertia were relatively small, so the angular momentum of the legs

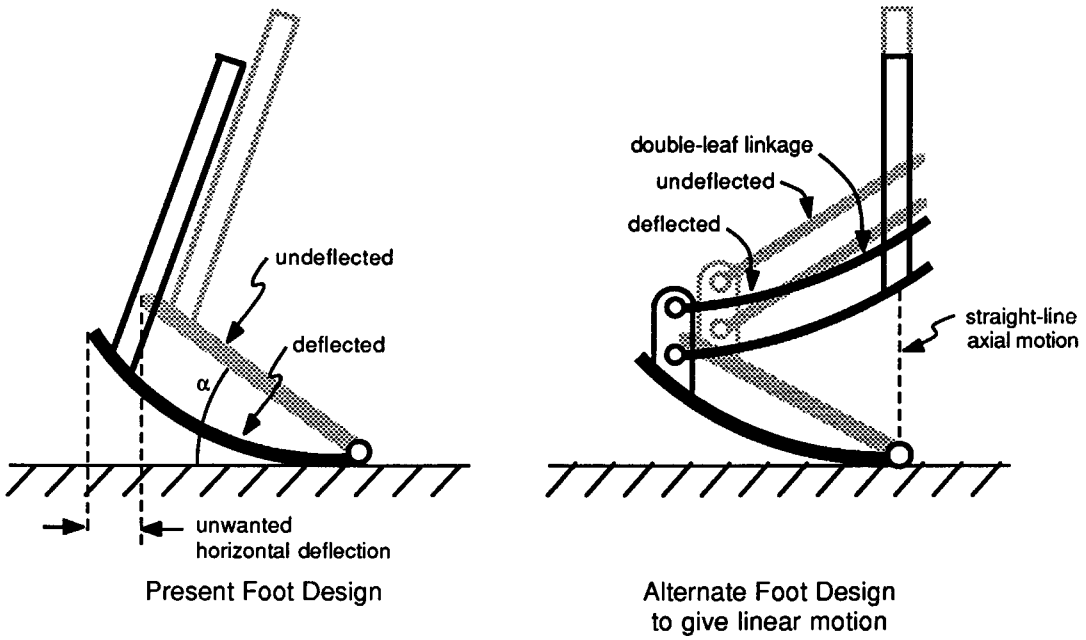

Figure 8–12: Left) Deflection of leafspring foot introduces an undesirable horizontal motion of the toe with respect to the ankle. Right) Introduction of an additional pair of leafsprings compensates for the horizontal motion, yielding a nearly vertical motion of the toe.

could be ignored in the attitude-control algorithm with little adverse affect. During two-legged running, the legs oscillate 180 deg out of phase, so the net angular momentum is approximately zero and may be neglected. On the monopod, the leg angular momentum is significant. Therefore we have recently incorporated an attitude-control algorithm that tries to servo to zero the total angular momentum and the weighted-average angular position of the body and leg. We define an average pitch angle

$$\bar{\phi} = \left(1 - \frac{J_{\text{leg}}}{J_{\text{sys}}}\right)\phi + \frac{J_{\text{leg}}}{J_{\text{sys}}}\theta_{\text{leg}} \tag{8.4}$$

where

- ϕ is the body pitch angle wrt horizontal,
- θ_{leg} is the leg angle wrt vertical,
- $\bar{\phi}$ is the weighted-average pitch angle,
- J_{leg} is the moment of inertia of the leg about the center of gravity of the system, and
- J_{sys} is the moment of inertia of the system about its center of gravity.

We then use $\bar{\phi}$ and its time derivative in place of pitch as a basis for a linear servo. This should minimize the attitude-control "effort", and result in a smooth, natural motion. Figure 8–11 shows that the weighted-average angular position goes through smaller oscillations than the body pitch angle, as expected due to counter rotation of the body and leg. Further tuning is needed to verify the success of this approach.

Unlike previous machines, the monopod is not symmetrical in the fore/aft direction. It has demonstrated a clear preference for traveling in the "forward" direction, that is, the direction in which the toe points. Because of the asymmetry, the mass of the leg is not aligned with the center of mass of the machine as it is with the telescoping legs used on the other machines. To offset the mass of the leg, we have a compensating mass on the body, so the center of mass of the entire machine is at the nominal center, the point above the toe.

The difference in leg-spring design between the monopod and previous machines raises the issue of how spring characteristics affect machine performance, and what characteristics are desirable. Some desirable characteristics are obvious: springs should be light in weight, compact, and rugged. They should have maximum energy storage capacity, good resilience, mechanical simplicity, and be easy to build. Other characteristics, however, are not obvious. Is a spring with a linear force/deflection characteristic preferable to the nonlinear characteristic of a gas spring? Should the spring be preloaded, and if so, how much? The system that is simplest to analyze is a linear spring with a preload that just equals the weight of the machine. In this case, the preload effectively negates the effect of gravity, and the system undergoes one-half cycle of pure harmonic motion during stance, assuming the spring acts vertically. Stance time will not vary with hopping height in this case. Whereas the nonlinear force/deflection function of a gas spring makes it analytically difficult, its inherent *hardness*, due to the asymptotically infinite forces near the end of travel, provides resistance to bottoming—a distinct advantage.

8.7 Monopod with Hoof

As a possible solution to the problem of the strong coupling between the sweeping motion of the hip and the thrusting motion of the ankle, an alternative foot design is proposed as shown in figure 8–13. This design places the toe on a platform that elevates it with respect to the ground. The platform is like a hoof. As mentioned previously, one solution to the coupling problem is to minimize the foot angle α. The proposed design reduces the foot angle without causing the ankle to collide with the ground. Although the motion of the ankle about the toe is still along a circular arc, it is now symmetrical with respect to the horizontal line passing through the toe joint. Therefore it induces less horizontal motion of the ankle.

The basic idea of this design was inspired by the mechanism of a horse's hoof (figure 8–14). Impact of the foot against the ground bends the fetlock joint and stretches an elastic ligament. The fetlock snaps back when the foot leaves the ground. Such motion induces an upward push to the leg. Because a suitable artificial tendon-like material for such a design has not been found, the fiberglass leafspring will be used in the new design as the energy storage element.

The alternative foot design with hoof-like structure discussed in the previous section was built as shown in figure 8–15. The toe of the original foot was replaced by a hinge joint and the hoof is connected. The angle of the hoof at rest was adjusted by changing

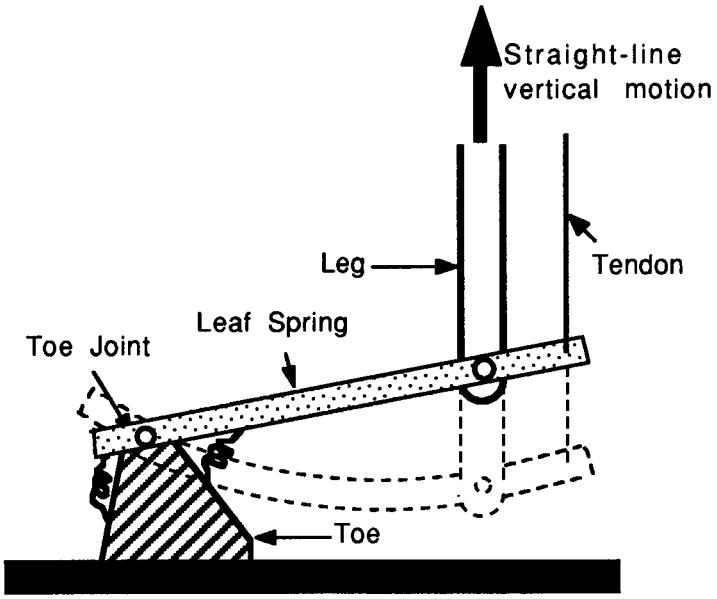

Figure 8–13: Drawing of alternative articulated leg design. This design places the toe on a hoof-like platform that elevates it with respect to the ground. It reduces the foot angle α without causing the ankle to collide with the ground, and thus minimizes the coupling between the vertical motion and the horizontal motion.

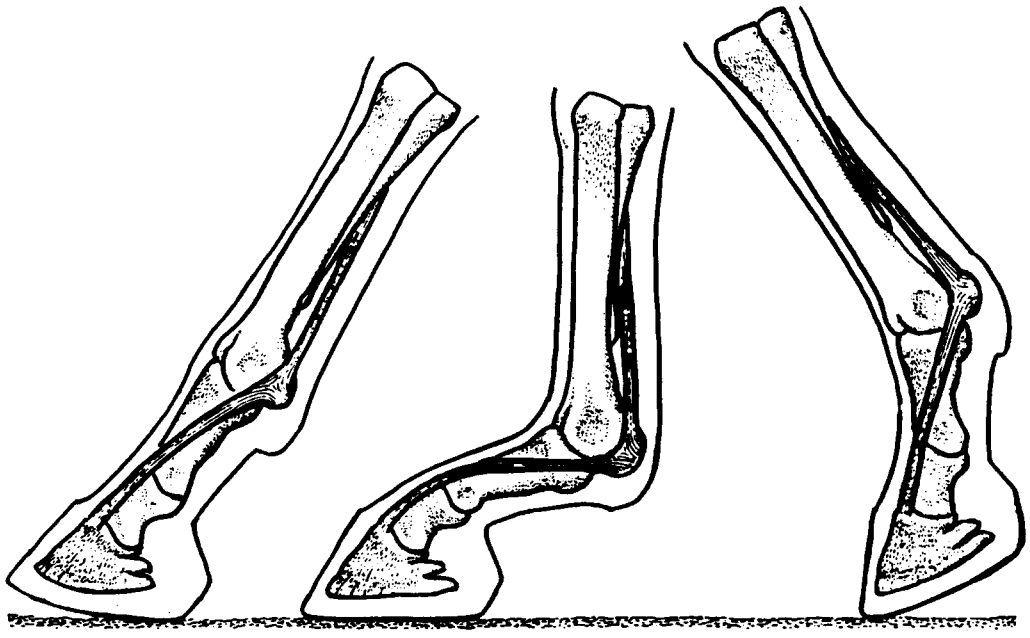

Figure 8–14: Horse's hoof. The basic idea of the alternative leg design was inspired by the mechanism of a horse's hoof. The hoof elevates the toe so the joint can move lower without touching the ground. Figure reprinted from (Hildebrand 1960).

Figure 8–15: Photograph of the monopod foot with hoof.

the tensions of the rubber springs. We set the spring so that the hoof was horizontal at landing. The angle of the hoof does not have to be actively controlled because the angle of the foot with respect to the body is kept constant by the four-bar linkage formed by the leg, heel lever, body, and tendon. The tension of the springs is set to the lowest value that will ensure the correct hoof angle. The hoof is made of wood with a layer of rubber padding on the bottom.

The addition of the hoof to the original foot design required no additional sensor mechanisms, but modification of the control system seems to be necessary for the reason to be explained in following section.

Monopod with Hoof Experiment

Figure 8–16 shows data from a run the monopod with hoof has made. The monopod ran at an average forward speed of 0.08 m/sec. The monopod also ran in place and backward. Although the latter task was very awkward, the original monopod could not perform these tasks well due to the fact that the heel made contact with the ground. As shown in figure 8–16, the single peak in foot deflection during each bounce, the absence of substantial single peak in pitch angle, and the absence of abrupt change in the vertical position of center of gravity, all indicate that there were no heel impacts with the ground. The body's pitch angle error was kept below 7 deg, typically with a nose-up posture. The hydraulic supply pressure used was 1500 psi.

Implementation of the hoof-like structure eliminated the problem of heel impact against the ground as planned, and thus also eliminated the cause of a substantial disturbance in

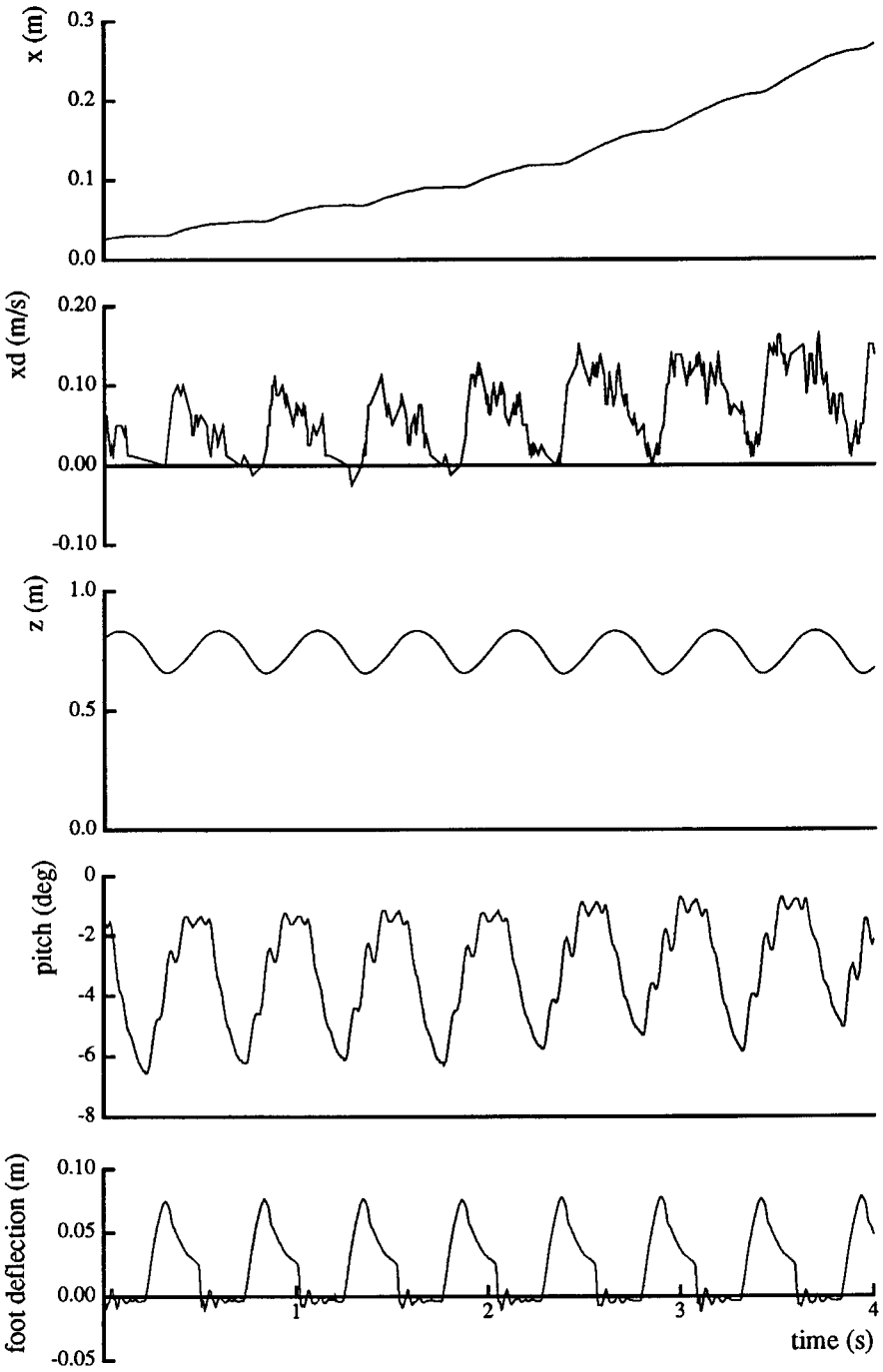

Figure 8–16: Running slowly, at approximately 0.08 m/sec. The single peaks in foot deflection indicate the absence of heel impacts with the ground. The absence of substantial single peaks in pitch angle and the abrupt change in vertical position of center of gravity also indicates no heel impacts with ground. The decrease of forward velocity during the flight phase is due to friction in the planarizer. (Data file M.235.10.)

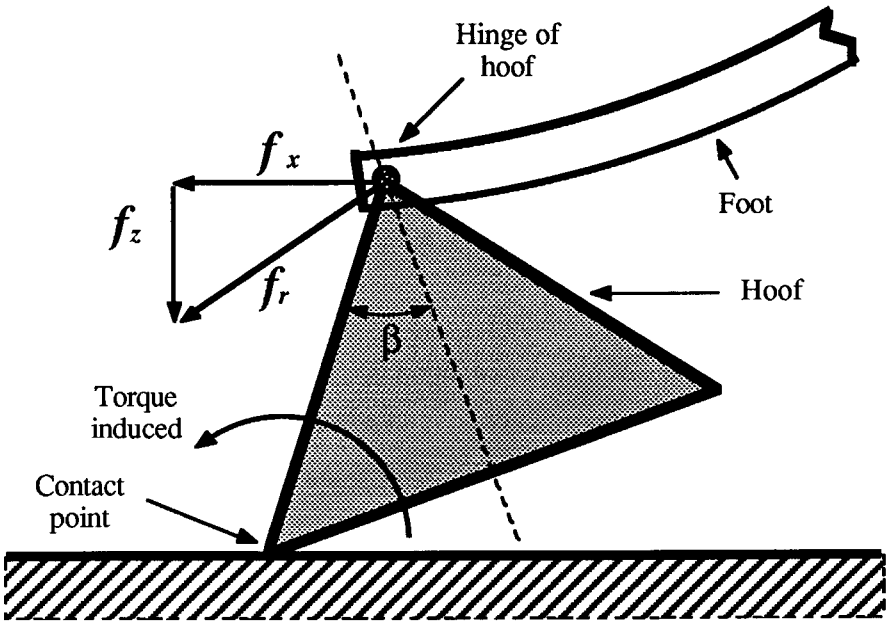

Figure 8–17: Free body diagram of the forces applied at the hinge of the hoof. The horizontal force f_x and the downward force f_z induce the resultant force f_r. The resultant force vector f_r has to pass below the bottom corner of the hoof. Otherwise, the torque induced about the bottom corner of the hoof will result in rolling of the hoof.

pitch. As the result, the monopod was able to run in place. However, the implementation of the hoof-like structure introduced a new problem to controlling the monopod; the rolling of the hoof. In the original foot design of the monopod, the toe was the single point of contact with the ground, and control was performed so that the slipping would not occur. The horizontal component of the force applied at the toe was smaller than the friction force between the toe and the ground. The source of the sweeping force during stance is torque applied at the hip to correct the body attitude. Conceptually, the problem with the rolling of the hoof is similar to the problem of slipping of the toe. The downward force f_z and sweeping force f_x applied at the hinge of the hoof induce a resultant force f_r as shown in figure 8–17. If f_r passes above the bottom corner of the hoof it will induce a torque and rolling of the hoof will occur. In order to avoid the rolling of the hoof the control system must satisfy the condition

$$f_x < f_z tan\beta \tag{8.5}$$

where

f_x is the horizontal force applied at the hinge of the hoof during stance,
f_z is the downward force applied at the hinge of the hoof during stance, and
β is bisected angle of the hoof at the hinged corner.

The horizontal force f_x satisfying the above condition is much smaller than the friction

force between the toe of the original foot and the ground. Because the torque applied at the hip to correct the body attitude is the source of the horizontal force f_x, the hip torque allowed for the attitude control for the hoofed monopod may be limited compared to the original monopod design. It may be possible to coordinate hip torque used for attitude control with the vertical loading of the hoof to avoid rolling the hoof.

The problem of rolling of the hoof is more serious when the forward velocity of the monopod increases, because the horizontal force applied at the hinge of the hoof will increase. At this point, further investigation of the problem is necessary.

Knees in the Future

We hope to replace telescoping legs with articulated legs in future running machines. However, because of its inability to retract substantially, the current articulated leg design is not adequate for running machines with more than one leg. With a single leg, the swing phase occurs during flight when the foot is clear off the ground. But for a machine with more than one leg, the idle leg must remain clear of the ground while the other leg is in stance—the idle leg must be able to shorten to less than the shortest length seen by the support legs during stance.

One way to obtain large retraction is to add a knee-like joint. The ankle pivot and tendon could then be eliminated because vertical thrust could be obtained by a combination of knee and hip motions. However, a complication then arises due to a kinematic coupling between hip and knee joints—both purely vertical movement and purely horizontal movement require use of the same joints. Therefore, use of the ankle as the primary actuator while using the knee joint mainly for gross changes in leg length during flight seems to be the best choice. However, the final mechanical design of such a ankle-knee articulated leg has not been considered yet. It will be the next step in the development of the project.

8.8 References

Alexander, R. McN. 1974. The mechanics of jumping by a dog. *J. Zoology (London)* 173:549–573.

Alexander, R. McN., Vernon, A. 1975. The mechanics of hopping by kangaroos (Macropodidas). *J. Zoology (London)* 177:265–303.

Cavagna, G. A. 1970. Elastic bounce of the body. *J. Applied Physiology* 29:279–282.

Cavagna, G. A., Heglund, N. C., Taylor, C. R. 1977. Mechanical work in terrestrial locomotion: Two basic mechanisms for minimizing energy expenditure. *American J. Physiology* 233:R243–R261.

Dawson, T. J., Taylor, C. R. 1973. Energetic cost of locomotion in kangaroos. *Nature* 246:313–314.

Hildebrand, M. 1960. How animals run. *Scientific American* 148–157.

Hirose, S., Umetani, Y. 1980. The basic motion regulation system for a quadruped walking vehicle. *ASME Conference on Mechanisms.*

Hodgins, J., Koechling, J., Raibert, M. H. 1986. Running experiments with a planar biped. *Third International Symposium on Robotics Research*, G. Giralt, M. Ghallab (eds.). Cambridge: MIT Press.

Lucas, E. 1894. Huitieme recreation—la machine a marcher. *Recreations Mathematiques* 4:198–204.

McMahon, T. A. 1984. *Muscles, Reflexes, and Locomotion.* Princeton: Princeton University Press.

Raibert, M. H., Brown, H. B., Jr. 1984. Experiments in balance with a 2D one-legged hopping machine. *ASME J. Dynamic Systems, Measurement, and Control* 106:75–81.

Raibert, M. H., Chepponis, M., Brown, H. B. Jr. 1986. Running on four legs as though they were one. *IEEE J. Robotics and Automation*, 2.

Song, S. M., Vohnout, V. J., Waldron, K. H., Kinzel, G. L. 1981. Computer-aided design of a leg for an energy efficient walking machine. *Proceedings of 7th Applied Mechanisms Conference*, Kansas City, pp. VII-1–VII-7.

Vohnout, V. J., Alexander, K. S., Kinzel, G. L. 1983. The structural design of the legs for a walking vehicle. *Proceedings of 8th Applied Mechanisms Conference*, St. Louis, pp. 50-1–50-8.

Waldron, K. J., Kinzel, G. L. 1983. The relationship between actuator geometry and mechanical efficiency in robots. In *Theory and Practice of Robots and Manipulators, Proceedings of RoManSy'81*, A. Morecki, G. Bianchi, K. Kedzior (eds.). Warsaw: Polish Scientific Publishers, 305–316.

Waldron, K. J., Vohnout, V. J., Pery, A., McGhee, R. B. 1984. Configuration design of the adaptive suspension vehicle. *International J. Robotics Research* 3:37–48.

8.9 Appendix A: Physical Parameters of the Monopod

Parameter	Metric Units	English Units
Lengths/angles		
Overall height	0.84 m	33 in
Overall length	1.02 m	40 in
Overall width	0.23 m	9 in
Hip height (leg fully extended)	0.74 m	29.2 in
Leg vertical travel	0.13 m	5.2 in
Leg sweep angle	±0.73 rad	±42 deg
Masses		
Total mass (body, leg, and boom)	7.9 kg	17.3 lbm
Body mass	5.4 kg	11.8 lbm
Leg mass	0.73 kg	1.61 lbm
Leg mass, unsprung	0.063 kg	0.14 lbm
Ratio of total mass to unsprung leg mass	125:1	125:1
Moments of Inertia		
Body moment of inertia (about CG)	0.22 kg-m^2	750 lbm-in^2
Leg moment of inertia (about hip)	0.097 kg-m^2	330 lbm-in^2
Ratio of body to leg moments of inertia	2.3:1	2.3:1
Performance		
Ideal no load stroke time†	0.023 s	0.023 s
Ideal no load sweep time†	0.037 s	0.037 s
Static thrust†	17.3 N	77 lb
Static hip torque†	67 N-m	590 in-lb
Ratio of static thrust to weight†	4.5:1	4.5:1
Work per Thrust Stroke†	49.9 N-m	442 in-lb
Work per Sweep Stroke†	82 N-m	724 in-lb
Leg spring stiffness	4060 N/m	23 lb/in

†Differential hydraulic pressure of 14mPa or 2000 psi.

8.10 Appendix B: Kinematics of the Monopod

Symbol	Variable Description
ϕ	Angle of the body wrt horizontal (pitch)
θ_1	Angle of foot actuator lever arm wrt leg normal
θ_2	Angle of leg wrt body normal
θ_{leg}	Angle of leg wrt vertical
θ_3	Angle of foot lever arm wrt leg normal
θ_{heel}	Angle of foot lever arm wrt horizontal
θ_{toe}	Angle of line joining ankle and toe wrt horizontal
α_1	Angle of foot actuator wrt leg
α_2	Angle of hip actuator wrt body normal
w_1	Foot actuator length, pivot to pivot
w_2	Hip actuator length, pivot to pivot
dw_1	Foot actuator displacement $(w_1 - w_{1\_0})$
dw_2	Hip actuator displacement $(w_2 - w_{2\_0})$
r_1	Effective moment arm of foot actuator about hip
r_2	Effective moment arm of hip actuator about hip
δ_f	Foot deflection $\perp$ to foot length
x	Horizontal position of the body CG
z	Height of the body CG above ground
legx	Horizontal distance from toe to body CG
legz	Vertical distance from toe to body CG

Table 8–1: Kinematic variables for monopod.

The kinematic configuration of the monopod is completely determined by four measured variables: ϕ, θ_1, θ_2, and δ_f. Given these four position variables, we want to find θ_{leg}, θ_{heel}, θ_{toe}, legx, and legz. By inspection of figure 8–1, we see at once that

$$\theta_{\text{leg}} = \theta_2 + \phi. \tag{8.6}$$

From the four-bar linkage defined by $a, c, b,$ and d, we see that

$$c + a\sin\theta_1 = d + b\sin\theta_3, \tag{8.7}$$

$$\sin\theta_3 = \frac{c-d}{b} + \frac{a}{b}\sin\theta_1 \tag{8.8}$$

$$= \sin\theta_{3\_0} + \frac{a}{b}\sin\theta_1, \tag{8.9}$$

where $\sin\theta_{3\_0} = (c-d)/b$ is the value of $\sin\theta_3$ when $\theta_1 = 0$. Therefore,

$$\theta_3 = \arcsin(\sin\theta_{3\_0} + \frac{a}{b}\sin\theta_1). \tag{8.10}$$

Symbol	Parameter	Metric Units	English Units
a	Foot-actuator lever arm length	0.0381 m	1.500 in
b	Foot lever arm length	0.0439 m	1.73 in
$c+h$	Leg length, hip to ankle	0.610 m	24.0 in
d	Tendon length	0.48 m	19.0 in
e	Hip-to-body-CG offset	0.1651 m	6.500 in
f	Foot length, ankle to toe	0.188 m	7.4 in
g	Body half length	0.51 m	20.0 in
h	Hip to foot-actuator-lever-pivot distance	0.1016 m	4.00 in
i	Hip actuator lever length	0.0381 m	1.500 in
k	Hip to hip-actuator-pivot distance	0.1091 m	4.295 in
w_{1_0}	Foot actuator length at center of travel	0.1016 m	4.000 in
w_{2_0}	Hip actuator length at center of travel	0.1022 m	4.025 in
θ_{3_0}	Value of θ_3 when $\theta_1 = 0$	0.19 rad	11 deg
θ_{toe_0}	Value of θ_{toe} when $\theta_{\text{heel}} = 0$ and $\delta_f = 0$	0.33 rad	19 deg
α_{2_0}	Value of α_2 when $\theta_2 = 0$	1.215 rad	69.6 deg

Table 8–2: Kinematic constants of the monopod.

Also by inspection

$$\theta_{\text{heel}} = \theta_{\text{leg}} + \theta_3. \tag{8.11}$$

If we assume that foot length f is constant, and foot deflection δ_f is measured along an arc about the ankle, then we can say

$$\theta_{\text{toe}} + \frac{\delta_f}{f} \approx \theta_{\text{heel}} + \theta_{\text{toe}\_0} \tag{8.12}$$

$$= \theta_{\text{leg}} + \theta_3 + \theta_{\text{toe}\_0}. \tag{8.13}$$

Therefore

$$\theta_{\text{toe}} \approx \theta_{\text{leg}} + \theta_3 + \theta_{\text{toe}\_0} - \frac{\delta_f}{f}. \tag{8.14}$$

We find the horizontal and vertical distances from toe to hip by adding components of each of the three link lengths:

$$\text{legx} = -f\cos\theta_{\text{toe}} + (c+h)\sin\theta_{\text{leg}} + e\cos\phi, \tag{8.15}$$

$$\text{legz} = f\sin\theta_{\text{toe}} + (c+h)\cos\theta_{\text{leg}} - e\sin\phi. \tag{8.16}$$

Actuator Kinematics

Given angles θ_1 and θ_2, we want to find the actuator lengths and displacements w_1, w_2 and dw_1, dw_2, and moment arms r_1 and r_2. With reference to figure 8–19, we add length

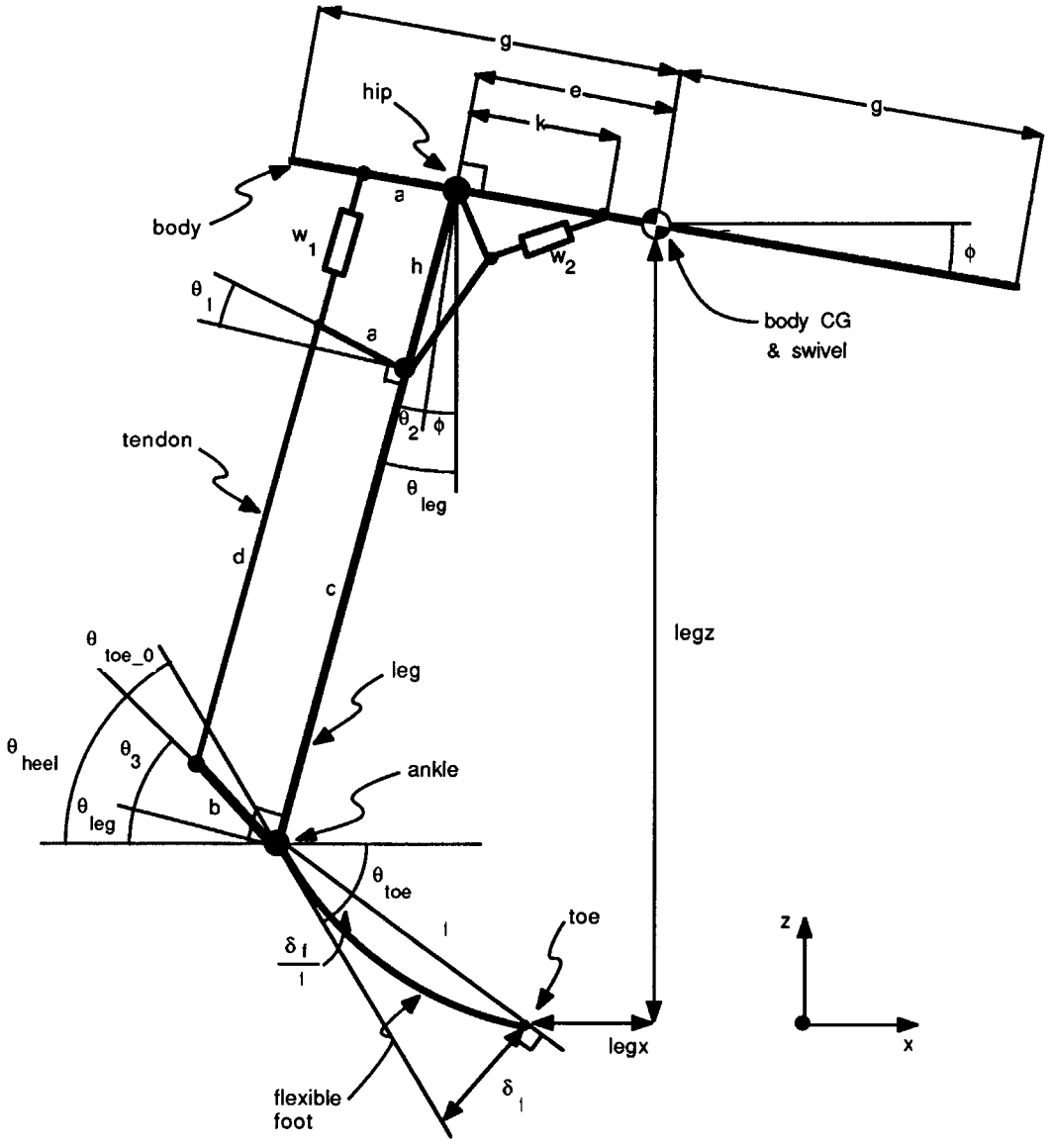

Figure 8–18: Monopod kinematics. The figure shows the overall configuration of the monopod with labels giving some of the nomenclature. Symbols are shown for the kinematic variables and parameters, which are further defined in tables 8–1 and 8–2.

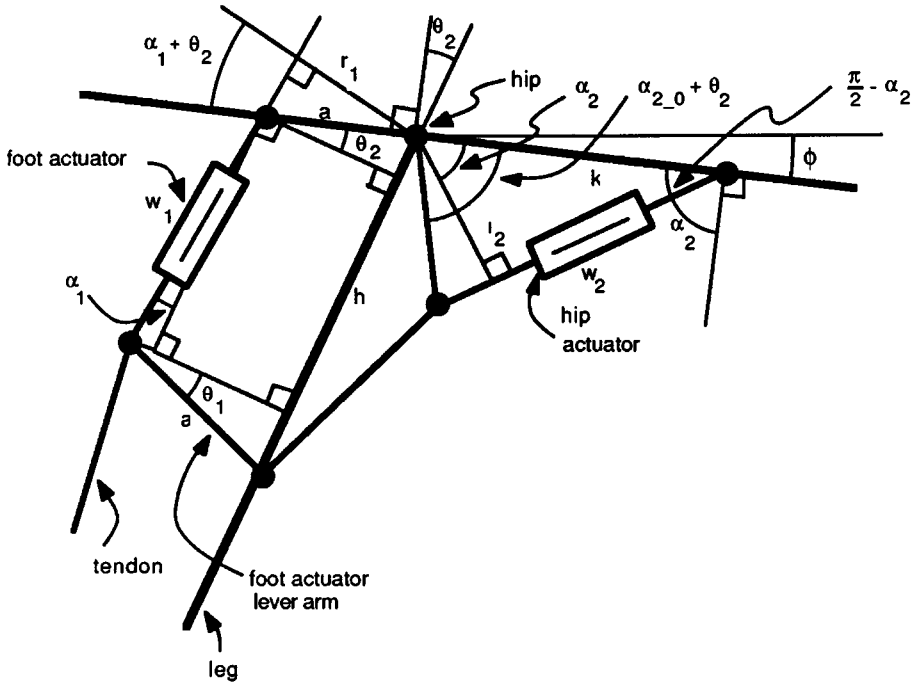

Figure 8–19: Actuator kinematics. The figure shows the geometry of the hip and actuator linkages.

components parallel to the leg for actuator 1 to get

$$w_1 \cos \alpha_1 + a \sin \theta_2 + a \sin \theta_1 = h. \tag{8.17}$$

Therefore

$$w_1 = \frac{h - a(\sin \theta_1 + \sin \theta_2)}{\cos \alpha_1}. \tag{8.18}$$

By considering length components perpendicular to the leg we get

$$a \cos \theta_1 = w_1 \sin \alpha_1 + a \cos \theta_2 \tag{8.19}$$

or

$$w_1 = \frac{a(\cos \theta_1 - \cos \theta_2)}{\sin \alpha_1}. \tag{8.20}$$

We combine this with (8.18) to get

$$\frac{h - a(\sin \theta_1 + \sin \theta_2)}{\cos \alpha_1} = \frac{a(\cos \theta_1 - \cos \theta_2)}{\sin \alpha_1} \tag{8.21}$$

or

$$\tan \alpha_1 = \frac{\cos \theta_1 - \cos \theta_2}{h/a - \sin \theta_1 - \sin \theta_2} \approx \alpha_1 \tag{8.22}$$

The maximum possible value of α is 0.12rad (6.9 deg), so $\tan \alpha_1 \approx \alpha_1$ with less than 0.5% error. Also $\cos \alpha_1 \approx 1$ within 1%, so (8.18) becomes

$$w_1 \approx h - a(\sin \theta_1 + \sin \theta_2). \tag{8.23}$$

By design, $w_{1\_0} = h$. Therefore

$$dw_1 = w_1 - w_{1\_0} = w_1 - h \approx -a(\sin\theta_1 + \sin\theta_2). \tag{8.24}$$

From figure 8–19 we see that

$$r_1 = a\cos(\alpha_1 + \theta_2). \tag{8.25}$$

For actuator 2, we apply the law of cosines to the triangle formed by i, k and w_2:

$$w_2^2 = i^2 + k^2 - 2ik\cos(\alpha_{2\_0} + \theta_2). \tag{8.26}$$

We see also that

$$r_2 = i\cos(\alpha_{2\_0} + \theta_2 - \alpha_2) \approx i\cos\theta_2 \tag{8.27}$$

for $\alpha_2 \approx \alpha_{2\_0}$. The worst error in r_2 due to this assumption is 14% which occurs only at the limit of hip travel. If necessary, we can find α_2 and use the exact form of (8.27). Law of cosines gives

$$i^2 = k^2 + w_2^2 - kw_2\cos(\pi/2 - \alpha_2) \tag{8.28}$$

from which

$$\alpha_2 = \pi/2 - \arccos\left(\frac{k^2 + w_2^2 - i^2}{kw_2}\right). \tag{8.29}$$

8.11 Appendix C: Moment of Inertia Determination

This appendix describes the analytical and experimental techniques that have been used to determine moments of inertia of several machines and legs. The polar moment of inertia about an axis is defined as

$$J = \int_m r^2 dm \tag{8.30}$$

where

- J is the polar moment of inertia,
- dm is an infinitesimal element of mass, and
- r is the distance from the axis to the element of mass.

The moment of inertia is related to the behavior of a rigid system by Newton's Second Law, in rotational terms:

$$\mathrm{T} = J\ddot{\phi} \tag{8.31}$$

where

- T is the torque about the system center of gravity, or about a point in the system fixed to an inertial reference,
- J is the polar moment of inertia about the same point, about an axis aligned with the torque vector, and
- $\ddot{\phi}$ is the angular acceleration of the system.

The parallel axis theorem arises from (8.30), and allows us to find moments of inertia about displaced parallel axes through a rigid body:

$$J_o = J_c + mr_o^2 \tag{8.32}$$

where

- J_o is the moment of inertia about a point o,
- J_c is the moment of inertia about the center of gravity,
- m is the mass of the body, and
- r_o is the displacement of point o from the center of gravity.

A planar, rigid body can be dynamically defined by three parameters: the mass, the location of the center of gravity, and the moment of inertia about the center of gravity. Its rotational behavior about any other (parallel) axis can be determined with the use of the parallel axis theorem. A three-dimensional body requires moments of inertia about three orthogonal axes through the center of gravity. Here we will consider only planar bodies, although the techniques are applicable to three-dimensional bodies as well.

The moment of inertia of a body can be determined by calculation or measurement. We have used both methods for finding moments of inertia of the leg and body subassemblies of the monopod and biped.

Calculation of Moments of Inertia

To find the moment of inertia of the biped's leg we assumed all individual components to be slender rods located on the leg axis. Using the parts lists and fabrication drawings, we tabulated the length, location, and mass of each component. A programmable calculator was used to determine the mass, location of the center of gravity and moment of inertia for each of the three leg subassemblies.

The biped leg comprises three subassemblies: (1) the upper leg, the parts that do not move axially; (2) the piston rod subassembly, the parts that move with the hydraulic piston and rod; and (3) the lower leg, the parts that move with the foot. We sum the masses and moments of inertia about the hip for all components of each subassembly, and locate the center of gravity relative to the hip.

We compute the moment-of-inertia contribution about the hip for each component, assumed to be a slender rod:

$$r_i = a_i + b_i/2 \tag{8.33}$$

$$J_{ci} = m_i b_i^2/12 \tag{8.34}$$

$$J_{oi} = J_{ci} + m_i r_i^2 \tag{8.35}$$

where

- a_i is the distance from the hip to the top end of the component,
- b_i is the length of the component,
- r_i is the distance from the hip to the center of gravity of the component,
- m_i is the the mass of the component,
- J_{ci} is the moment of inertia of the component about its own center of gravity,
- J_{oi} is moment of inertia of the component about the hip, and
- i identifies the component.

Then we total the contributions to obtain a total moment of inertia about the hip for a subassembly:

$$J_{ok} = \sum_i J_{oi} = \sum_i m_i b_i^2/12 + \sum_i m_i r_i^2, \tag{8.36}$$

where k denotes the subassembly. We also need the center of gravity of the subassembly, which we get by averaging first moments of mass:

$$r_k = \frac{\sum_i m_i r_i}{\sum_i m_i} \tag{8.37}$$

where r_k is the distance from the hip to the center of gravity of the subassembly. We can then find the moment of inertia of the subassembly about its own center of gravity using the parallel axis theorem:

$$J_{ck} = J_{ok} - m_k r_k^2 \tag{8.38}$$

where $m_k = \sum_i m_i$ is the mass of the subassembly k.

This technique is valid only when the system can be modeled as a group of coaxial, slender rods.

Measurement of Moments of Inertia

When geometric complexities, the presence of a large number of components, and/or the absence of adequate information preclude calculating moments of inertia, values can be obtained by measurement. The following technique has been found useful for our planar machines which have a low-friction pivot built into the system.

Consider a subassembly or system having its center of gravity suspended below a low-friction pivot. We can relate the moment of inertia about the pivot to the period of pendulum oscillation:

$$J_o = mgr(\tau/2\pi)^2$$

where

- J_o is the moment of inertia of the system about the pivot,
- m is the mass of the system,
- g is the gravitational acceleration,
- r is the distance from the pivot to the center of gravity of the system, and
- τ is the period of pendulum oscillation.

We can measure τ precisely by recording data from a potentiometer attached to the pivot (e.g. the pitch potentiometer), or, less desirably, by using a stopwatch. We may not know m or r precisely, but can get a good value of the product by measuring the torque needed to hold the assembly at 90 deg to its idle position:

$$\mathrm{T} = mgr$$

where T is the torque required to balance the moment generated by the weight of the system at 90 deg. We can find T by using a spring-scale or other force-measuring device at a known radius from the pivot. Care should be taken to keep the scale vertical, and the system at 90 deg to its idle position.

We used this method to find the moment of inertia of the biped (body plus legs) about the pivot by wiring the legs to the body so the whole system behaved as a rigid body. We then found the moment of inertia of the body alone by subtracting the moment of inertia of the two legs about the pivot.

This method was also used to measure the leg moment of inertia of the monopod. To do this we disconnected both hydraulic actuators so the leg could swing freely. We wired the foot in the desired position.

8.12 Appendix D: Planarizer

We have designed a mechanism that will permit the Monopod to run on a treadmill, while constraining its motion to the plane. The main function of the planarizer is to restrict motion of the Monopod in all degrees of freedom, except those in the sagittal plane—fore and aft, up and down, and pitch rotation. In fact, the function of the planarizer is same as of the tether boom used to constrain the planar biped described in earlier chapters of this report. However, the tether boom turns the machine as the machines moves fore and aft. If the monopod were to travel forward on the treadmill while tethered by a boom, the legs would no longer sweep in the direction of the moving belt.

The planarizer should be rigid enough to eliminate non-planar motions, and should have minimum influence on the dynamics of the Monopod. Low friction is thus very desirable. It is also important that the size of the planarizer permits it to be mounted on the treadmill. The major criteria for design of the planarizer are that it

- Allows motions within the sagittal plane, while preventing motions out of the plane.
- Does not disturb dynamics.
- Adequate size.

We have considered several designs, some of which are shown in figure 8–20—the arm structure, the X-Y table, and the linear-sliding boom. However, none of these designs satisfied all the criteria mentioned above. For example, the arm structure is vulnerable to the side thrust applied by the robot due to its long arm, and requires a bulky and heavy arm in order to be rigid enough. Furthermore, the distribution of inertia is even only over a limited range of orientations, and otherwise it disturbs the dynamics of the robot. The X-Y table satisfies the first and third criteria, but it does not satisfy the second criterion because of its uneven distribution of mass. The linear-sliding boom meets all the criteria. However, the arm has to be relatively long, and the space available is thus the limiting factor.

The schematic of the design we have selected is shown in figure 8–21. This mechanism operates in Cartesian coordinates. It consists of two vertical linear slides and rails, two horizontal linear slides and rails, pulleys, and cables. The running machine is mounted on the vertical linear slide #1, which rides on the vertical rail #1. The vertical rail #1, in turn, is mounted on the two horizontal linear slides as shown, whereas the vertical rail #2 is stationary. The force transmitting elements are the pulleys and cables. They are mounted in such a way that the vertical movement of vertical slide #1 will cause exactly the same movement in vertical slide #2, but the horizontal movement will not affect the vertical slide #2. Therefore the inertia of the machine's vertical movement can be adjusted to be the same as the inertia of horizontal movement by adding weights on the vertical slide #2. The major drawback is friction in the cables and pulleys. The design permits measurement of location of the machine by measuring the rotation of the pulleys using rotary digital encoders.

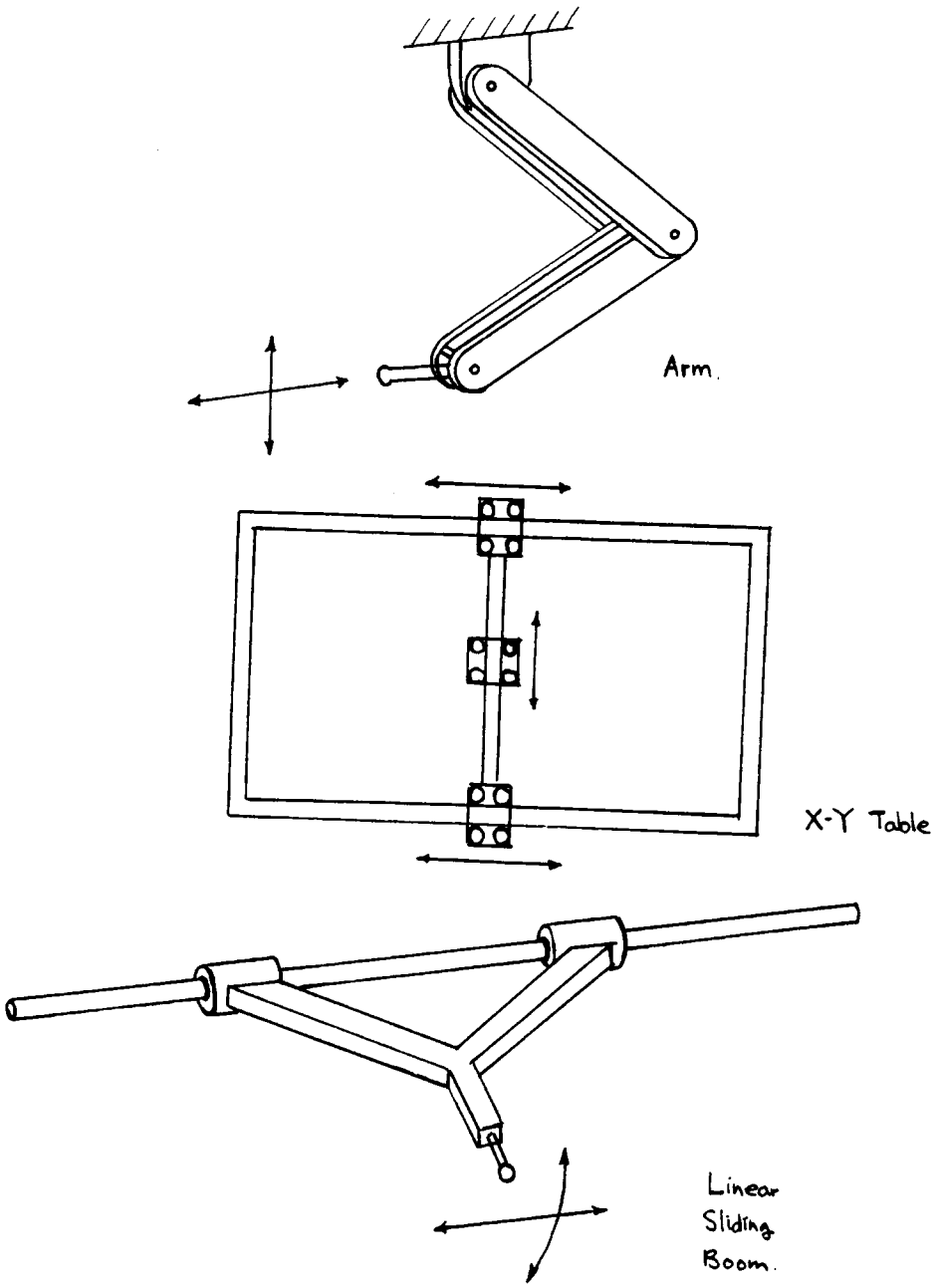

Figure 8–20: Three designs of planarizer: A) Arm structure: It is vulnerable to the side thrust applied by the robot due to its long arm, and requires a bulky and heavy arm in order to be rigid enough. The distribution of inertia is even only over a limited range of orientations, and otherwise it disturbs the dynamics of the robot. B) X-Y table: The distribution of inertia is uneven. C) Linear-sliding boom: The arm has to be relatively long, and the space available is thus the limiting factor.

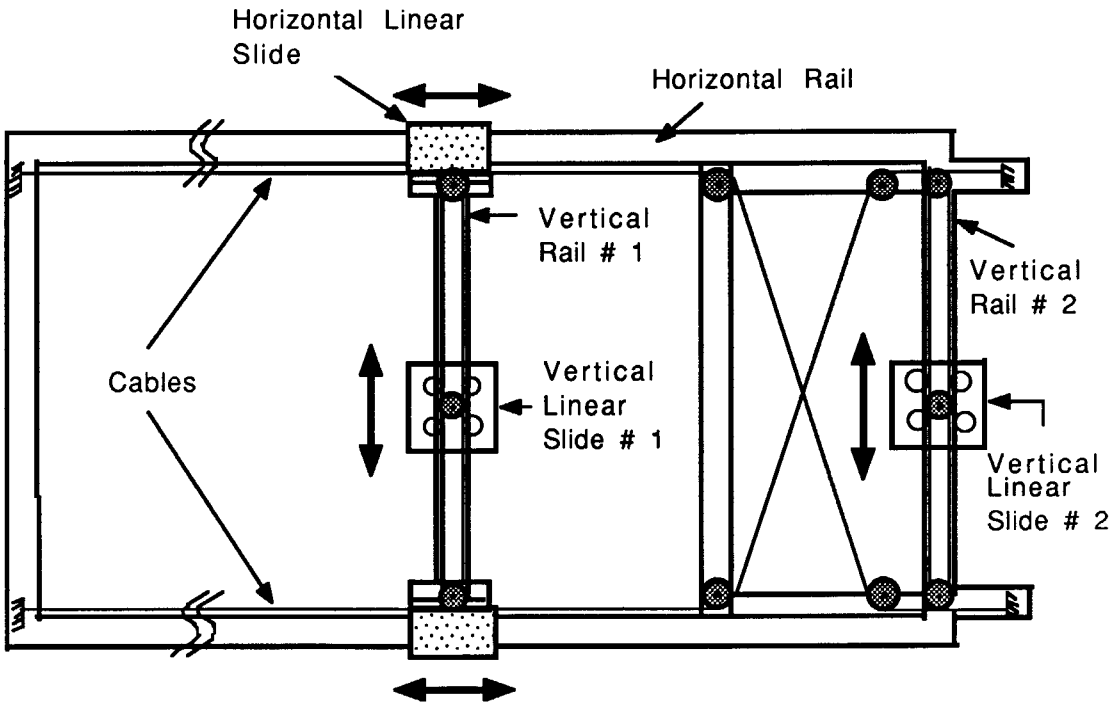

Figure 8–21: Schematic of planarizer as constructed. The inertia of the machine's vertical movement can be adjusted to be the same as the inertia of horizontal movement by adding weights to the vertical slide #2. The major drawback is friction in the cables and pulleys.

This empty page was substituted for a blank page in the original document.

Chapter 9

Internal Combustion Actuators

David S. Barrett and Marc H. Raibert

9.1 Introduction

We are exploring a new kind of actuator to use in systems that are self-contained and must carry their own power. A conventional self-contained power system, like the one shown in figure 9–1a, incorporates a chain of energy conversions that intermediates between combustion of a fluid fuel such as gasoline, and the controlled delivery of force and power to the mechanism. The present idea is to improve the power to weight ratio of the overall system by eliminating links in the conversion chain. The proposed system, shown in figure 9–1b, will combust fuel directly in the actuator. The fuel and fuel supply tank remain unchanged. The carburetor and servovalve merge into a single fuel-valving mechanism. The engine, shafts, couplings, and hydraulic pump are eliminated.

The actuator is similar in form to conventional actuators, but it must dissipate heat and match the impedance of the exploding fuel to the driving load of the output linkage. Additional valves may be required to exhaust hot gasses at high rate. Techniques for providing fuel and exhaust valving are at the heart of the proposed development. Initial designs will perform these functions using conventional mechanical and electromagnetic valves, including servovalves. Future designs may use specially designed micro fuel injectors fabricated with integrated technology. Computing will play a role in providing suitable operation of fuel and exhaust valves.

The advantages of the internal combustion actuator over conventional designs would be its high power to size and power to weight ratios, and the simplicity gained from eliminating major sets of moving parts. Improved fuel efficiency might also be possible at some scales, although probably not at large scale.

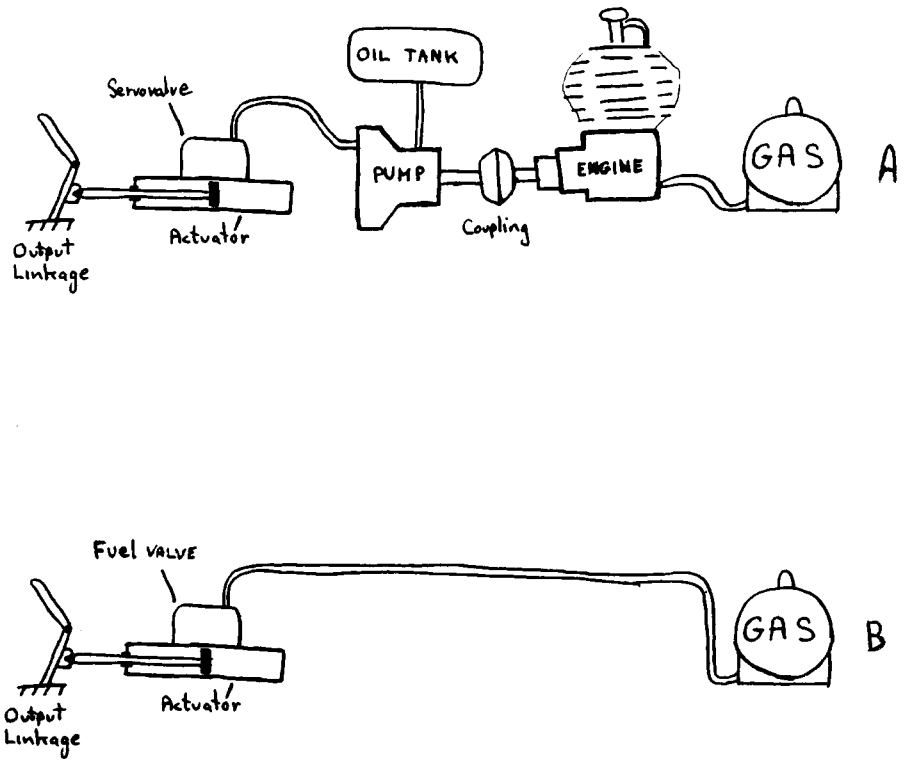

Figure 9–1: A) A conventional power system employing an internal combustion engine, a hydraulic pump, and hydraulic servoactuators. B) An *internal combustion actuator.* The engine, coupling linkages, and hydraulic pump are eliminated, since the fuel is combusted directly in the linear actuator.

Direct Actuation

The idea behind the internal combustion actuator is to avoid a long chain of energy conversions, each of which reduces efficiency and adds weight. There is an increasingly direct connection between combustion and propulsion as one proceeds through the vehicles in the following list:

- diesel train, steam ship
- automobile
- propeller aircraft
- jet aircraft
- rocket

The coupling between combustion and thrust is quite tight in the jet aircraft and rocket, though both rely on conventional actuation to move control surfaces. Space systems with reaction-jet attitude control use internal combustion actuation for motion control. We are

left with a central question of this study: Can the extremely high energy density and rapid response of combustible fluid fuels such as gasoline be harnessed to produce controlled motion without a lot of mechanical overhead?

Use of Internal Combustion Actuators in Running Machines

We are exploring the internal combustion actuator in the context of legged locomotion. The application to legged robots is ideal because legged systems will require self-contained power to be practical, and there is a high penalty for size and weight. Legged systems are a particularly good application for internal combustion actuators because they use rhythmic motions, which should be simpler to control with an internal combustion actuator than the discrete motions found in manipulation. Internal combustion actuators may eventually be useful in other self-contained applications that use servoactuators.

Internal combustion actuators are suited for two functions in legged locomotion. One function is to power the vertical thrust that each leg delivers to make the machine rebound from the ground†. A second function is to power the fore and aft sweeping motions of the legs. The vertical motion is particularly good for internal combustion actuation, because each vertical thrust is preceded by a compression phase, in which the legs shorten under the weight of the body. This compression phase can be used to prepare for actuation as does the compression stroke in a conventional internal combustion engine. Some other means will be required to provide compression for the sweeping motions of the legs, especially to get started. Pairs of actuators, return springs, and temporary gas storage elements are possibilities. For both the vertical and sweeping motions of the legs, springs in series with actuators will be required to match impedances.

In evaluating the internal combustion actuators, both on the bench and in the context of running machines, we expect to reach one of the following conclusions:

- Internal combustion actuators are totally unworkable with existing or near term technology.
- Internal combustion actuators can be used for main power delivery, but control must be exercised through conventional actuators.
- Internal combustion actuators can provide a crude control at low bandwidth, but they must be used in conjunction with a low power/high-bandwidth actuation system for precise motions.
- Internal combustion actuators can deliver controlled output at high bandwidth.

This list of possibilities comes from the expectation that internal combustion actuation will be easy when the required motion is repetitive, but more difficult when the required output of force, amplitude, and rate vary from motion to motion and within each motion. Another likely possibility is that we can trade some of the simplicity shown in figure 9–1b for improved control.

† A gasoline powered pogo-stick using internal combustion actuation to power the vertical motion was sold through magazines in the early 1970's. That design suffered from a poor match between the rate of vertical acceleration of the rider and the duration of the vertical thrust, and because there was no means for controlling the magnitude of the combustion.

9.2 Progress on the Internal Combustion Actuator

We have built a series of four bench-top hydrogen engines that have allowed us to experiment with various overall configurations, fuel/air mixtures, compression arrangements, seals, and instrumentation.

We chose to use hydrogen as the fuel for these experiments because it has a higher energy mass density (142 MJ/kg) than propane (50 MJ/kg) or gasoline (47 MJ/kg). Hydrogen is convenient because the principal combustion byproduct is water vapor, permitting us to run indoor experiments without special exhaust handling equipment. Hydrogen is also safer to store in the laboratory than either gasoline or propane.

One-Sided Test Actuator

We built a one-sided internal combustion actuator and an actuator system controller, to determine the relationship between system input variables, such as fuel/air ratio and pre-combustion pressure preload, and system output.

The one-sided actuator shown by figure 9–2 consists of:

1. A brass power piston tightly fitted into the bore of a thick-walled aluminum cylinder head. The small annular gap (0.001 inch) between the piston and the cylinder acts as a dynamic seal to protect the O-ring riding at the top of the piston from the hot combustion gasses.
2. A manifold block to carry the fuel/air mixture to the cylinder and to mechanically support the other assemblies.
3. A fuel/air mix chamber that acts as a carburetor and allows precise control of the ratio of air and hydrogen. The chamber holds enough fuel/air mixture charge for 6 piston firings.
4. A simple sensor and control system consisting of a high resolution pressure sensor (0.01 psi) in the carburetor, a high pressure (5000 psi) pressure sensor in the combustion chamber, and a single board computer as a local controller. The processor was a Motorola 6811 micro-controller.
5. A glow plug was used for detonation.
6. A high-pressure stainless steel check valve and a single failsafe normally closed commercially purchased external charge injection valve protected the input fuel line.
7. A pressure regulateable double acting air cylinder was attached to the actuator piston through a shock absorbing coupling to both position the actuator piston during the motoring parts of a cycle, and to act as a load during the firing parts of a cycle.
8. The control program performed all of the cycle sequence and experimental data recording functions automatically.

We installed O-ring seals on the piston and at all juncture points and used commercial high pressure valving wherever possible. The fixture holds pressure for a few minutes. The

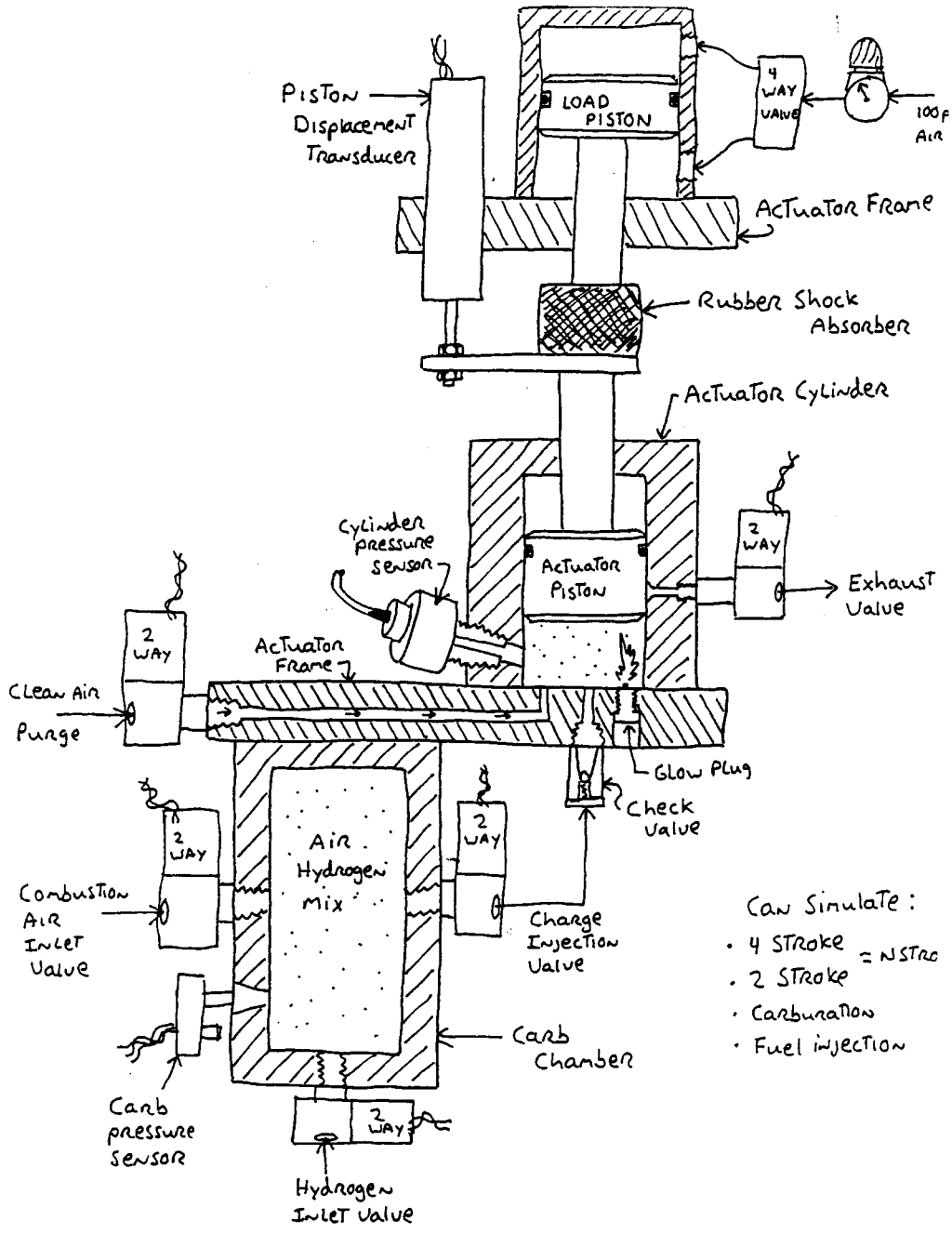

Figure 9–2: One-sided internal combustion test bench.

operation of the test station varied depending on which firing cycle was under investigation. When operated with a four stroke cycle, the controller executes the following steps:

1. Charge the carburetor to the correct mix.
2. Void the piston chamber by drawing the piston down with the exhaust valve open.
3. Induct a fresh explosive charge by closing the exhaust valve opening the injection valve and driving the piston up, creating a partial vacuum that pulls in the charge from the carburetor.
4. Compress the charge by closing all valves and driving the piston down. The more the charge is compressed, the more explosive it becomes because of the proximity between fuel and oxidant.
5. Fire by turning on the glowplug at a preset pressure level.
6. Record data during the power stroke, as the hot expanding gasses formed by the explosion push against the actuator piston which in turn, is loaded by the air cylinder. The pressure rise in the cylinder caused by the interaction of the two is recorded from the onset of fuse activation for about 1.2 sec. During this interval 512 cylinder pressure and piston displacement data samples are recorded.
7. Open the exhaust valve after the last data point is recorded, releasing the cylinder gasses. Because of the low frequency of firing, the actuator body never gets hot enough to keep the combustion byproducts (in this case water vapor) in a gaseous form. As the vapor hits the cold cylinder walls it condenses and a significant fouling problem occurs. Clean air at 100 psi is injected through a purge valve to blow out any accumulation of liquid between cycles. At higher firing rates, the vapor stays vapor and steam can be seen issuing from the exhaust valve.

Results

The internal combustion test station has 5 major parameters that can be experimentally varied to study its feasibility for use as a controllable actuator:

1. Air/fuel mix ratio, which controls force generated
2. Compression ratio, which controls energy return for energy invested
3. Type of combustion cycle, 0, 2, or 4 strokes
4. Frequency of firing
5. Type of load applied to piston

Experiment 1: Effect of Air/Fuel Mix

Hydrogen is a very flexible fuel to use for internal combustion actuation because it is explosive over a wider range of fuel/air mixture ratios than any other fuel. To get an idea of how force output could be controlled by selectivity altering this ratio, a series of experiments

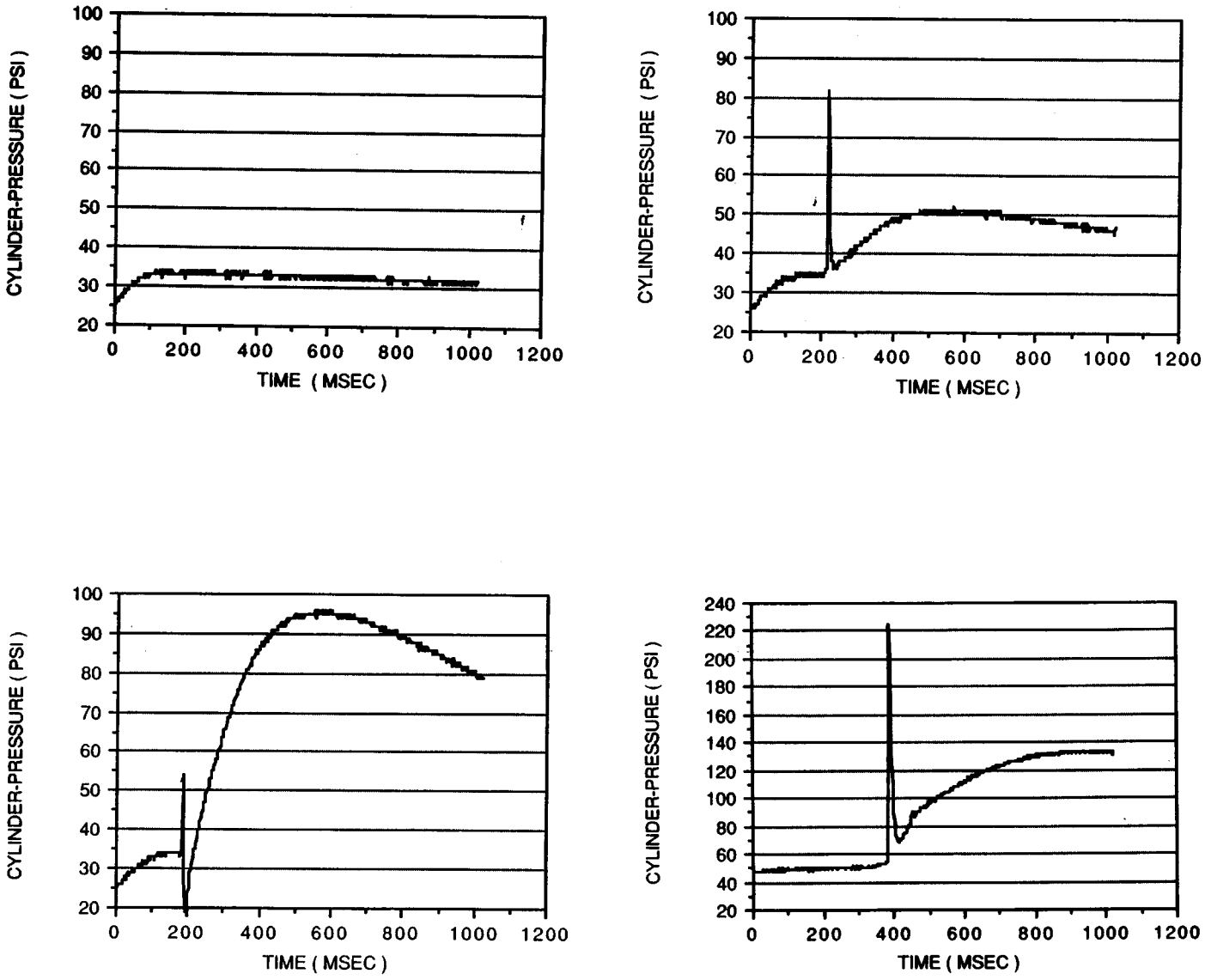

Figure 9–3: Pressure vs time for various mixtures of air and hydrogen, and for two settings of the pressure fuse. Top left: 20% hydrogen, 25 psi fuse, top right: 40% hydrogen, 25 psi fuse, bottom left: 60% hydrogen, 25 psi fuse, bottom right: 60% hydrogen, 50 psi fuse.

were run in which the ratio was varied from 10% hydrogen to 90% hydrogen air with the explosion pressure profile measured for each one. These ratios were those present in the carburetor and not those present in the cylinder. The ratio in the cylinder was probably considerably leaner because of mixing with air entrained in the manifold block passages. All other variables were held constant. With a ration of 10% (figure 9–3 top left) the pressure time curve shows a slight pressure rise caused by the piston compressing the fuel/air mixture, but no explosion takes place. With a mixture ratio of 40% (figure 9–3 top right) an explosive peak that followed ignition was followed by a pressure rise that could be attributed to hot expanding gasses. With a ratio of 60% (figure 9–3 bottom left) the explosive peak is followed by a pressure rise that almost triples the pressure developed by compression of the charge alone. The surplus pressure (the area under the 60% curve and above the 20% curve) is excess energy capable of doing useful work (see figure 9–3 bottom right).

The complete family of explosion curves shows a symmetry of form that rises from no explosion at 20% to a maximum at 60% and then down to no explosion again at 80%. Varying other parameters causes the family of curves to shift and distort in unpredictable ways. However, for a given set of parameters, the actuators force output might be controlled by varying the mix ratio. This would require the development of a precise high-speed mixing system if the actuator were to operate at high frequencies.

Experiment 2

The compression ratio relates the volume of the cylinder when it is first filled with charge to the volume of the cylinder when the charge is ignited. If the piston does not move the ratio is 1:1. If the piston moves halfway down the cylinder the ratio is 2:1, etc. Commercial engines operate with compression ratios between 8:1 and 12:1. At low compression ratios the molecules of fuel and oxidant are relatively far apart and tend to burn rather than explode. At high compression ratios the molecules are crowded together and combustion takes place almost instantaneously.

To determine the effect of the compression ratio on the performance of an internal combustion actuator, the pressure fuse trip point was increased from 0 to 50 psi holding all other variables constant. The pressure fuse trip point is measured relative to the cylinder pressure before the piston moves. At 0 psi, the compression ratio was 1:1, and there was a slightly audible pop but no significant pressure rise. At 50 psi the high pressure spikes were between 200 and 300 psi, and they sometimes ruptured hoses. No higher pressures were tried because we did not want to destroy the apparatus. Compare the data in figure 9–3 bottom left, which was produced with a 25 psi fuse, with that in figure 9–3 bottom right, which had a 50 psi fuse. The same amount of hydrogen and air (and thus the same potential energy content) was present in the cylinder in all cases. There is more "bang for the buck" at higher compression ratios. The charge could be injected into the cylinder at these high pressures negating the need for a compression stroke and releasing the same energy.

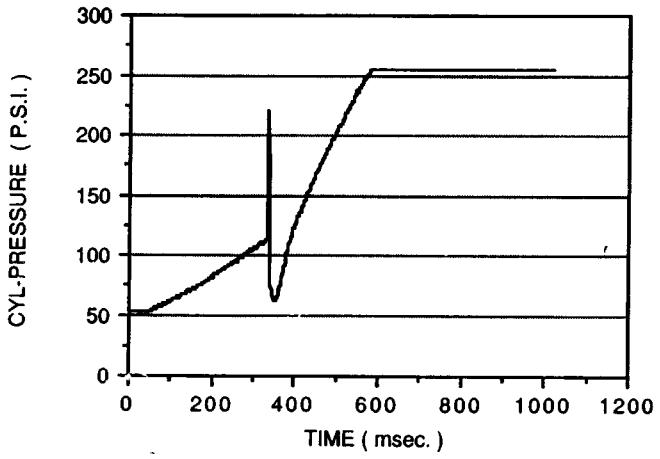

Figure 9–4: Pressure vs time for two stroke cycle.

Experiment 3: Combustion Cycle

Three types of combustion cycles were tested: 4 stroke, 2 stroke and 1 stroke. The four stroke cycle consisted of 4 sequential steps: 1) exhaust the cylinder 2) induct a fresh charge 3) compress the charge 4) explode the charge

Of all the cycles tried, this one was the easiest to implement. The shuttling of gasses from carburetor to cylinder and from cylinder to exhaust was straight forward with only a single state present in the cylinder at a time. The viability of the cycle did not seem to sensitively depend on small changes in parameters. Correspondingly, this cycle was chosen for most of the experimentation.

The two stroke cycle consisted of two steps: 1) exhaust water vapor and induct fresh charge 2) compress charge and explode

This cycle was difficult to implement because by its very definition exhaust gasses are exiting the cylinder at the same time a fresh charge is being drawn in. Timing is crucial. If the exhaust valve stays open too long all the new charge blows out with the old exhaust. If it closes too quickly the old exhaust dampens and smothers the explosion of the new charge. This cycle seemed to be very dependent on small changes of parameters and was prone to misfiring and drowning in liquid residue of previous explosions. Although the actuator was eventually able to run consistently, a change in port design and location would greatly boost its reliability.

The one stroke cycle consisted of directly injecting a high pressure charge into the piston cylinder with the piston in the position of normal full compression and then exploding the charge. Although this cycle worked, producing reliable repetitive cycles was difficult because of the exhaust port placement.

Experiment 4: Frequency of Firing

The frequency of firing is the total time elapsed between subsequent explosions. It is a function of the response time of the solenoid valves used, the size of the internal passages and orifices, and the pressures in the carburetor and cylinder. It is also a function of

the chosen combustion cycle. In practice, the maximum frequency of firing of this internal combustion actuator was one cycle every three seconds. This was caused by the time needed to recharge the carburetor chamber and the flow restrictions that limited the speed of the load simulating air cylinder. This firing speed is probably too slow for practical actuation. Replacing the carburetor with direct fuel injection into the piston chamber could reduce the cycle time measurably.

Experiment 5: Type of Load Applied

The type of load applied to the actuator piston is governed by the valving and regulation driving the load-simulating air cylinder. For most of the experiments this cylinder simply supplied a constant pressure to the actuator piston during an explosion. However, close observation revealed significant short term dynamic oscillations at the junction of the actuator piston and the rubber shock absorber that attaches it to the load cylinder. Other valving schemes were tried but the fundamental question of whether any of these faithfully represent a true load remains unanswered. Probably the best solution would be to replace the load air cylinder with an actual swinging mass leg.

Direct Fuel Injection

In order to address the problem of low firing frequency the carburetor on the test fixture was removed and replaced with a direct fuel injection system, shown in figure 9–5. This system consisted of two, two-way highspeed normally-closed solenoid valves and two manually adjustable flow regulators. In theory, for a 4-stroke cycle, the system should work in the following way:

1. Exhaust stroke—during the exhaust stroke as the piston descends both the exhaust and the air injection valve open forcing out the combustion byproducts and any water vapor that condensed on the cylinder walls.
2. Intake stroke—as the piston rises, both the air and hydrogen valves open allowing both gasses to rush into the chamber created as the piston moves. The fuel/air mix ratio achieved is governed by the pressure regulator and flow regulator setting for each of the component gasses.
3. Compression stroke—as the piston descends all valves close and pressure rises sharply in the cylinder.
4. Power stroke—at a given preset pressure the glowplug ignites the charge driving the piston up in the cylinder.

Results

The installation of a fuel injection system increased the firing frequency of the actuator, which now seems to be limited only by the response time of the load simulating air cylinder.

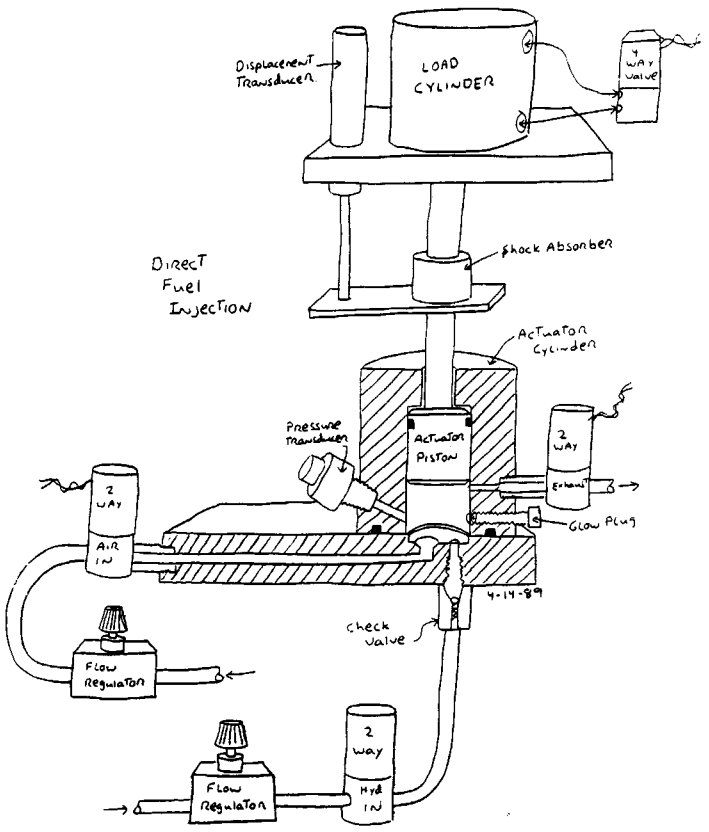

Figure 9–5: One-sided internal combustion actuator with direct fuel injection.

However, the addition of the four manually adjusted analog pressure and flow regulators considerably reduced the capability of precisely controlling the air/fuel mix ratio. It seems as though the pressure and flow settings for each gas (air and hydrogen) are tightly coupled to each other and to the firing frequency in as yet undetermined ways. Small changes in one variable (1/8 turn on a flow regulator) are enough to spell the difference between no explosion and large explosions. A 4-stroke cycle was started fairly quickly with a lot of knob tweaking (see figure 9–4), but the 2-stroke was not consistently firing. Further work needs to be done to improve the control of this system.

9.3 What Next?

We are considering the next step in the development of the internal combustion actuator. One plan would be to build a system coupled to a leg-like mechanism. One concept is shown in figure 9–6. The device consists of three main parts:

1. A swinging mass leg driven by a torsion spring. This leg could have variable length and mass and the corresponding drive spring could be easily replaceable so that a reasonable

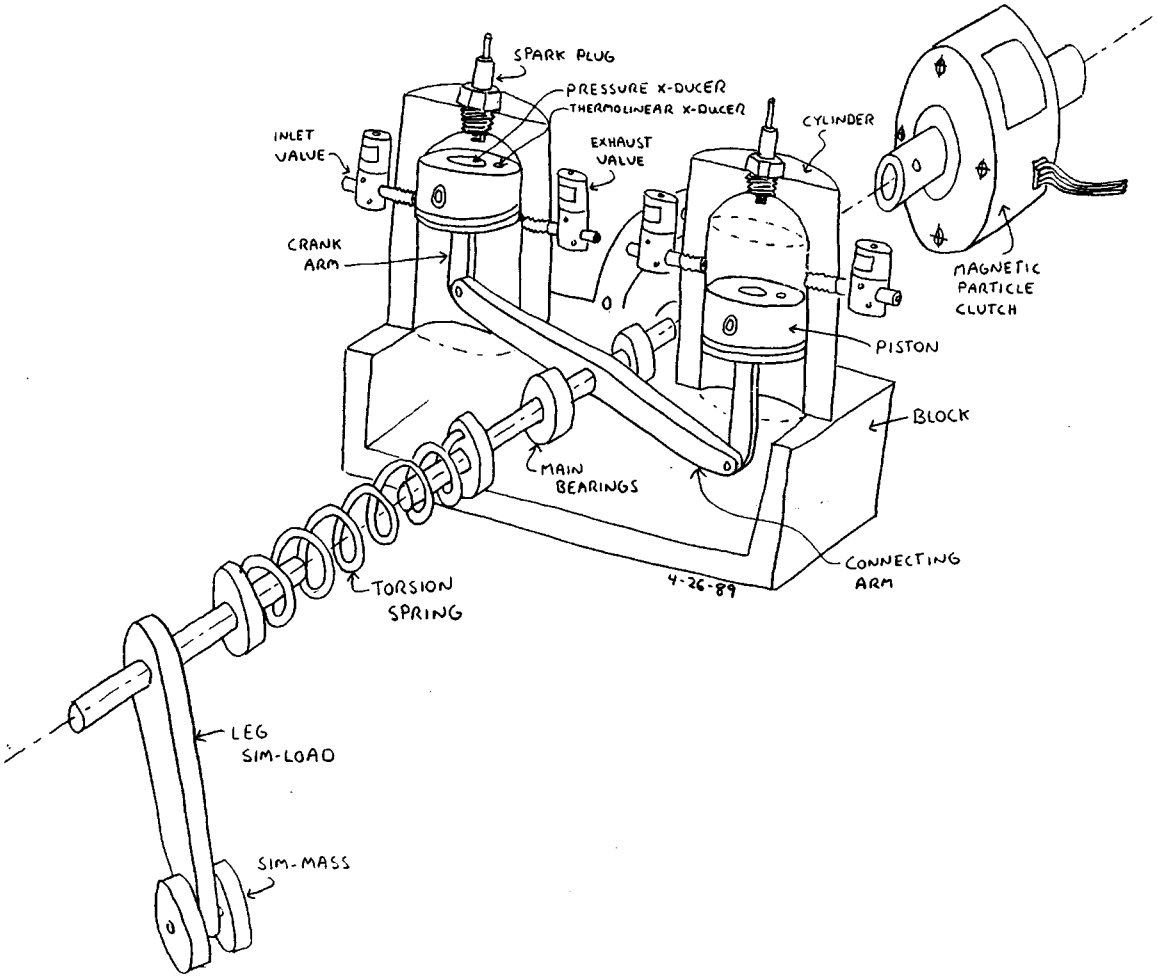

Figure 9–6: Concept for actuator driving leg oscillation.

spectrum of leg loads could be simulated. As an actual swung mass load, this system would accurately simulate real leg loads where the previous high friction air piston failed.

2. A double acting internal combustion actuator.
3. High speed magnetic particle clutch that will allow the actuator to be instantly frozen in a desired location and held there as long as necessary.

Some of the design features and goals of the system are

- Two pistons for 2-way motion.
- High compression cylinder heads, with no fittings, hoses, or valves in the high compression zone.
- High flow opposing port design to combat fouling and promote water vapor purging.
- Better piston stroke to bore ratio to promote heat retention for water vaporization.

- Integral piston pressure and temperature sensors for accurate chamber state measurements.
- Spark ignition system for rapid controllable firing.
- A controllable fuel injection system using massflow sensors and a closed loop control.
- A precision potentiometer to measure the displacement of the piston in the cylinder.

9.4 Summary and Conclusions

Two internal combustion actuators were designed, fabricated and tested in order to determine the feasibility of using combustion as a primary driver for locomotion. In the process of experimentation, the actuators were modified considerably to improve their performance. The results of this experimentation are listed as follows:

1. Explosions in a cylinder with hydrogen as a fuel are fairly easy to produce.
2. The force produced by the explosion is directly linked to the fuel/air mix ratio in a repeatable, predictable way.
3. For a given mass of fuel/air charge, the higher its compression before ignition, the more energy is released in its explosion.
4. 4-stroke combustion cycles are inherently easier to implement than 2 or fewer strokes. However, the lower strokes produce more power per piston cycle.
5. Port location and configuration is crucial to a workable 2-stroke design.
6. The load the actuator sees is a major contributor to its dynamic explosion response.

In short it appears possible to produce controlled explosions of a given force at potentially high frequencies in an internal combustion actuator with existing technology.

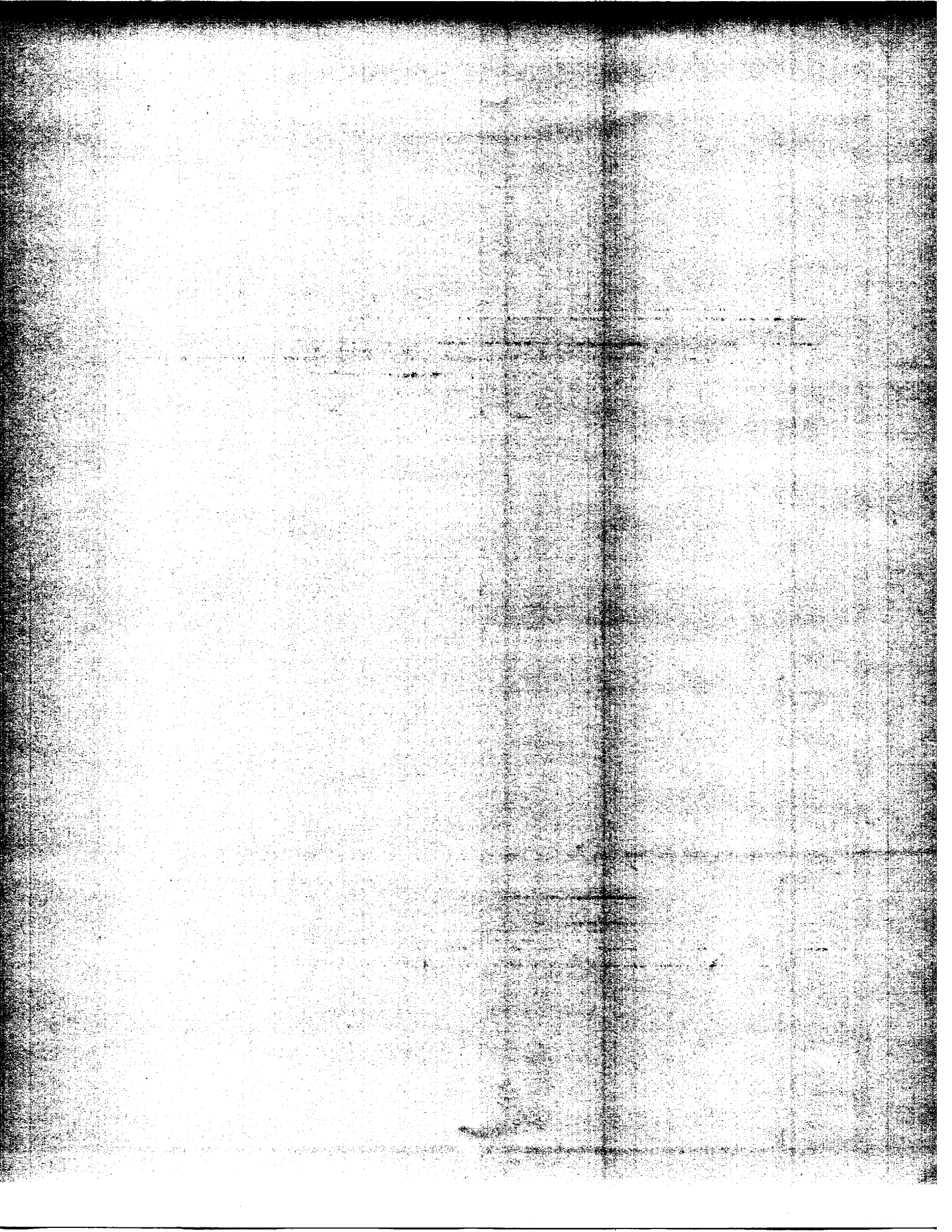

Chapter 10

Zero-Gravity Running

John Daniell Hebert, Lance Borvansky, and
David S. Barrett

10.1 Introduction

Legged locomotion is usually associated with an environment having a gravitational field. Normally it is not possible to run without gravity, because the upward motion that initiates the flight phase cannot be reversed once contact with the ground is lost. One solution would be to use sticky or prehensile feet. In this case the flight phase would be replaced by a "tension phase" during which the vertical motion of the body would be reversed as tension in the legs pulled the body downward toward the support surface.

Another solution, first suggested us by Robert H. Cannon, is to run between two floors. In this case, the supporting forces generated in the collision with one floor reverses the vertical velocity of the previous collision with the other floor. Such a configuration for running might exist in a space station where the walls, floors, and ceilings could act as rebounding surfaces.

We studied a machine designed for running in zero-gravity. The machine has one leg and two feet, and it is restricted to move in plane. The machine uses a control strategy developed for control of hopping machines. Algorithms that control running in zero-gravity can be similar to those used in one-g, to the extent that behavior during ground collision in normal running is dominated by the need to reverse the vertical velocity of the body, rather than oppose the acceleration of gravity. This paper reports computer and laboratory simulations that test this idea.

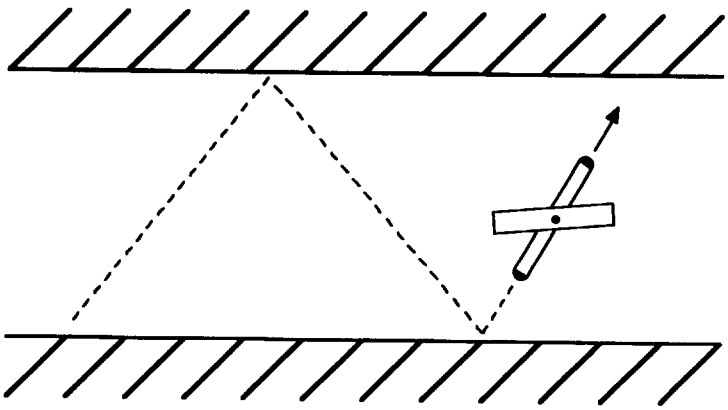

Figure 10–1: The zero-gravity running machine rebounds from two parallel floors as it travels down the corridor.

10.2 Similarities Between Biped Running and Zero-Gravity Running

The basic approach to controlling the running in zero-gravity is to use algorithms originally developed for a one-gravity biped. The two tasks are similar in three respects. First, the phases of the running cycle are identical. Four consecutive phases complete one cycle (see diagram):

- stance phase on leg one
- first flight phase
- stance phase on leg two
- second stance phase
- repeat cycle.

Second, the flight phases of the two systems are similar. For the system running in one-gravity environment, the velocity just after take-off is equivalent to the velocity just prior to touchdown because the flight is ballistic. Likewise, in a zero-gravity environment, the corresponding velocities are also equivalent because the velocity is constant throughout the flight phase.

The stance phases are also similar. Behavior during the stance phase for hopping with or without gravity is similar to the behavior of a mass-spring oscillator. The velocity at the beginning of the stance phase is equivalent to the velocity at the end of the stance phase. Also, for both systems, there is a change in direction during the stance phase.

10.3 Control of Zero-Gravity Running

The similarities between the two systems allowed us to use the same control algorithm. This control algorithm is responsible for maintaining balance and for alternating active and idle legs. It is robust enough such that the absence of gravity does not introduce any additional control problems.

The control algorithm uses a state machine to synchronize control actions with the events in the running cycle. After each unloading state, the idle leg becomes active and the active leg becomes idle. Because the zero-gravity running machine has only one leg, the idle leg cannot be moved independently and thus it automatically opposes the motion of the active leg. This motion, like the mirroring motion of the biped, positions the idle leg near the correct leg position for the next stance cycle. Also the idle leg does not have to retract since there is no danger of striking the ground as it swings forward for the next touchdown.

10.4 Computer Simulation of Zero-Gravity Running

A model of the zero-gravity running machine was simulated. The dynamic model consisted of a body, an upper leg, a massless lower leg, and two massless feet. A drawing of the model is shown in figure 10–2. The massless lower leg slides into the upper leg like a pogo stick. The feet attached to the ends of the lower leg were used to model ground interaction. The machine has two actuators, one on the hip and one on the leg. The hip actuator was modeled as a torque source that acts between the body and the leg. The leg actuator was modeled as a force source that acts between the upper and lower parts of the leg. The output torque and force were calculated by the control program.

A computer program performed control calculations and numerical integration of the dynamic equations derived from the model. The control calculations monitored sensor data from the dynamic model to synchronize the controller state machine with the model, and to calculate the actuator torque and force. A variable step Runga-Kutta algorithm integrated the dynamic equations of the model with initial conditions and control calculations from the previous cycle. Data from the simulation was recorded for future playback as plots or animated cartoons.

The bouncing motion of the machine between two walls can be seen in the path of the body in figure 10–1.

10.5 Zero-Gravity Running Machine

The successful simulation of zero-gravity running encouraged us to design and build a physical machine demonstration of zero-gravity running. The machine has a single leg with a telescoping airspring on each end. The leg is connected to the body by a pivot joint that forms the hip. A pneumatic cylinder actuator at the hip positions the leg. The air springs on the leg make the leg springy and also serve as thrust actuators. A two dimensional zero-gravity environment was created by floating the machine on a smooth table with air bearings. The table was placed in a hallway where the walls acted as rebound surfaces for the legs.

An onboard computer monitors the sensors, performs the control calculations, and sends commands to the actuators. As in the simulation, the control program synchronizes the state machine with the actuators via sensor inputs. In each state, the appropriate servo

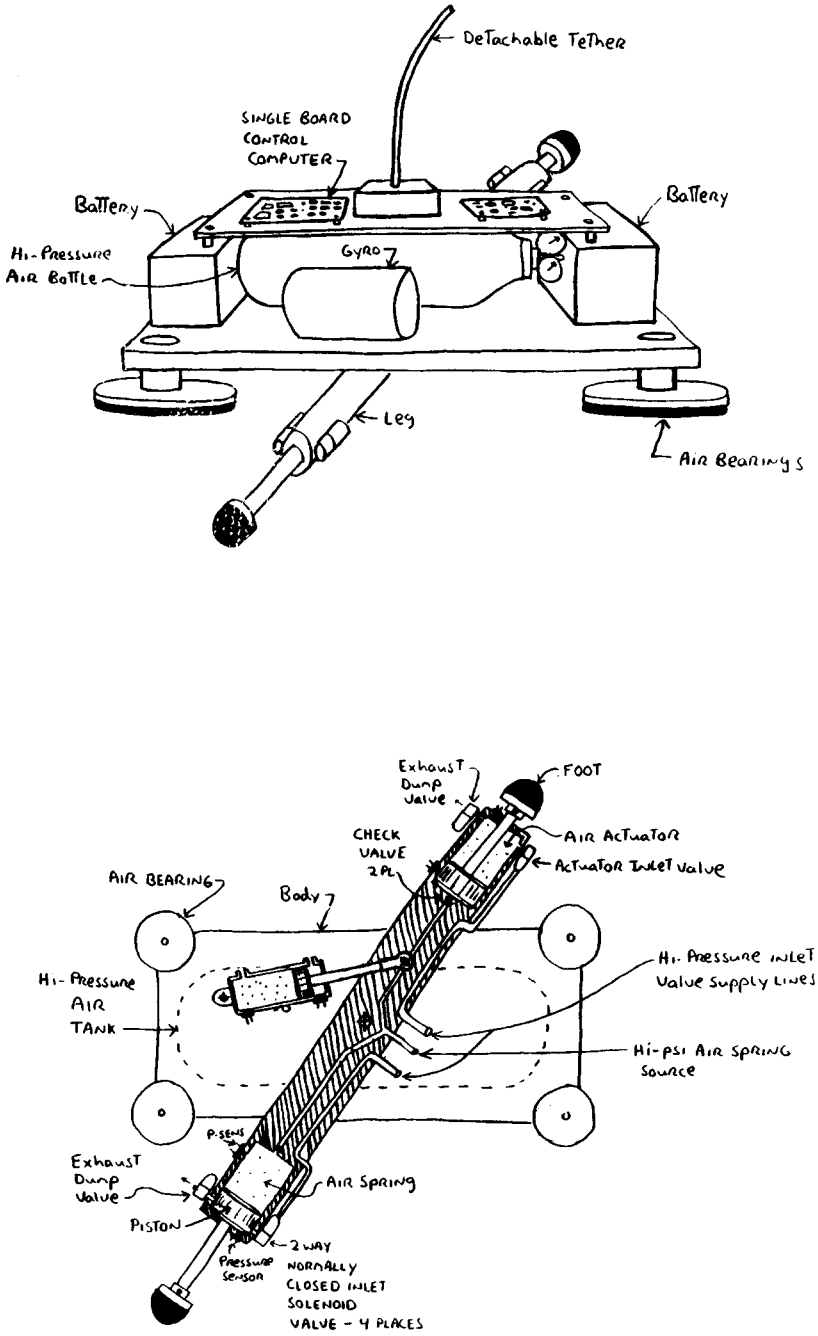

Figure 10–2: Diagram of planar zero-gravity running machine.

calculation is performed and results are output to the actuator.

10.6 Summary

Running can take place in an environment without gravity if there are two support surfaces to bounce between. The control algorithm developed for a bipedal running machine are adequate to control running in zero-gravity. This is possible because the running cycles of both machines are the same, and the absence of gravity has a small effect on the dynamics of the machine.

10.7 Appendix: Detailed Description of the Zero-Gravity Running Machine

A frame made out of half inch birch plywood separated by 6 inch aluminum dowels holds electronics and sensors on the top level, air tank, batteries, and hip actuator on the middle level, and air bearings, leg and thrust actuators on the bottom level.

The hip, a steel dowel supported by two bearing pillow blocks attached to the plywood frame, supports the leg. A rotary potentiometer attached to the top of the hip dowel measures hip angle. The hip actuator is a single ended cylinder attached to the dowel through a lever arm. The cylinder is controlled by a servo valve which creates a pressure difference across the cylinder proportional to input current.

The leg has two double-ended pneumatic cylinders which act as both air springs and thrust actuators during the stance phase. Two rubber feet are attached to the ends of the cylinder rods. Switches inside the feet close when ground contact is made. Pneumatic valves control the thrusting of the leg.

Six sensors were used: two foot switches to sense ground contact, two linear potentiometers to measure leg length, a rotary potentiometer to measures hip angle, and a free gyroscope to measure body angle relative to the orientation of the support surface. The control computer calculates derivatives to find the hip rate, body pitch rate, and leg length rate.

Three air bearings attached to the bottom of the frame float the machine on the floor and allow it to slide with very little friction. The air bearings are 6 inch diameter discs cut from 1/2 inch aluminum plate. Flow control valves regulate the flow of air through 1/4 inch holes drilled in the center of the plates.

The electronics interface and control computer for the zero-gravity hopper are all located on the machine. The electronics interface has an analog and digital component. The a 16 channel analog to digital converter and a four channel digital to analog converter. All control calculations for the zero-gravity hopper are done on board with a general purpose digital signal processor computer. The development interface is a dual port ram connected to a VAX 785 computer.

Power for the zero-gravity running machine is both electric and pneumatic. The machine is designed to operate without a tether for control or power. The electrical power system was designed to be autonomous and an attempt was made to make the pneumatic system autonomous. The electrical power system consists of a bank of thirty 4.5 amp-hour nickel cadmium batteries connected in series, which provide 36V-30V during discharge. DC to DC converters provide 5V@5A and +/- 15V@750mA for the computer and analog electronics. The solenoid valves use an unregulated centertap 24V from the batteries. A 30V DC to 115VAC 400Hz converter powers the gyroscope. Fully charged batteries are capable of powering the system for approximately half an hour, if the gyroscope is not caged frequently.

Due to the properties of the servo valve and the air bearings, the pneumatic system is far from autonomous. A 2.5 gallon high pressure tank was placed on board to provide autonomous pressure, but it was found that the charge in the cylinder was enough to provide

lift for only 40 seconds. Much lower flow rates could be attained if both the air bearings and the floor surfaces were smoother. Another source of air loss is the pneumatic servo valve for the hip actuator, which uses a high flow, even when the actuator is stationary. The performance of the system could also be improved if the total weight were reduced. The batteries and high pressure steel tank with regulators add about twenty five pounds bringing the total system weight to sixty pounds.

To run the machine and record data, the onboard computer was connected to a VAX computer. The computer provided parameters like joystick input, servo gains, and start and stop signals. The VAX recorded data from all the sensors.

This empty page was substituted for a blank page in the original document.

CS-TR Scanning Project
Document Control Form

Date : 6/29/95

Report # AI-TR-1179

Each of the following should be identified by a checkmark:
Originating Department:

☒ Artificial Intellegence Laboratory (AI)
☐ Laboratory for Computer Science (LCS)

Document Type:

☒ Technical Report (TR) ☐ Technical Memo (TM)
☐ Other:_____

Document Information

Number of pages: 212 (220-IMAGES)
Not to include DOD forms, printer instructions, etc... original pages only.

Originals are:
☒ Single-sided or
☐ Double-sided

Intended to be printed as :
☐ Single-sided or
☒ Double-sided

Print type:
☐ Typewriter ☐ Offset Press ☒ Laser Print
☐ InkJet Printer ☐ Unknown ☐ Other:_____

Check each if included with document:

☒ DOD Form ☐ Funding Agent Form ☒ Cover Page
☒ Spine ☐ Printers Notes ☐ Photo negatives
☐ Other: _____

Page Data:

Blank Pages (by page number): FOLLOWING PAGES, V, 26, 47, 78, 105, 181

Photographs/Tonal Material (by page number): 3-5, 11, 28, 68, 81, 109, 156, 165, 195, 203

Other (note description/page number):

Description : Page Number:

(A) IMAGE MAP: (1-8) UN#'ED TITLE, COPYRIGHT, iii-vii, UN#'ED BLANK
(9-212) PAGES #'ED 1-25, UN#'ED BLANK, 27-47, UN#'ED BLANK, 49-78, UN#'ED BLANK, 80-105, UN#'ED BLANK, 107-181, UN#BLANK, 183-203, UN#BLANK
(213-220) SCANNING TRGT, COVER, SPINE, DOP(2), TAGTS(3)

(B) CUT+PASTE FIGS ON PAGES: 3-6, 11, 17-18, 28, 33, 68, 80-82, 84, 92, 109, 111-112, 139, 150-152, 156, 164-165, 180, 184, 187, 189, 191, 193, 194, 198, 200

Scanning Agent Signoff:

Date Received: 6/29/95 Date Scanned: 7/17/95 Date Returned: 7/20/95

Scanning Agent Signature: Michael W. Cook

SECURITY CLASSIFICATION OF THIS PAGE (When Data Entered)

REPORT DOCUMENTATION PAGE

READ INSTRUCTIONS BEFORE COMPLETING FORM

1. REPORT NUMBER: AI-TR 1179	2. GOVT ACCESSION NO.: AD-A225713
3. RECIPIENT'S CATALOG NUMBER:	
4. TITLE (and Subtitle): Dynamically Stable Legged Locomotion	5. TYPE OF REPORT & PERIOD COVERED: technical report
	6. PERFORMING ORG. REPORT NUMBER:
7. AUTHOR(s): Marc H. Raibert, H. Benjamin Brown, Jr., Michael Chepponis, Jeff Koechling, Jessica K. Hodgins, Diane Dustman, W. Kevin Brennan, David S. Barrett, Clay M. Thompson, John Daniell Hebert, Woojin Lee, Lance Borvanksy	8. CONTRACT OR GRANT NUMBER(s):
9. PERFORMING ORGANIZATION NAME AND ADDRESS: Artificial Intelligence Laboratory, 545 Technology Square, Cambridge, MA 02139	10. PROGRAM ELEMENT, PROJECT, TASK AREA & WORK UNIT NUMBERS:
11. CONTROLLING OFFICE NAME AND ADDRESS: Advanced Research Projects Agency, 1400 Wilson Blvd., Arlington, VA 22209	12. REPORT DATE: September 1989 13. NUMBER OF PAGES: 203
14. MONITORING AGENCY NAME & ADDRESS (if different from Controlling Office): Office of Naval Research, Information Systems, Arlington, VA 22217	15. SECURITY CLASS. (of this report): UNCLASSIFIED 15a. DECLASSIFICATION/DOWNGRADING SCHEDULE:

16. DISTRIBUTION STATEMENT (of this Report)

Distribution is unlimited

17. DISTRIBUTION STATEMENT (of the abstract entered in Block 20, if different from Report)

18. SUPPLEMENTARY NOTES

None

19. KEY WORDS (Continue on reverse side if necessary and identify by block number)

Robotics
Legged Locomotion
Dynamic Stability
Gymnastics
Legged Robots
Robot Control

20. ABSTRACT (Continue on reverse side if necessary and identify by block number)

This report documents our study of active balance in dynamic legged systems. The purpose of this research is to build a foundation of knowledge that can lead both to the construction of useful legged vehicles and to a better understanding of animal locomotion. In this report we focus on the control of biped locomotion, the use of terrain footholds, running at high speed, biped gymnastics, symmetry in running, and the mechanical design of articulated legs:

(cont. on back)

DD FORM 1 JAN 73 1473 EDITION OF 1 NOV 65 IS OBSOLETE S/N 0102-014-6601

UNCLASSIFIED

SECURITY CLASSIFICATION OF THIS PAGE (When Data Entered)

- Planar Biped—Control principles originally developed for one-legged hopping were extended to control biped running. A planar biped machine uses this approach to run with an alternating gait, to hop on one leg, and to switch between gaits.
- Rough Terrain—The ability to place the feet on specific footholds is essential to locomotion on rough terrain. We have explored three methods for controlling the length of the step in order to control foot placement. This work allows the planar biped to negotiate obstacles and climb stairs.
- Top Running Speed—The running speed of a legged system can be limited by the strength, length, and stiffness of the legs, the range of joint motion, and the actuator force-velocity characteristics. In the course of experimenting with these parameters, the planar two-legged robot has reached a top speed of 5.9 m/s (13.1 mph).
- Biped Gymnastics—The planar biped has done front flips and aerials. The control program that produces flips uses open-loop actuation patterns in conjunction with the algorithms for normal running.
- Trot, Pace, Bound—We have generalized algorithms for one-legged running to the control of a four-legged running machine. One set of control programs generates three running gaits: trotting, pacing, and bounding. The machine can switch between some of the gaits while running.
- Articulated Legs—We expect legs that use rotary joints to be better than telescoping legs. They will have lower moment of inertia, less unsprung mass, a larger range of motion, better ruggedness, and will be easier to build. Tests on a simple articulated leg indicate that it has superior mechanical characteristics, but it is more difficult to control.
- Passive Dynamic Running—We are interested in the possibility of designing legged systems whose intrinsic mechanical behavior is very close to the behavior needed for locomotion. We have simulated a passive legged system composed entirely of springs, masses, and linkages. It runs passively when supplied with suitable initial conditions.

- Internal Combustion Actuators—A typical mobile hydraulic power supply consists of an engine, pump, drivetrain, and actuators. Can the combustions that normally occur in the engine be moved to the actuator, thereby eliminating the engine, pump, and drivetrain?
- Zero Gravity Running—It is possible to run in the absence of gravity by traveling between two rebound surfaces. We have explored zero-gravity running for the case of a planar one-legged, two-footed machine. The one-g balance algorithms are effective in zero-g without fundamental modification.

Scanning Agent Identification Target

Scanning of this document was supported in part by the **Corporation for National Research Initiatives,** using funds from the **Advanced Research Projects Agency** of the **United states Government** under Grant: **MDA972-92-J1029.**

The scanning agent for this project was the **Document Services** department of the **M.I.T Libraries.** Technical support for this project was also provided by the **M.I.T. Laboratory for Computer Sciences.**

Scanned

Date: 7/17/1995

M.I.T. Libraries
Document Services